Studies Toward the Reactivity of Hydrazones for the Synthesis of Functionalized Pyrazoles and Nitromethyl Sulfones and the Application of Pyrazoles Thereof

A Thesis Submitted
in Partial Fulfillment of the Requirements
for the Degree of

DOCTOR OF PHILOSOPHY

by

Dinabandhu Sar
Roll No. 11612201

Department of Chemistry
Indian Institute of Technology Guwahati
Guwahati- 781039
August 2016

Dedicated

To

My Family Members

INDIAN INSTITUTE OF TECHNOLOGY GUWAHATI

Department of Chemistry

STATEMENT

I hereby declare that the matter embodied in this thesis is the result of investigations carried out by me in the Department of Chemistry, Indian Institute of Technology Guwahati, Guwahati, India under the supervision of Prof. Tharmalingam Punniyamurthy.

In keeping with the general practice of reporting scientific observations, due acknowledgement has been made wherever the work described is based on the findings of other investigators.

Guwahati — Dinabandhu Sar

August 2016

INDIAN INSTITUTE OF TECHNOLOGY GUWAHATI

Department of Chemistry

CERTIFICATE

This is to certify that Mr. Dinabandhu Sar has been working under my supervision since July 2011. I am forwarding his thesis entitled "*Studies Toward the Reactivity of Hydrazones for the Synthesis of Functionalized Pyrazoles and Nitromethyl Sulfones and the Application of Pyrazoles Thereof*" being submitted for the Ph.D. degree of this institute. I certify that he has fulfilled all the requirements according to the rules of this institute, and regarding the investigations embodied in his thesis and this work has not been submitted elsewhere for a degree.

Guwahati

August 2016

Prof. Tharmalingam Punniyamurthy

Supervisor

ACKNOWLEDGEMENT

It would have not been possible to write this doctoral thesis without the help and support of the kind people around me, to only some of whom it is possible to give particular mention here.

First and foremost, my heartfelt thanks to my advisor Prof. Tharmalingam Punniyamurthy for his continuous support, motivation, expert guidance and suggestions throughout my Ph.D. His true scientific spirit has helped me a lot during my research work. I am also thankful to him for giving me the freedom to explore organic chemistry and nurturing my love for the subject. I shall remain indebted to him forever.

I would like to thank my doctoral committee members Dr. Subhendu Sekhar Bag, Dr. Bhubaneswar Mandal, and Prof. Arun Goyal for their evaluation and valuable suggestions during the entire period of my doctoral studies. My honest regards to all the faculty of the Department of Chemistry for their motivation and encouragement.

I am very greatful to CSIR for fellowship for the entire period of the Ph.D. program. I also thank Central Instrument Facility (CIF), IIT Guwahati for providing the instrument facility and DST for providing the X-ray facility.

Further, I would like to thank all my past and present group members, Dr. Prasenjit Saha, Dr. S. Sakthivel, Dr. Tamminana Ramana, Dr. Rajesh Paul, Dr. Md Ashif Ali, Dr. Murali Mohan Guru, Dr. Rapolu Kiran Kumar, Dr. Santosh Kumar Alla, Dr. G. Sathish Kannan, M. Kannan, M. Sengoden, G. Murgavel, G. Bharathiraja, Pradeep Sadhu, D. Mahesh, M. Vijay, V. Satheesh, Raghunath Bag, Pinaki Bhusan De, Sourav Pradhan, Ritesh Pal, Abhisikta Bhowmick and Rinki Nag for the stimulating discussions, pleasant and helpful company and for all the fun we have had in the last five years.

I extend my sincere thanks to other friends in IITG, especially Subhashis Jana, Afsana Yashmeen for their help and support in all aspects.

I also take this opportunity to thank all of my Ph.D. batchmates (July, 11), the other research scholars in the chemistry department and all my IITG friends, who have shared their thoughts and views with me.

My special thanks also go to my dearest friends from outside IITG, Somenath Datta, Debnath Datta, Chanchal Mallik and Amrita Saha for their constant support and encouragement in all respects.

I would like to express my sincere gratitude to my aunty (Aditi Dutta Bag), sister (Shreyasi) and brother (Saswata) for their lovingly inspiration and encouragement throughout my doctoral study.

Finally, I want to thank all of my family members. Without their love and support throughout the past 28 years, none of this would have been possible. They have been nothing short of incredible. I wish to convey my profound gratitude to my beloved parents (Dhanapati Sar & Ita Sar), brother (Anathbandhu Sar) and I dedicate this work to them.

Dinabandhu Sar

LIST OF ABBREVIATIONS

Ar	aryl
aq	aqueous
acac	acetylacetone
Å	angstrom (10^{-8}cm)
λ_{max}^{abs}	absorption maxima
MeCN	acetonitrile
K	association constant
APCI	atmospheric-pressure chemical ionization
bpy	2,2'-bipyridine
B3LYP	Becke, three-parameter, Lee-Yang-Parr
Bu	butyl
BOC	*t*-butyloxycarbonyl
BSA	bovine serum albumin proteins
NBS	*N*-bromosuccinimide
Bn	benzyl
calcd	calculated
CD	circular dichroism
NCS	*N*-chlorosuccinimide
CCDC	cambridge crystallographic data centre
DME	1,2-dimethoxyethane
DMSO	dimethylsulfoxide
DMF	*N*,*N*-dimethylformamide
o-DCB	1,2-dichlorobenzene
DFT	density functional theory
DDQ	2,3-dichloro-5,6-dicyano-1,4-benzoquinone
DPPH	2,2-diphenyl-1 picrylhydrazyl
DABCO	1,4-diazabicyclo[2.2.2]octane
DNA	deoxyribonucleic acid
DIB	(diacetoxyiodo)benzene

DMAPPDN	5-(4-dimethylamino-phenyl)-penta-2,4-dienenitrile
DCE	1,2-dichloroethane
DCM	dichloromethane
Et	ethyl
ee	enantiomeric excess
er	enantiomeric ratio
EWG	electron wthdrawing group
EDG	electron donating group
equiv	equivalent
eV	electron volt
ESI	electrospray ionization
λ_{max}^{fl}	fluorescence maxima
ΔG_r	Gibbs free energy
HSA	human serum albumin protein
ICT	intramolecular charge transfer
IR	infrared
^{i}Pr	isopropyl
ICl	iodine monochloride
NIS	*N*-iodosuccinimide
kcal	kilocalories
Me	methyl
*m*CPBA	*meta*-chloroperbenzoic acid
mp	melting point
MS	molecular sieves
m/z	mass to charge ratio
mM	milimolar
μM	micromolar
nm	nanometer
NMR	nuclear magnetic resonance
ORTEP	oak ridge thermal ellipsoid plot
PDC	pyridinium dichromate

Φ	quantum yield
Q-TOF	quadrupole-time-of-flight
ΔH_r	reaction enthalpy
rt	room temperature
DP-TPPNa	sodium4,4′4″-(3,4-diphenyl-1*H*-pyrrole-1,2,5-triyl)tribenzoate
Δf	solvent polarity parameter
TEMPO	2,2,6,6-tetramethylpiperidine-1-oxyl
TMS	tetramethylsilane
Ts	*p*-toluenesulfonyl
Et_3N	triethylamine
TLC	thin layer chromatography
OTf	trifluoromethanesulfonate
THF	tetrahydrofuran
UV	ultraviolet
λ	wavelength

Abbreviations for intensities of ^{1}H-NMR signals

s	singlet
d	doublet
dd	doublet of doublet
J	spin-spin coupling constant
δ	chemical shifts
MHz	megahertz
t	triplet
q	quartet
m	multiplet
Hz	hertz

Abstract

The thesis contains four chapters. The first chapter focuses on synthesis of bisarylnitromethyl sulfones via iron-mediated radical nitration of bisarylsulfonyl hydrazones followed by elimination of N_2. The second chapter deals with vanadium-catalyzed *C-N* bond formation of alkenyl hydrazones via dehydrogenative cross-coupling for the synthesis of highly substituted pyrazoles. The third chapter contains 2,2,6,6-tetramethylpiperi-dine-1-oxyl (TEMPO)/*N*-bromosuccinimide (NBS) mediated C-H oxidative cyclization of vinylhydrazones for the synthesis of functionalized pyrazoles. The fourth chapter describes UV-visible and fluorescence photophysical properties of some of the synthesized pyrazoles and interaction of two of the pyrazole compounds with BSA protein.

Chapter I. Iron-Mediated Nitration of Bisarylsulfonyl Hydrazones: Synthesis of Bisarylnitromethyl Sulfones

The chemistry of nitroalkanes and sulfones continues to attract the research interest as they generate pharmaceutically important class of compounds. They are widely used in carbon-carbon bond forming reactions, and subsequent several functional group transformations. This chapter report the synthesis of bisarylnitromethyl sulfones using $Fe(NO_3)_3{\cdot}9H_2O$-mediated radical nitration of bisarylsulfonyl hydrazones, generated in situ by the condensation of aryl aldehydes with arylsulfonyl hydrazides at moderate temperature (Scheme 1). The mild reaction conditions, broad substrate scope and use of non-toxic iron salt are the significant practical features.

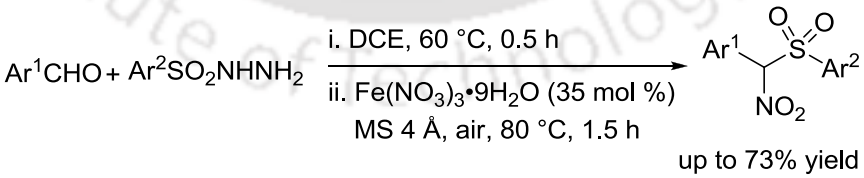

Scheme 1. Synthesis of Bisarylnitromethyl Sulfones

Chapter II. Vanadium-Catalyzed *C-N* Cross-Dehydrogenative Coupling (CDC): Synthesis of Substituted Pyrazoles

Pyrazoles are an important class of *N*-heterocyclic compounds that are extensively used in biological and medicinal sciences. Compounds containing pyrazole scaffold have been

used for the synthesis of many drugs such as Celebrex, Fipronil and Acomplia. This chapter describes the condensation of *α,β*-unsaturated ketones and aryl hydrazines followed by *C-N* cross-dehydrogenative coupling of alkenyl hydrazones using vanadium catalyst for the synthesis of varied substituted pyrazoles at ambient condition (Scheme 2). The substrates bearing electron donating as well as electron withdrawing groups are compatible to provide the pyrazoles with good yields.

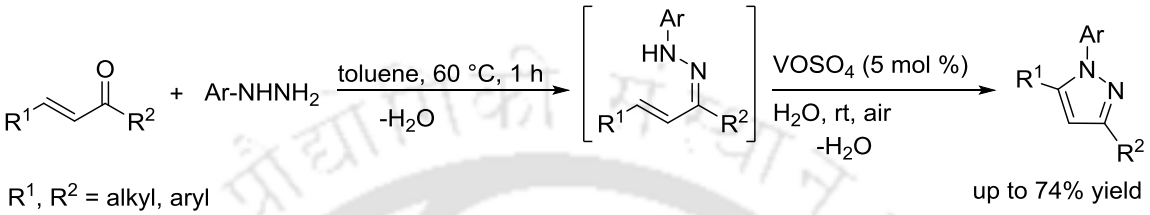

Scheme 2. Vanadium-Catalyzed Synthesis of Substituted Pyrazoles

Chapter III. TEMPO/NBS Mediated C-H Oxidative Cyclization of Vinylhydrazones: Synthesis of Substituted Pyrazoles

Pyrazole is a privileged structural motif present in many compounds that are important in biological, medicinal, material and agricultural sciences. This chapter focuses on a metal-free oxidative synthesis of highly substituted pyrazoles and 4-bromo pyrazoles from (*Z*)-1-allylidene-2-arylhydrazines via C-H amination in presence of TEMPO/NBS as well as NBS (Scheme 3). The metal-free protocol is simple, general and provides a potential route for the synthesis of a library of substituted pyrazoles in short time under mild reaction conditions.

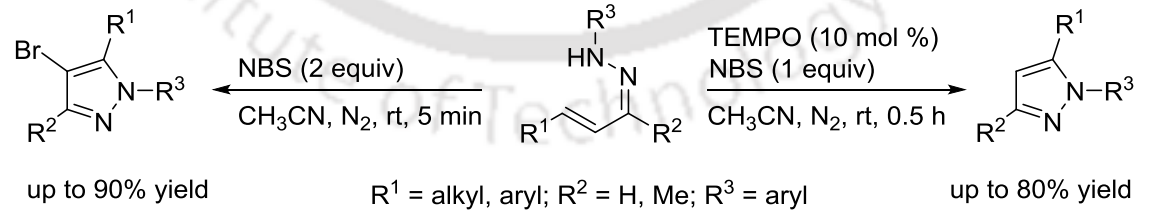

Scheme 3. Synthesis of Substituted Pyrazoles and 4-Bromopyrazoles via Metal Free Condition

Chapter IV. Photophysical Properties and Application of Pyrazoles: Fluorescence Switch-On Sensing of BSA Protein

Functionalized pyrazoles are the subject of recent research interest due to their biological and medicinal applications. Furthermore, pyrazoles are known to bind strongly with biomolecules. This chapter describes the UV-visible and fluorescence photophysical properties of some of the synthesized pyrazoles and also binding studies of two of the pyrazoles towards biomolecule such as bovine serum albumin (BSA) protein.

Contents

Chapter I

Iron-Mediated Nitration of Bisarylsulfonyl Hydrazones: Synthesis of Bisarylnitromethyl Sulfones

Iron has recently attracted significant interests in synthetic community as non-toxic, environmentally benign, inexpensive and second most abundant (4.7 wt %) metal on the earth crust.[1] It is also present in various biological systems. For examples, it takes part in immune system, enzyme production (cytochrome P450), binding and transport of oxygen in the blood, and various electron transfer reaction.[2] In addition, iron complexes have been used as replacements for the expensive transition-metal catalysts such as Pd and Rh for the formation of carbon-heteroatom bonds.[3] Furthermore, a numerous organic transformations are known to be initiated by Fe(III) through single-electron transfer (SET) mechanism.[4] Besides this, several iron salts are known to produce radical species, which are utilized to produce organic derivatives.[5] Moreover, $Fe(NO_3)_3{\cdot}9H_2O$ is well known to produce NO_2 radical on heating,[6,7] which is generally utilized for the production of nitroalkanes.[8]

The development of new reactions for the synthesis of diverse building blocks that can lead to a broad range of utilities is a challenging task in the field of modern organic chemistry. The chemistry of nitroalkanes[9] and sulfones[10] continues to attract the attention of chemists as they comprise a synthetically important class of compounds for the generation of molecules of pharmaceutical importance.[11] They are widely used in different efficient stereoselective carbon-carbon bond forming reactions, and subsequent numerous functional group transformations. For examples, nitroalkanes are utilized in stereoselective Henry reaction[12] and Michael addition,[13] and for the generation of oximes, amines and carbonyl compounds,[14] while aryl sulfones are substrate precursors for Julia olefination,[15] aldol reaction[16] and Michael addition,[17] and for the generation of ketones and alkanes by desulfonylation.[18] Aryl nitroalkanes are demonstrated as key intermediates in the total synthesis of manzamine A[19] and (-)-nutlin-3.[20] Thus, development of effective methods for the construction of nitromethane[21,22] with aryl and sulfonyl groups[23] would be valuable as they may serve as precursor to an array of useful structural scaffolds (Scheme1).[24] In this chapter, we disclose Fe(III)-mediated synthesis of bisarylnitromethyl sulfones from bisarylsulfonyl hydrazones.

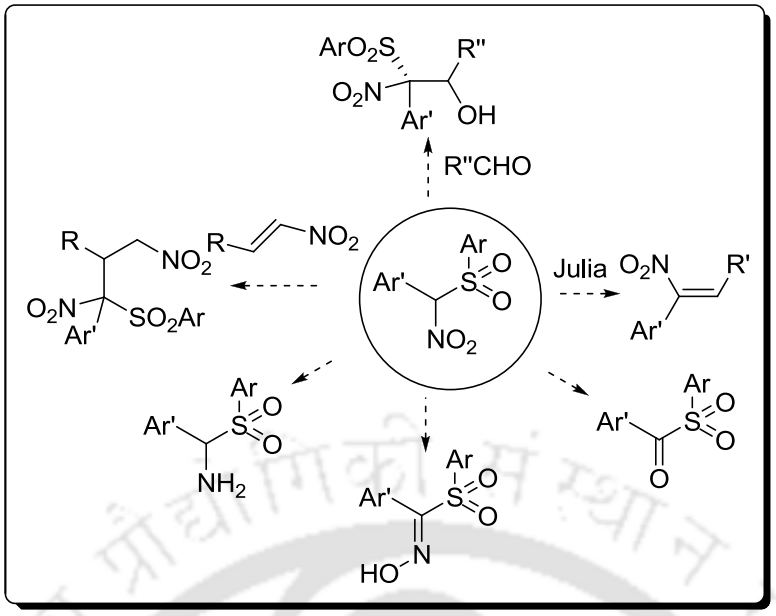

Scheme 1. Application of Nitromethyl Sulfones

1.1 Strategies for the Synthesis of Nitromethyl Sulfones

1.1.1 Traditional Method

The common method used for synthesis of *α*-nitrosulfones is base induced nitration of sulfones in presence of amyl nitrates (Scheme 2).[24] However, this protocol has several limitations involving harsh reaction conditions such as the use of strong bases/acids and inaccessibility of the suitable starting materials.

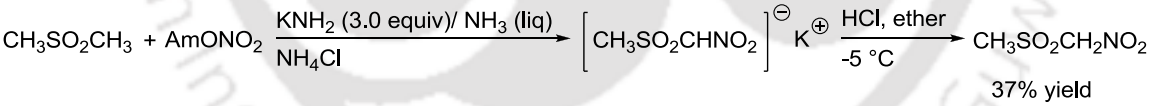

Scheme 2. Base Mediated Synthesis of *α*-Nitrosulfones

1.2 Strategies for the Synthesis of Nitroalkanes

The following schemes illustrate the methods for the synthesis of alkyl/aryl substituted nitroalkanes. For example, the synthesis of nitroalkanes is reported from alkyl halides using $AgNO_2$ as a mediator as well as nitro source in aqueous medium (Scheme 3).[25]

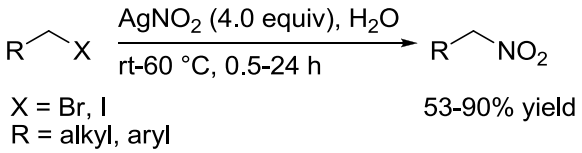

Scheme 3. Synthesis of Nitroalkanes under Aqueous Medium

The synthesis of halo-nitro products has been shown from alkenes employing $Fe(NO_3)_3{\cdot}9H_2O$ as the nitro source and $FeCl_3$ as halogen source under reflux (Scheme 4).[8a] The protocol involves a radical mediated nitration of alkenes by NO_2 radical followed by halogenation of the resultant radical to afford the corresponding halo-nitro products.

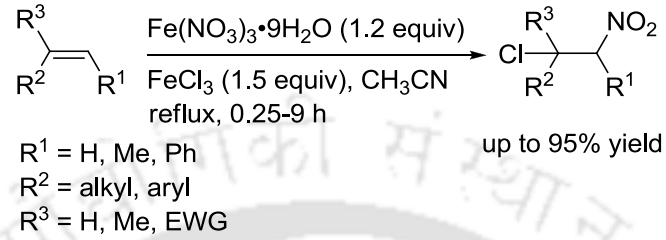

Scheme 4. Synthesis of Halo-Nitro Alkanes/Arenes

Kozlowski and co-workers developed a protocol for the synthesis of arylnitromethane via cross-coupling reaction of aryl halides with nitromethane in presence of Pd catalyst in good yields (Scheme 5).[22b]

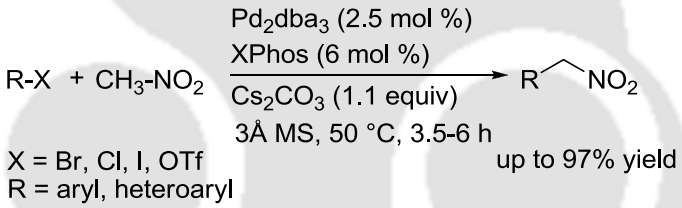

Scheme 5. Pd-Catalyzed Synthesis of Arylnitromethane via Cross-Coupling Reaction

The same group also disclosed the route for the construction of arylnitromethane from 2-aryl-2-nitroacetate via decarboxylation process (Scheme 6).[22c] Substrates with neutral and electron-poor aryl groups vs electron-donating aryl groups afford aryl nitromethanes via decarboxylation process.

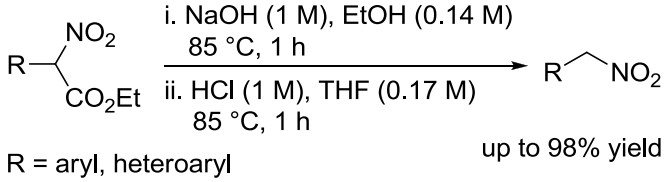

Scheme 6. Synthesis of Arylnitromethane from 2-Aryl-2-Nitroacetate

1.3 Strategies for the Synthesis of Sulfones

There are several methods available for the synthesis of sulfones. For examples, Jørgensen and co-workers explored the synthesis of optically active cyclohexanone by the reaction of *α,β*-unsaturated carbonyl compounds with phenylsulfonylacetophenone in presence of chiral imidazolidine (*S*)-1 via domino Michael-aldol reaction (Scheme 7).[23a]

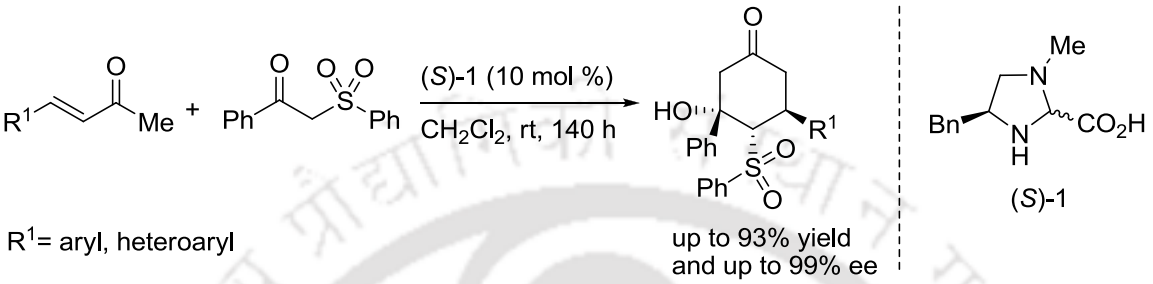

Scheme 7. Synthesis of Optically Active Cyclohexanone Building Blocks

Cinchona alkaloids have been employed for the synthesis of optically pure *α,α*-disubstituted cyanosulfones by the reaction of *α*-substituted cyanosulfones with vinyl ketones via organocatalytic enantioselective Michael addition reaction (Scheme 8).[23b]

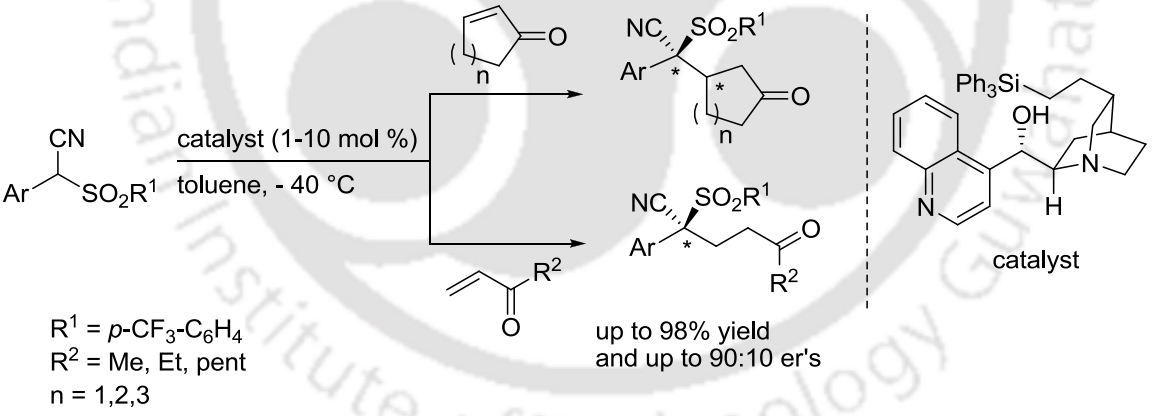

Scheme 8. Synthesis of *α,α*-Disubstituted Cyanosulfones

Reaction of heterocyclic sulfones and acyl or alkoxy carbonyl derivatives has been reported for the synthesis of *β*-acyl and *β*-alkoxycarbonyl heterocyclic sulfones in good to excellent yields (Scheme 9).[26a]

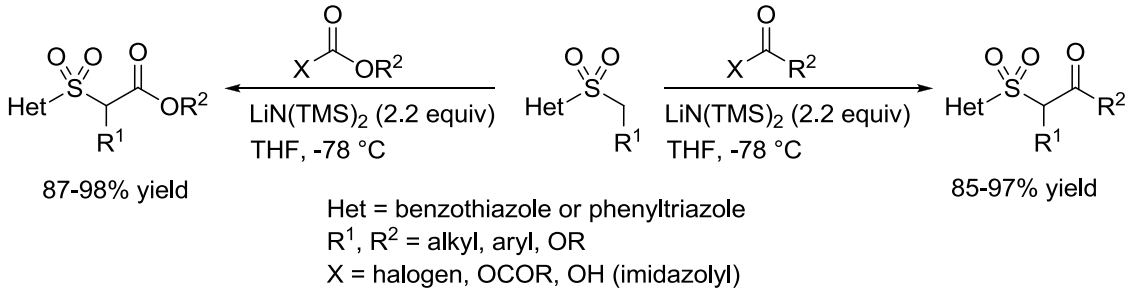

Scheme 9. Synthesis of *β*-Acyl and *β*-Alkoxycarbonyl Heterocyclic Sulfones

Chang and co-workers reported aerobic Wacker-type aminocyclization of *α*-allyl-*β*-ketosulfones followed by 1,4-sulfonyl migration to afford sulfonylmethyl arylpyrroles in good yields (Scheme 10).[26b]

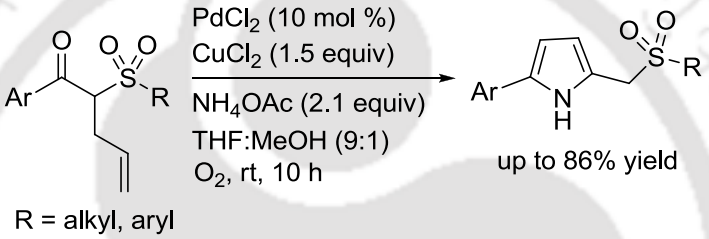

Scheme 10. Synthesis of Sulfonylmethyl Arylpyrrole Derivatives

They also established an efficient protocol for the *m*-CPBA mediated stereoselective synthesis of sulfonyl tetrahydropyrans via ring closure of *β*-hydroxy sulfones (Scheme 11).[26c] Cinnamylation of *β*-keto sulfones in presence of K_2CO_3 produces the product with *α*-cinnamyl side arm which on reduction with $NaBH_4$ affords *β*-hydroxy sulfones.

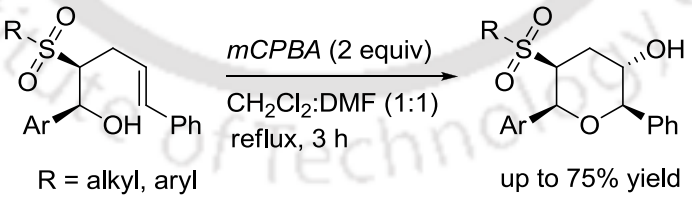

Scheme 11. Synthesis of Sulfonyl Tetrahydropyrans

The synthesis of *β*-keto sulfones has been achieved from *β*-dicarbonyl compounds using iodine mediated sulfonation followed by deacetylation using Na_2SO_3 in water (Scheme 12).[26d]

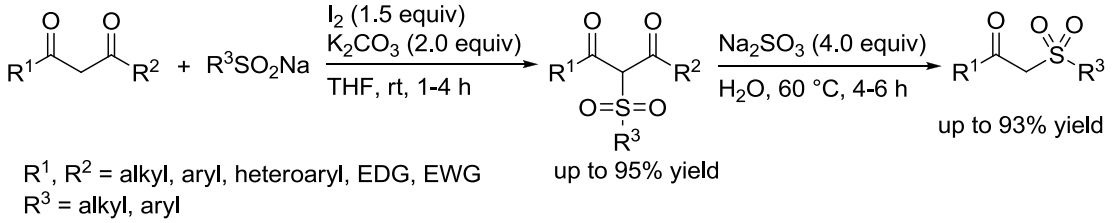

Scheme 12. Synthesis of *β*-Dicarbonyl Sulfones and *β*-Keto Sulfones

1.4 Present Study

We present here $Fe(NO_3)_3·9H_2O$-mediated radical nitration of bisarylsulfonyl hydrazones to afford bisarylnitromethyl sulfones at moderate temperature. The optimization of the reaction conditions was performed using aldehyde **1a** and *p*-toluenesulfonyl hydrazide **2a** as standard substrates employing a series of nitro sources in different solvents at varied temperature (Table 1). The reaction readily underwent to produce bisarylnitromethyl sulfone **3a** in 63% yield when the substrates **1a** and **2a** were stirred at 60 ^oC for 0.5 h in DCE followed by addition of $Fe(NO_3)_3·9H_2O$ and stirring the resultant mixture at 80 ^oC for 1.5 h. In a set of nitro sources screened, $Fe(NO_3)_3·9H_2O$ gave **3a** in 51% yield, while $Cu(NO_3)_2·3H_2O$ afforded the product in 38% yield (entries 1 and 6). In contrast, $Ca(NO_3)_2·4H_2O$, $Bi(NO_3)_3·5H_2O$, ^{t}BuONO and $AgNO_3$ showed no reaction and target product formation was not observed (entries 2-5). DCE was found to be solvent choice, whereas CH_3CN, toluene and 1,4-dioxane gave **3a** in 36-47% yields (entries 7-9). In contrast, THF and DMF yielded inferior results (entries 10-11). The optimum temperature was found to be 80 ^oC, and the addition of the molecular sieves 4Å led to an increase the yield to 63% (entries 12-14). Control experiment confirmed that, in the absence of $Fe(NO_3)_3·9H_2O$, the formation of **3a** was not observed (entry 15).

With the optimized conditions in hand, the scope of the protocol was explored for the reactions of aldehydes **1b-r** with *p*-toluenesulfonyl hydrazide **2a** as a standard substrate (Table 2). The reaction of benzaldehyde **1b** afforded bisarylnitromethyl sulfone **3b** in 66% yield. *o*-Tolualdehyde **1c** underwent reaction to provide **3c** in 57% yield. The reactions of the aldehydes **1d-g** with 3-chloro, 3-methyl, 3-nitro and 3-trifluoromethyl substituents afforded the corresponding substituted bisarylnitromethyl sulfones **3d-g** in 51-61% yields. The aldehydes **1h-m** bearing 4-bromo, 4-chloro, 4- cyano, 4-fluoro, 4-methoxy and 4-ester substituents underwent reaction to produce the target products **3h-m** in 52-69% yields. In addition, the aldehyde **1n** with 2-methoxy and 3-bromo substituents

Table 1. Optimization of the Reaction Conditions[a]

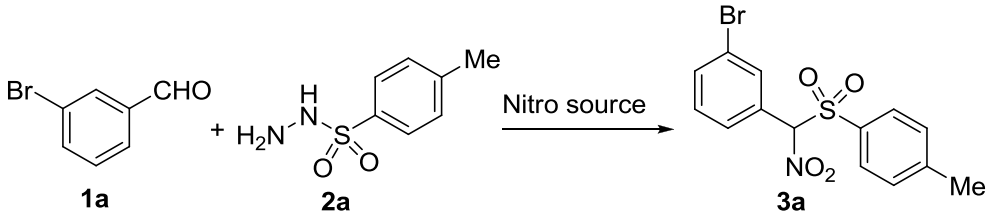

Entry	Nitro source (mol %)	Solvent	Yield (%)[b]
1	$Cu(NO_3)_2{\cdot}3H_2O$ (50)	DCE	38
2	$Ca(NO_3)_2{\cdot}4H_2O$ (50)	DCE	n.o.
3	$Bi(NO_3)_3{\cdot}5H_2O$ (35)	DCE	n.o.
4	^{t}BuONO (100)	DCE	n.o.
5	$AgNO_3$ (100)	DCE	n.o.
6	$Fe(NO_3)_3{\cdot}9H_2O$ (35)	DCE	51
7	$Fe(NO_3)_3{\cdot}9H_2O$ (35)	toluene	47
8	$Fe(NO_3)_3{\cdot}9H_2O$ (35)	CH_3CN	38
9	$Fe(NO_3)_3{\cdot}9H_2O$ (35)	dioxane	36
10	$Fe(NO_3)_3{\cdot}9H_2O$ (35)	THF	trace
11	$Fe(NO_3)_3{\cdot}9H_2O$ (35)	DMF	trace
12	$Fe(NO_3)_3{\cdot}9H_2O$ (35)	DCE	36[c]
13	$Fe(NO_3)_3{\cdot}9H_2O$ (35)	DCE	32[d]
14	**$Fe(NO_3)_3{\cdot}9H_2O$ (35)**	**DCE**	**63**[e]
15	-	DCE	n.o.

[a] Reaction conditions: aldehyde **1a** (1.0 mmol), sulfonyl hydrazide **2a** (1.2 mmol), DCE (3 mL), 60 ^{o}C, 0.5 h; $Fe(NO_3)_3{\cdot}9H_2O$ (35 mol %), 80 ^{o}C, air, 1.5 h. [b] Isolated yield. [c] Temp. 60 ^{o}C. [d] Temp. 100 ^{o}C. [e] MS 4Å (50 mg) used. n.o. = not observed.

produced the desired **3n** in 65% yield, while the reactions of the aldehydes **1o** and **1p** with 2,4,5-trimethoxy and 3,4,5-trimethoxy groups furnished **3o** and **3p** in 72% and 70%

yields, respectively. Furthermore, 2-naphthaldehyde **1q** underwent reaction to give **3q** in 73% yield. However, the reaction of aliphatic aldehyde **1r** was not successful due to decomposition of the hydrazone generated from the aldehyde and sulfonyl hydrazide. Recrystallization of **3o** yielded single crystals in CH_3CN whose structure was determined by single crystal X-ray analysis (Fig 1).

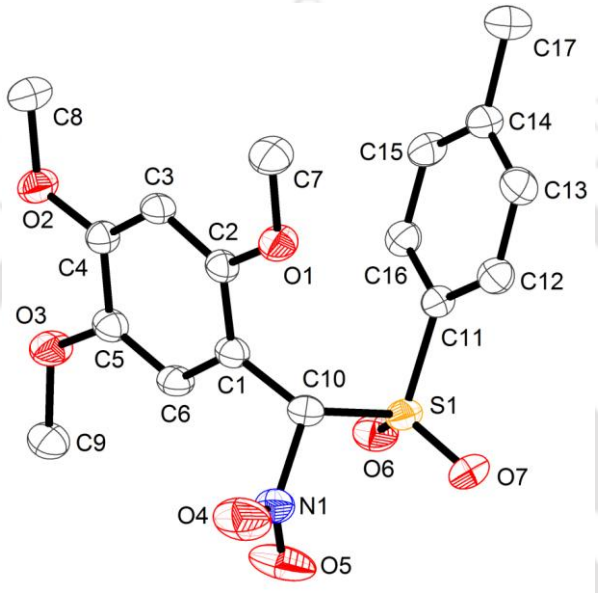

Figure 1. ORTEP diagram of **3o** with 50% ellipsoid. H-Atoms are omitted for clarity (CCDC 1031493).

Next, the protocol was investigated for the reaction of arylsulfonyl hydrazides with the aldehydes **1i** and **1l** having 4-chloro and 4-methoxy substituents as the representative examples (Table 3). Arylsulfonyl hydrazide **2b** underwent reaction to furnish the target bisarylnitromethyl sulfones **3s** and **3t** in 66% and 68% yields, respectively. Similarly, the reactions of the arylsulfonyl hydrazides **2c-e** bearing 4-chloro, 4-methoxy and 4-nitro substituents occurred with 54-64% yields. Furthermore, arylsulfonyl hydrazide **2f** with 2,4,6-trimethyl substituents underwent reaction with 66% and 64% yields, respectively. These results suggest that the protocol has broad substrate scope to afford an effective route for the construction of functionalized bisarylnitromethyl sulfones.

Table 2. Reaction of Various Aldehydes with *p*-Toluenesulfonyl Hydrazide[a]

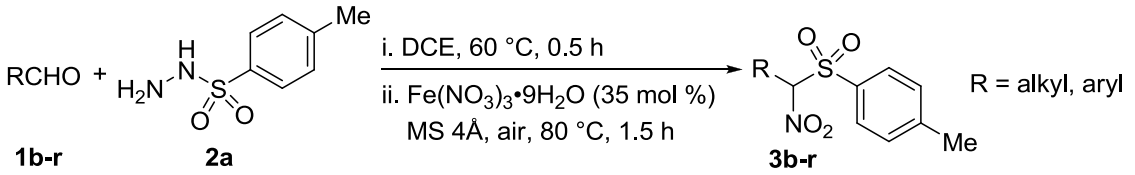

1b-r **2a** **3b-r**

Entry	Aldehyde	Product	Yield (%)[b]
1	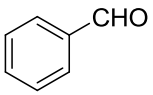 **1b**	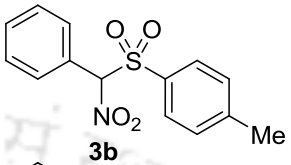 **3b**	66
2	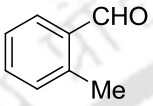 **1c**	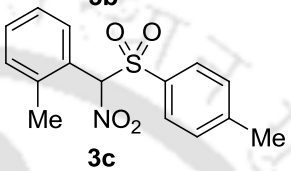 **3c**	57
3	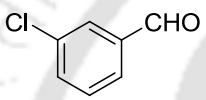 **1d**	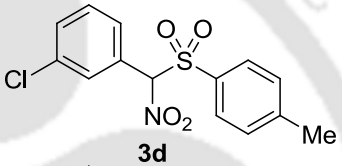 **3d**	61
4	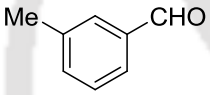 **1e**	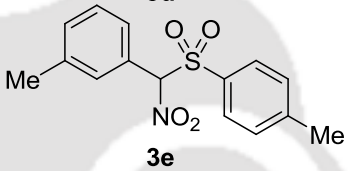 **3e**	58
5	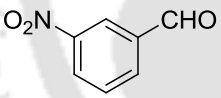 **1f**	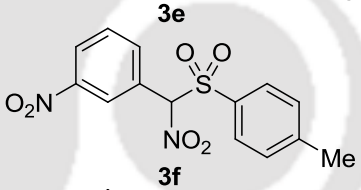 **3f**	55
6	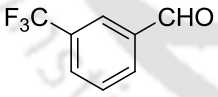 **1g**	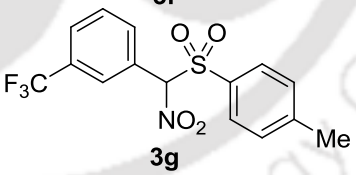 **3g**	51
7	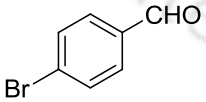 **1h**	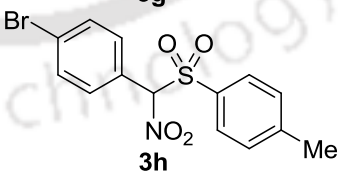 **3h**	60
8	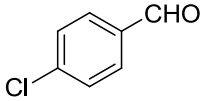 **1i**	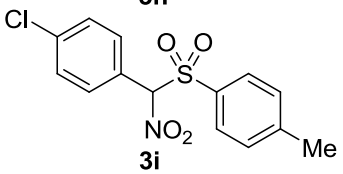 **3i**	62
9	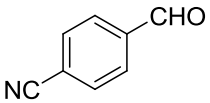 **1j**	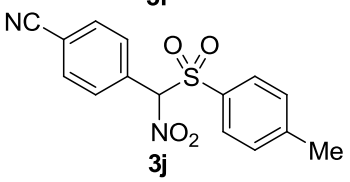 **3j**	52

Table 2 continues.....

10	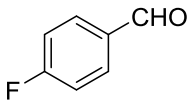 **1k**	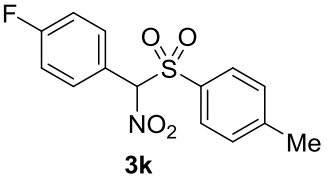 **3k**	59
11	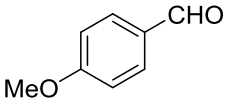 **1l**	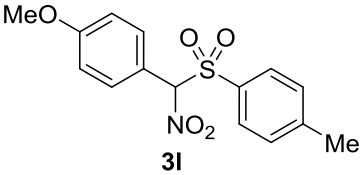 **3l**	69
12	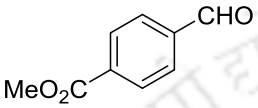 **1m**	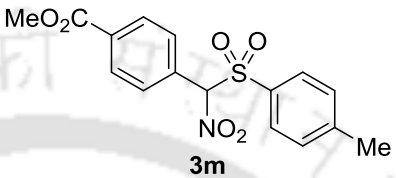 **3m**	58
13	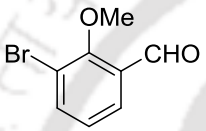 **1n**	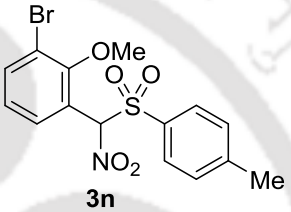 **3n**	65
14	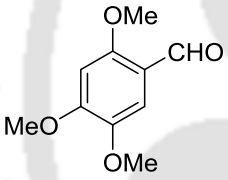 **1o**	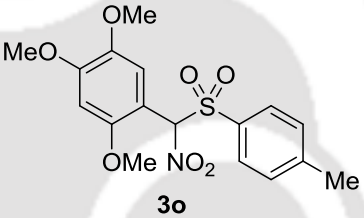 **3o**	72
15	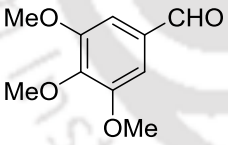 **1p**	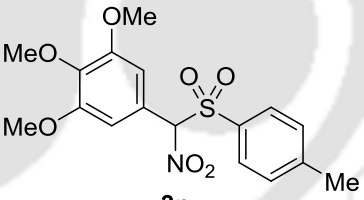 **3p**	70
16	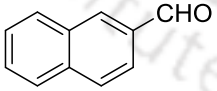 **1q**	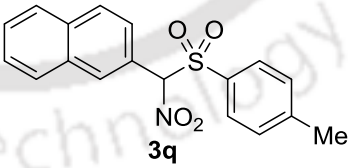 **3q**	73
17	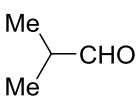 **1r**	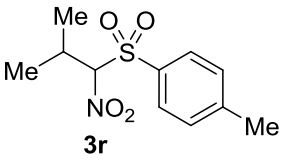 **3r**	n.o.

[a] Reaction conditions: aldehyde (1.0 mmol), sulfonyl hydrazide **2a** (1.2 mmol), DCE (3 mL), 60 ^{o}C, 0.5 h; $Fe(NO_3)_3 \cdot 9H_2O$ (35 mol %), MS 4Å (50 mg), air, 80 ^{o}C, 1.5 h. n.o. = not observed. [b] Isolated yield.

Table 3. Reaction of Different Sulfonyl Hydrazides with Aldehydes **1i** and **1l**[a]

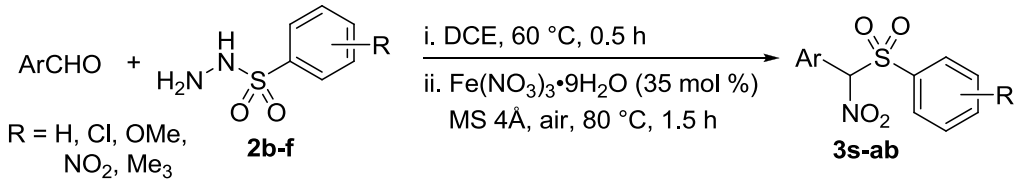

Entry	Aldehyde	Sulfonyl hydrazide	Product	Yield (%)[b]
1	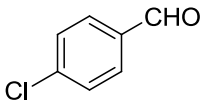 **1i**	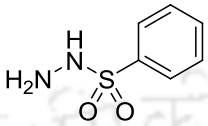 **2b**	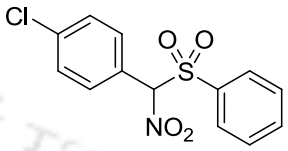 **3s**	66
2	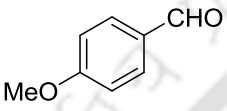 **1l**	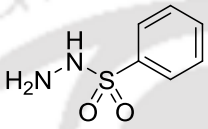 **2b**	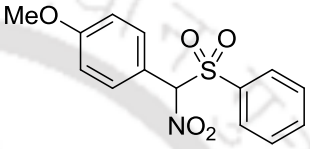 **3t**	68
3	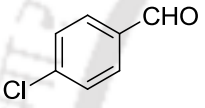 **1i**	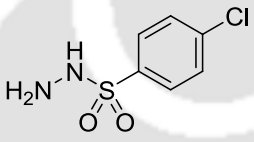 **2c**	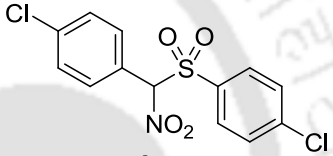 **3u**	57
4	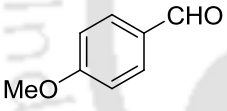 **1l**	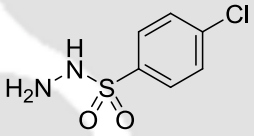 **2c**	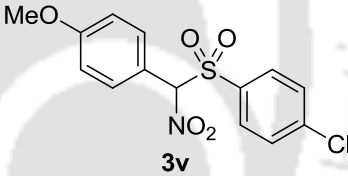 **3v**	61
5	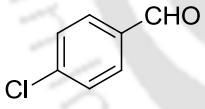 **1i**	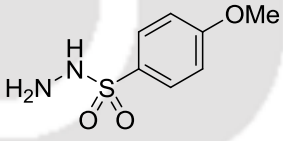 **2d**	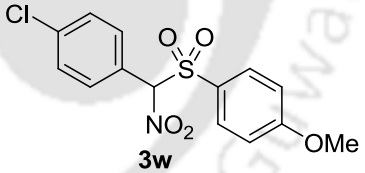 **3w**	64
6	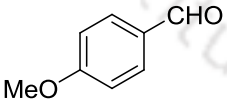 **1l**	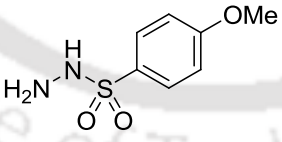 **2d**	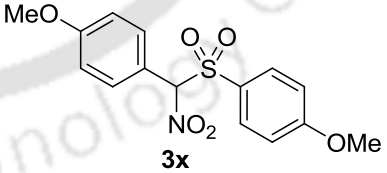 **3x**	63
7	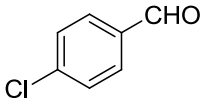 **1i**	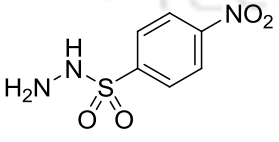 **2e**	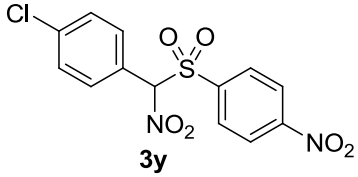 **3y**	54
8	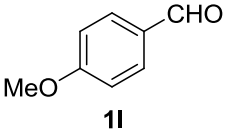 **1l**	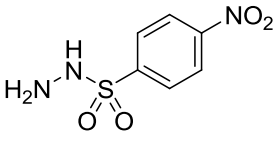 **2e**	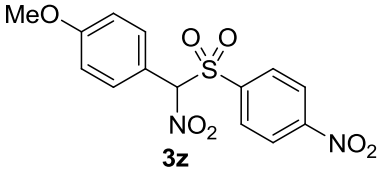 **3z**	58

Table 3 continues.....

9	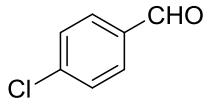 **1i**	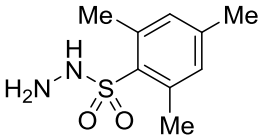 **2f**	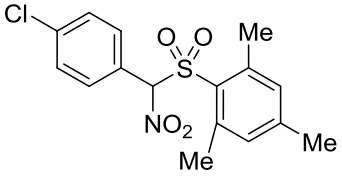 **3aa**	66
10	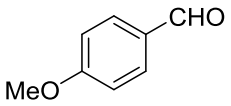 **1l**	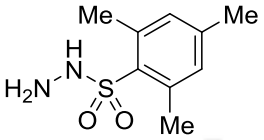 **2f**	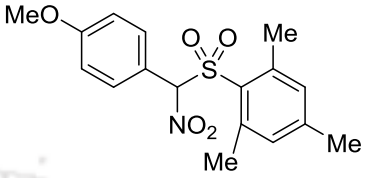 **3ab**	64

[a] Reaction conditions: aldehyde (1.0 mmol), sulfonyl hydrazide (1.2 mmol), DCE (3 mL), 60 ^{o}C, 0.5 h; $Fe(NO_3)_3{\cdot}9H_2O$ (35 mol %), MS 4Å (50 mg), air, 80 ^{o}C, 1.5 h. [b] Isolated yield.

Gram-Scale Synthesis. Finally, the reaction of the aldehyde **1a** and sulfonyl hydrazide **2a** was examined in gram-scale as representative examples (Scheme 13). The reaction readily took place to afford **3a** in good yields, which suggests that the protocol is scalable.

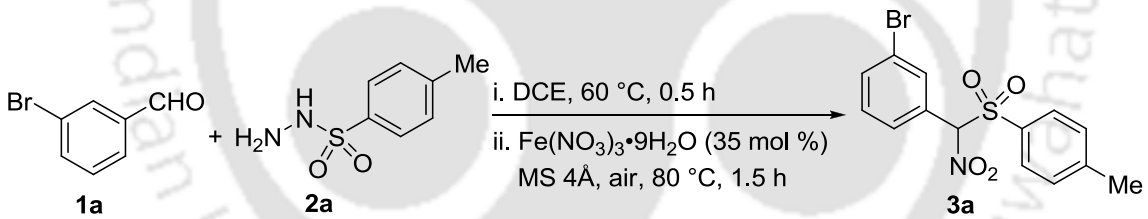

1a	**2a**	**3a**
5.40 mmol (1.0 g)	6.48 mmol (1.2 g)	(56%, 1.12 g)
27.0 mmol (5.0 g)	32.4 mmol (6.0 g)	(41%, 4.10 g)

Scheme 13. Gram-Scale Synthesis

Synthesis of Oximes. The products can be readily converted into oximes in high yields (Table 4). For examples, Sn-mediated reaction of **3b**, **3h** and **3l** afforded the oximes **4a-c** in high yields. The compound **4a** afforded single crystals in $CHCl_3$ whose structure was determined by single crystal X-ray analysis (Fig 2).

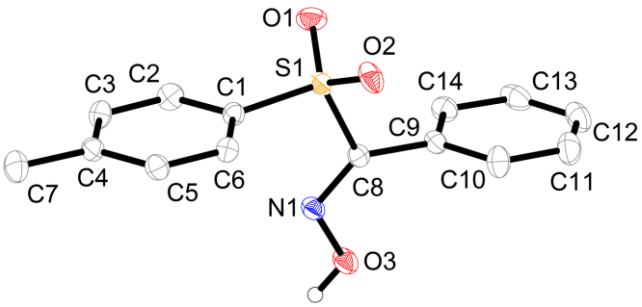

Figure 2. ORTEP diagram of (*E*)-Phenyl(tosyl)methanone oxime **4a** with 50% ellipsoid. H-Atoms are omitted for clarity (CCDC 1052905).

Table 4. Synthesis of Oximes

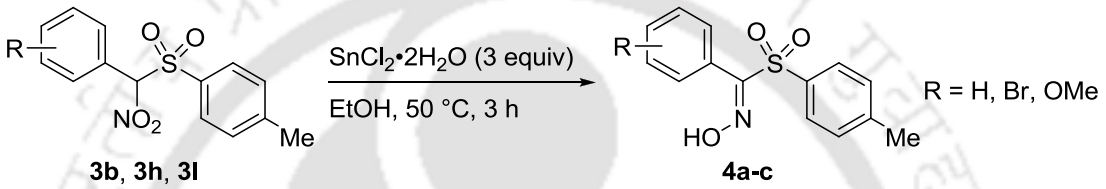

Entry	Bisarylnitromethyl sulfone	Oxime	Yield (%)[b]
1	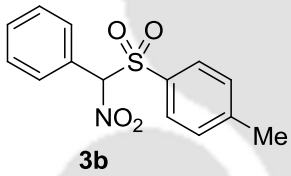 **3b**	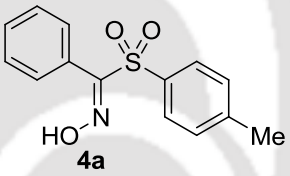 **4a**	90
2	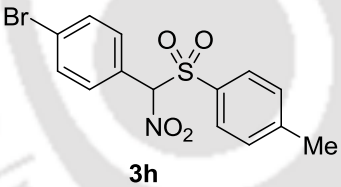 **3h**	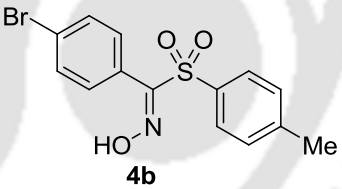 **4b**	86
3	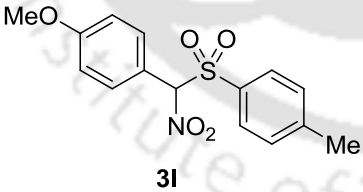 **3l**	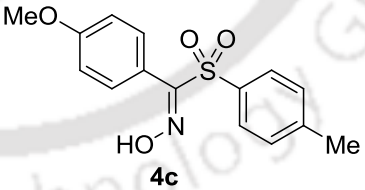 **4c**	83

[a] Reaction conditions: bisarylnitromethyl sulfone (0.25 mmol), $SnCl_2 \cdot 2H_2O$ (0.75 mmol), EtOH (1 mL), air, 50 °C, 3.0 h. [b] Isolated yield

Mechanistic Studies. The reaction of bisarylsulfonyl hydrazone **5** was independently investigated (Scheme 14). The nitration took place efficiently to afford **3a** in 64% yield, which suggests that the condensation of the aldehyde with sulfonyl hydrazide may first give bisarylsulfonyl hydrazone that may undergo nitration to afford the target products.

Next, the reaction of the aldehyde **1b** and arylsulfonyl hydrazide **2a** was examined with $Fe(NO_3)_3{\cdot}9H_2O$ as the representative examples in the presence of radical scavengers, 1,1-diphenylethyelene and *N*-*tert*-butyl-α-phenylnitrone (Scheme 15).[27] However, no reaction was observed, which suggests that the reaction may involve the radical intermediates. Furthermore, the substrates showed no nitration in the presence of base, which suggests that the reaction may not proceed via a carbene intermediate (Scheme 16).[28] In addition, *N*-benzyl bisarylsulfonyl hydrazone failed to react and the substrate was isolated intact, which suggests that N-H is essential for the reaction (Scheme 17).

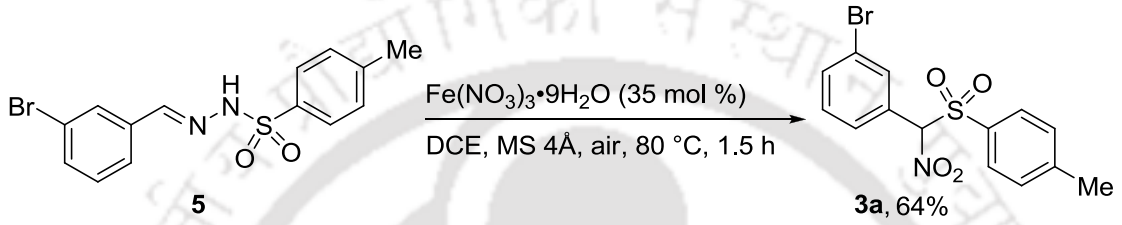

Scheme 14. Nitration of Bisarylsulfonyl Hydrazone

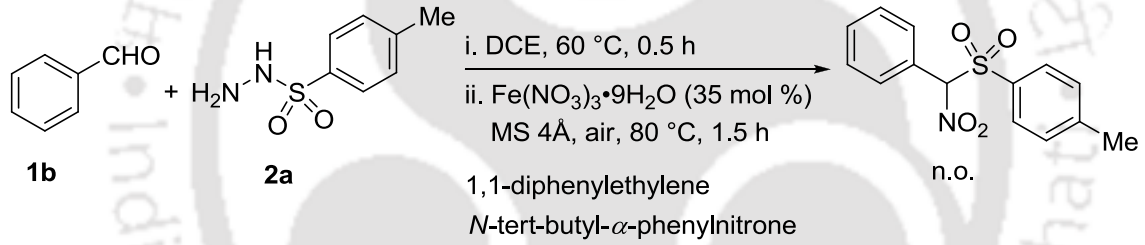

Scheme 15. Effect of Radical Scavengers

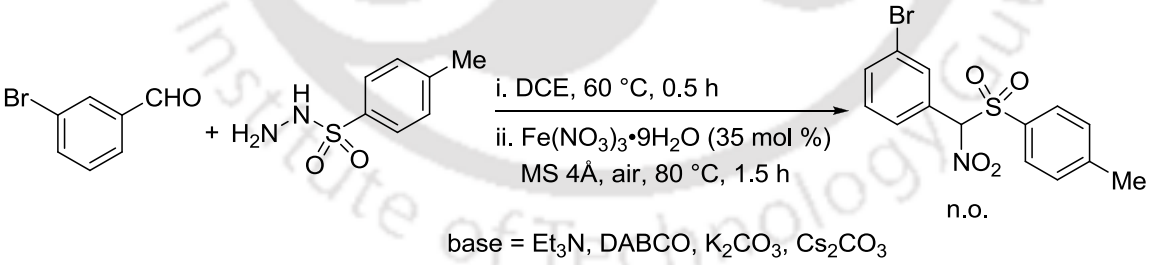

Scheme 16. Effect of Base

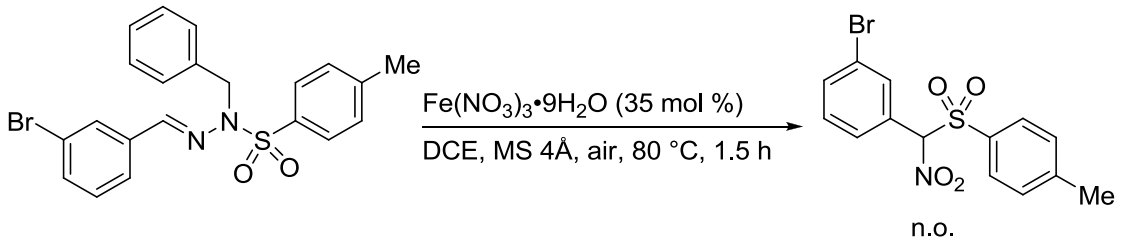

Scheme 17. Effect of *N*-Protecting Group

These results reveal that the reaction of the aldehyde with arylsulfonyl hydrazide can give sulfonyl hydrazone ***a*** that can react with $Fe(NO_3)_3$ via single electron transfer to produce $Fe(NO_3)_2$, NO_3^- and intermediate ***b*** (Scheme 18).[29] Isomerization of ***b*** can give ***c*** that can react with NO_2 radical[6,7] to give **d** and the target products **3** via path ***a***. Alternatively, the intermediate ***c*** may give ***e*** via path ***b***, which with NO_2 radical can give the target product.[6,7] Oxidation of the Fe(II) species with HNO_3 can regenerate Fe(III) species to complete the catalytic cycle.

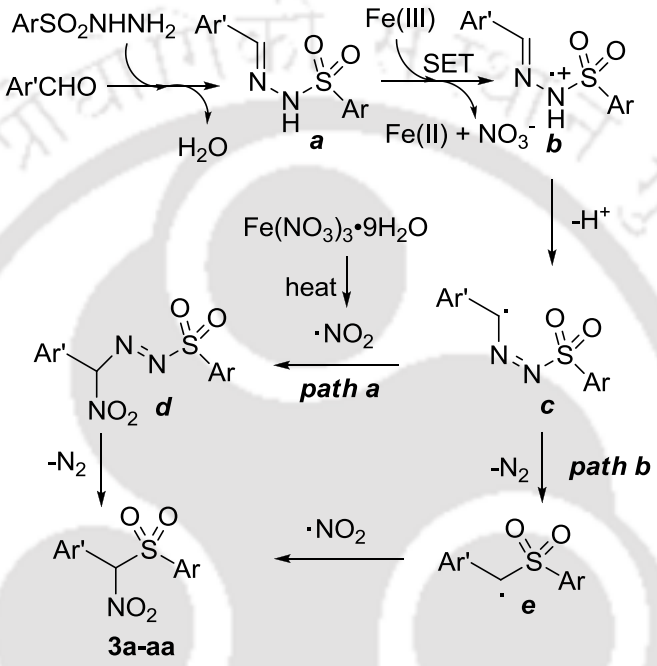

Scheme 18. Proposed Reaction Pathway for the synthesis of Bisarylnitromethyl Sulfones

DFT Study. To understand the feasibility of the reaction paths, we have calculated the standard reaction enthalpy (ΔH_r) and Gibbs free energy (ΔG_r) for both the paths including zero point correction. In the frame work of density functional theory (DFT), hybrid B3LYP functional was used to explore the stationary points on the potential energy surfaces. All the atoms were treated with the 6-311G+(d,p) basis sets. In order to determine the nature of different stationary points on the potential energy surface and to calculate the zero-point vibrational energies (ZPEs), vibrational frequency calculations were also performed using the same level of theory at which the optimization was made. The vibrational frequencies of all the optimized structures are found to be positive confirming them to be at energy minima.[30,31] The thermochemical parameters like standard reaction enthalpy (ΔH_r) and Gibbs free energy (ΔG_r) at temperature T were

estimated from the difference of H and G values of products and reactants at that temperature. All the calculations are carried out using Gaussian 09 suits of program.

From the calculation, the ΔG_r value for the path ***a*** is found to be -1.76 eV, which indicates that this path is feasible. The ΔH_r value is found also to be negative (-13.95eV) indicating that the path is exothermic in nature. For path ***b***, both the thermochemical parameters ΔG_r and ΔH_r are found to be highly positive, which reveals that this pathway is not feasible. Hence, path ***a*** may be predominant in nature. The optimized structures of different species involved in the reactions are shown in Figure 3.

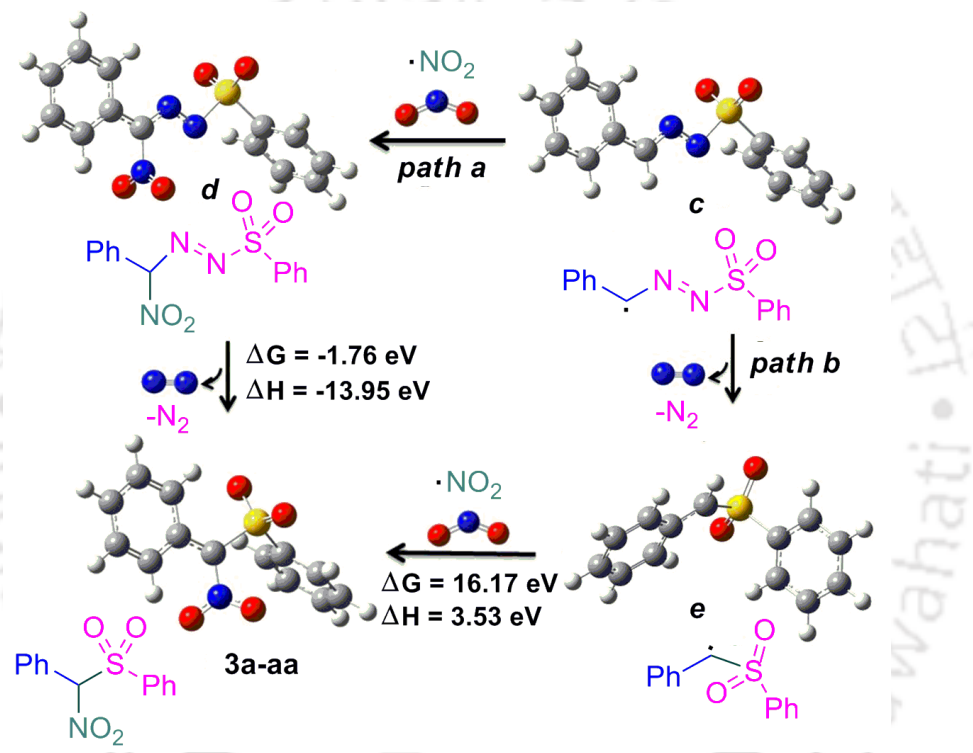

Figure 3. Optimized structures of organic species (white: hydrogen, grey: carbon, yellow: sulphur, red: oxygen and blue: nitrogen)

In summary, Fe(III)-mediated radical nitration of bisarylsulfonyl hydrazones followed by elimination of N_2 is developed for the synthesis of bisarylnitromethyl sulfones at moderate temperature. The reaction is free from the use of additives and effective under neutral conditions. The mild reaction conditions, broad substrate scope, the readily availability of substrate precursors and the use of non-toxic iron salt as catalyst as well act as a nitro source are the important practical advantages. The products can be converted into oximes using $SnCl_2{\cdot}2H_2O$ in high yields. Further, we have also analyzed reaction pathway by using DFT, which reveals that first nitration followed by elimination of N_2 is

the preferred pathway over the second proposed path of elimination of N_2 followed by nitration.

1.5 Experimental Section

General Information: Arylsulfonyl chlorides, aryl aldehydes, hydrazine hydrate (99-100%), and $SnCl_2 \cdot 2H_2O$ (97%) were purchased from commercial source and used as received. $Fe(NO_3)_3 \cdot 9H_2O$ (98%) was purchased from Merck and used as received. Sulfonyl hydrazides,[32] aryl aldehydes[33] and sulfonyl hydrazones[34] were prepared according to reported procedure. TLC analysis was performed on silica gel G/GF 254 plates. Silica gel (60-120 mesh) was used for column chromatography. NMR spectra were recorded on 400 and 600 MHz spectrometers using Me_4Si as an internal standard. Melting points were determined with a melting point apparatus and are uncorrected. FT-IR spectra were collected using IR spectrometer. Q-Tof ESI-MS instrument was used for recording high-resolution mass spectra (HRMS). Single crystal X-ray data were collected using CCD diffractometer, which is equipped with 1.75 kW sealed-tube Mo-Kα irradiation (λ = 0.71073 Å) at 298(2) K. The crystal structure was solved by direct method using SHELXL-97 (Göttingen, Germany).

General Procedure for the Nitration of Bisarylsulfonyl Hydrazones. Aryl aldehyde **1** (1 mmol) and arylsulfonyl hydrazide **2** (1.2 mmol) were stirred in 1,2-dichloroethane (3 mL) for 0.5 h at 60 ^oC under air. The reaction mixture was cooled to room temperature and then treated with $Fe(NO_3)_3 \cdot 9H_2O$ (35 mol %, 0.35 mmol, 141 mg) and molecular sieves (4Å, 50 mg). The resultant mixture was stirred for 1.5 h at 80 ^oC under air. The progress of the reaction was monitored by TLC using ethyl acetate and hexane as eluent. After completion, the reaction mixture was cooled to room temperature and the solvent was evaporated under reduced pressure. The residue was treated with saturated $NaHCO_3$ (3 mL) and extracted with ethyl acetate (3 x 15 mL). The combined organic solution was successively washed with brine (1 x 10 mL) and water (1 x 10 mL). Drying (Na_2SO4) and evaporation of the solvent gave a residue that was purified on silica gel column chromatography using hexane and ethyl acetate as eluent.

General Procedure for the Synthesis of Oximes. To a solution of bisarylnitromethyl sulfone (0.25 mmol) in ethanol (1 mL) was added $SnCl_2 \cdot 2H_2O$ (0.75 mmol, 169 mg). The reaction mixture was stirred for 3 h at 50 ^oC under air. The progress of the reaction was

monitored by TLC using ethyl acetate and hexane as eluent. After completion, the reaction mixture was cooled to room temperature and the solvent was evaporated under reduced pressure. The residue was treated with saturated $NaHCO_3$ (3 mL) and extracted with ethyl acetate (3 x 15 mL). The combined organic solution was successively washed with brine (1 x 10 mL) and water (1 x 10 mL). Drying (Na_2SO_4) and evaporation of the solvent gave a residue that was purified by column chromatography using hexane and ethyl acetate as eluent.

1.6 Characterization Data of Products

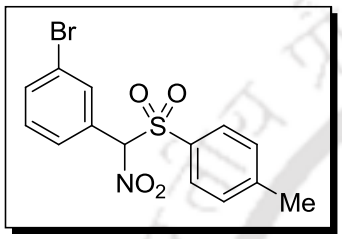

1-Bromo-3-(nitro(tosyl)methyl)benzene 3a. Analytical TLC on silica gel, 1:3 ethyl acetate/hexane R_f = 0.41; white solid; yield: 63% (231 mg); mp 79-80 °C. ^{1}H NMR (400 MHz, $CDCl_3$) δ 7.65 (d, *J* = 7.6 Hz, 1H), 7.62 (d, *J* = 8.0 Hz, 2H), 7.56 (s, 1H), 7.45 (d, *J* = 7.6 Hz, 1H), 7.35 (d, *J* = 8.0 Hz, 2H), 7.29 (t, *J* = 8.4 Hz, 1H), 6.40 (s, 1H), 2.48 (s, 3H); ^{13}C{^{1}H} NMR (100 MHz, $CDCl_3$) δ 147.4, 135.0, 132.6, 130.7, 130.5, 130.1, 128.5, 127.1, 123.0, 103.0, 22.0; FT-IR (KBr) 2982, 1594, 1561, 1473, 1337, 1257, 1188, 1153, 1081, 1039, 1014, 661 cm^{-1}; HRMS (APCI) *m/z* [M-H]$^-$ calcd for $C_{14}H_{12}BrNO_4S$: 367.9598, found: 367.9591.

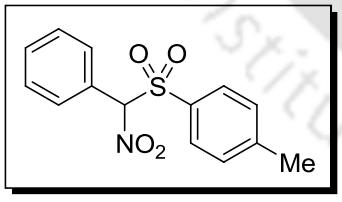

1-Methyl-4-(nitro(phenyl)methylsulfonyl)benzene 3b. Analytical TLC on silica gel, 1:9 ethyl acetate/hexane R_f = 0.52; white solid; yield: 66% (192 mg); mp 163-164 °C. ^{1}H NMR (600 MHz, $CDCl_3$) δ 7.59 (d, *J* = 7.8 Hz, 2H), 7.51 (t, *J* = 7.8 Hz, 1H), 7.47 (d, *J* = 7.2 Hz, 2H), 7.39 (t, *J* = 7.8 Hz, 2H), 7.31 (d, *J* = 8.4 Hz, 2H), 6.46 (s, 1H), 2.46 (s, 3H); ^{13}C{^{1}H} NMR (150 MHz, $CDCl_3$) δ 147.0, 131.8, 131.2, 130.7, 130.0, 129.7, 129.1, 125.3, 103.9, 22.0; FT-IR (KBr) 2984, 2359, 1592, 1559, 1488, 1454, 1333, 1303, 1184, 1155, 1083, 1030, 1016 cm^{-1}; HRMS (APCI) *m/z* [M-H]$^-$ calcd for $C_{14}H_{13}NO_4S$: 290.0493, found: 290.0486.

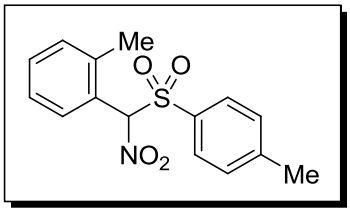

1-Methyl-2-(nitro(tosyl)methyl)benzene 3c. Analytical TLC on silica gel, 1:3 ethyl acetate/hexane R_f = 0.38; white solid; yield: 57% (173 mg); mp 198-199 °C. ^{1}H NMR (600 MHz, $CDCl_3$) δ 7.64 (d, *J* = 7.8 Hz, 2H), 7.54 (d, *J* = 7.8 Hz, 1H), 7.37 (t, *J* = 7.8 Hz, 1H), 7.33 (d, *J* = 7.8 Hz, 2H), 7.26 (d, *J* = 8.4 Hz, 1H), 7.18 (t, *J* = 7.8 Hz, 1H), 6.81 (s, 1H), 2.47 (s, 3H), 2.39 (s, 3H); ^{13}C{^{1}H} NMR (150 MHz, $CDCl_3$) δ 147.0, 138.9, 131.8, 131.7, 131.2, 130.8, 130.0, 128.4, 126.8, 124.2, 99.2, 22.0, 19.8; FT-IR (KBr) 2999, 1689, 1595, 1557, 1491, 1456, 1406, 1355, 1331, 1292, 1264, 1153, 1084, 1037, 1018 cm^{-1}; HRMS (APCI) *m/z* [M-H]$^-$ calcd for $C_{15}H_{15}NO_4S$: 304.0649, found: 304.0658.

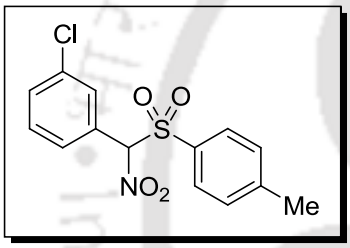

1-Chloro-3-(nitro(tosyl)methyl)benzene 3d. Analytical TLC on silica gel, 1:4 ethyl acetate/hexane R_f = 0.39; white solid; yield: 61% (198 mg); mp 82-84 °C. ^{1}H NMR (600 MHz, $CDCl_3$) δ 7.62 (d, *J* = 7.8 Hz, 2H), 7.50 (d, *J* = 7.8 Hz, 1H), 7.45 (s, 1H), 7.40 (d, *J* = 7.8 Hz, 1H), 7.36-7.34 (m, 3H), 6.41 (s, 1H), 2.48 (s, 3H); ^{13}C{^{1}H} NMR (150 MHz, $CDCl_3$) δ 147.4, 135.2, 132.0, 130.9, 130.7, 130.3, 130.1, 129.8, 128.1, 127.0, 103.1, 22.0; FT-IR (KBr) 2990, 1597, 1562, 1477, 1408, 1384, 1340, 1261, 1187, 1157, 1083, 1017, 663 cm^{-1}; HRMS (APCI) *m/z* [M-H]$^-$ calcd for $C_{14}H_{12}ClNO_4S$: 324.0103, found: 324.0110.

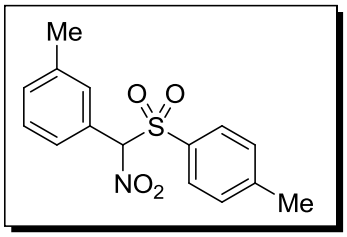

1-Methyl-3-(nitro(tosyl)methyl)benzene 3e. Analytical TLC on silica gel, 1:6 ethyl acetate/hexane R_f = 0.49; white solid; yield: 58% (177 mg); mp 116-117 °C. ^{1}H NMR (400 MHz, $CDCl_3$) δ 7.61(d, *J* = 7.6 Hz, 2H), 7.32 (d, *J* = 7.6

Hz, 2H), 7.26-7.23 (m, 4H), 6.42 (s, 1H), 2.47 (s, 3H), 2.33 (s, 3H); $^{13}C\{^{1}H\}$ NMR (100 MHz, $CDCl_3$) δ 146.9, 139.1, 132.6, 131.2, 130.8, 130.2, 129.9, 128.9, 126.8, 125.1, 103.9, 22.0, 21.4; FT-IR (KBr) 2983, 1633, 1592, 1554, 1484, 1333, 1305, 1155, 1083, 1039, 1017 cm^{-1}; HRMS (APCI) *m/z* $[M-H]^-$ calcd for $C_{15}H_{15}NO_4S$: 304.0649, found: 304.0641.

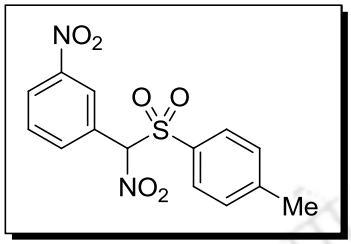

1-Nitro-3-(nitro(tosyl)methyl)benzene 3f. Analytical TLC on silica gel, 1:3 ethyl acetate/hexane R_f = 0.28; yellow solid; yield: 55% (184 mg); mp 132-133 °C. ^{1}H NMR (400 MHz, $CDCl_3$) δ 8.41 (d, *J* = 8.4 Hz, 1H), 8.33 (s, 1H), 8.00 (d, *J* = 7.2 Hz, 1H), 7.70-7.66 (m, 3H), 7.39 (d, *J* = 7.6 Hz, 2H), 6.59 (s, 1H), 2.49 (s, 3H); $^{13}C\{^{1}H\}$ NMR (100 MHz, $CDCl_3$) δ 148.3, 147.9, 135.9, 130.5, 130.4, 130.3, 127.0, 126.6, 125.2, 102.3, 22.0; FT-IR (KBr) 2925, 1707, 1618, 1533, 1481, 1446, 1352, 1291, 1158, 1124, 1035, 1010, 815, 720, 668 cm^{-1}; HRMS (APCI) *m/z* $[M-H]^-$ calcd for $C_{14}H_{12}N_2O_6S$: 335.0343, found: 335.0349.

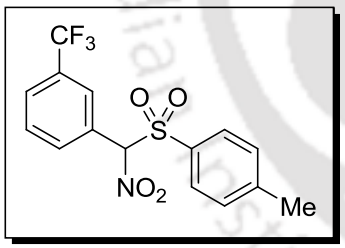

1-(Nitro(tosyl)methyl)-3-(trifluoromethyl)benzene 3g. Analytical TLC on silica gel, 1:4 ethyl acetate/hexane R_f = 0.29; yellow liquid; yield: 51% (183 mg). ^{1}H NMR (600 MHz, $CDCl_3$) δ 7.78 (d, *J* = 7.8 Hz, 2H), 7.60-7.58 (m, 4H), 7.34 (d, *J* = 8.4 Hz, 2H), 6.51 (s, 1H), 2.47 (s, 3H); $^{13}C\{^{1}H\}$ NMR (150 MHz, $CDCl_3$) δ 147.6, 133.5, 133.3, 130.7, 130.2, 129.8, 129.4, 128.6, 127.3, 126.6, 126.3, 103.1, 22.0; FT-IR (neat) 2926, 1596, 1566, 1452, 1384, 1332, 1261, 1159, 1133, 1101, 1081, 814, 703, 659 cm^{-1}; HRMS (APCI) *m/z* $[M-H]^-$ calcd for $C_{15}H_{12}F_3NO_4S$: 358.0361, found: 358.0367.

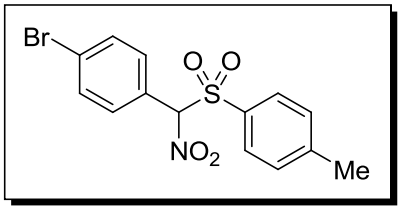

1-Bromo-4-(nitro(tosyl)methyl)benzene 3h. Analytical TLC on silica gel, 1:4 ethyl acetate/hexane R_f = 0.40; white solid; yield: 60% (222 mg); mp 129-130 °C. ^{1}H NMR (600 MHz, $CDCl_3$) δ 7.62 (d, *J* = 8.4 Hz, 2H), 7.55 (d, *J* = 8.4 Hz, 2H), 7.37-7.33 (m, 4H), 6.41 (s, 1H), 2.47 (s, 3H); ^{13}C{^{1}H} NMR (150 MHz, $CDCl_3$) δ 147.3, 132.5, 131.3, 131.0, 130.7, 130.2, 126.8, 124.2, 103.2, 22.0; FT-IR (KBr) 2923, 1626, 1562, 1488, 1408, 1384, 1340, 1155, 1075, 1012, 707, 658 cm^{-1}; HRMS (APCI) *m/z* [M-H]$^-$ calcd for $C_{14}H_{12}BrNO_4S$: 367.9598, found: 367.9591.

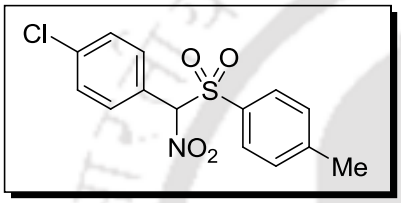

1-Chloro-4-(nitro(tosyl)methyl)benzene 3i. Analytical TLC on silica gel, 1:3 ethyl acetate/hexane R_f = 0.50; white solid; yield: 62% (201 mg); mp 128-129 °C. ^{1}H NMR (600 MHz, $CDCl_3$) δ 7.62 (d, *J* = 7.8 Hz, 2H), 7.44 (d, *J* = 8.4 Hz, 2H), 7.39 (d, *J* = 8.4 Hz, 2H), 7.34 (d, *J* = 8.4 Hz, 2H), 6.43 (s, 1H), 2.47 (s, 3H); ^{13}C{^{1}H} NMR (150 MHz, $CDCl_3$) δ 147.3, 138.5, 131.2, 131.0, 130.6, 130.2, 129.5, 123.7, 103.1, 22.0; FT-IR (KBr) 2979, 1665, 1594, 1568, 1494, 1413, 1340, 1310, 1291, 1177, 1152, 1082, 1018, 818, 662 cm^{-1}; HRMS (APCI) *m/z* [M-H]$^-$ calcd for $C_{14}H_{12}ClNO_4S$: 324.0103, found: 324.0108.

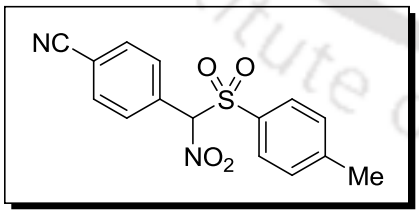

4-(Nitro(tosyl)methyl)benzonitrile 3j. Analytical TLC on silica gel, 1:2 ethyl acetate/hexane R_f = 0.40; white solid; yield: 52% (164 mg); mp 125-126 °C. ^{1}H NMR (600 MHz, $CDCl_3$) δ 7.72 (d, *J* = 8.4 Hz, 2H), 7.66 (d, *J* = 8.4 Hz, 2H), 7.63 (d, *J* = 7.8 Hz, 2H), 7.36 (d, *J* = 7.8 Hz, 2 H), 6.49 (s, 1H), 2.48 (s, 3H); ^{13}C{^{1}H} NMR (150 MHz, $CDCl_3$) δ 147.8, 132.8, 130.8, 130.7, 130.4, 129.7, 117.7, 115.9, 102.9, 22.1; FT-IR (KBr) 2924, 2853, 2231, 1741, 1628, 1563, 1462, 1338, 1152,

1081, 1017, 812 cm^{-1}; HRMS (APCI) *m/z* $[M-H]^-$ calcd for $C_{15}H_{12}N_2O_4S$: 315.0445, found: 315.0451.

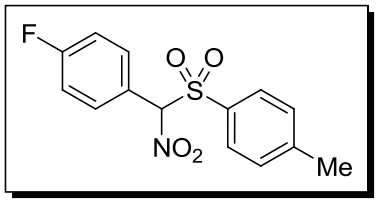

1-Fluoro-4-(nitro(tosyl)methyl)benzene 3k. Analytical TLC on silica gel, 1:2 ethyl acetate/hexane R_f = 0.56; yellow solid; yield: 59% (182 mg); mp 107-108 °C. ^1H NMR (600 MHz, $CDCl_3$) δ 7.62 (d, *J* = 7.8 Hz, 2H), 7.52-7.49 (m, 2H), 7.34 (d, *J* = 8.4 Hz, 2H), 7.10 (t, *J* = 8.4 Hz, 2H), 6.44 (s, 1H), 2.47 (s, 3H); $^{13}C\{^1H\}$ NMR (100 MHz, $CDCl_3$) δ 166.1 (J_{C-F} = 251.7 Hz), 147.2, 132.2 (J_{C-F} = 9.2 Hz), 131.0, 130.6, 130.1, 121.2 (J_{C-F} =3.8 Hz), 116.5 (J_{C-F} = 22.1 Hz), 103.0, 22.0; FT-IR (KBr) 2979, 1605, 1566, 1512, 1406, 1384, 1339, 1233, 1154, 1083, 1016, 820, 665 cm^{-1}; HRMS (APCI) *m/z* $[M-H]^-$ calcd for $C_{14}H_{12}FNO_4S$: 308.0398, found: 308.0396.

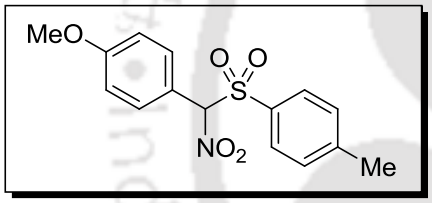

1-Methoxy-4-(nitro(tosyl)methyl)benzene 3l. Analytical TLC on silica gel, 1:4 ethyl acetate/hexane R_f = 0.51; yellow solid; yield: 69% (221 mg); mp: 126-127 °C. ^1H NMR (600 MHz, $CDCl_3$) δ 7.61 (d, *J* = 8.4 Hz, 2H), 7.41 (d, *J* = 8.4 Hz, 2H), 7.32 (d, *J* = 7.8 Hz, 2H), 6.89 (d, *J* = 9.0 Hz, 2H), 6.40 (s, 1H), 3.83 (s, 3H), 2.46 (s, 3H); $^{13}C\{^1H\}$ NMR (150 MHz, $CDCl_3$) δ 162.4, 146.9, 131.5, 131.4, 130.7, 130.0, 117.0, 114.5, 103.6, 55.6, 22.0; FT-IR (KBr) 2995, 1609, 1596, 1552, 1515, 1460, 1341, 1309, 1278, 1263, 1182, 1157, 1085, 1019 cm^{-1}; HRMS (APCI) *m/z* $[M-H]^-$ calcd for $C_{15}H_{15}NO_5S$: 320.0598, found: 320.0599.

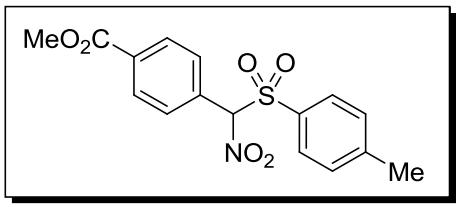

Methyl-4-(nitro(tosyl)methyl)benzoate 3m. Analytical TLC on silica gel, 1:4 ethyl acetate/hexane R_f = 0.22; white solid; yield: 58% (202 mg); mp 110-111 °C. ^1H NMR (600 MHz, $CDCl_3$) δ 8.05 (d, *J* = 8.4 Hz, 2H), 7.59-

7.54 (m, 4H), 7.32 (d, *J* = 8.4 Hz, 2H), 6.52 (s, 1H), 3.94 (s, 3H), 2.46 (s, 3H); $^{13}C\{^{1}H\}$ NMR (150 MHz, $CDCl_3$) δ 166.1, 147.4, 133.2, 130.9, 130.7, 130.2, 130.1, 129.8, 129.5, 103.4, 52.7, 22.0; FT-IR (KBr) 2995, 1714, 1593, 1555, 1432, 1341, 1291, 1187, 1154, 1114, 1083, 1018 cm^{-1}; HRMS (APCI) *m/z* $[M-H]^-$ calcd for $C_{16}H_{15}NO_6S$: 348.0547, found: 348.0541.

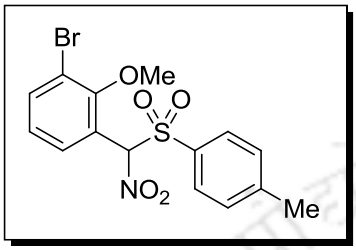

1-Bromo-2-methoxy-3-(nitro(tosyl)methyl)benzene 3n. Analytical TLC on silica gel, 1:3 ethyl acetate/hexane R_f = 0.35; white solid; yield: 65% (260 mg); mp 153-154 °C. ^{1}H NMR (600 MHz, $CDCl_3$) δ 7.76 (d, *J* = 2.4 Hz, 1H); 7.69 (d, *J* = 7.8 Hz, 2H), 7.56 (dd, *J* = 9.0, 2.4 Hz, 1H), 7.37 (d, *J* = 8.4 Hz, 2H), 7.12 (s, 1H), 6.80 (d, *J* = 9.0 Hz, 1H), 3.76 (s, 3H), 2.48 (s, 3H); $^{13}C\{^{1}H\}$ NMR (150 MHz, $CDCl_3$) δ 157.0, 147.0, 136.0, 132.9, 131.8, 130.5, 130.0, 115.7, 113.3, 112.9, 95.1, 56.5, 22.0; FT-IR (KBr) 2981, 1595, 1556, 1487, 1462, 1441, 1403, 1352, 1329, 1305, 1282, 1260, 1213, 1186, 1155, 1116, 1085, 1019, 820, 647 cm^{-1}; HRMS (APCI) *m/z* $[M-H]^-$ calcd for $C_{15}H_{14}BrNO_5S$: 397.9703, found: 397.9710.

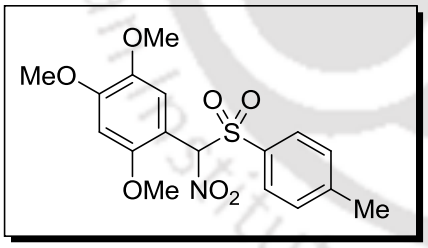

1,2,4-Trimethoxy-5-(nitro(tosyl)methyl)benzene 3o. Analytical TLC on silica gel, 1:2 ethyl acetate/hexane R_f = 0.64; yellow solid; yield: 72% (274 mg); mp 148-149 °C. ^{1}H NMR (600 MHz, $CDCl_3$) δ 7.69 (d, *J* = 8.4 Hz, 2H), 7.34 (d, *J* = 8.4 Hz, 2H), 7.15 (s, 1H), 7.11 (s, 1H), 6.46 (s, 1H), 3.91 (s, 3H), 3.74 (s, 3H), 3.73 (s, 3H), 2.46 (s, 3H); $^{13}C\{^{1}H\}$ NMR (150 MHz, $CDCl_3$) δ 153.5, 153.0, 146.5, 143.4, 132.4, 130.5, 129.9, 112.1, 104.4, 96.6, 95.9, 56.9, 56.4, 56.2, 21.9; FT-IR (KBr) 2977, 1599, 1525, 1406, 1384, 1332, 1305, 1232, 1214, 1153, 1112, 1083, 1039, 1027 cm^{-1}; HRMS (APCI) *m/z* $[M-H]^-$ calcd for $C_{17}H_{19}NO_7S$: 380.0809, found: 380.0807.

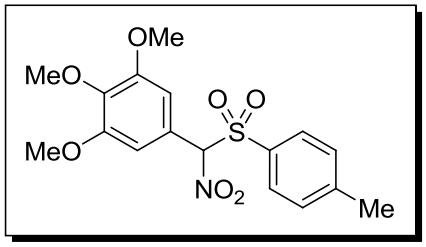

1,2,3-Trimethoxy-5-(nitro(tosyl)methyl)benzene 3p. Analytical TLC on silica gel, 1:2 ethyl acetate/hexane R_f = 0.59; yellow solid; yield: 70% (267 mg); mp 150-151 °C. ^{1}H NMR (600 MHz, $CDCl_3$) δ 7.64 (d, *J* = 8.4 Hz, 2H), 7.34 (d, *J* = 7.8 Hz, 2H), 6.63 (s, 2H), 6.37 (s, 1H), 3.86 (s, 3H), 3.75 (s, 6H), 2.46 (s, 3H); ^{13}C{^{1}H} NMR (150 MHz, $CDCl_3$) δ 153.4, 147.0, 140.9, 131.1, 130.8, 129.9, 120.1, 107.0, 103.8, 61.1, 56.3, 21.9; FT-IR (KBr) 2945, 1593, 1557, 1509, 1465, 1424, 1336, 1277, 1244, 1230, 1155, 1129, 1079, 1018 cm^{-1}; HRMS (APCI) *m/z* [M-H]$^-$ calcd for $C_{17}H_{19}NO_7S$: 380.0809, found: 380.0815.

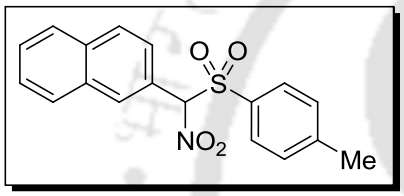

2-(Nitro(tosyl)methyl)naphthalene 3q. Analytical TLC on silica gel, 1:4 ethyl acetate/hexane R_f = 0.71; white solid; yield: 73% (249 mg); mp 175-176 °C. ^{1}H NMR (600 MHz, $CDCl_3$) δ 7.95 (s, 1H), 7.86 (t, *J* = 9.0 Hz, 2H), 7.82 (d, *J* = 7.8 Hz, 1H), 7.61-7.52 (m, 5H), 7.29 (d, *J* = 8.4 Hz, 2H), 6.63 (s, 1H), 2.45 (s, 3H); ^{13}C{^{1}H} NMR (150 MHz, $CDCl_3$) δ 147.0, 134.6, 132.7, 131.3, 130.9, 130.7, 130.0, 129.0, 128.8, 128.4, 127.9, 127.3, 125.3, 122.5, 104.2, 22.0; FT-IR (KBr) 2987, 1593, 1559, 1507, 1338, 1306, 1211, 1156, 1125, 1083, 1018, 818, 665 cm^{-1}; HRMS (APCI) *m/z* [M-H]$^-$ calcd for $C_{18}H_{15}NO_4S$: 340.0649, found: 340.0653.

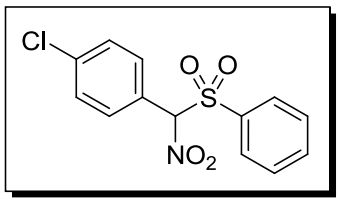

1-Chloro-4-(nitro(phenylsulfonyl)methyl)benzene 3s. Analytical TLC on silica gel, 1:6 ethyl acetate/hexane R_f = 0.29; white solid; yield: 66% (205 mg); mp 117-118 °C. ^{1}H NMR (400 MHz, $CDCl_3$) δ 7.76-7.74 (m, 3H), 7.56 (t, *J* = 7.6 Hz, 2H), 7.44-7.38 (m, 4H), 6.46 (s, 1H); ^{13}C{^{1}H} NMR (100 MHz, $CDCl_3$) δ 138.6, 135.7, 134.0, 131.1, 130.6, 129.6, 129.5, 123.5, 103.0; FT-IR (KBr) 2979, 1565, 1488,

1448, 1411, 1355, 1337, 1289, 1180, 1154, 1080, 1012, 770, 728 cm^{-1}; HRMS (APCI) *m/z* $[M-H]^-$ calcd for $C_{13}H_{10}ClNO_4S$: 309.9941, found: 309.9943.

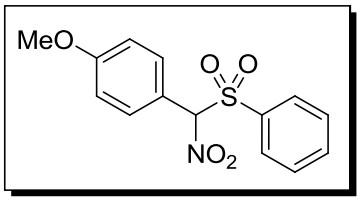

1-Methoxy-4-(nitro(phenylsulfonyl)methyl)benzene 3t. Analytical TLC on silica gel, 1:6 ethyl acetate/hexane R_f = 0.31; white solid; yield: 68% (209 mg); mp 143-144 °C. ^1H NMR (600 MHz, $CDCl_3$) δ 7.73 (d, *J* = 8.4 Hz, 2H), 7.70 (d, *J* = 8.4 Hz, 1H), 7.52 (t, *J* = 7.8 Hz, 2H), 7.39 (d, *J* = 8.4 Hz, 2H), 6.89 (d, *J* = 9.0 Hz, 2H), 6.43 (s, 1H), 3.82 (s, 3H); $^{13}C\{^1H\}$ NMR (150 MHz, $CDCl_3$) δ 162.4, 135.4, 134.4, 131.4, 130.6, 129.3, 116.8, 114.5, 103.5, 55.6; FT-IR (KBr) 2990, 1607, 1578, 1554, 1513, 1460, 1445, 1338, 1309, 1276, 1262, 1181, 1160, 1113, 1084, 1018 cm^{-1}; HRMS (APCI) *m/z* $[M-H]^-$ calcd for $C_{14}H_{13}NO_5S$: 306.0442, found: 306.0448.

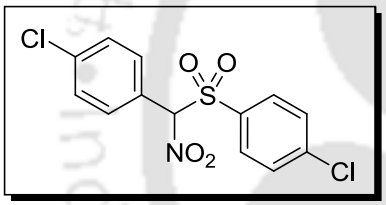

1-Chloro-4-(((4-chlorophenyl)(nitro)methyl)sulfonyl)benzene 3u. Analytical TLC on silica gel, 1:4 ethyl acetate/hexane R_f = 0.45; white solid; yield: 57% (197 mg); mp 117-118 °C. ^1H NMR (600 MHz, $CDCl_3$) δ 7.67 (d, *J* = 9.0 Hz, 2H), 7.53 (d, *J* = 8.4 Hz, 2H), 7.41 (s, 4H), 6.44 (s, 1H); $^{13}C\{^1H\}$ NMR (150 MHz, $CDCl_3$) δ 143.0, 138.8, 132.4, 132.1, 131.0, 129.9, 129.7, 123.3, 103.1; FT-IR (KBr) 2901, 2072, 1639, 1430, 1372, 1339, 1319, 1282, 1205, 1163, 1059, 1032, 896, 707 cm^{-1}; HRMS (APCI) *m/z* $[M-H]^-$ calcd for $C_{13}H_9Cl_2NO_4S$: 343.9557, found: 343.9550.

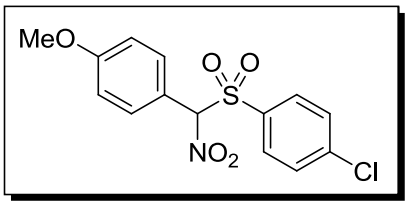

1-Chloro-4-(((4-methoxyphenyl)(nitro)methyl)sulfonyl)benzene 3v. Analytical TLC on silica gel, 1:4 ethyl acetate/hexane R_f = 0.40; yellow solid; yield: 61% (208 mg); mp 113-114 °C. ^1H

NMR (400 MHz, $CDCl_3$) δ 7.63 (d, *J* = 8.4 Hz, 2H), 7.49 (d, *J* = 8.4 Hz, 2H), 7.35 (d, *J* = 8.4 Hz, 2H), 6.89 (d, *J* = 8.4 Hz, 2H), 6.39 (s, 1H), 3.82 (s, 3H); $^{13}C\{^1H\}$ NMR (100 MHz, $CDCl_3$) δ 162.5, 142.5, 132.7, 132.1, 131.3, 129.6, 116.6, 114.7, 103.6, 55.6; FT-IR (KBr) 2958, 1608, 1579, 1556, 1513, 1469, 1447, 1427, 1395, 1356, 1339, 1310, 1182, 1152, 1142, 1116, 1090, 1077, 1028, 657 cm^{-1}; HRMS (APCI) *m/z* $[M-H]^-$ calcd for $C_{14}H_{12}ClNO_5S$: 340.0052, found: 340.0057.

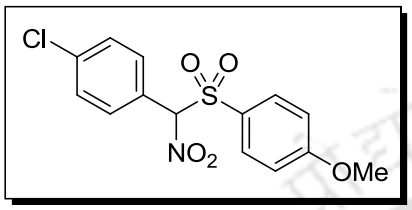

1-Chloro-4-((4-methoxyphenylsulfonyl)(nitro)methyl)benzene 3w. Analytical TLC on silica gel, 1:4 ethyl acetate/hexane R_f = 0.34; yellow solid; yield: 64% (218 mg); mp 112-113 °C. ^1H NMR (600 MHz, $CDCl_3$) δ 7.65 (d, *J* = 9.0 Hz, 2H), 7.43 (d, *J* = 8.4 Hz, 2H), 7.39 (d, *J* = 8.4 Hz, 2H), 6.99 (d, *J* = 9.0 Hz, 2H), 6.42 (s, 1H), 3.91 (s, 3H); $^{13}C\{^1H\}$ NMR (150 MHz, $CDCl_3$) δ 165.5, 138.4, 133.1, 131.1, 129.5, 124.9, 123.9, 114.7, 103.2, 56.1; FT-IR (KBr) 2992, 1594, 1562, 1496, 1461, 1409, 1332, 1316, 1263, 1150, 1083, 1019, 830, 663 cm^{-1}; HRMS (APCI) *m/z* $[M-H]^-$ calcd for $C_{14}H_{12}ClNO_5S$: 340.0052, found: 340.0057.

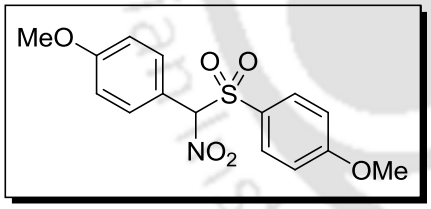

1-Methoxy-4-((4-methoxyphenyl)(nitro)methylsulfonyl)benzene 3x. Analytical TLC on silica gel, 1:4 ethyl acetate/hexane R_f = 0.50; yellow solid; yield: 63% (212 mg); mp 118-119 °C. ^1H NMR (400 MHz, $CDCl_3$) δ 7.63 (d, *J* = 6.8 Hz, 2H), 7.39 (d, *J* = 7.2 Hz, 2H), 6.96 (d, *J* = 6.8 Hz, 2H), 6.88 (d, *J* = 6.8 Hz, 2H), 6.41(s, 1H), 3.88 (s, 3H), 3.81 (s, 3H); $^{13}C\{^1H\}$ NMR (100 MHz, $CDCl_3$) δ 165.2, 162.3, 133.0, 131.3, 125.3, 117.2, 114.5, 114.4, 103.7, 55.9, 55.6; FT-IR (KBr) 2993, 2389, 1609, 1592, 1561, 1513, 1499, 1461, 1441, 1330, 1310, 1267, 1179, 1148, 1084, 1023 cm^{-1}; HRMS (APCI) *m/z* $[M-H]^-$ calcd for $C_{15}H_{15}NO_6S$: 336.0547, found: 336.0542.

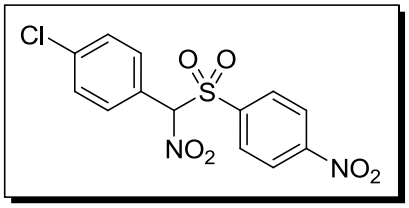

1-Chloro-4-(nitro((4-nitrophenyl)sulfonyl)methyl)benzene 3y. Analytical TLC on silica gel, 1:4 ethyl acetate/hexane R_f = 0.29; yellow solid; yield: 54% (192 mg); mp 198-199 °C. ^{1}H NMR (600 MHz, $CDCl_3$) δ 8.39 (d, *J* = 9.0 Hz, 2H), 7.95 (d, *J* = 9.0 Hz, 2H), 7.44-7.40 (m, 4H), 6.51 (s, 1H); ^{13}C{^{1}H} NMR (150 MHz, $CDCl_3$) δ 152.0, 139.7, 139.2, 132.3, 130.9, 129.9, 124.4, 122.7, 103.1; FT-IR (KBr) 2989, 1639, 1593, 1554, 1533, 1491, 1412, 1341, 1315, 1290, 1157, 1108, 1093, 1080, 1030, 740 cm^{-1}; HRMS (APCI) *m/z* [M-H]$^-$ calcd for $C_{13}H_9ClN_2O_6S$: 354.9792, found: 354.9799.

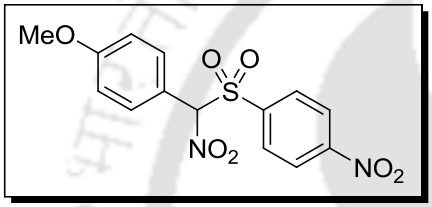

1-Methoxy-4-(nitro((4-nitrophenyl)sulfonyl)methyl)benzene 3z. Analytical TLC on silica gel, 1:4 ethyl acetate/hexane R_f = 0.28; white solid; yield: 58% (204 mg); mp 172-173 °C. ^{1}H NMR (600 MHz, $CDCl_3$) δ 8.35 (d, *J* = 9.0 Hz, 2H), 7.92 (d, *J* = 9.0 Hz, 2H), 7.35 (d, *J* = 8.4 Hz, 2H), 6.91 (d, *J* = 9.0 Hz, 2H), 6.48 (s, 1H), 3.84 (s, 3H); ^{13}C{^{1}H} NMR (150 MHz, $CDCl_3$) δ 162.8, 151.8, 140.0, 132.4, 131.2, 124.2, 116.0, 114.9, 103.6, 55.7; FT-IR (KBr) 2959, 1610, 1582, 1556, 1526, 1513, 1402, 1344, 1307, 1252, 1179, 1144, 1111, 1079, 1026 cm^{-1}; HRMS (APCI) *m/z* [M-H]$^-$ calcd for $C_{14}H_{12}N_2O_7S$: 351.0292, found: 351.0289.

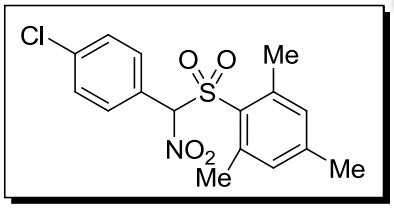

2-((4-Chlorophenyl)(nitro)methylsulfonyl)-1,3,5-trimethylbenzene 3aa. Analytical TLC on silica gel, 1:4 ethyl acetate/hexane R_f = 0.36; white solid; yield: 66% (233 mg); mp 164-165 °C. ^{1}H NMR (600 MHz, $CDCl_3$) δ 7.59 (d, *J* = 9.0 Hz, 2H), 7.44 (d, *J* = 8.4 Hz, 2H), 7.00 (s, 2H), 6.43 (s, 1H), 2.53 (s, 6H), 2.33 (s, 3H); ^{13}C{^{1}H} NMR (150 MHz, $CDCl_3$) δ 145.8, 142.1, 138.5, 132.9, 132.1, 129.4, 129.2,

123.3, 102.5, 23.2, 21.4; FT-IR (KBr) 2997, 1598, 1567, 1489, 1443, 1411, 1350, 1322, 1288, 1144, 1089, 714, 651 cm^{-1}; HRMS (APCI) *m/z* $[M-H]^-$ calcd for $C_{16}H_{16}ClNO_4S$: 352.0416, found: 352.0420.

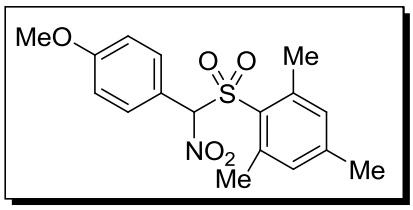

2-((4-Methoxyphenyl)(nitro)methylsulfonyl)-1,3,5-trimethylbenzene 3ab. Analytical TLC on silica gel, 1:4 ethyl acetate/hexane R_f = 0.54; yellow solid; yield: 64% (223 mg); mp 134-135 °C. ^1H NMR (600 MHz, $CDCl_3$) δ 7.56 (d, *J* = 9.0 Hz, 2H), 6.98 (s, 2H), 6.95 (d, *J* = 9.0 Hz, 2H), 6.40 (s, 1H), 3.84 (s, 3H), 2.52 (s, 6H), 2.32 (s, 3H); $^{13}C\{^1H\}$ NMR (150 MHz, $CDCl_3$) δ 162.5, 145.4, 142.0, 132.8, 132.3, 129.6, 116.7, 114.5, 103.1, 55.6, 23.2, 21.3; FT-IR (KBr) 2979, 1608, 1556, 1515, 1443, 1410, 1384, 1357, 1329, 1267, 1176, 1153, 1025 cm^{-1}; HRMS (APCI) *m/z* $[M-H]^-$ calcd for $C_{17}H_{19}NO_5S$: 348.0911, found: 348.0905.

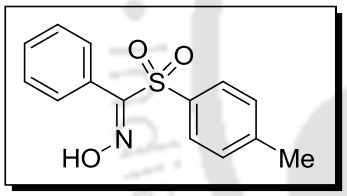

(*E*)-Phenyl(tosyl)methanone oxime 4a. Analytical TLC on silica gel, 1:4 ethyl acetate/hexane R_f = 0.49; white solid; yield: 90% (61 mg); mp 145-146 °C. ^1H NMR (600 MHz, $CDCl_3$) δ 9.52 (s, 1H), 7.67 (d, *J* = 7.8 Hz, 2H), 7.46-7.44 (m, 1H), 7.41-7.40 (m, 4H), 7.27 (d, *J* = 7.8 Hz, 2H), 2.41 (s, 3H); $^{13}C\{^1H\}$ NMR (150 MHz, $CDCl_3$) δ 158.6, 145.6, 134.7, 130.9, 130.0, 129.6, 129.3, 128.6, 125.7, 21.9; FT-IR (KBr) 3373, 2922, 2854, 1593, 1443, 1385, 1289, 1145, 1086, 1014, 970 cm^{-1}; HRMS (ESI) *m/z* $[M+H]^+$ calcd for $C_{14}H_{13}NO_3S$: 276.0694, found: 276.0698.

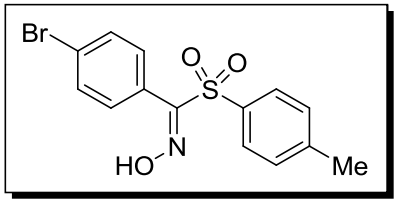

(*E*)-(4-Bromophenyl)(tosyl)methanone oxime 4b. Analytical TLC on silica gel, 1:4 ethyl acetate/hexane R_f = 0.42; white solid; yield: 86% (76 mg); mp 160-161 °C. ^1H NMR (600 MHz, $CDCl_3$) δ 9.13 (s, 1H), 7.68 (d, *J* = 8.4 Hz,

2H), 7.56 (d, *J* = 8.4 Hz, 2H), 7.32 (d, *J* = 8.4 Hz, 2H), 7.31 (d, *J* = 7.8 Hz, 2H), 2.43 (s, 3H); $^{13}C\{^{1}H\}$ NMR (150 MHz, $CDCl_3$) δ 158.5, 145.8, 134.5, 132.0, 131.2, 130.1, 129.4, 125.8, 124.4, 21.9; FT-IR (KBr) 3325, 2921, 2851, 1594, 1586, 1484, 1315, 1215, 1147, 1073, 1019, 998, 810, 674 cm^{-1}; HRMS (ESI) *m/z* $[M+H]^+$ calcd for $C_{14}H_{12}BrNO_3S$: 353.9800, found: 353.9796.

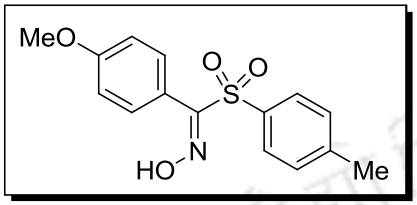

(*E*)-(4-Methoxyphenyl)(tosyl)methanone oxime 4c. Analytical TLC on silica gel, 1:4 ethyl acetate/hexane R_f = 0.48; white solid; yield: 83% (63 mg); mp 143-144 °C. ^{1}H NMR (600 MHz, $CDCl_3$) δ 7.69 (d, *J* = 8.4 Hz, 2H), 7.46 (d, *J* = 9.0 Hz, 2H), 7.28 (d, *J* = 7.8 Hz, 2H), 6.92 (d, *J* = 9.0 Hz, 2H), 3.83 (s, 3H), 2.41 (s, 3H); $^{13}C\{^{1}H\}$ NMR (150 MHz, $CDCl_3$) δ 161.5, 158.5, 145.4, 135.0, 131.4, 129.9, 129.2, 117.5, 114.1, 55.5, 21.9; FT-IR (KBr) 3448, 2961, 2924, 2854, 1604, 1507, 1455, 1314, 1293, 1258, 1173, 1149, 1088, 1019, 969, 835 cm^{-1}; HRMS (ESI) *m/z* $[M+H]^+$ calcd for $C_{15}H_{15}NO_4S$: 306.0800, found: 306.0800.

Crystal Data and Structure Refinement for 3o at 298(2) K.

Identification code	**3o**
Empirical formula	$C_{17}H_{19}NO_7S$
Formula weight	381.39
Temperature	298(2)
Wavelength	0.71073 Å
Crystal system	Monoclinic

Space group	P 21/n
	Loop xyz
	'x, y, z'
	'-x, y+1/2, -z+1/2'
	'-x, -y, -z'
	'x, -y-1/2, z-1/2'
Unit cell dimensions	*a* = 9.4930(5) Å α(°) = 90.00
	b = 8.0554(4) Å β(°) = 94.040(3)
	c = 23.9965(12)Å γ(°) = 90.00
Volume	1830.45(16) $Å^3$
Z	4
Density (calculated)	1.384Mg/m^3
Absorption coefficient	0.216 mm^{-1}
F(000)	800
Crystal size	0.42 x 0.38 x 0.24 mm
Theta range for data collection	2.36 to 24.990°
Index ranges	-11<=h<=10, -9<=k<=9, -28<=l<=24
Reflections collected	3208
Independent reflections	2643 [R (int) = 0.0828]
Completeness to theta = 29.07°	99.3 %
Absorption correction	Multi-scan
Refinement method	Full-matrix least-squares on F^2
Data / restraints / parameters	3226/ 0 /239
Goodness-of-fit on F^2	1.046
Final R indices [I>2sigma (I)]	*R1* = 0.0404, *wR2* = 0.1135
R indices (all data)	*R1* = 0.0481, *wR2* = 0.1200

Crystal Data and Structure Refinement for 4a at 298(2) K.

Identification code	**4a**
Empirical formula	$C_{14}H_{13}NO_3S$
Formula weight	275.31
Temperature	298(2)

Wavelength	0.71073 Å
Crystal system	Orthorhombic
Space group	P c a 21
	Loop xyz
	'x, y, z'
	'-x, y+1/2, -z+1/2'
	'-x, -y, -z'
	'x, -y-1/2, z-1/2'
Unit cell dimensions	*a* = 15.2114(14) Å α(°) = 90.00
	b = 7.1506(7) Å β(°) = 90.00
	c = 12.2547(12) Å γ(°) = 90.00
Volume	1333.0(2) $Å^3$
Z	4
Density (calculated)	1.372 Mg/m^3
Absorption coefficient	0.246 mm^{-1}
F(000)	576
Crystal size	0.42 x 0.22 x 0.18 mm
Theta range for data collection	1.34 to 26.00°
Index ranges	-18<=h<=18, -8<=k<=8, -14<=l<=15
Reflections collected	2620
Independent reflections	1995 [R (int) = 0.0561]
Completeness to theta = 29.07°	99.1%
Absorption correction	Multi-scan
Refinement method	Full-matrix least-squares on F^2
Data / restraints / parameters	2559 / 1 / 175
Goodness-of-fit on F^2	1.114
Final R indices [I>2sigma (I)]	*R1* = 0.0406, *wR2* = 0.0922
R indices (all data)	*R1* = 0.0576, *wR2* = 0.1023

Energy Minimized Structures of Organic Species Calculated at the B3LYP/ 6-311G+(d,p) Level.

Coordinates of R1

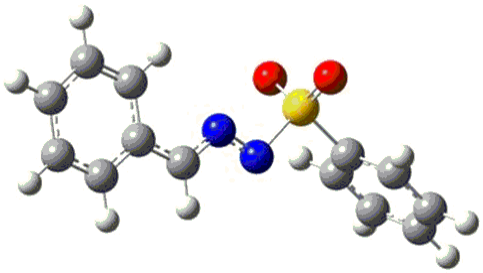

	X	Y	Z
C	6.032954	0.005756	-0.000024
C	5.10274	1.051562	-0.000011
C	3.74474	0.780746	-0.000031
C	3.289089	-0.558563	-0.000059
C	4.238965	-1.603857	-0.000074
C	5.596957	-1.321569	-0.000057
H	7.094393	0.226036	-0.000012
H	5.446277	2.079498	0.000015
H	3.015176	1.58032	-0.00003
H	3.895934	-2.632983	-0.000095
H	6.318537	-2.130135	-0.000073
C	1.893572	-0.881629	-0.000055
H	1.579042	-1.926805	-0.000077
C	-2.916027	0.131383	0.000013
C	-3.502821	-0.205496	-1.21724
C	-3.502741	-0.205881	1.217194
C	-4.707997	-0.903884	-1.210189
H	-3.029556	0.0892	-2.14532
C	-4.707917	-0.904268	1.210001
H	-3.029424	0.088517	2.145342
C	-5.306661	-1.253795	-0.00013
H	-5.180617	-1.169366	-2.148632
H	-5.18048	-1.170044	2.148389
H	-6.245643	-1.795742	-0.000183
N	0.963303	0.072889	-0.000005
N	-0.248738	-0.368783	0.000105
S	-1.358064	1.023324	0.000099
O	-1.217832	1.729863	-1.273189
O	-1.217878	1.729705	1.273487

EB3LYP+ZPE = -1160.018887 Hartree

Coordinates of R2

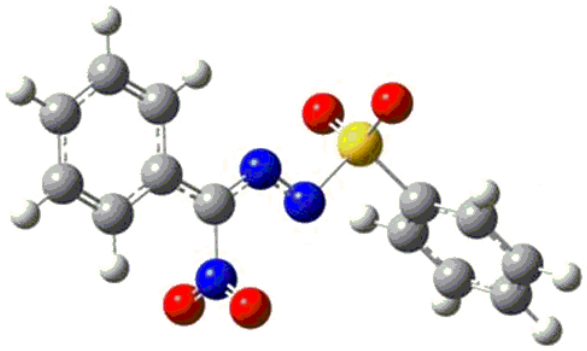

	X	Y	Z
C	-5.46499	0.627866	-0.08712
C	-4.13902	1.027214	-0.039218
C	-3.108836	0.060834	-0.030705
C	-3.447733	-1.312863	-0.072077
C	-4.777024	-1.695385	-0.119514
C	-5.78942	-0.730608	-0.127111
H	-6.250114	1.374275	-0.092464
H	-3.90037	2.083156	-0.005381
H	-2.655018	-2.049123	-0.066641
H	-5.030814	-2.748223	-0.151289
H	-6.828448	-1.036886	-0.164197
C	3.135866	-0.381402	0.000625
C	3.725269	0.135875	1.152038
C	3.683828	-0.18137	-1.264151
C	4.895653	0.879352	1.026422
H	3.280469	-0.051842	2.121003
C	4.855433	0.563544	-1.373675
H	3.20642	-0.610297	-2.135991
C	5.456624	1.093658	-0.232538
H	5.369729	1.287819	1.911051
H	5.298493	0.72693	-2.348969
H	6.368021	1.673456	-0.324047
N	-0.732636	-0.434603	0.04511
N	0.460697	0.042296	0.096114
S	1.616766	-1.317012	0.150088
O	1.534093	-1.897298	1.48891
O	1.433059	-2.137926	-1.044195
C	-1.728028	0.439129	0.019887
N	-1.403573	1.90406	0.045317
O	-1.344779	2.430708	1.142075
O	-1.220345	2.440213	-1.032723

EB3LYP+ZPE = -1364.56357 Hartree

Coordinates of E

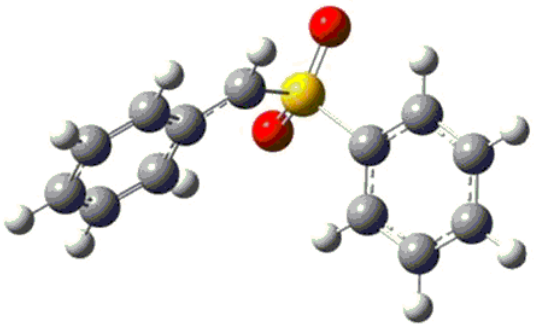

	X	Y	Z
C	-4.359218	-1.161142	-0.066431
C	-3.513445	-0.83317	-1.131806
C	-2.318635	-0.16862	-0.914698
C	-1.925607	0.192224	0.406457
C	-2.808029	-0.146153	1.475837
C	-3.996814	-0.810077	1.239482
H	-5.292674	-1.67987	-0.251338
H	-3.797872	-1.096113	-2.144429
H	-1.68154	0.101465	-1.744835
H	-2.530472	0.125393	2.488353
H	-4.649477	-1.057369	2.068966
C	-0.729485	0.864949	0.739833
H	-0.518197	1.126486	1.770115
C	1.843489	0.083112	-0.090503
C	2.783756	0.225421	0.929356
C	1.846905	-1.025754	-0.935821
C	3.737816	-0.772864	1.111188
H	2.775234	1.114056	1.548251
C	2.80682	-2.016174	-0.744418
H	1.124565	-1.096227	-1.739255
C	3.747405	-1.891806	0.278507
H	4.478758	-0.671562	1.895718
H	2.825593	-2.879908	-1.398898
H	4.493721	-2.664915	0.421911
S	0.599275	1.372486	-0.318773
O	1.138693	2.60182	0.274227
O	0.173086	1.333067	-1.72374

EB3LYP+ZPE = -1050.528053 Hartree

Coordinates of Product

	X	Y	Z
C	4.363278	1.085398	-0.151991
C	2.997017	1.256633	-0.037963
C	2.113928	0.137235	-0.092566
C	2.693361	-1.15298	-0.267348
C	4.064384	-1.300062	-0.381625
C	4.910376	-0.189934	-0.325838
H	5.011657	1.952371	-0.103429
H	2.599488	2.252743	0.088132
H	2.055843	-2.021709	-0.329143
H	4.479035	-2.291755	-0.519145
H	5.983043	-0.315219	-0.416729
C	-2.078294	-0.453345	-0.021589
C	-2.436529	-0.397164	-1.367562
C	-2.960727	-0.100753	0.996243
C	-3.71619	0.040575	-1.698691
H	-1.736982	-0.706978	-2.133712
C	-4.239731	0.324046	0.649181
H	-2.643293	-0.159427	2.028771
C	-4.613122	0.399331	-0.692741
H	-4.013339	0.092243	-2.739342
H	-4.941736	0.601072	1.426572
H	-5.609357	0.736179	-0.955807
S	-0.450791	-1.08162	0.408663
O	-0.414958	-1.397232	1.83534
O	-0.105677	-2.110507	-0.579557
C	0.708809	0.303462	0.085315
N	0.136064	1.620881	0.255054
O	0.425403	2.489192	-0.565466
O	-0.625207	1.781744	1.206296

EB3LYP+ZPE = -1255.070461 Hartree

1.7 References

1. For reviews on iron-catalyzed reactions, see: (a) *Iron-catalysis in Organic Chemistry*; Plietker, B.; Ed.; Wiley-VCH: Weinheim, 2008. (b) Bolm, C.; Legros, J.; LePaih, J.; Zani, L. *Chem. Rev.* **2004**, *104*, 6217. (c) Enthaler, S.; Junge, K.; Beller, M. *Angew. Chem., Int. Ed.* **2008**, *47*, 3317. (d) Fürstner, A. *Angew. Chem., Int. Ed.* **2009**, *48*, 1364. (e) Sahan, A. A.; Bolm, C. *Chem. Soc. Rev.* **2009**, *38*, 2730.
2. (a) Bertini, I.; Gray, H. B.; Lippard, S. J.; Valentine, J. S. *Bioinorganic Chemistry*, University Science Books, Mill Valley, 1994. (b) Rosenzweig, A. C.; Brandstetter, H.; Whittington, D. A.; Nordlund, P.; Lippard, S. J.; Frederick, C. A. *Proteins: Struct., Funct., Genet.*, **1997**, *29*, 141.
3. For examples, see: (a) Sylvester, K. T.; Chirik, P. J. *J. Am. Chem. Soc.* **2009**, *131*, 8772. (b) Wu, J. Y.; Moreau, B.; Ritter, T. *J. Am. Chem. Soc.* **2009**, *131*, 12915. (c) Junge, K.; Wundt, B.; Shaikh, N.; Beller, M. *Chem. Commun.* **2010**, 1769. (d) D'Souza, B. R.; Lane, T. K.; Louie, J. *Org. Lett.* **2011**, *13*, 2936. (e) Wang, C.; Wang, D.; Xu, F.; Pan, B.; Wan, B. *J. Org. Chem.* **2013**, *78*, 3065. (f) Tseng, K.-N. T.; Kampf, J. W.; Szymczak, N. K. *Acs Catal.* **2015**, *5*, 411. (g) Bag, R.; Sar, D.; Punniyamurthy, T. *Org. Biomol. Chem.* **2016**, *14*, 3246.
4. (a) Li, Y.-Z.; Li, B.-J.; Lu, X.-Y.; Lin, S.; Shi, Z.-J. *Angew. Chem., Int. Ed.* **2009**, *48*, 3817. (b) Monir, K.; Bagdi, A. K.; Ghosh, M.; Hajra, A. *Org. Lett.* **2014**, *16*, 4630. (c) Wei, W.; Wen, J.; Yang, D.; Wu, M.; You, J.; Wang, H. *Org. Biomol. Chem.* **2014**, *12*, 7678. (d) Bag, R.; Sar, D.; Punniyamurthy, T. *Org. Biomol. Chem.* **2016**, *14*, 3246.
5. (a) Schareina, T.; Zapf, A.; Beller, M. *Chem. Commun.* **2004**, 1388. (b) Pinto, A.; Jia, Y.; Neuville, L.; Zhu, J. *Chem.-Eur. J.* **2007**, *13*, 961. (c) Franz, A. W.; Popa, L. N.; Müller, T. J. J. *Tetrahedron let.* **2008**, *49*, 3300. (d) Li, X.; Shi, X.; Fang, M.; Xu, X. *J. Org. Chem.* **2013**, *78*, 9499.
6. (a) Hill, W. D. Jr. *Inorg. Chem. Acta* **1986**, *121*, L33. (b) Wieczorek-Ciurowa, K.; Kozak, A. J. *J. Therm. Anal. Calorim.* **1999**, *58*, 647.
7. Varma, R. S.; Naicker, K. P.; Liesen, P. J. *Tetrahedron Lett.* **1998**, *39*, 3977.
8. (a) Taniguchi, T.; Fujii, T.; Ishibashi, H. *J. Org. Chem.* **2010**, *75*, 8126. (b) Taniguchi, T.; Ishibashi, H. *Org. Lett.* **2010**, *12*, 124.
9. For examples, see: (a) Feuer, H.; Nielsen, A. T. *Nitro Compounds: Recent Advances in Synthesis and Chemistry*; VCH: New York, 1990. (b) Ono, N. *The Nitro group in*

Organic Synthesis; Wiley-VCH: New York, 2001. (c) Kudyba, I.; Raczko, J.; Jurczak, J. *J. Org. Chem.* **2004**, *69*, 2844. (d) Ballini, R.; Bosica, G.; Fiorini, D.; Palmieri, A.; Petrini, M. *Chem. Rev.* **2005**, *105*, 933. (e) Fioravanti, S.; Pellacani, L.; Tardella, P. A.; Vergari, M. C. *Org. Lett.* **2008**, *10*, 1449. (f) Bui, T.; Syed, S.; Barbas, C. F., III. J. *Am. Chem. Soc.* **2009**, *131*, 8758. (g) Marques-Lopez, E.; Merino, P.; Tejero, T.; Herrera, R. P. *Eur. J. Org. Chem.* **2009**, 2401. (h) Ando, K.; Shimazu, Y.; Seki, N.; Yamataka, H. *J. Org. Chem*. **2011**, *76*, 3937.

10. For examples, see: (a) Simpkins, N. S. *Sulfones in Organic Synthesis*; Pergamon: Oxford, 1993. (b) Toru, T.; Bolm, C. *Organosulfur Chemistry in Asymmetric Synthesis*; Wiley-VCH: Weinheim, 2008. (c) El-Awa, A.; Noshi, M. N.; Mollat du Jourdin, X.; Fuchs, P. L. *Chem. Rev.* **2009**, *109*, 2315. (d) Liu, C.-R.; Li, M.-B.; Cheng, D.-J.; Yang, C.-F.; Tian, S.-K. *Org. Lett.* **2009**, *11*, 2543. (e) Prakash, G. K. S.; Chacko, S.; Vaghoo, H.; Shao, N.; Gurung, L.; Mathew, T.; Olah, G. A. *Org. Lett.* **2009**, *11*, 1127.
11. For examples, see: (a) Mulzer, J.; Zuhse, R.; Schmiechen, R. *Angew. Chem., Int. Ed.* **1992**, *31*, 870. (b) Lovejoy, B.; Welch, A. R.; Carr, S.; Luong, C.; Broka, C.; Hendricks, R. T.; Campbell, J. A.; Walker, K. A. M.; Martin, R.; Van Wart, H.; Browner, M. F. *Nat. Struct. Biol.* **1999**, *6*, 217. (c) Lakshmaiah, G.; Kawabata, T.; Shang, M.; Fuji, K. *J. Org. Chem.* **1999**, *64*, 1699. (d) Mulzer, J.; Riether, D. *Org. Lett.* **2000**, *2*, 3139. (e) Kudyba, I.; Raczko, J.; Jurczak, J. *J. Org. Chem.* **2004**, *69*, 2844.
12. For some selected examples, see: (a) Bulut, A.; Aslan, A.; Dogan, O. *J. Org. Chem.* **2008**, *73*, 7373. (b) Kowalczyk, R.; Kwiatkowski, P.; Skarżewski, J.; Jurczak, J. *J. Org. Chem.* **2009**, *74*, 753. (c) Fabris, M.; Noè, M.; Perosa, A.; Selva, M.; Ballini, R. *J. Org. Chem.* **2012**, *77*, 1805. (d) Hashimoto, K.; Kumagai, N.; Shibasaki, M. *Org. Lett.* **2014**, *16*, 3496.
13. For some selected examples, see: (a) Ballini, R.; Bosica, G.; Fiorini, D.; Palmieri, A.; Petrini, M. *Chem. Rev.* **2005**, *105*, 933. (b) Zhu, Q.; Lu, Y. *Org. Lett.* **2009**, *11*, 1721. (c) García, J. M.; Maestro, M. A.; Oiarbide, M.; Odriozola, J. M.; Razkin, J.; Palomo, C. *Org. Lett.* **2009**, *11*, 3826. (d) Sahu, B.; Gururaja, G. N.; Mobin, S. M.; Namboothiri, I. N. N. *J. Org. Chem.* **2009**, *74*, 2601. (e) Ogawa, T.; Mouri, S.; Yazaki, R.; Kumagai, N.; Shibasaki, M. *Org. Lett.* **2012**, *14*, 110. (f) Qian, H.; Yu, X.; Zhang, J.; Sun, J. *J. Am. Chem. Soc.* **2013**, *135*, 18020. (g) Quintavalla, A.;

Lanza, F.; Montroni, E.; Lombardo, M.; Trombini, C. *J. Org. Chem.* **2013**, *78*, 12049.

14. (a) Kurti, L.; Czako, B. *Strategic Applications of Named Reactions in Organic Synthesis*: Elsevier Academic Press: Amsterdam, 2005. (b) Ballini, R.; Palmieri, A.; Righi, P. *Tetrahedron* **2007**, *63*, 12099.
15. For recent examples, see: (a) Julia, M.; Paris, J.-M. *Tetrahedron Lett.* **1973**, *14*, 4833. (b) Kelly, S. E. *Comp. Org. Syn.* **1991**, *1*, 792. (c) Aïssa, C. *J. Org. Chem.* **2006**, *71*, 360. (d) Aleman, J.; Reyes, E.; Richter, B.; Overgaard, J.; Jorgensen, K. A. *Chem. Commun.* **2007**, 3921. (e) Rodrigo, E.; García Ruano, J. L.; Cid, M. B. *J. Org. Chem.* **2013**, *78*, 10737. (f) Ando, K.; Kobayashi, T.; Uchida, N. *Org. Lett.* **2015**, *17*, 2554.
16. For examples, see: (a) Ni, C.; Wang, F.; Hu, J. *Beilstein J. Org. Chem.* **2008**, *4*, 21. (b) Cassani, C.; Bernardi, L.; Fini, F.; Ricci, A. *Angew. Chem., Int. Ed.* **2009**, *48*, 5694.
17. Nielsen, M.; Jacobsen, C. B.; Holub, N.; Paixao, M. W.; Jorgensen, K. A. *Angew. Chem., Int. Ed.* **2010**, *49*, 2668.
18. For examples, see: (a) Najera, C.; Yus, M. *Tetrahedron* **1999**, *55*, 10547. (b) Mosse, S.; Alexakis, A. *Org. Lett.* **2005**, *7*, 4361. (c) Zhu, Q.; Lu, Y. *Org. Lett.* **2008**, *10*, 4803.
19. Jakubec, P.; Hawkins, A.; Felzmann, W.; Dixon, D. J. *J. Am. Chem. Soc.* **2012**, *134*, 17482.
20. Davis, T. A.; Johnston, J. N. *Chem. Sci.* **2011**, *2*, 1076.
21. For the synthesis of aryl nitromethane via nucleophilic substitution, see: Greger, J. G.; Yoon-Miller, S. J. P.; Bechtold, N. R.; Flewelling, S. A.; MacDonald, J. P.; Downey, C. R.; Cohen, E. A.; Pelkey, E. T. *J. Org. Chem.* **2011**, *76*, 8203.
22. For the synthesis aryl nitromethane via cross-coupling, see: (a) Fox, J. N.; Huang, X.; Chieffi, A. Buchwald, S. L. *J. Am. Chem. Soc.* **2000**, *122*, 1360. (b) Walvoord, R.; Berritt, S.; Kozlowski, M. C. *Org. Lett.* **2012**, *14*, 4086. (c) Metz, A. E.; Kozlowski, M. C. *J. Org. Chem.* **2013**, *78*, 717. (d) Walvoord, R. R.; Kozlowski, M. C. *J. Org. Chem.* **2013**, *78*, 8859.
23. For examples, see: (a) Pulkkinen, J.; Aburel, P. S.; Halland, N.; Jorgensen, K. A. *Adv. Synth. Catal.* **2004**, *346*, 1077. (b) Cid, M. B.; Lopez-Cantarero, J.; Duce, S.; Garcia Ruano, J. L. *J. Org. Chem.* **2009**, *74*, 431.

24. For base mediated synthesis of bisarylnitromethyl sulfone, see: Truce, W. E.; Klingler, T. C.; Paar, J. E.; Feuer, H.; Wu, D. K. *J. Org. Chem.* **1969**, *34*, 3104.
25. Ballini, R.; Barboni, L.; Giarlo, G. *J. Org. Chem.* **2004**, *69*, 6907.
26. (a) Pospísil, J.; Sato, H. *J. Org. Chem.* **2011**, *76*, 2269. (b) Chang, M.-Y.; Cheng, Y.-C.; Lu, Y.-J. *Org. Lett.* **2014**, *16*, 6252. (c) Chang, M.-Y.; Lu, Y.-J.; Cheng, Y.-C. *Tetrahedron* **2015**, *71*, 1192. (d) Gao, W.-C.; Zhao, J.-J.; Hu, F.; Chang, H.-H.; Li, X.; Wei, W.-L. *RSC Adv.* **2015**, *5*, 25222.
27. (a) Antonchick, A. P.; Samanta, R.; Kulikov, K.; Lategahn, *J. Angew. Chem., Int. Ed.* **2011**, *50*, 8605. (b) Huang, J.; He,Y.; Wang,Y.; Zhu, Q. *Chem. Eur. J.* **2012**, *18*, 13964.
28. For examples see: (a) Barluenga, J.; Tomas-Gamasa, M.; Aznar, F.; Valdes, C. *Angew. Chem., Int. Ed.* **2010**, *49*, 4993. (b) Yin, B.; Zhang, X.; Zhang, X.; Peng, H.; Zhou, W.; Liu, B.; Jiang, H. *Chem. Commun.* **2015**, *51*, 6126. (c) Su, N.; Theorell, J. A.; Wink, D. J.; Driver, T. G. *Angew. Chem., Int. Ed.* **2015**, *54*, 12942. (d) Xu, P.; Han, F.-S.; Wang, Y.-H. *Adv. Synth. Catal.* **2015**, *357*, 3441. (e) Zhang, Z.; Zhou, Q.; Yu, W.; Li, T.; Wu, G.; Zhang, Y.; Wang, J. *Org. Lett.* **2015**, *17*, 2474.
29. Taniguchi, T.; Sugiura, Y.; Zaimoku, H.; Ishibashi, H. *Angew. Chem., Int. Ed.* **2010**, *49*, 10154.
30. (a) Lee, C.; Yang, W.; Parr, R. G. *Phys. Rev. B* **1988**, *37*, 785. (b) Becke, A. D. *J. Chem. Phys*. **1992**, *96*, 2155.
31. Frisch, M. J.; Trucks, G. W.; Schlegel, H. B.; Scuseria, G. E.; Robb, M. A.; Cheeseman, J. R.; Scalmani, G.; Barone, V.; Mennucci, B.; Petersson, G. A.; Nakatsuji, H.; Caricato, M.; Li, X.; Hratchian, H. P.; Izmaylov, A. F.; Bloino, J.; Zheng, G.; Sonnenberg, J. L.; Hada, M.; Ehara, M.; Toyota, K.; Fukuda, R.; Hasegawa, J.; Ishida, M.; Nakajima, T.; Honda, Y.; Kitao, O.; Nakai, H.; Vreven, T.; Montgomery, J. A., Jr.; Peralta, J. E.; Ogliaro, F.; Bearpark, M.; Heyd, J. J.; Brothers, E.; Kudin, K. N.; Staroverov, V. N.; Kobayashi, R.; Normand, J.; Raghavachari, K.; Rendell, A.; Burant, J. C.; Iyengar, S. S.; Tomasi, J.; Cossi, M.; Rega, N.; Millam, J. M.; Klene, M.; Knox, J. E.; Cross, J. B.; Bakken, V.; Adamo, C.; Jaramillo, J.; Gomperts, R.; Stratmann, R. E.; Yazyev, O.; Austin, A. J.; Cammi, R.; Pomelli, C.; Ochterski, J. W.; Martin, R. L.; Morokuma, K.; Zakrzewski, V. G.; Voth, G. A.; Salvador, P.; Dannenberg, J. J.; Dapprich, S.; Daniels, A. D.; Farkas, Ö.; Foresman, J. B.; Ortiz, J. V.; Cioslowski, J.; Fox, D. J. Gaussian, Inc., Wallingford CT, 2009.

32. Yang, F.-L.; Ma, X.-T.; Tian, S.-K. *Chem. Eur. J*. **2012**, *18*, 1582.
33. Doshi, J. M.; Tian, D.; Xing, C. *J. Med. Chem*. **2006**, *49*, 7731.
34. Guru, M. M.; Ali, M. A.; Punniyamurthy, T. *J. Org. Chem*. **2011**, *76*, 5295.

1.8 Selected Spectra

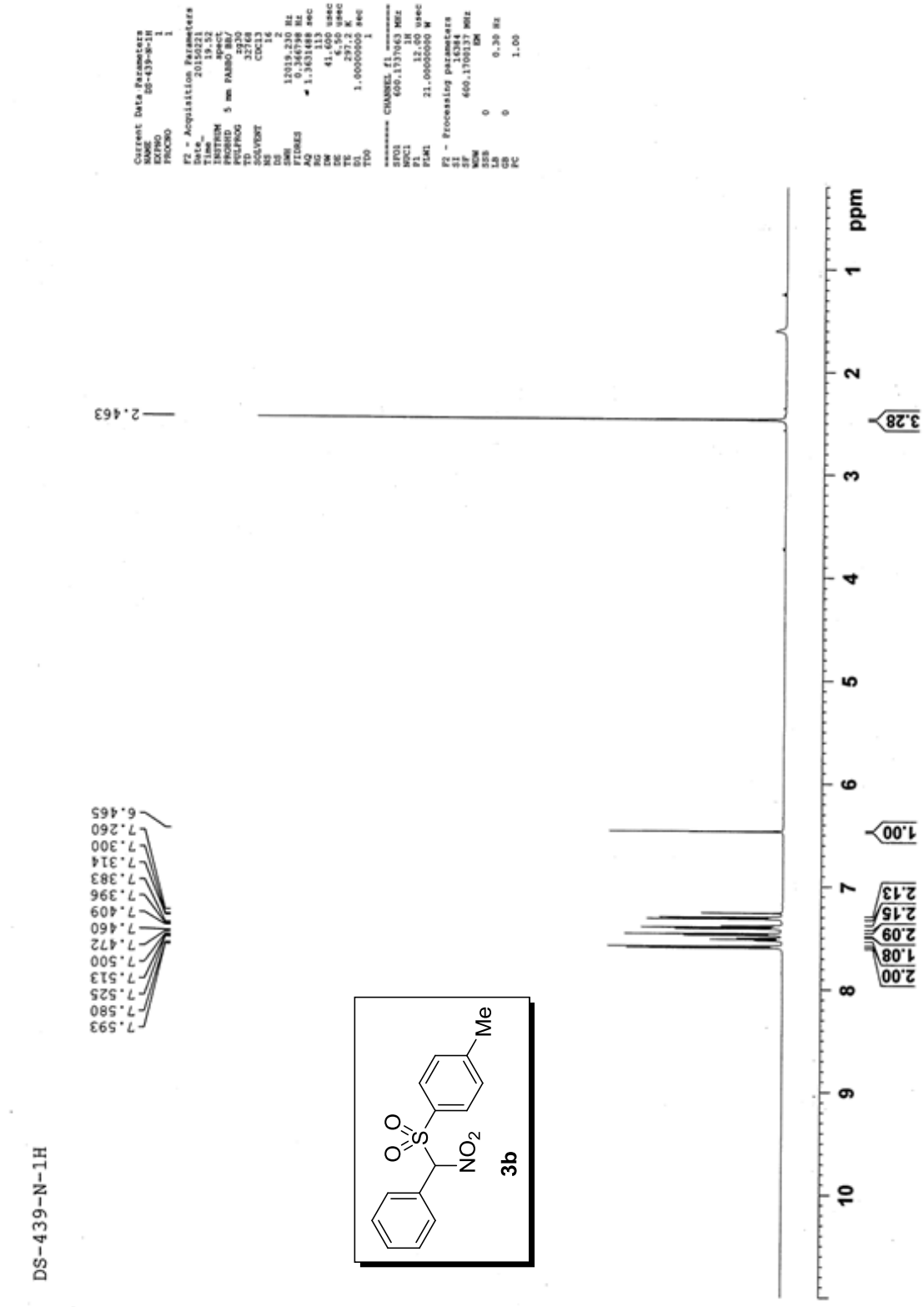

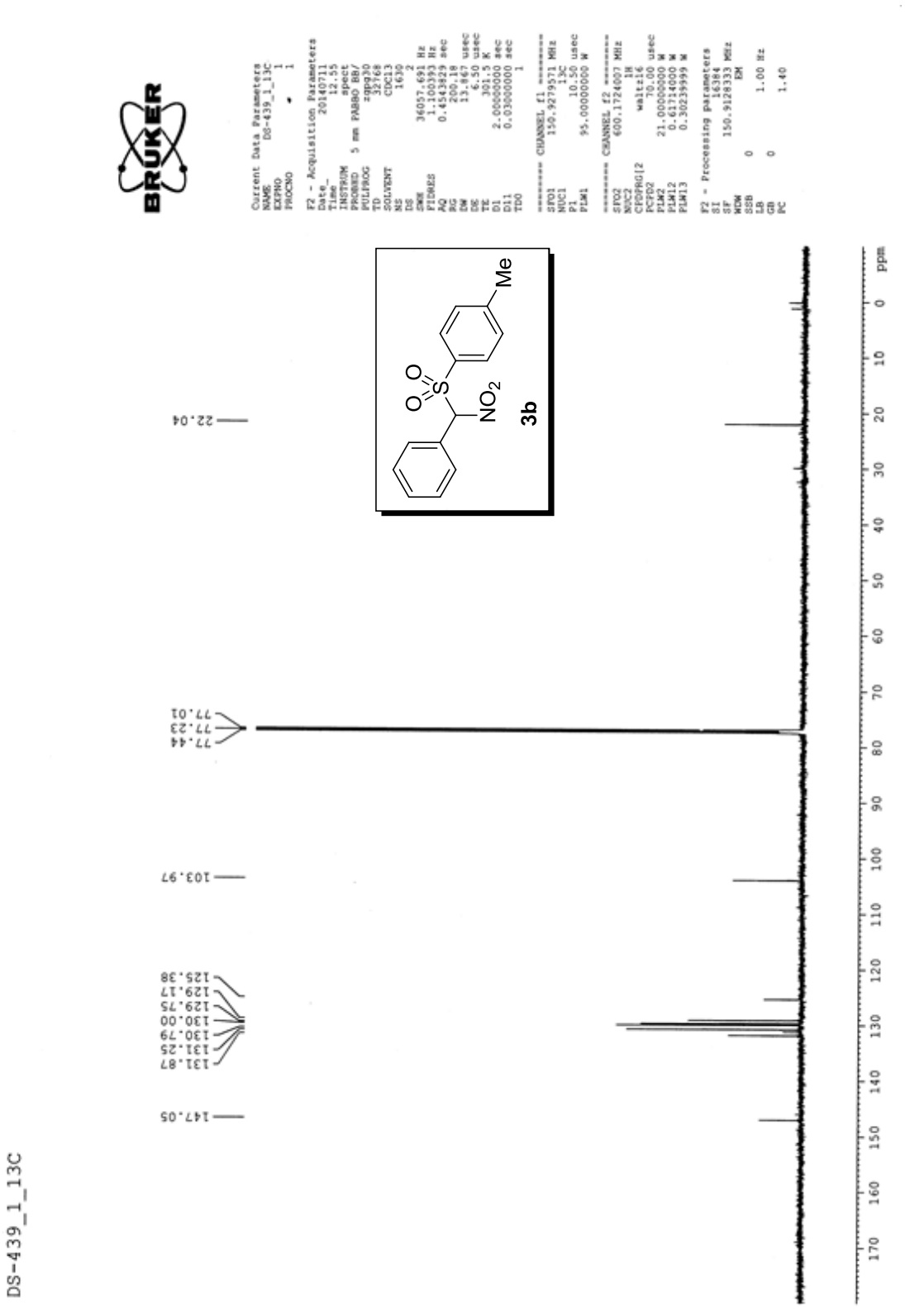
DS-439_1_13C
Current Data Parameters
NAME DS-439_1_13C
EXPNO 1
PROCNO 1
F2 - Acquisition Parameters
Date_ 20140711
Time 12.35
INSTRUM spect
PROBHD 5 mm PABBO BB/
PULPROG zgpg30
TD 32768
SOLVENT CDCl3
NS 1630
DS 2
SWH 36057.691 Hz
FIDRES 1.100393 Hz
AQ 0.4543829 sec
RG 200.18
DW 13.867 usec
DE 6.50 usec
TE 301.3 K
D1 2.00000000 sec
D11 0.03000000 sec
TD0 1
======== CHANNEL f1 ========
SFO1 150.9279571 MHz
NUC1 13C
P1 10.50 usec
PLW1 95.00000000 W
======== CHANNEL f2 ========
SFO2 600.1724007 MHz
NUC2 1H
CPDPRG[2 waltz16
PCPD2 70.00 usec
PLW2 21.00000000 W
PLW12 0.61714000 W
PLW13 0.30239999 W
F2 - Processing parameters
SI 65536
SF 150.9128333 MHz
WDW EM
SSB 0
LB 1.00 Hz
GB 0
PC 1.40
Me
O
O
S
NO2
3b
22.04
77.44
77.23
77.01
103.97
125.38
129.17
129.75
130.00
130.79
131.25
131.87
147.05
ppm

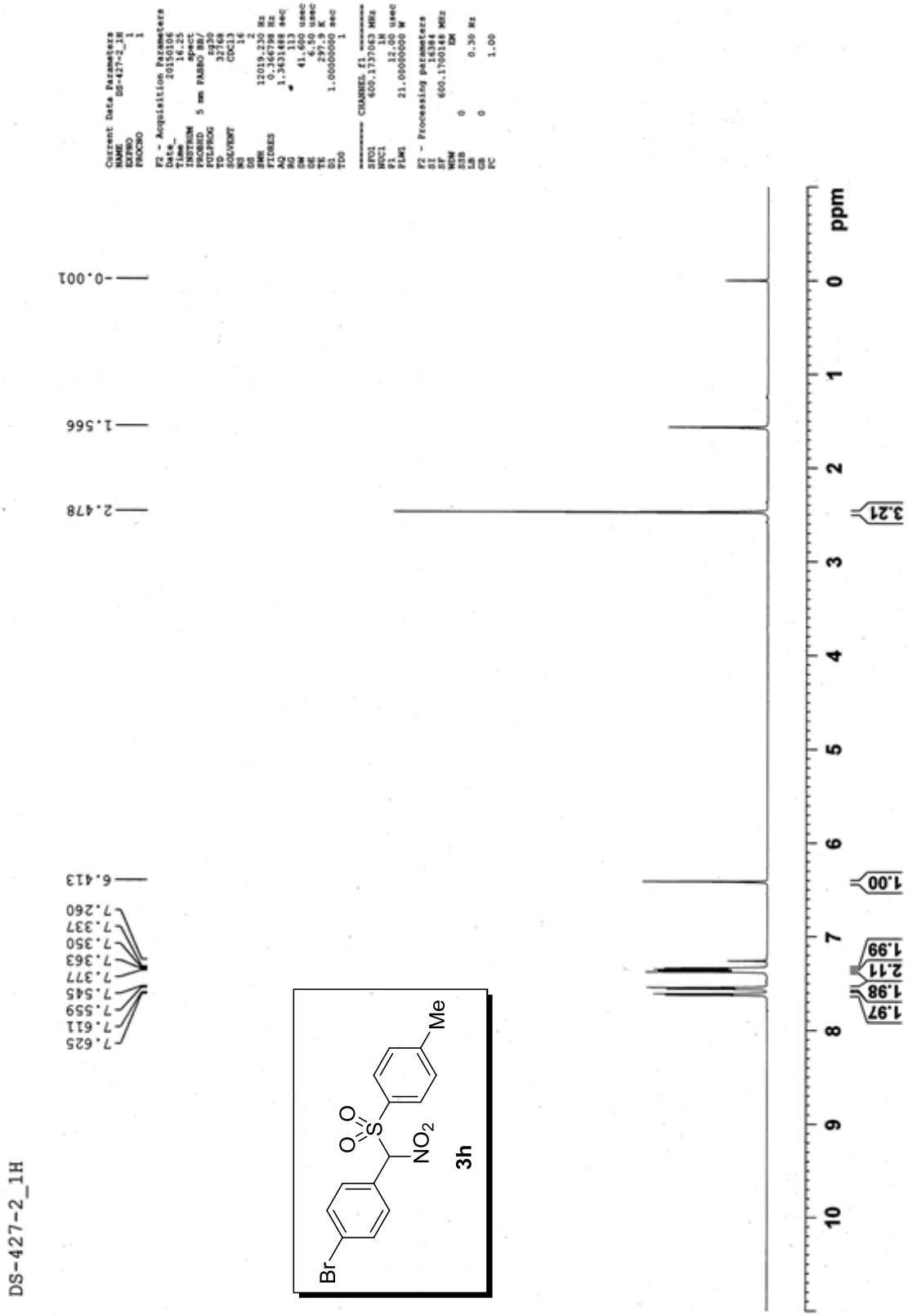
DS-427-2_1H
Current Data Parameters
NAME DS-427-2_1H
EXPNO 1
PROCNO 1
F2 - Acquisition Parameters
Date_ 20150106
Time 16.25
INSTRUM spect
PROBHD 5 mm PABBO BB/
PULPROG zg30
TD 32768
SOLVENT CDCl3
NS 16
DS 2
SWH 12019.230 Hz
FIDRES 0.366798 Hz
AQ 1.3631488 sec
RG 133
DW 41.600 usec
DE 6.50 usec
TE 297.0 K
D1 1.00000000 sec
TD0 1
======== CHANNEL f1 ========
SFO1 600.1737063 MHz
NUC1 1H
P1 12.00 usec
PLW1 21.00000000 W
F2 - Processing parameters
SI 16384
SF 600.1700148 MHz
WDW EM
SSB 0
LB 0.30 Hz
GB 0
PC 1.00
0.001
1.566
2.478
6.413
7.260
7.337
7.350
7.363
7.377
7.545
7.559
7.611
7.625
3.21
1.00
1.99
2.11
1.98
1.97
ppm
Me
Br
O
O
S
NO2
3h

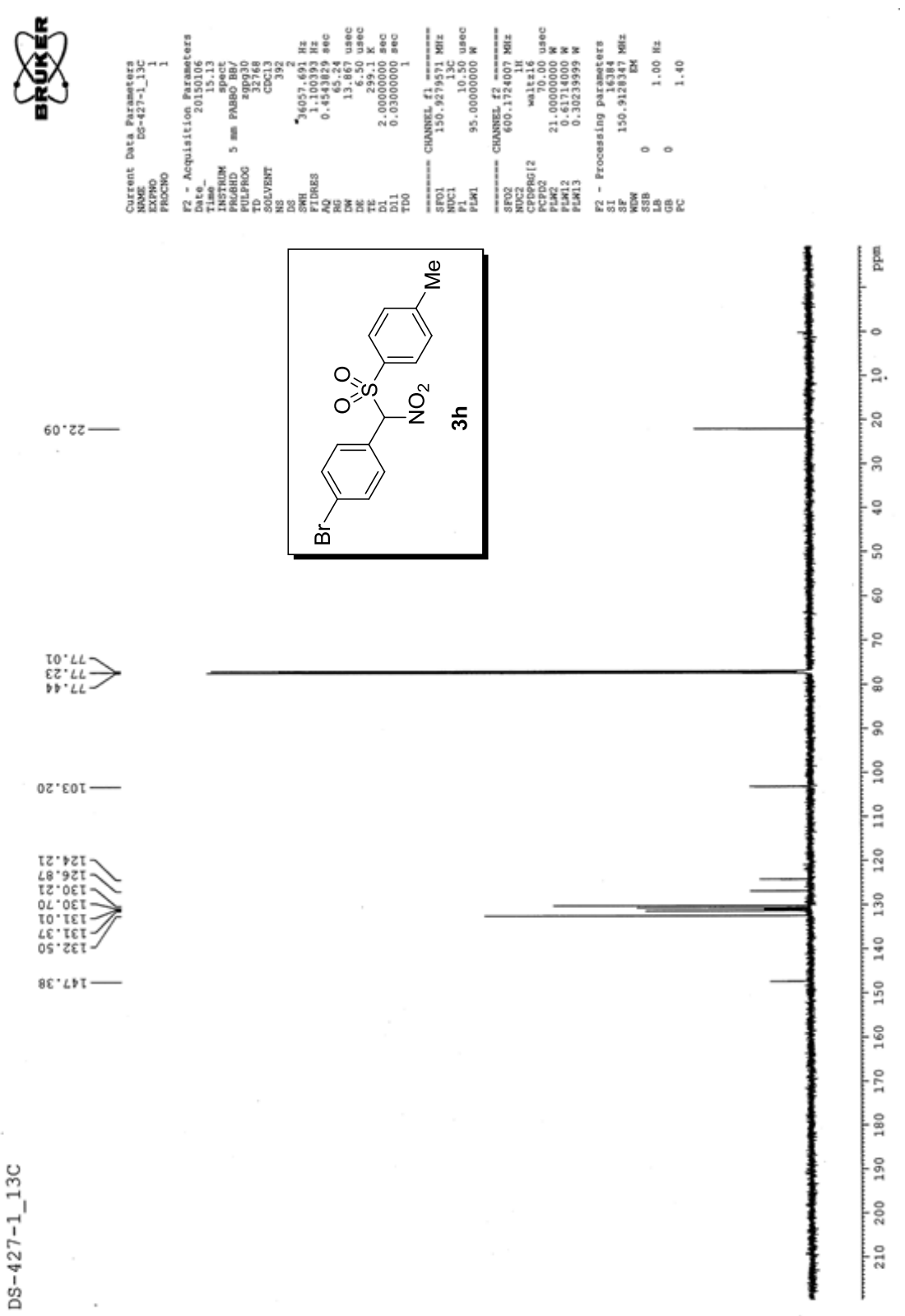
DS-427-1_13C
Current Data Parameters
NAME DS-427-1_13C
EXPNO 1
PROCNO 1
F2 - Acquisition Parameters
Date_ 20150106
Time 15.13
INSTRUM spect
PROBHD 5 mm PABBO BB/
PULPROG zgpg30
TD 32768
SOLVENT CDCl3
NS 392
DS 2
SWH 36057.691 Hz
FIDRES 1.100393 Hz
AQ 0.4543829 sec
RG 65.24
DW 13.867 usec
DE 6.50 usec
TE 299.1 K
D1 2.00000000 sec
D11 0.03000000 sec
TD0 1
======== CHANNEL f1 ========
SFO1 150.9279571 MHz
NUC1 13C
P1 10.50 usec
PLW1 95.00000000 W
======== CHANNEL f2 ========
SFO2 600.1724007 MHz
NUC2 1H
CPDPRG[2 waltz16
PCPD2 70.00 usec
PLW2 21.00000000 W
PLW12 0.61714000 W
PLW13 0.30239999 W
F2 - Processing parameters
SI 16384
SF 150.9128347 MHz
WDW EM
SSB 0
LB 1.00 Hz
GB 0
PC 1.40
Br
O
O
S
NO2
Me
3h
22.09
77.01
77.23
77.44
103.20
124.21
126.87
130.21
130.70
131.01
131.37
132.50
147.38
ppm

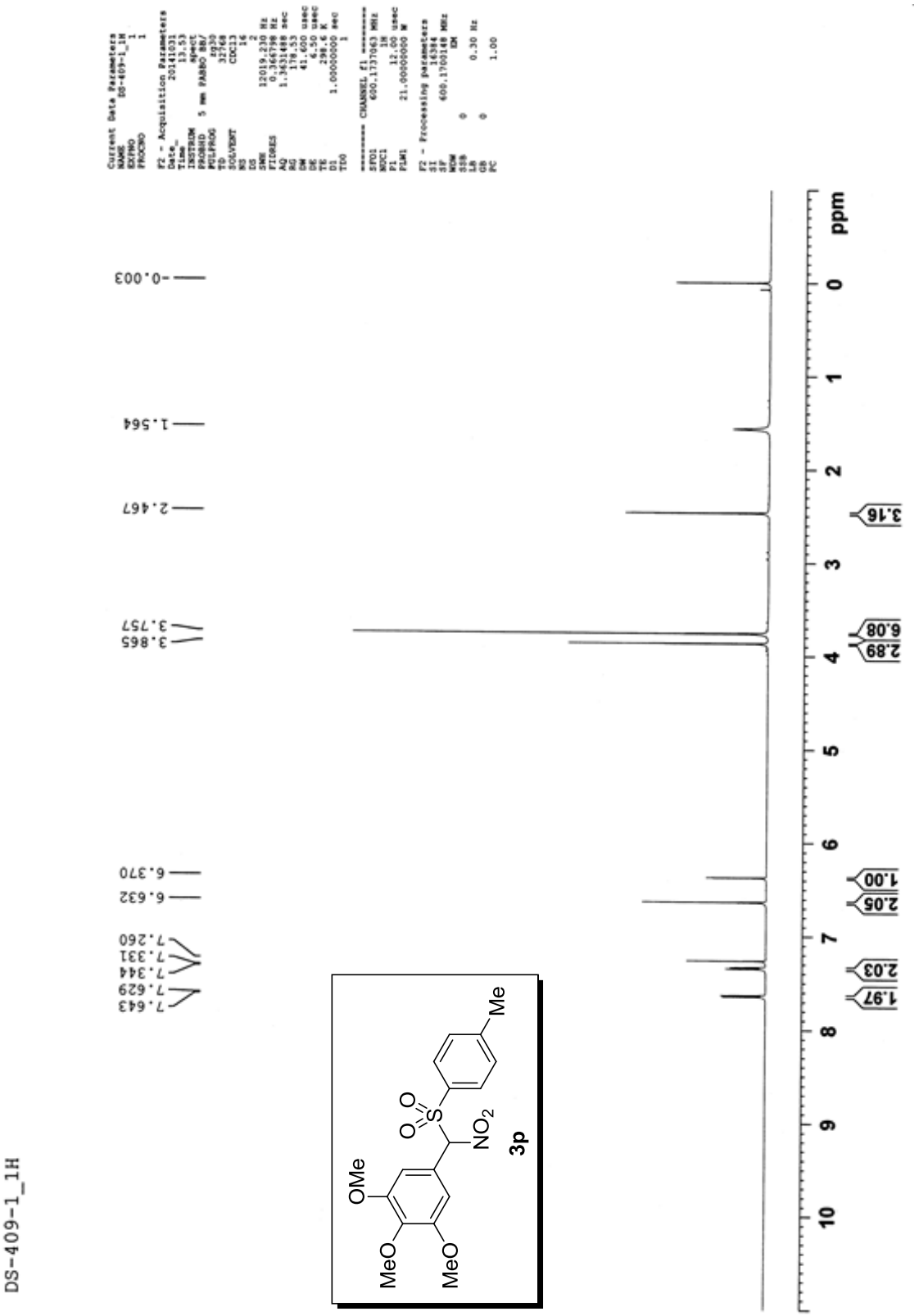
DS-409-1_1H
3p
OMe
MeO
MeO
Me
NO_2
ppm
7.643
7.629
7.344
7.331
7.260
6.632
6.370
3.865
3.757
2.467
1.564
0.003
1.97
2.03
2.05
1.00
2.89
6.08
3.16

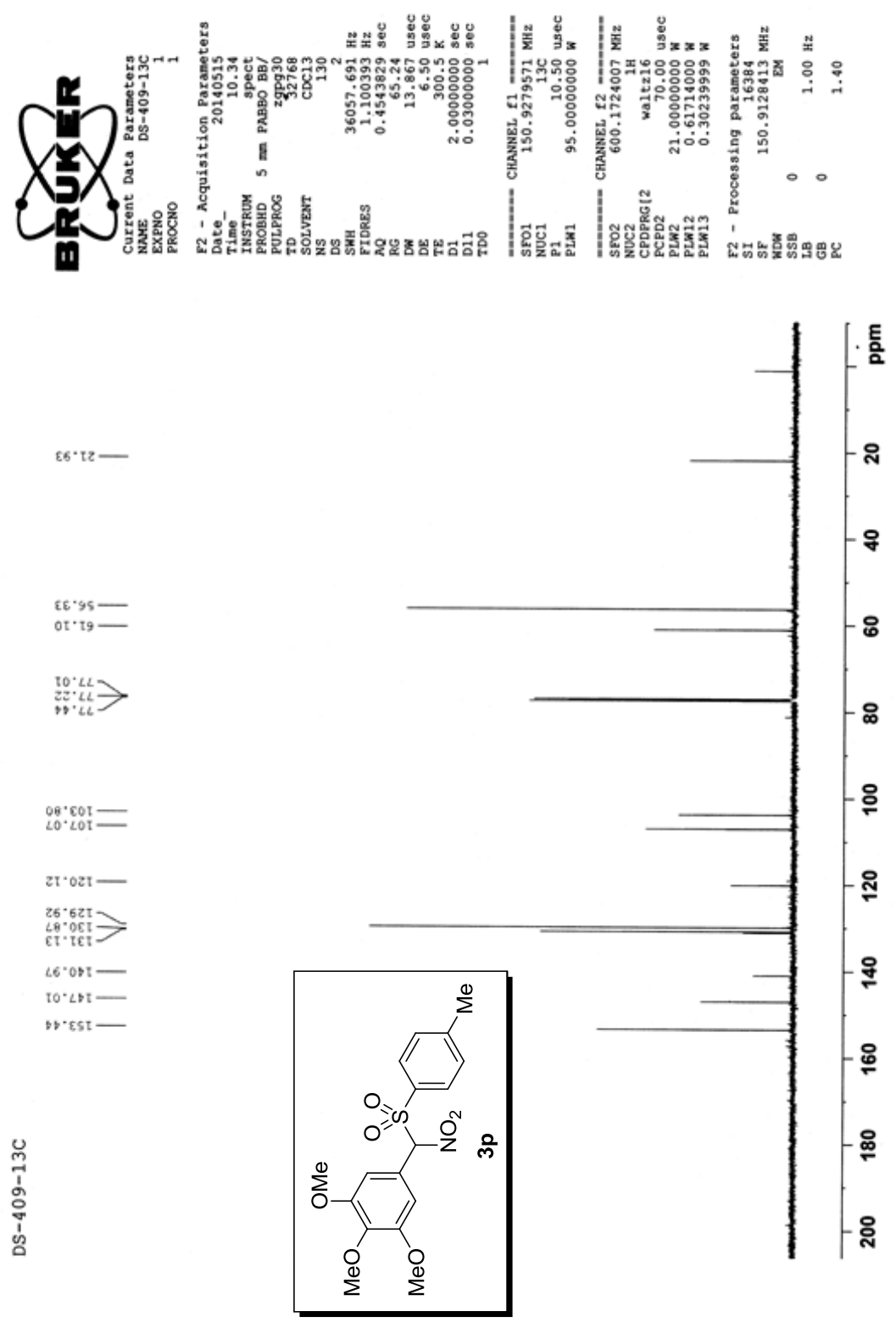
DS-409-13C
Current Data Parameters
NAME DS-409-13C
EXPNO 1
PROCNO 1
F2 - Acquisition Parameters
Date_ 20140515
Time_ 10.34
INSTRUM spect
PROBHD 5 mm PABBO BB/
PULPROG zgpg30
TD 32768
SOLVENT CDCl3
NS 130
DS 2
SWH 36057.691 Hz
FIDRES 1.100393 Hz
AQ 0.4543829 sec
RG 65.24
DW 13.867 usec
DE 6.50 usec
TE 300.5 K
D1 2.00000000 sec
D11 0.03000000 sec
TD0 1
======== CHANNEL f1 ========
SFO1 150.9279571 MHz
NUC1 13C
P1 10.50 usec
PLW1 95.00000000 W
======== CHANNEL f2 ========
SFO2 600.1724007 MHz
NUC2 1H
CPDPRG[2 waltz16
PCPD2 70.00 usec
PLW2 21.00000000 W
PLW12 0.61714000 W
PLW13 0.30239999 W
F2 - Processing parameters
SI 16384
SF 150.9128413 MHz
WDW EM
SSB 0
LB 1.00 Hz
GB 0
PC 1.40
21.93
56.33
61.10
77.01
77.22
77.44
103.80
107.07
120.12
129.92
130.87
131.13
140.97
147.01
153.44
OMe
MeO
MeO
NO2
S
O
O
Me
3p
ppm

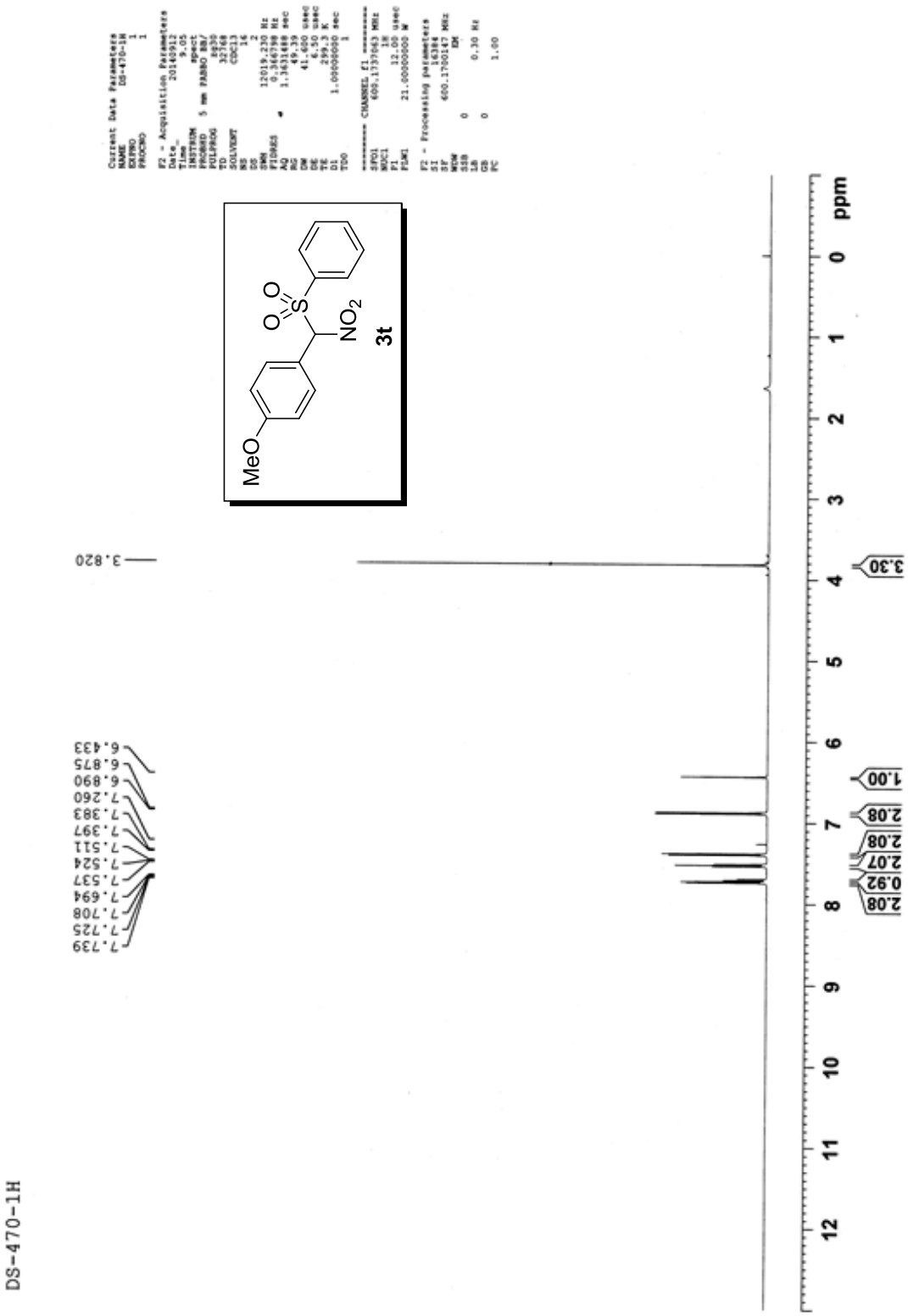
DS-470-1H
3t
MeO
NO_2
3.820
6.433
6.875
6.890
7.260
7.383
7.397
7.511
7.524
7.537
7.694
7.708
7.725
7.739
3.30
1.00
2.08
2.08
2.07
0.92
2.08
ppm

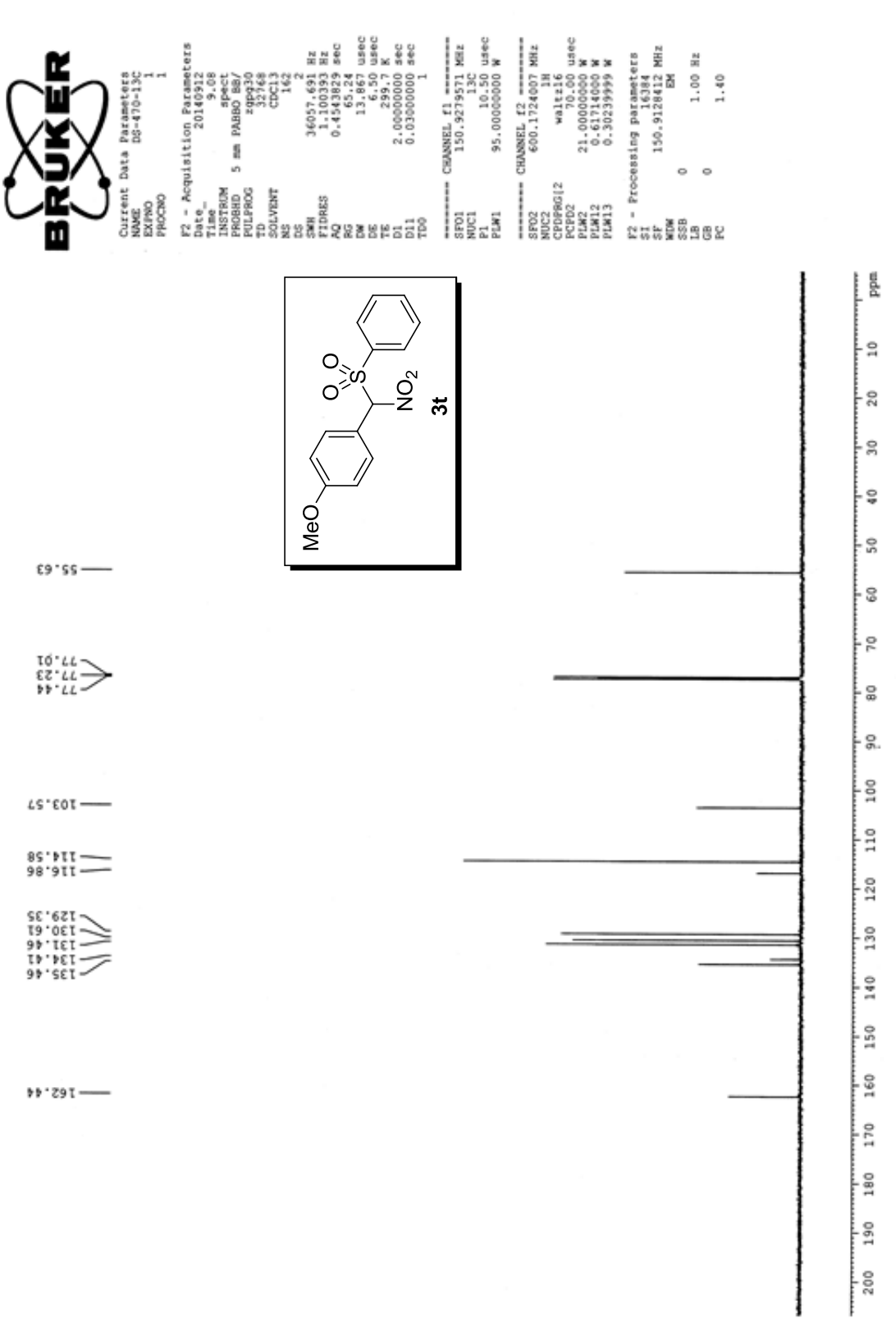
Current Data Parameters
NAME DS-470-13C
EXPNO 1
PROCNO 1
F2 - Acquisition Parameters
Date_ 20140912
Time 9.08
INSTRUM spect
PROBHD 5 mm PABBO BB/
PULPROG zgpg30
TD 32768
SOLVENT CDCl3
NS 162
DS 2
SWH 36057.691 Hz
FIDRES 1.100393 Hz
AQ 0.4543829 sec
RG 65.24
DW 13.867 usec
DE 6.50 usec
TE 299.7 K
D1 2.00000000 sec
D11 0.03000000 sec
TD0 1
CHANNEL f1
SFO1 150.9279571 MHz
NUC1 13C
P1 10.50 usec
PLW1 95.00000000 W
CHANNEL f2
SFO2 600.1724007 MHz
NUC2 1H
CPDPRG[2 waltz16
PCPD2 70.00 usec
PLW2 21.00000000 W
PLW12 0.61714000 W
PLW13 0.30239999 W
F2 - Processing parameters
SI 16384
SF 150.9128412 MHz
WDW EM
SSB 0
LB 1.00 Hz
GB 0
PC 1.40
MeO
O
O
S
NO2
3t
55.63
77.44
77.23
77.01
103.57
114.58
116.86
129.35
130.61
131.46
134.41
135.46
162.44
ppm

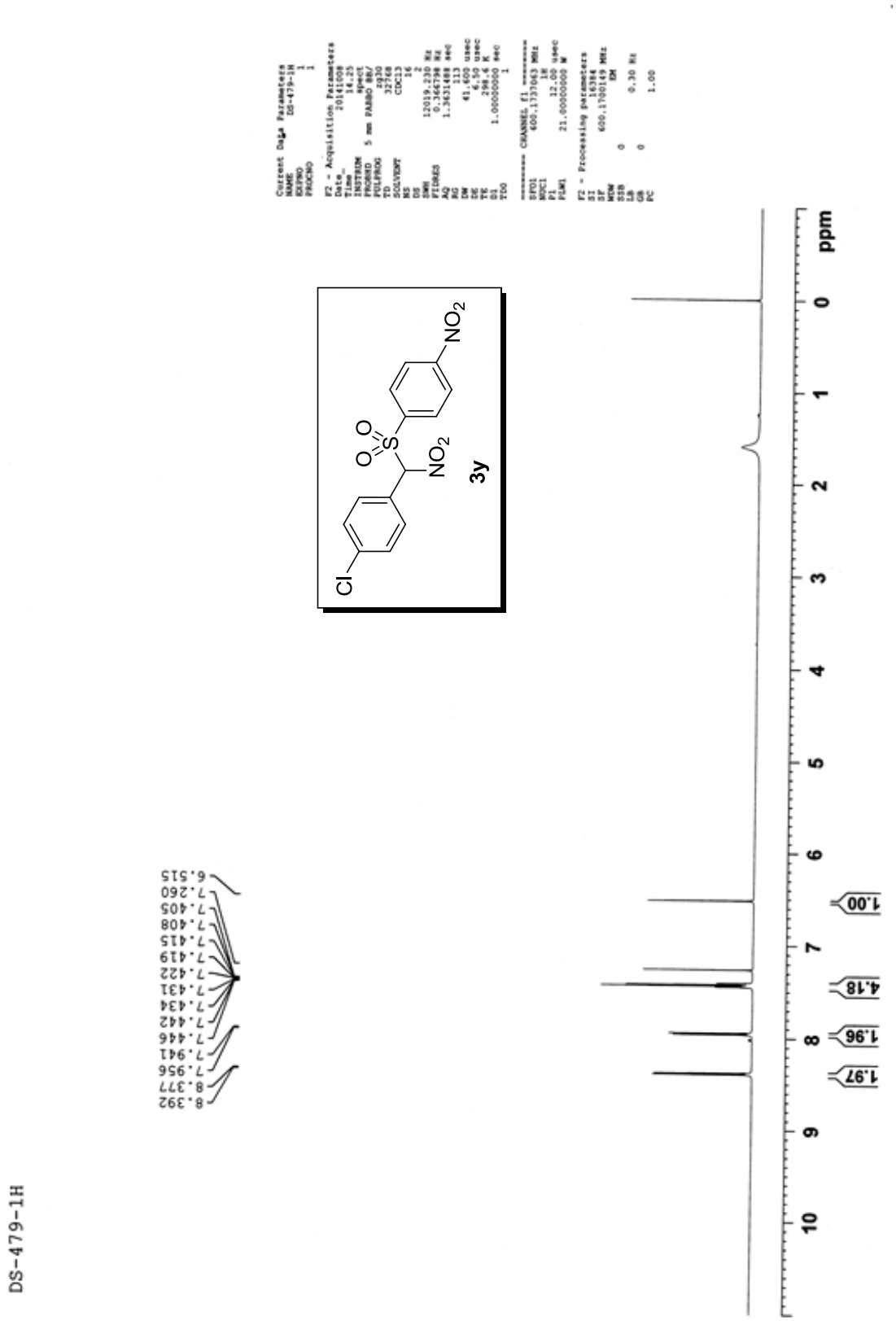
DS-479-1H
8.392
8.377
7.956
7.941
7.446
7.442
7.434
7.431
7.422
7.419
7.415
7.408
7.405
7.260
6.515
1.00
4.18
1.96
1.97
ppm
3y
Cl
NO2
NO2
S
O
O

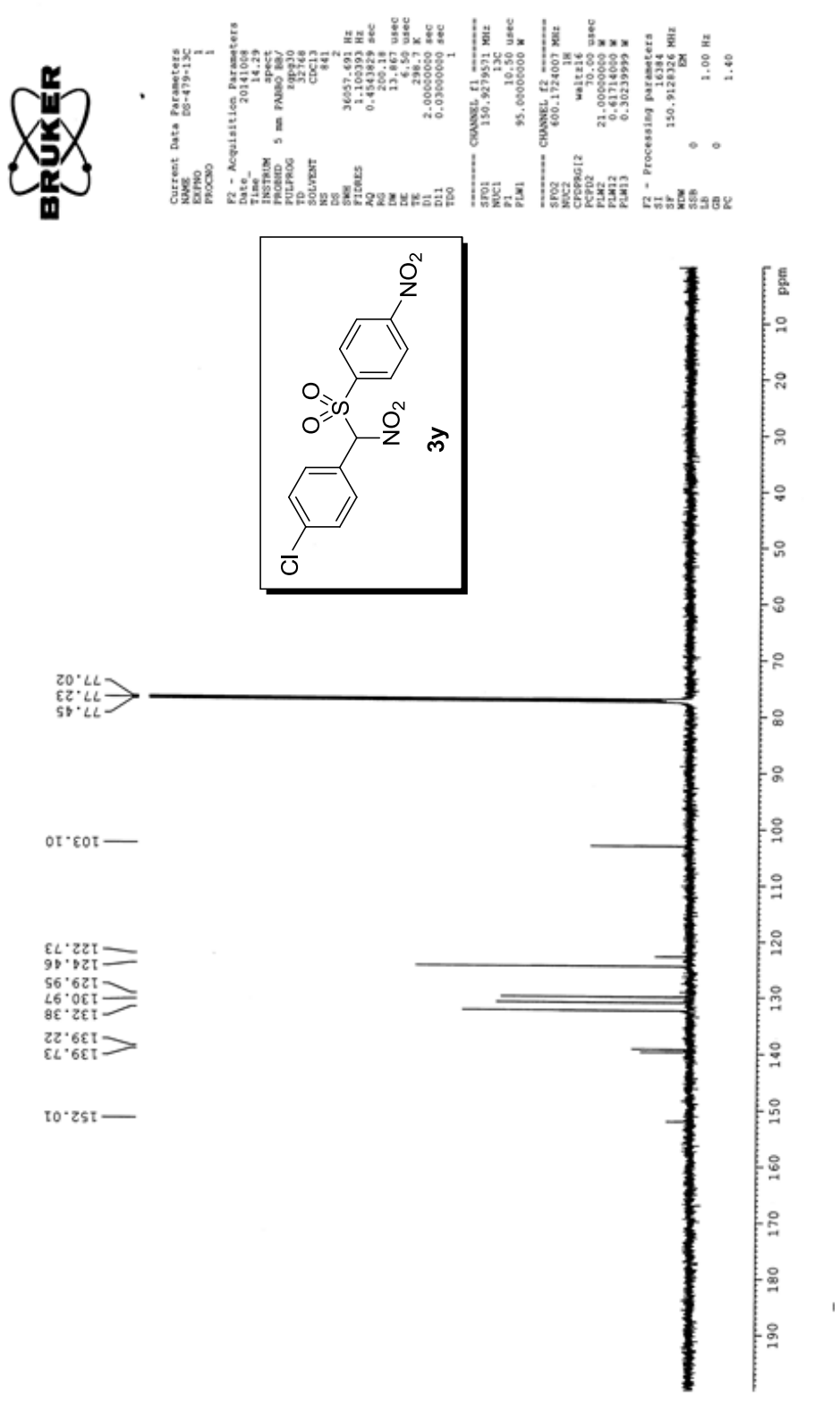
BRUKER
Current Data Parameters
NAME 85-479-13C
EXPNO 1
PROCNO 1
F2 - Acquisition Parameters
Date_ 20141004
Time 14.29
INSTRUM spect
PROBHD 5 mm PABBO BB/
PULPROG zgpg30
TD 32768
SOLVENT CDCl3
NS 641
DS 2
SWH 36057.691 Hz
FIDRES 1.100393 Hz
AQ 0.4543629 sec
RG 200.18
DW 13.867 usec
DE 6.50 usec
TE 298.7 K
D1 2.00000000 sec
D11 0.03000000 sec
TD0 1
CHANNEL f1
SFO1 150.9279571 MHz
NUC1 13C
P1 10.50 usec
PLW1 95.00000000 W
CHANNEL f2
SFO2 600.1724007 MHz
NUC2 1H
CPDPRG12 waltz16
PCPD2 70.00 usec
PLW2 21.00000000 W
PLW12 0.47116000 W
PLW13 0.30239999 W
F2 - Processing parameters
SI 16384
SF 150.9128326 MHz
WDW EM
SSB 0
LB 1.00 Hz
GB 0
PC 1.40
3y
77.02
77.23
77.45
103.10
122.73
124.46
129.95
130.97
132.38
139.22
139.73
152.01
ppm

Chapter II

Vanadium-Catalyzed *C-N* Cross-Dehydrogenative Coupling (CDC): Synthesis of Substituted Pyrazoles

Heterocyclic compounds are important structural motifs of several biologically active natural products[1] and, thus, attracted immense research interest in medicinal chemistry[2] as well as material sciences.[3] As a consequence, since more than a century, a vast majority of research work in organic community has been devoted for the construction of heterocyclic scaffold through carbon-carbon and carbon-heteroatom bond formations.[4-6] The recent advances in the transition-metal-catalyzed cross-coupling, cycloaddition and C-H activation methods are viable synthetic tools for the construction of heterocyclic compounds.[7] Among these, transition-metal-catalyzed oxidative C-H functionalization affords a powerful tool for regioselective carbon-carbon and carbon-heteroatom bond formation.[8] Transition-metals such as Rh, Ru, Pd and Cu have been significantly investigated for this purpose.[8] However, development of cost effective, simple, non-hazardous, mild and novel catalytic synthetic methodologies would be highly desirable. Vanadium is being non-toxic, readily available, cheap, having good catalytic activity and suitably positioned in electrochemical series.[9] Its exploration for the selective C-H functionalization via cross-dehydrogenative coupling,[10] employing air[11] as the oxidant under environmentally benign aqueous organic reaction conditions,[12] would be thus valuable. In this chapter, we describe an efficient protocol for the construction of pyrazole skeleton via C-H functionalization using V(IV) catalyst in aerobic condition at room temperature.

Out of various *N*-heterocycles, pyrazole has been used as scaffolds for synthesis of many blockbuster drugs.[13] Pyrazole derivatives have been shown to have significant pharmacological activities with respect to analgesic,[13b] antimicrobial,[13c] anti-cancer (COX-1 inhibitor SC-560),[13e] anti-viral (measles virus RdRp inhibitor AS-136A)[13h] and anti-inflammatory[13i] properties. In fact, pyrazole derivatives are present in many man made drugs including sildenafil (Viagra), celecoxib (Celebrex), rimonabant (Acomplia), and Fipronil (Figure 1).[14] In addition, the substituted pyrazoles find applications as bifunctional ligands for metal catalysis[15a] and are also present in various functional materials such as optical brighteners, ultraviolet stabilizers, etc.[15] Thus, the construction

of biologically and medicinally important pyrazole moiety by effective methods is of great interest in organic synthesis.[16]

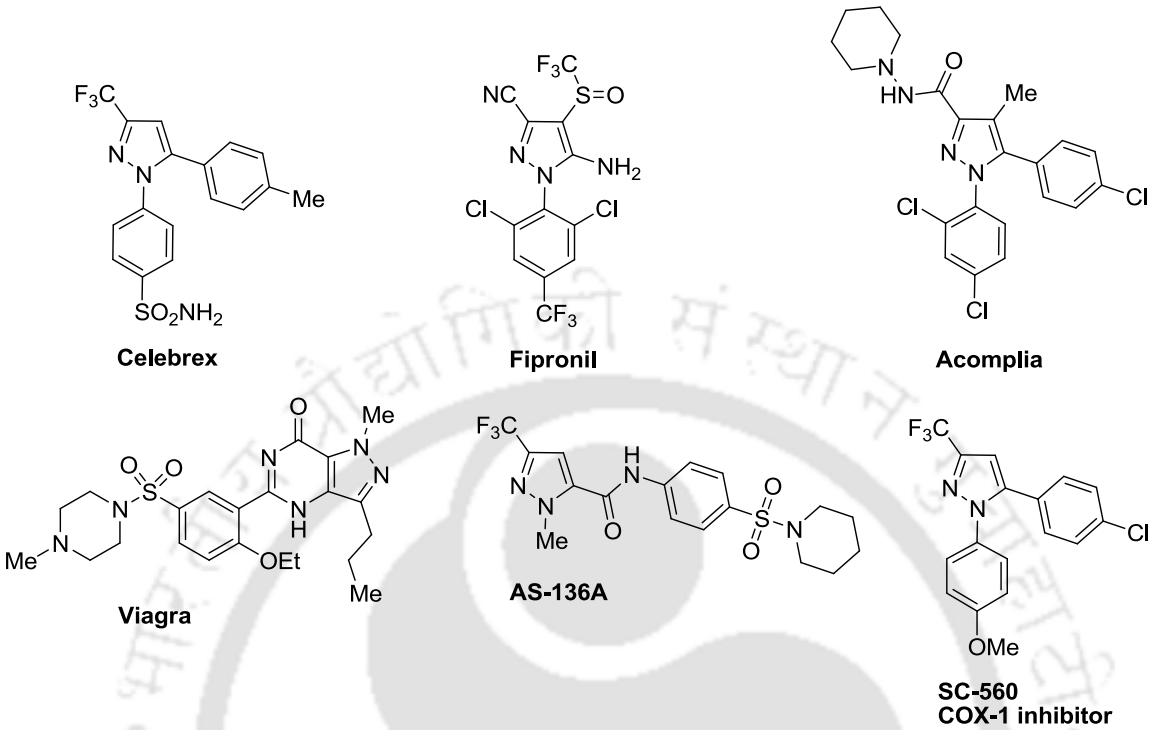

Figure 1. Examples of some medicinally active compounds

2.1 Strategies for the Synthesis of Pyrazoles

2.1.1 Classical Method

The traditional method used for the construction of pyrazole framework includes the condensation of 1,3-dicarbonyl compounds or their derivatives with hydrazine derivatives using acid catalyst (Scheme 1).[17] However, the lack of regiospecificity, narrow substrate scope and use of harsh reaction conditions such as involvement of strong acids in combination with high temperature are the disadvantages of this methods.

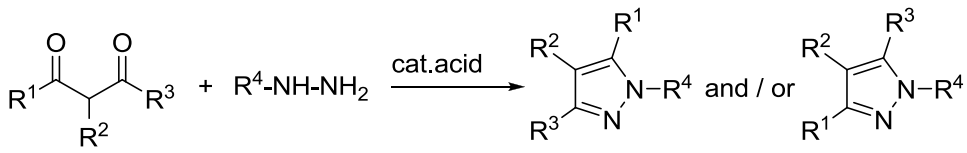

Scheme 1. Common Method of Synthesis of Substituted Pyrazoles

To overcome these drawbacks, immense efforts have thus been invested to develop more sustainable greener path for the synthesis of biologically important pyrazoles under relatively mild reaction condition. In this purpose, the 1,3-dipolar cycloaddition of diazoalkane, nitrilimine and sydnones as azomethine imine with alkene or alkyne, electrophilic cyclizations of *α,β*-alkynic hydrazones and multicomponent reaction have been used for the regioselective construction of pyrazoles scaffold. Furthermore, transition-metal-catalyzed cross-coupling method has also been used for the synthesis of functionalized pyrazoles from pre-existing pyrazoles containing precursors.

2.1.2 1,3-Dipolar Cycloadditions

1,3-Dipolar cycloaddition reactions are the valuable synthetic strategies for the synthesis of pyrazole scaffolds. These methods are highly regioselective compared to the classical cyclocondensation reaction between 1,3-diketones with hydrazines.

2.1.2.1 Diazoalkanes as 1,3-Dipoles

The 1,3-dipolar cycloaddition of diazo compounds with alkenes or alkynes are useful strategies for the construction of pyrazoles motifs. Aggarwal and co-workers reported the construction of pyrazoles skeleton in one-pot from diazo compounds (Scheme 2).[18a] Diazo compounds synthesized in situ from aldehydes and tosyl hydrazines, reacted with terminal alkynes and *N*-vinylimidazole via 1,3-dipolar cycloaddition to yield 3,5-disubstituted pyrazoles and 3-substituted pyrazoles.

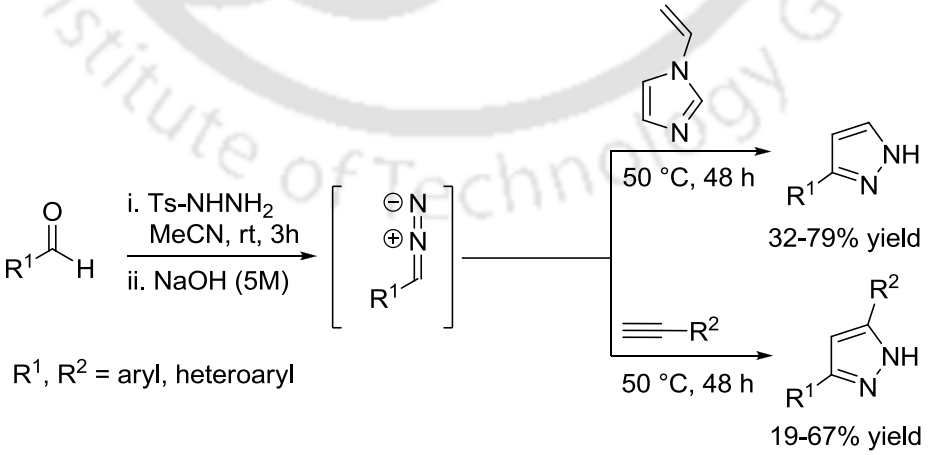

Scheme 2. Synthesis of Substituted Pyrazoles via 1,3-Dipolar Cycloaddition Reaction

1,3-Dipolar cycloaddition of diazocarbonyl compounds with alkynones or alkynoates is described using catalytic amount of $InCl_3$ in water at ambient temperature for the synthesis of pyrazoles (Scheme 3).[18b] The reaction involves 1,3-dipolar cycloaddition followed by hydrogen migration.

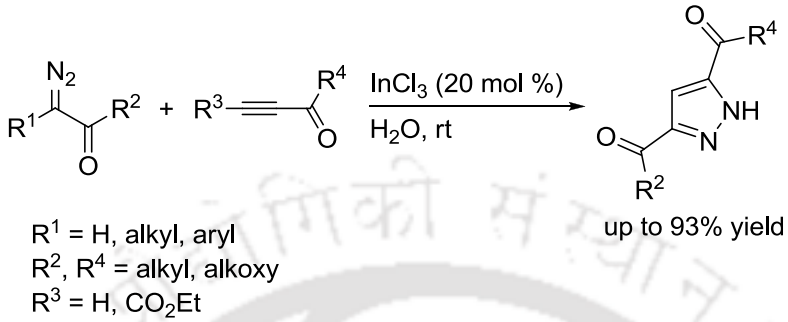

Scheme 3. In-Catalyzed Synthesis of Substituted Pyrazoles in Water

The synthesis of highly functionalized phosphonylpyrazoles is reported using the reaction of the anion of diethyl 1-diazomethylphosphonates with conjugated nitroalkenes at room temperature (Scheme 4).[18c] Diethyl 1-diazomethylphosphonate or its corresponding anion is synthesized in situ from diethyl 1-diazo-2-oxopropylphosphonate in presence of base (NaOEt). This protocol is used for phosphonylpyrazoles synthesis by the spontaneous elimination of nitro group. This methodology has been utilized for the synthesis of nitropyrazoles by using *α*-bromonitroalkenes.

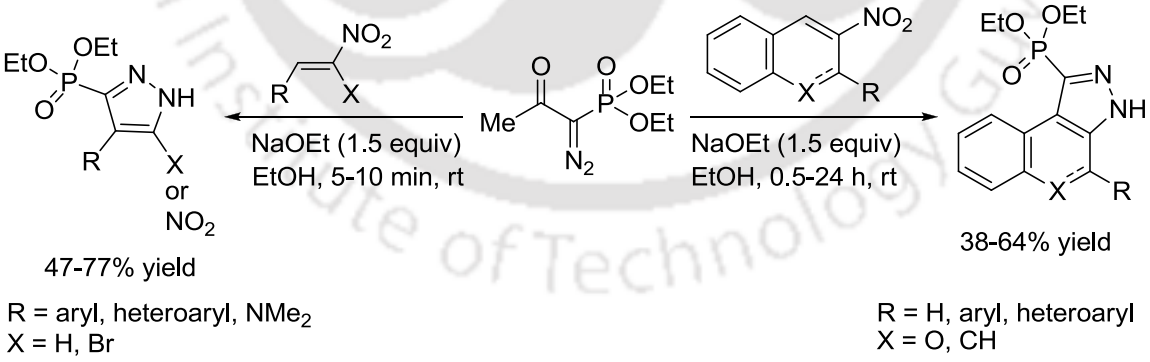

Scheme 4. Base-Mediated One-Pot Synthesis of Phosphonylpyrazoles

Cu-mediated the synthesis of substituted pyrazoles is accomplished through inverse-electron-demand cycloaddition of in situ generated copper acetylides with diazocarbonyl compounds (Scheme 5).[18d]

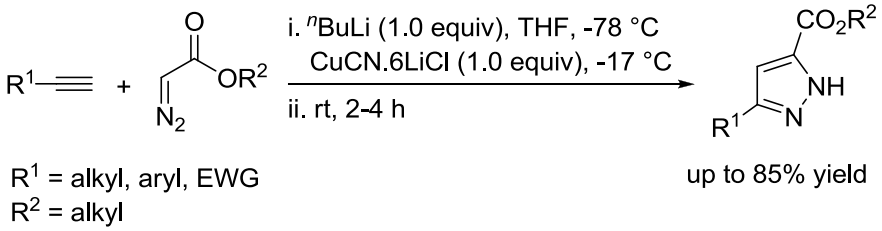

Scheme 5. Cu-Mediated Synthesis of 3,5-Disubstituted Pyrazoles

The synthesis of functionalized pyrazoles is achieved by the 1,3-dipolar cycloaddition of α-diazocarbonyls compound with ethyl propiolate and diethyl acetylene dicarboxylate (Scheme 6).[18e] This method is scalable up to multi gram synthesis of pyrazoles.

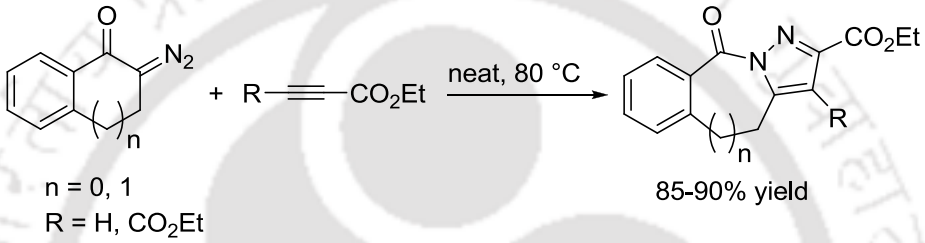

Scheme 6. Synthesis of Pyrazoles under Solvent-Free condition

Substituted pyrazole derivatives have been synthesized under catalyst-free tandem cycloaddition of nitroalkene with ethyl diazoacetate at ambient condition (Scheme 7).[18f]

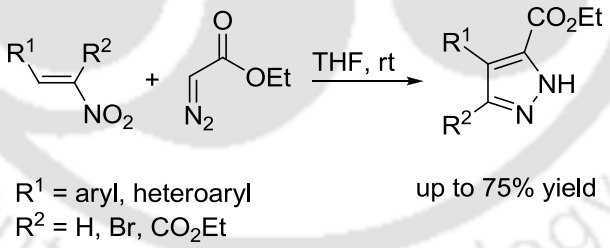

Scheme 7. Catalyst-Free One-Pot Synthesis of Substituted Pyrazoles

2.1.2.2 Nitrilimines as 1,3-Dipoles

1,3-Dipolar cycloadditions between nitrilimines and alkene or alkyne as dipolarophiles are the useful strategy for the construction of substituted pyrazoles. Nitrilimines are generated in situ from hydrazonoyl halides in presence of base. For example, McCarthy and co-workers reported the cycloaddition of nitrilimines with resin-bound enamines for

the solid phase regioselective synthesis of substituted pyrazoles high purity (Scheme 8).[19a] This protocol involves pyrazoles synthesis through cleavage of the resin-bound pyrazoline intermediate under mild acidic condition.

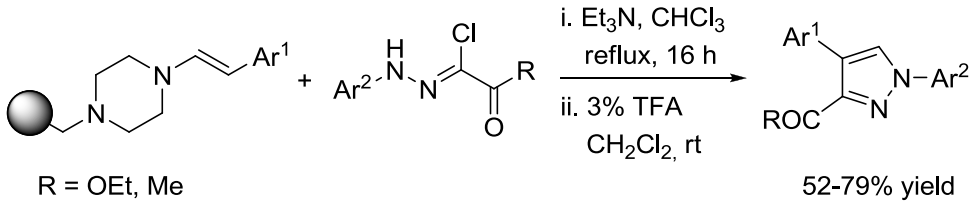

Scheme 8. Solid Phase Synthesis of Substituted Pyrazoles

Conti and co-workers demonstrated the preparation of synthetically demanding *N*-phenyl-5-substituted-3-dimethyoxyphosphono-pyrazoles via 1,3-dipolar cycloaddition of nitrilimine with monosubstituted alkynes/alkenes (Scheme 9).[19b] Nitrilimines are formed in situ from the dehydrohalogenation of hydrazonoyl bromides using sodium bicarbonate as a base.

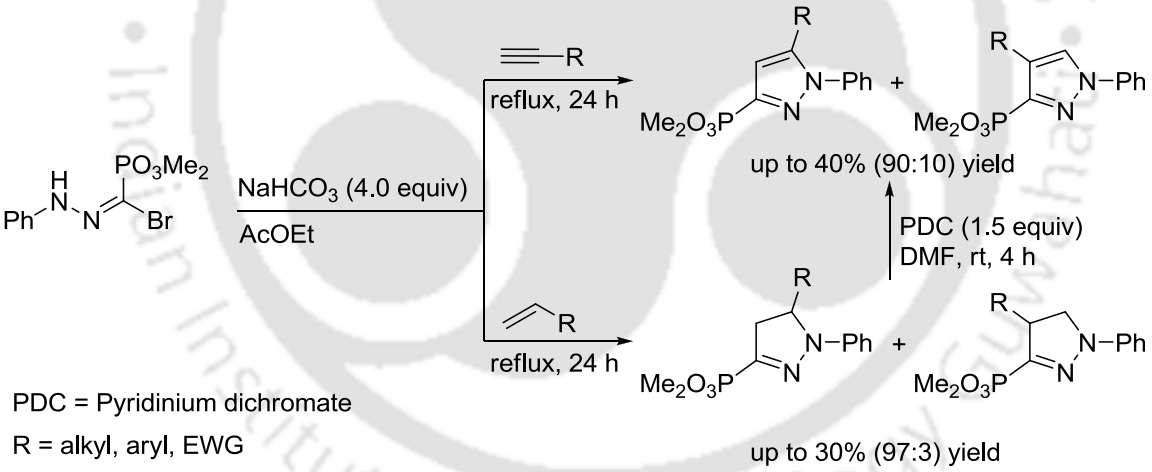

Scheme 9. 1,3-Dipolar Cycloaddition of Nitrilimine with Alkynes/Alkenes

Tetrasubstituted pyrazoles have been synthesized by the cycloaddition of nitrilimine generated in situ from hydrazonoyl bromides with active methylene compounds (Scheme 10).[19c]

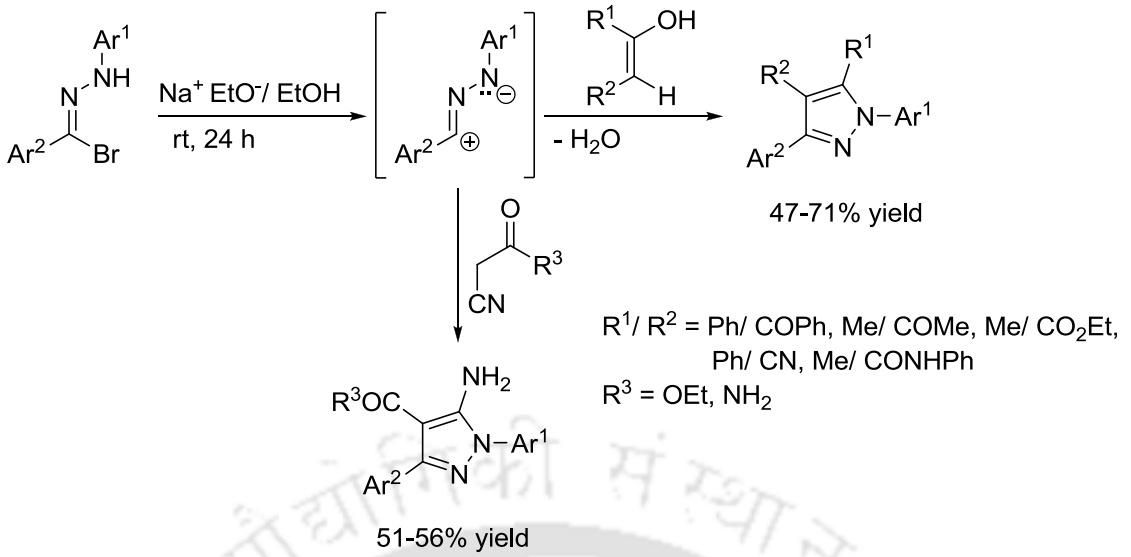

Scheme 10. Synthesis of Tetrasubstituted Pyrazoles

Cycloaddition of nitrilimines with *β*-oxophosphonates is reported for the synthesis of 1,3,5-trisubstituted pyrazoles (Scheme 11).[19d] The functional group compatibility is the salient feature of this protocol.

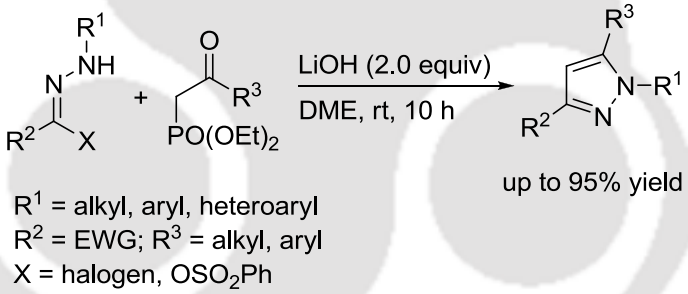

Scheme 11. Synthesis of 1,3,5-Trisubstituted Pyrazoles from *β*-Oxophosphonates

2.1.2.3 Sydnones as Azomethine Imine-type 1,3-Dipoles

Sydnones are mesoionic compounds. They are considered as azomethine imine treated as a 1,3-dipoles, which undergoes cycloaddition with electron deficient alkynes to form biologically important pyrazoles scaffold via the elimination of carbon dioxide. Highly substituted unsymmetrical *α,β*-acetylenic ketone containing nitrofuran moiety (X = O) undergoes cycloaddition with 3-arylsydnones to afford substituted pyrazole derivatives in high yields (Scheme 12).[20a] Similarly, *α,β*-acetylenic ketone containing nitrothiophene moiety (X = S) undergoes same reaction path way to give the corresponding substituted pyrazoles. Alkyne partners used as a dipolarophile in this reaction.

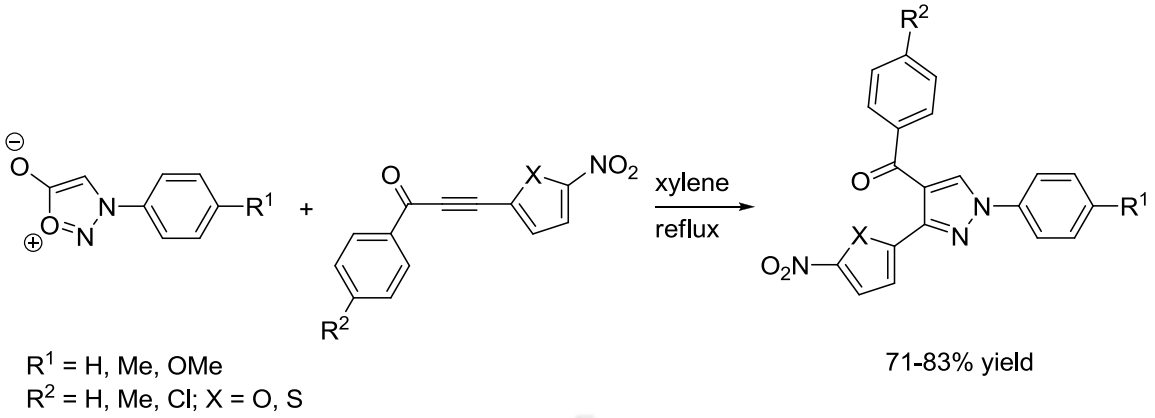

Scheme 12. Regiospecific Synthesis of 1,3,4-Trisubstituted Pyrazoles from *α,β*-Acetylenic Ketones

Cycloaddition of 4-trifluoromethylsydnones with alkynes have been demonstrated for the synthesis of 5-trifluoromethyl pyrazoles in good yields (Scheme 13).[20b] This protocol has been used for the synthesis of herbicide fluazolate as a bioactive fluorinated pyrazole.

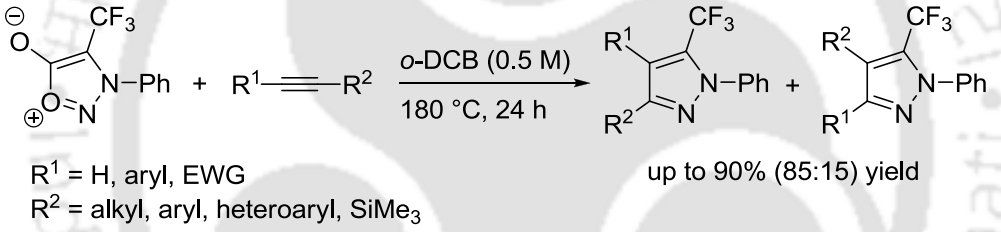

Scheme 13. Synthesis of 5-Trifluoromethyl Pyrazoles

2.1.3 Electrophilic Cyclization

Electrophilic cyclization of functionally substituted alkynes is a useful strategy for the synthesis of pyrazoles. CuI-mediated electrophilic cyclization of *α,β*-alkynic hydrazones have been investigated for the preparation of pyrazoles in good yields (Scheme 14).[21a] *α,β*-Alkynic hydrazones are synthesized by the condensation of hydrazines with propargyl aldehydes or ketones. The reaction appears to be simple and general for the synthesis of varied substituted pyrazoles.

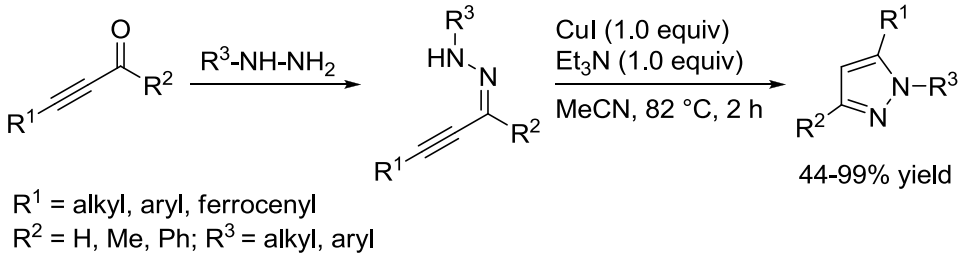

Scheme 14. Cu-Mediated Synthesis of Substituted Pyrazoles via electrophilic cyclization

Highly substituted fluoropyrazoles have been synthesized by Au-catalyzed tandem aminofluorination of alkyne in presence of selectfluor at ambient temperature (Scheme 15).[21b] This protocol is the first report for the synthesis of fluorinated pyrazoles using Au catalyst.

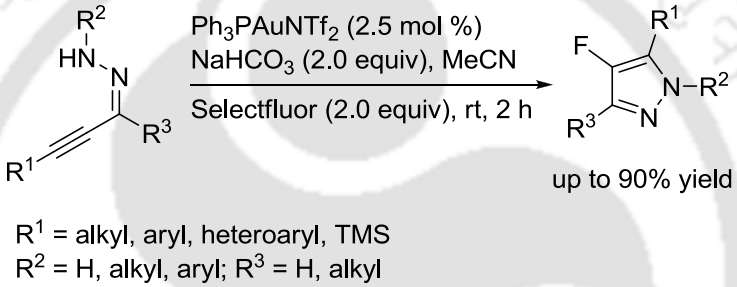

Scheme 15. Au-Catalyzed Synthesis of Fluorinated Pyrazoles

Our group showed the synthesis of tetrasubstituted pyrazoles via Cu-catalyzed cascade electrophilic cyclization of nitro substituted 1,3-enynes with hydrazines at room temperature (Scheme 16).[21c]

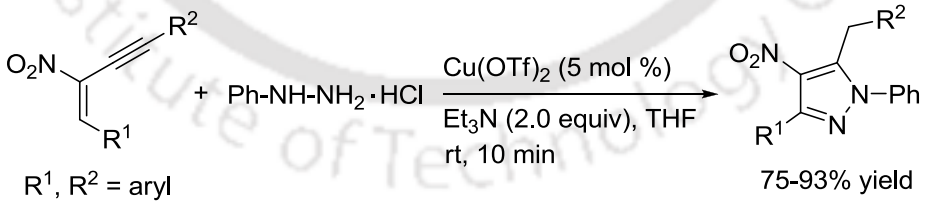

Scheme 16. Cu-Catalyzed Synthesis of Nitro Pyrazoles

Cycloisomerization of *α,β*-acetylenic hydrazones generated from reaction of acetylenic ketones with hydrazines have been accomplished for the synthesis of pyrazole derivatives in presence of Au catalyst (Scheme 17).[21d]

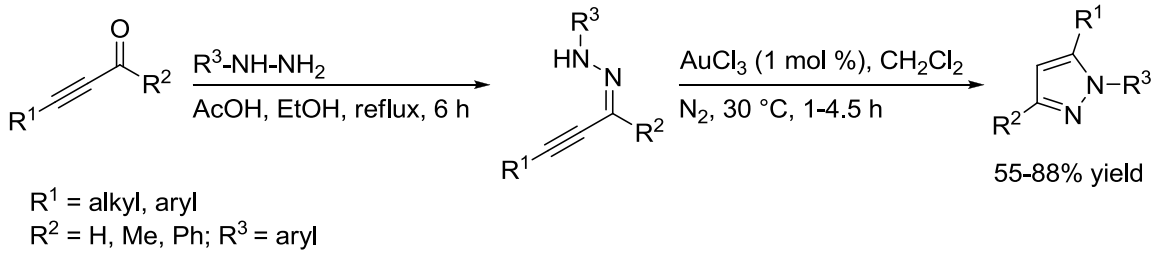

Scheme 17. Au-Catalyzed Synthesis of Trisubstituted Pyrazoles from *α,β*-acetylenic hydrazones

2.1.4 Multicomponent Reactions

Multicomponent reactions (MCRs) are desirable methods for the construction of heterocyclic compounds because they can form two or more bonds in single step without isolating the intermediate by combining more than two starting materials. For instance, Pyrazole derivatives could be prepared by a Pd-catalyzed four-component coupling of a terminal alkyne with hydrazine and carbon monoxide in presence of aryl iodide under an ambient pressure of carbon monoxide at room temperature in an aqueous solvent system (Scheme 18).[22a]

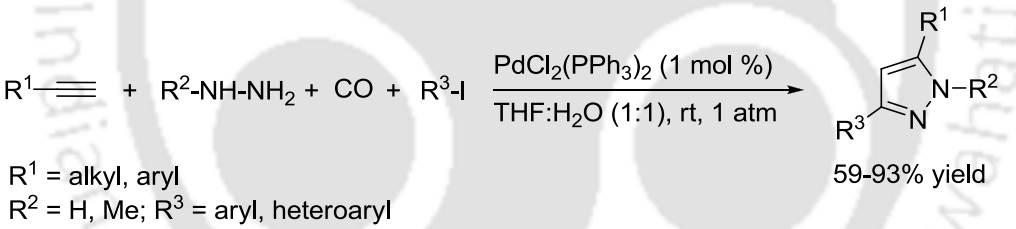

Scheme 18. Pd-Catalyzed Multicomponent Reaction for the Synthesis of Substituted Pyrazoles

Ma and co-workers reported Cu-mediated synthesis of tetrasubstituted pyrazoles from three component reaction of 2,3-allenoates or 2-alkynoates, amines and nitriles (Scheme 19).[22b] The reaction proceeds via tandem conjugate addition, 1,2-addition and *N-N* bond formation process from readily available starting materials.

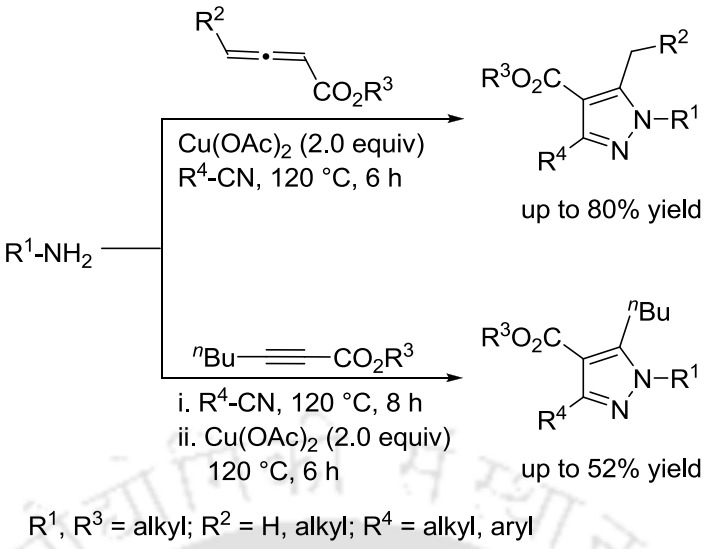

Scheme 19. Cu-Mediated Synthesis of Tetrasubstituted Pyrazoles via Tandem Reaction

2.1.5 Cross-Coupling Reactions

Transition-metal-catalyzed cross-coupling reactions are straightforward methods for the synthesis of heterocyclic compounds via carbon-carbon and carbon-nitrogen bonds formations.

2.1.5.1 Cu-Catalyzed Synthesis of Pyrazoles

Synthesis of *N*-aryl pyrazoles via carbon-nitrogen bond formation in presence of low cost and readily available Cu salt is a convenient method. Cu-diamine-catalyzed cross-coupling of pyrazoles has been developed with aryl iodides or aryl bromides (Scheme 20).[23a] This method has been applied to prepare varied pyrazole derivatives having elcron-donating and electron-withdrawing groups.

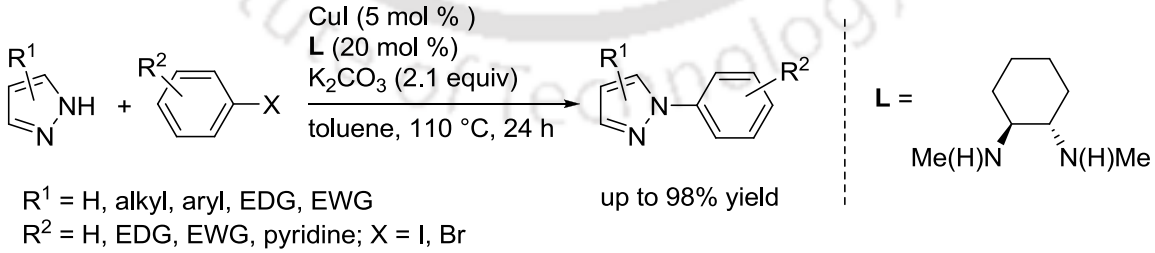

Scheme 20. Cu-Diamine-Catalyzed Synthesis of *N*-Arylation of Pyrazoles

Ila and co-workers reported the synthesis of pyrazolo[1,5-*a*]benzimidazoles via Cu-catalyzed intramolecular *C*−*N* bond formation of 5-(2-bromoanilino)-1*H*-pyrazole

precursors (Scheme 21).[23b] Electron-donating or electron-withdrawing group at the 3-position of pyrazoles are compatible to furnish the pyrazolo[1,5-*a*]benzimidazoles.

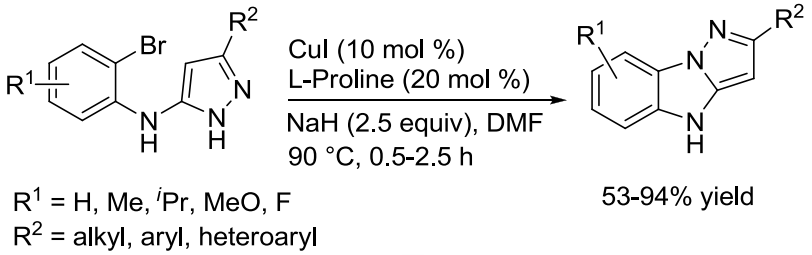

Scheme 21. Cu-Catalyzed Intramolecular Synthesis of Pyrazolo[1,5-*a*]benzimidazoles

2.1.5.2 Pd-Catalyzed Synthesis of Pyrazoles

Pd-catalyzed carbon-carbon cross-coupling reaction is a powerful tool for the synthesis of *N*-aryl pyrazoles. The synthesis of aryl pyrazoles from pyrazole triflates has been performed by Dvorak and co-workers (Scheme 22).[24a] Pyrazole triflates react with aryl boronic acids via Pd-catalyzed Suzuki cross-coupling reaction to form corresponding aryl pyrazoles. Pyrazole triflates could be prepared from corresponding pyrazolones and *N*-phenyl-bis(trifluoromethanesulfonamide).

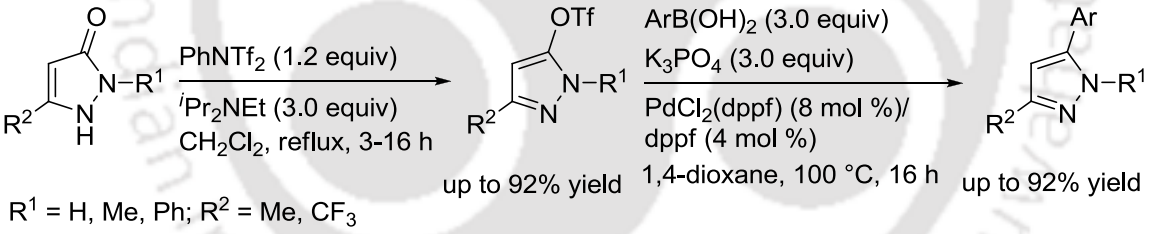

Scheme 22. Pd-Catalyzed Synthesis of *N*-Aryl Pyrazoles

Pd-catalyzed microwave assisted Stille cross-coupling has been demonstrated for the construction of 1,4,5-trisubstituted-3-trifluoromethylpyrazoles from 1,5-substituted-4-bromo-3-trifluoromethylpyrazoles and allylstannane or arylstannanes (Scheme 23).[24b]

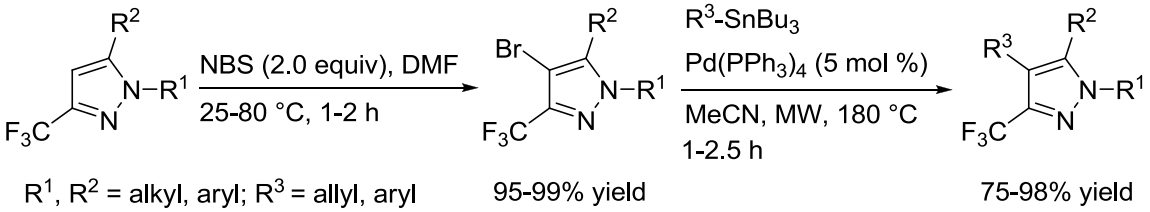

Scheme 23. Pd-Catalyzed Stille cross-coupling to the Synthesis of Substituted Pyrazoles

2.1.6 C-H Functionalization Reactions

Recent advances in the functionalization of C-H bonds through transition-metal-catalysts are valuable atom-economical synthetic tool for the synthesis of pyrazole derivatives. For example, Rao and co-workers showed the synthesis of tri- and tetrasubstituted pyrazoles by aerobic oxidative *C-N* bond formation in presence of Ru catalyst (Scheme 24).[25a] Dioxygen has been incorporated as an oxidant for this transformation.

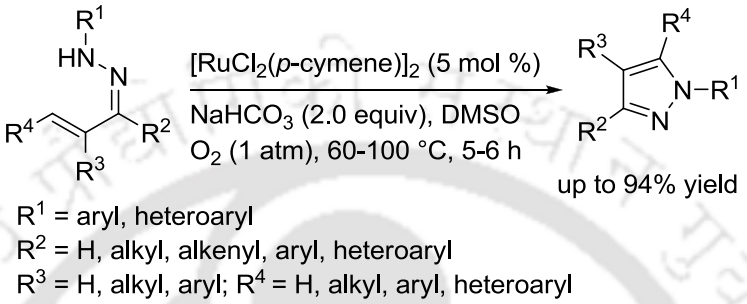

Scheme 24. Ru-Catalyzed Synthesis of Substituted Pyrazoles via C-H Functionalization

Jiang and co-workers reported Cu-catalyzed synthesis of trisubstituted pyrazoles via C-H functionalization followed by *C-N* bond formation (Scheme 25).[25b]

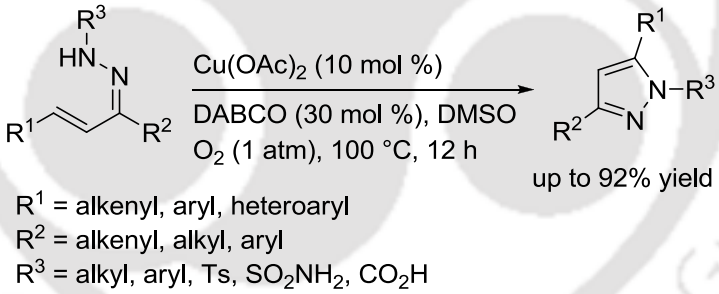

Scheme 25. Cu-Catalyzed C-H Functionalization of Alkenyl Hydrazones

2.2 Present Study

Herein we present the synthesis of trisubstituted pyrazoles using V(IV) catalyst via *C-N* cross-dehydrogenative coupling of alkenyl hydrazones at room temperature.

Synthesis of 4-Alkyl/Aryl Substituted *α,β*-Unsaturated Methyl Ketones (1a-q). *α,β*-Unsaturated methyl ketones were prepared from aldehydes and acetone in presence of aqueous solution of NaOH (10%) at 40 ^{o}C (Scheme 26). [25a]

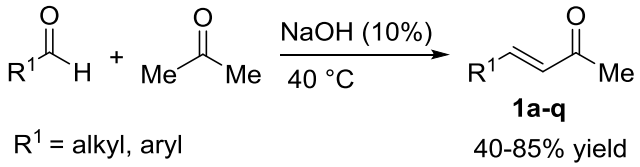

Scheme 26. Synthesis of *α,β*-Unsaturated Ketones

Synthesis of (*E*)-1-phenyl-3-(3,4,5-trimethoxyphenyl)prop-2-en-1-one (1r). (*E*)-1-Phenyl-3-(3,4,5-trimethoxyphenyl)prop-2-en-1-one was prepared from aldehyde and acetophenone in the presence of NaOH in ethanol-water (1:1) at room temperature (Scheme 27).[25a]

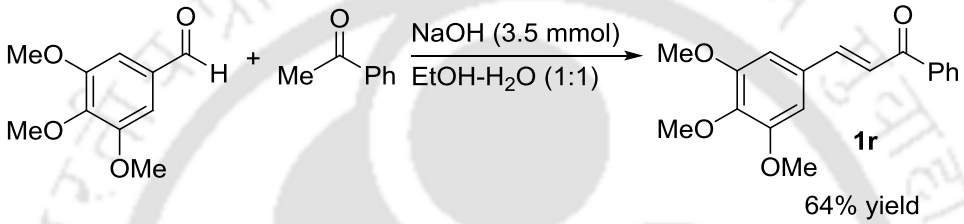

Scheme 27. Synthesis of (*E*)-1-phenyl-3-(3,4,5-trimethoxyphenyl)prop-2-en-1-one

Synthesis of (*E*)-1,1,1-trifluoro-4-p-tolylbut-3-en-2-one (1s). The titled precursor **1s** was prepared from 4-methylbenzaldehyde and trifluoroacetone in dry toluene at 0 ^{o}C to room temperature (Scheme 28).[25a]

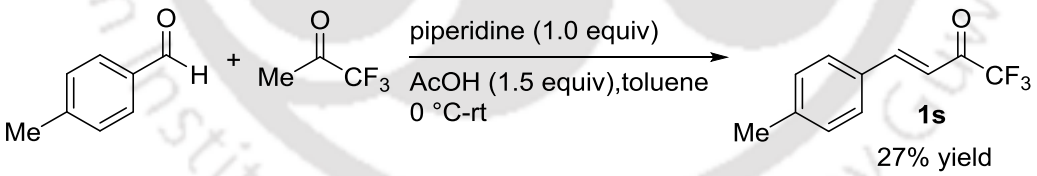

Scheme 28. Synthesis of (*E*)-1,1,1-trifluoro-4-*p*-tolylbut-3-en-2-one

Synthesis of Aryl Hydrazine Hydrochlorides (2b-f). Scheme 29 shows the synthesis of aryl hydrazine hydrochlorides.[26] Substituted anilines first reacted with $NaNO_2$/HCl at 0 °C to form aryl diazonium salts, which was then treated with $SnCl_2 \cdot 2H_2O$/HCl at 0 °C to afford the corresponding aryl hydrazine salts.

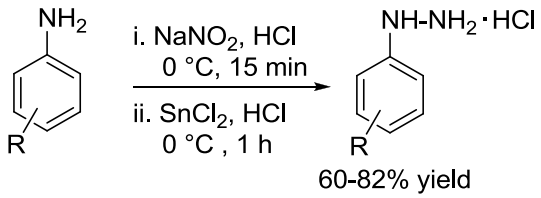

Scheme 29. Synthesis of Aryl hydrazine Hydrochlorides

The Synthesis of Pyrazoles: First, we optimized the reaction condition using *α,β*-unsaturated ketone **1a** and phenylhydrazine hydrochloride **2a** as model substrates with vanadium catalysts (Table 1). Gratifyingly, the reaction readily occurred to provide the functionalized pyrazole **3a** in 70% yield when the substrates **1a** and **2a** were stirred with NaOAc in a 1:1 mixture of toluene:H_2O at 60 °C for 1 h followed by addition of 20 mol % $VOSO_4$ and stirring at room temperature for 18 h using air as an oxidant (entry 1). Subsequent screening of $VO(acac)_2$ and V_2O_5 as the catalysts produced the target heterocycle **3a** in 55 and 54% yield, respectively (entries 2 and 3). However, lowering the quantity of $VOSO_4$ to 5 mol % led to an increase in the yield to 73% (entries 4-5). The reaction under a N_2 atmosphere provided **3a** in trace amount (entry 6). Control experiment confirmed that in the absence of vanadium catalyst the target heterocycle **3a** was not formed (entry 7).

Having the optimal reaction conditions, the scope of the procedure was explored. The reaction of a series of methyl alkenyl ketones **1b-p** was screened with phenylhydrazine **2a** (Table 2). The substrate **1b** underwent reaction to afford **3b** in 48% yield. The reactions of substrates **1c-j** bearing substituted aryl rings with 2-bromo, 2-methoxy, 2-methyl, 4-bromo, 4-cyano, 4-fluoro, 4-methyl and 4-methyl carboxylate functionalities produced the corresponding pyrazoles **3c-j** in 38-66% yields, while **1k-l** having 2,4-dimethoxy and 3,4,5-trimethoxy substituents in the aryl ring underwent reaction to furnish **3k-l** in good yields. In addition, the reaction of **1m-p** bearing cyclohexyl, isobutyl, sec-butyl and isopropyl substituents in the alkenyl position occurred to furnish the corresponding pyrazoles **3m-p** in 54-64% yields. Recrystallization of pyrazoles product **3a** from CH_3CN gave a single crystal whose structure was determined by X-ray analysis (Figure 2).

Table 1: Optimization of the Reaction Condition[a]

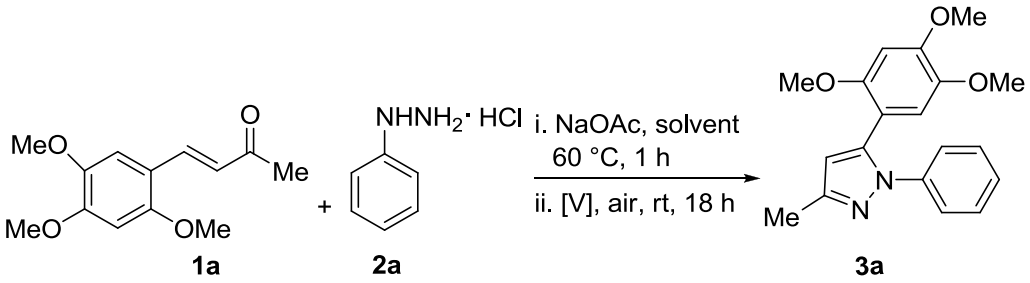

Entry	[V] (mol %)	Solvent	Yield (%)[b,c]
1	$VOSO_4$ (20)	toluene-H_2O (1:1)	70
2	$VO(acac)_2$ (20)	toluene-H_2O (1:1)	55
3	V_2O_5 (20)	toluene-H_2O (1:1)	54
4	$VOSO_4$ (10)	toluene-H_2O (1:1)	72
5	**$VOSO_4$ (5)**	**toluene-H_2O (1:1)**	**73**
6	$VOSO_4$ (5)	toluene-H_2O (1:1)	trace[d]
7	-	toluene-H_2O (1:1)	n.o.

[a] Reaction conditions: **1a** (1.0 mmol), **2a** (1.2 mmol), NaOAc (2.9 mmol), toluene:H_2O (1:1, 3 mL), 60 ^oC, 1 h; [V], rt, 18 h, air. [b] Isolated yield. [c] Accompanied ~10% unreacted **1a** and **2a**. [d] N_2 used. n. o. = not observed.

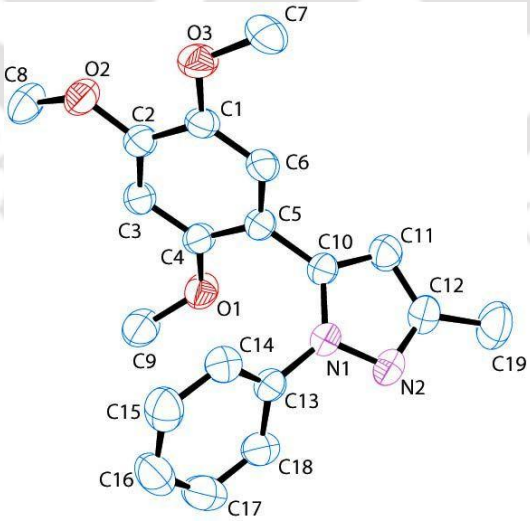

Figure 2. ORTEP diagram of 3-Methyl-1-phenyl-5-(2,4,5-trimethoxyphenyl)-1*H*-pyrazole **3a** with 50% ellipsoid. H-Atoms are omitted for clarity (CCDC 949193).

Table 2. Reaction of Methyl Alkenyl Ketones **1b-p** with Phenylhydrazine **2a**[a-c]

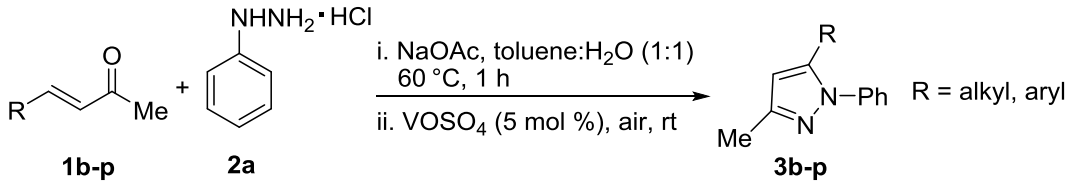

Entry	Methyl alkenyl ketone	Time (h)	Product	Yield (%)[b]
1	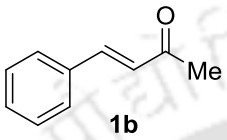 **1b**	17	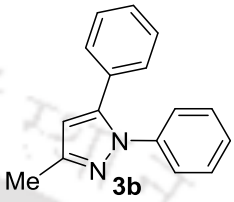 **3b**	48
2	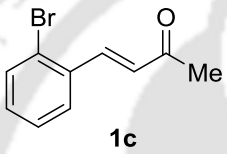 **1c**	20	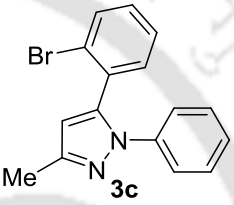 **3c**	45
3	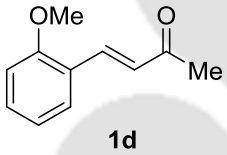 **1d**	18	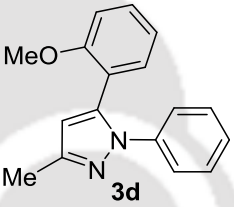 **3d**	66
4	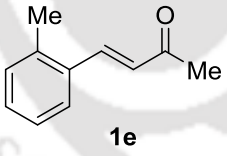 **1e**	18	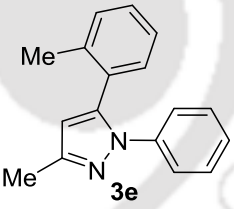 **3e**	53
5	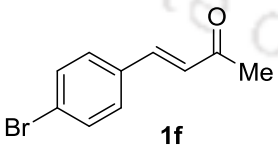 **1f**	17	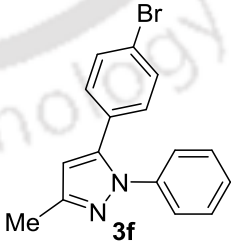 **3f**	41
6	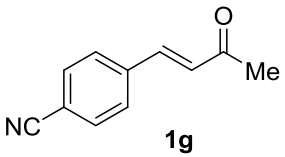 **1g**	21	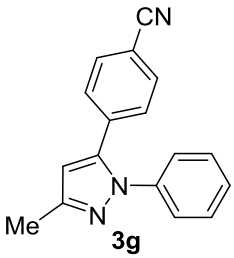 **3g**	38

Table 2 continues.....

7	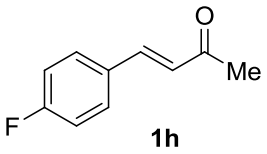 **1h**	24	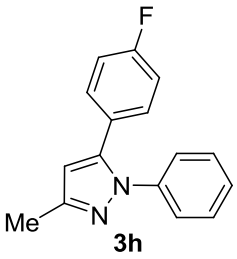 **3h**	39
8	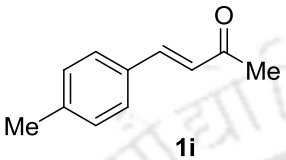 **1i**	19	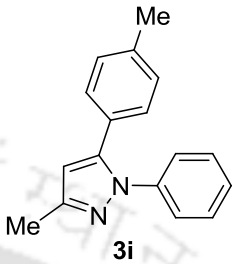 **3i**	62
9	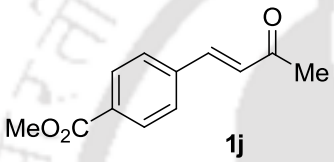 **1j**	19	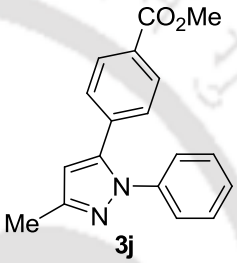 **3j**	66
10	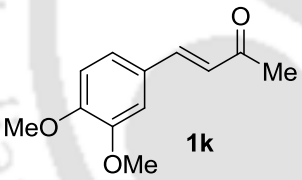 **1k**	19	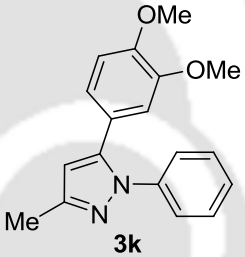 **3k**	59
11	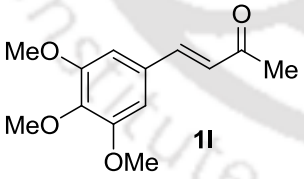 **1l**	17	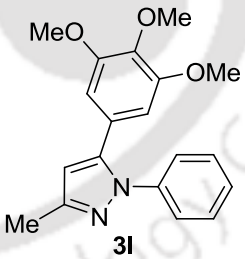 **3l**	68
12	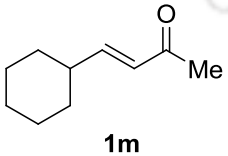 **1m**	17	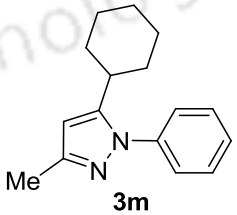 **3m**	62
13	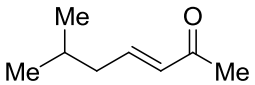 **1n**	19	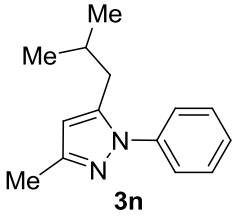 **3n**	54

Table 2 continues.....

14	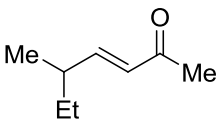 **1o**	19	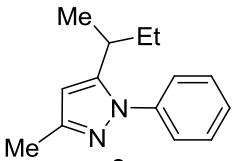 **3o**	58
15	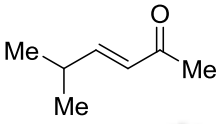 **1p**	18	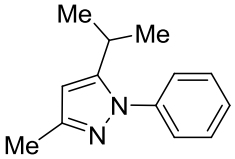 **3p**	64

[a] Reaction conditions: **1b-p** (1.0 mmol), **2a** (1.2 mmol), NaOAc (2.9 mmol) toluene:H_2O (1:1, 3 mL), 60 ^oC, 1 h; $VOSO_4$ (0.05 mmol), rt, air. [b] Isolated yield. [c] Accompanied ~5-10% unreacted **1b-p** and **2a**.

Next, the utility of the protocol was extended to the reaction of methyl alkenyl ketones **1a-b**, **1i**, **1f**, **1l-m** and **1q** with different aryl hydrazines **2b-e** (Table 3). Ketones **1i** and **1m** underwent reaction with (4-bromophenyl)hydrazine **2b** to give pyrazoles **3q** and **3r** in 74 and 61% yields, respectively, while **1b**, **1q** and **1l** with (4-chlorophenyl)hydrazine **2c** produced the desired pyrazole derivatives **3s-u** in 48-71% yields. The reaction of the ketone **1i** with (4-methoxyphenyl)hydrazine **2d** gave **3v** in 68% yield, whereas **1f** and **1a** with (2,4-dichlorophenyl)hydrazine **2e** furnished pyrazoles **3w** and **3x** in 58 and 63% yields, respectively. Furthermore, the reaction of the chalcone **1r** with **2a** produced pyrazole **3y** in 72% yield (Scheme 30), whereas trifluoromethyl ketone with *p*-tolyl substituent in the alkenyl position **1s** underwent reaction with hydrazine **2f** to produce celebrex **3z** in 45% yield. These results suggest that this procedure can be employed for the reactions of a broad range of substrates to afford diverse functionalized pyrazoles in good yields.

Gram-Scale Synthesis. To reveal the scalability of the reaction, the reaction of **1a** with **2a** was also studied in gram-scale as a representative example (Scheme 31). The reaction took place readily to produce **3a** in 65% yield.

Table 3. Reaction of Methyl Alkenyl Ketones with Different Aryl Hydrazines **2b-e**[a-c]

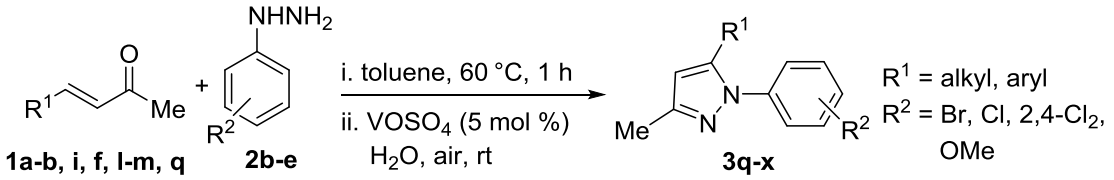

1a-b, i, f, l-m, q 2b-e 3q-x

Entry	Methyl alkenyl ketone	Hydrazine	Time (h)	Product	Yield (%)[b]
1	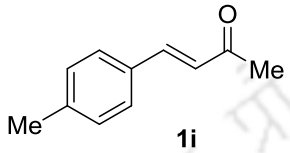 **1i**	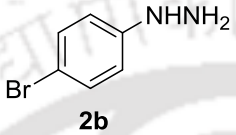 **2b**	20	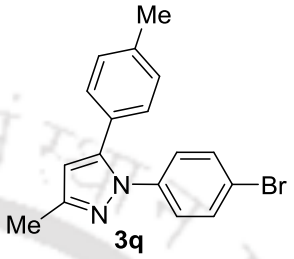 **3q**	74
2	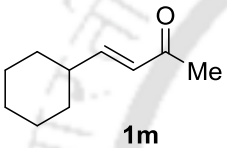 **1m**	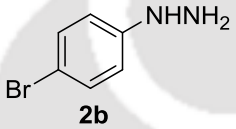 **2b**	19	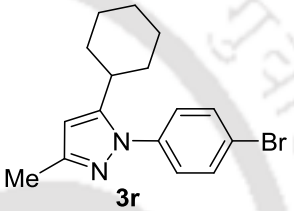 **3r**	61
3	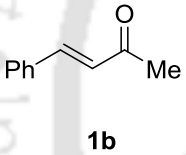 **1b**	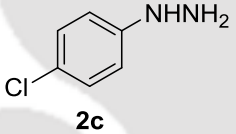 **2c**	16	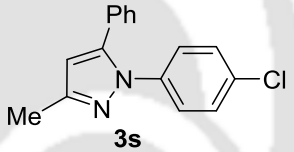 **3s**	71
4	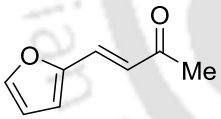 **1q**	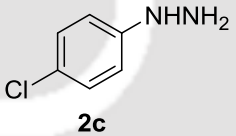 **2c**	19	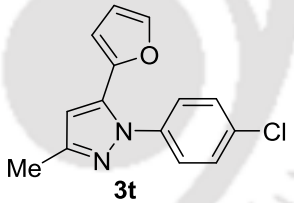 **3t**	60
5	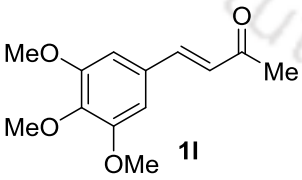 **1l**	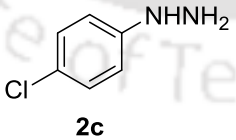 **2c**	18	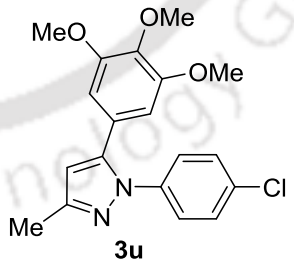 **3u**	48
6	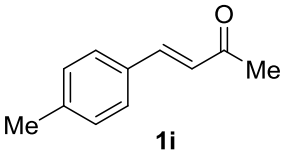 **1i**	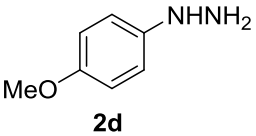 **2d**	17	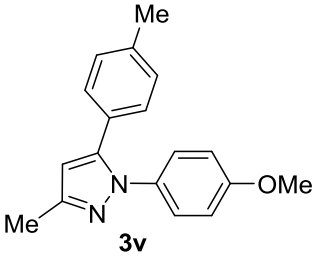 **3v**	68

Table 3 continues.....

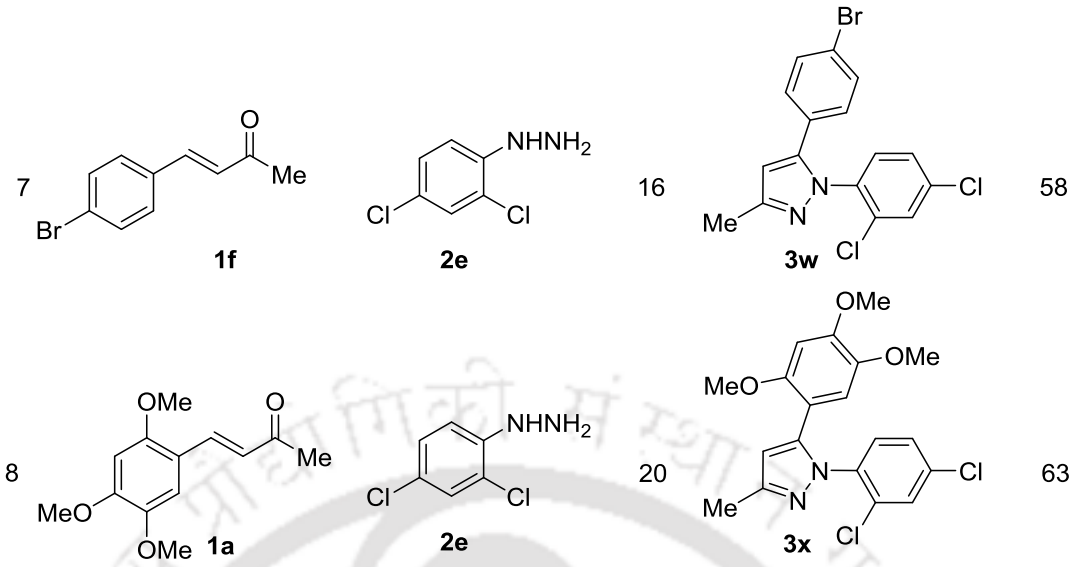

[a] Reaction conditions: ketone (1.0 mmol), aryl hydrazines **2b-e** (1.2 mmol), toluene (1.5 mL), 60 °C, 1 h; $VOSO_4$ (0.05 mmol), H_2O (1.5 mL), rt, air. [b] Isolated yield. [c] Accompanied ~5-10% unreacted substrates.

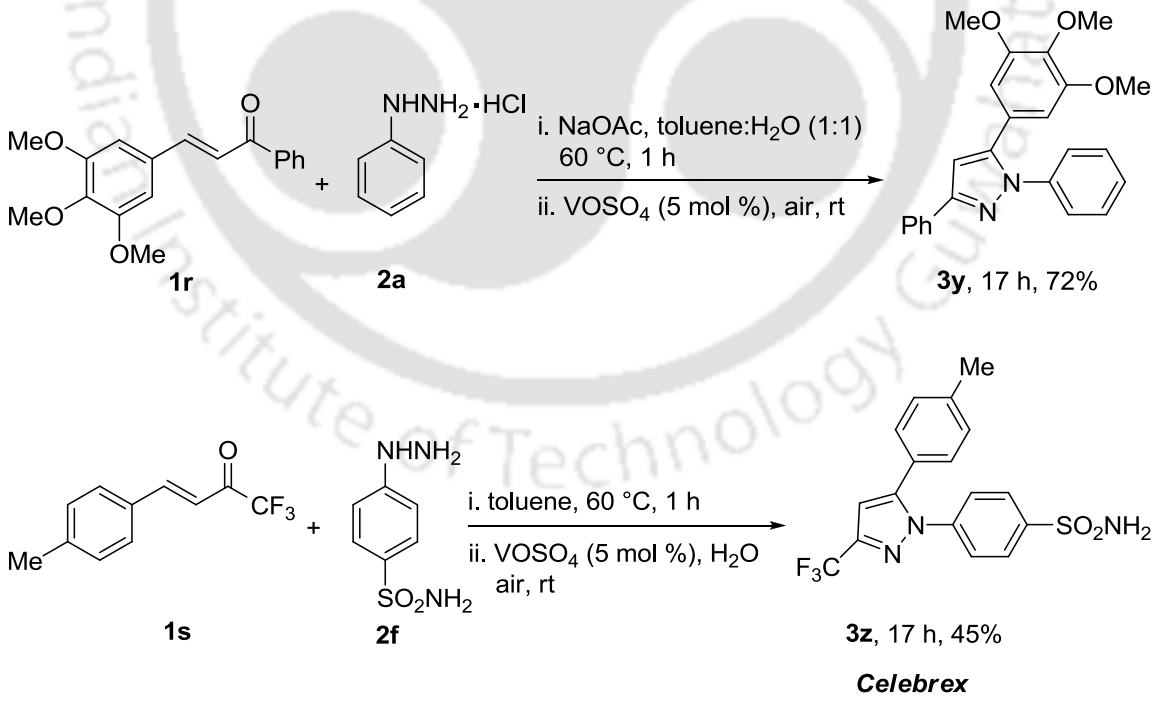

Scheme 30. Reaction of *α,β*-Unsaturated Ketones **1r-s** with Hydrazines **2a** and **2f**

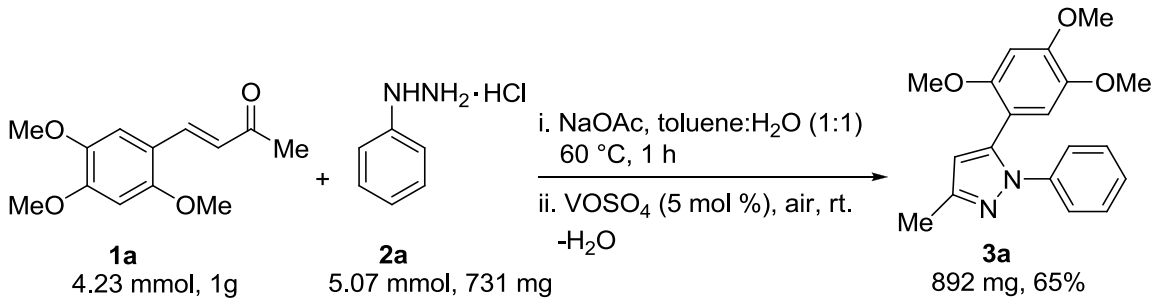

Scheme 31. Gram-Scale Synthesis

Recyclability Experiments. The aqueous layer having the vanadium catalyst could be easily separated and recycled. For example, the reaction of **1a** with **2a** was studied over three runs with >64% yield (Scheme 32).

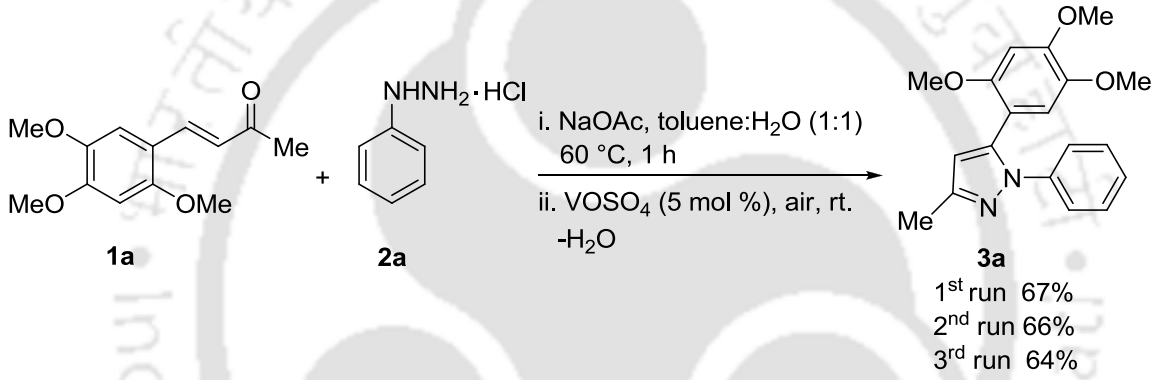

Scheme 32. Recyclability Experiments

Proposed catalytic cycle is shown in Scheme 33. Condensation of the ketones with aryl hydrazines may give hydrazones ***a***, which may react with $VOSO_4$ to yield the intermediate ***b***.[9a] Concerted metalation-deprotonation (CMD) of ***b*** may give the cyclic vanadium intermediate ***c***, which may undergo reductive elimination to produce the target pyrazole derivatives and V(II) species. The latter with air may oxidize to active catalysts via the peroxo species ***d*** and ***e*** to complete the catalytic cycle.

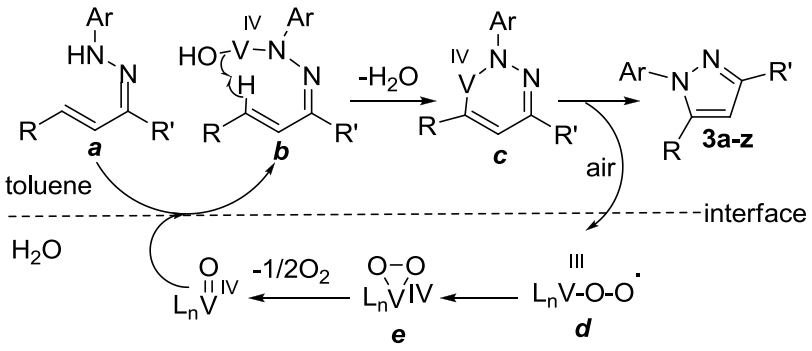

Scheme 33. Proposed Reaction Pathway

In summary, V-catalyzed *C-N* cross-dehydrogenative coupling of alkenyl hydrazones leading to highly functionalized pyrazoles is presented in a 1:1 mixture of toluene/water under air at ambient temperature. In this protocol, $VOSO_4$ can be recovered and recycled. Simplified product isolation, mild reaction conditions and the broad substrate scope are the significant practical features.

2.3 Experimental Section

General Information: Aryl amines and V_2O_5 (98%) of Aldrich, $VOSO_4$ (97%) and $VO(acac)_2$ (99%) of Otto and $SnCl_2{\cdot}2H_2O$ (97%) of Merck were used as received. Analytical TLC was performed on Merck silica gel G/GF 254 plates for progress of the reaction. NMR (^1H and ^{13}C) spectra were recorded on DRX-400 Varian spectrometer, Bruker Avance III 600, and Bruker Ultrashield^{TM} 300 using $CDCl_3$ as a solvent and TMS as an internal standard. Chemical shifts (δ) are reported in ppm for all ^1H NMR and ^{13}CNMR spectra and other data are reported as follows: s = singlet, d = doublet, m = multiplet and *J* = spin-spin coupling constant (Hz). Melting points were determined with a Büchi B-540 apparatus and are uncorrected. Perkin Elmer IR spectrometer was used for recording FT-IR spectra. Mass spectra were recorded on a Q-Tof ESI-MS instrument (model HAB 273). Single crystal X-ray data were collected using Bruker SMART APEX-II CCD diffractometer, which is equipped with 1.75 kW sealed-tube Mo-Kα irradiation (λ = 0.71073 Å) at 298(2) K. The crystal structure was solved by direct method using *SHELXL-97* (Göttingen, Germany) and refined with full-matrix least squares on F^2 using SHELXL-97.

General Procedure for the Synthesis of *α,β*-Unsaturated Methyl Ketones 1a-q.[25a] Aqueous solution of NaOH (3 mL, 10%) was added dropwise to a stirred solution of aldehydes (5 mmol) and acetone (50 mmol) in 1.0 mL of water, and the mixture was stirred at 40 ^{o}C. The progress of the reaction was monitored by TLC using ethyl acetate and hexane as solvent. After completion, the reaction mixture was cooled to room temperature and quenched with HCL (1N) and adjusted the pH to 7. The solution was extracted with ethyl acetate (3 x 15 mL) and washed with brine (1 x 10 mL). Drying (Na_2SO_4) and evaporation of the solvent gave a residue that was purified on silica gel column chromatography using *n*-hexane and ethyl acetate as an eluent.

Synthesis of (*E*)-1-phenyl-3-(3,4,5-trimethoxyphenyl)prop-2-en-1-one[25a] **1r.** To a stirred solution of aldehyde (1.0 mmol) and acetophenone (1.0 mmol) in 4 mL of EtOH was added NaOH (1.2 mmol) dissolved in 4 mL of ethanol-water (1:1). The mixture was stirred at room temperature and the progress of the reaction was monitored by TLC using ethyl acetate and hexane. After completion, EtOH was evaporated and the resultant mixture was extracted with ethyl acetate (3 x 15 mL) and washed with brine (1 x 10 mL). Drying (Na_2SO_4) and evaporation of the solvent gave a residue that was purified on silica gel column chromatography using *n*-hexane and ethyl acetate as an eluent.

Synthesis of (*E*)-1,1,1-trifluoro-4-*p*-tolylbut-3-en-2-one[25a] **1s.** To a solution of 4-methylbenzaldehyde (0.59 mL, 5.0 mmol), acetic acid (0.43 mL, 7.5 mmol) and piperidine (0.50 mL, 5.0 mmol) in dry toluene (5.0 mL) at 0 ^{o}C was added dropwise trifluoroacetone (1.79 mL, 20 mmol) in dry benzene (5.0 mL). The mixture was allowed to sir for 2 h at 0 ^{o}C and for overnight at room temperature. The reaction was mixture was quenched with saturated NH_4Cl and the organic layer was washed with water (1 x 10 mL). Drying (Na_2SO_4) and evaporation of the solvent gave a residue that was purified on silica gel column chromatography using *n*-hexane and ethyl acetate as an eluent.

Synthesis of Aryl Hydrazine Hydrochlorides[26] **(2b-f).** An ice cold solution of $NaNO_2$ (6.38 mmol, 0.44 g) in water (3.0 mL) was added dropwise to a solution of anilines (6.0 mmol) in conc. HCl (10.4 mL) at 0 °C for 15 min, and then the solution of $SnCl_2{\cdot}2H_2O$ (13.3 mmol, 3.0 g) in conc. HCl (3.0 mL) was added dropwise for 10 min. The reaction mixture was allowed to stir at room temperature for 1 h. The precipitate was filtered and dried to give the titled compounds, which were used without further purification.

General Procedure for the Synthesis of Pyrazoles 3a-p. *α,β*-Unsaturated ketones **1a-p** (1.0 mmol) and aryl hydrazines **2a** (1.2 mmol) were stirred with NaOAc (2.9 mmol) in toluene:H_2O (1:1, 3.0 mL) at 60 ^oC for 1 h under air. The reaction mixture was cooled at room temperature and then treated with $VOSO_4$ (5 mol %). The resultant reaction mixture was stirred at room temperature under air. The progress of the reaction was monitored by TLC. After completion, toluene layer was separated and the aqueous solution was extracted with EtOAc (3 x 5 mL). The combined organic solution was washed with brine (1 x 10 mL) and water (1 x 10 mL). Drying (Na_2SO_4) and evaporation of the solvent gave a residue that was purified on silica gel column chromatography using hexane and ethyl acetate as eluent.

General Procedure for the Synthesis of Pyrazoles 3q-z. *α,β*-Unsaturated ketones **1** (1 mmol), and aryl hydrazines **2b-f** (1.2 mmol) were stirred in toluene (1.5 mL) at 60 ^oC for 1 h under air. The reaction mixture was cooled at room temperature and then treated with solution of $VOSO_4$ (5 mol %) in H_2O (1.5 mL). The resultant reaction mixture was stirred at room temperature under air. The progress of the reaction was monitored by TLC. The work up and purification of the pyrazoles were performed as described above.

2.4 Characterization Data of Substituted Pyrazoles 3a-z

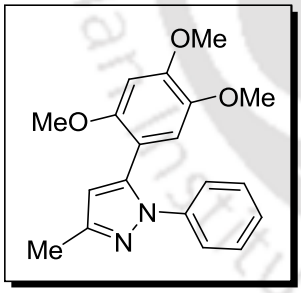

3-Methyl-1-phenyl-5-(2,4,5-trimethoxyphenyl)-1*H*-pyrazole 3a. Analytical TLC on silica gel, 1:4 ethyl acetate/hexane R_f = 0.44; white solid; yield: 73% (236 mg); mp 142-143 ^oC. ^1H NMR (600 MHz, $CDCl_3$) δ 7.28-7.19 (m, 5H), 6.73 (s, 1H), 6.42 (s, 1H), 6.27 (s, 1H), 3.89 (s, 3H), 3.73 (s, 3H), 3.37 (s, 3H), 2.39 (s, 3H); $^{13}C\{^1H\}$ NMR (100 MHz, $CDCl_3$) δ 151.0, 150.2, 149.1, 142.9, 141.1, 140.1, 128.5, 126.5, 123.7, 114.4, 111.3, 108.4, 97.6, 56.4, 56.0, 55.8, 13.7; FT-IR (KBr) 2999, 2961, 2935, 2837, 1613, 1596, 1502, 1474, 1454, 1438, 1383, 1361, 1277, 1260, 1213, 1192, 1140, 1020, 856, 809, 762, 692 cm^{-1}; HRMS (APCI) *m/z* $[M+H]^+$ calcd for $C_{19}H_{20}N_2O_3$: 325.1547, found: 325.1551.

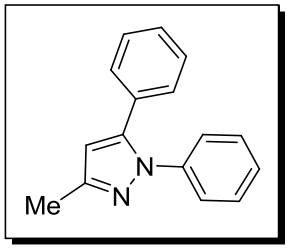

3-Methyl-1,5-diphenyl-1*H*-pyrazole[27a] **3b.** Analytical TLC on silica gel, 1:9 ethyl acetate/hexane R_f = 0.41; yellow liquid; yield: 48% (112 mg). ^{1}H NMR (400 MHz, $CDCl_3$) δ 7.33-7.20 (m, 10H), 6.31 (s, 1H), 2.39 (s, 3H); $^{13}C\{^1H\}$ NMR (150 MHz, $CDCl_3$) δ 149.6, 143.8, 140.3, 130.8, 128.9, 128.7, 128.5, 128.2, 127.2, 125.2, 107.8, 13.7; FT-IR (neat) 3060, 2925, 1950, 1669, 1596, 1553, 1504, 1455, 1439, 1417, 1377, 1364, 1195, 1072, 1013, 969, 695 cm^{-1}; HRMS (APCI) *m/z* $[M+H]^+$ calcd for $C_{16}H_{14}N_2$: 235.1230, found: 235.1232.

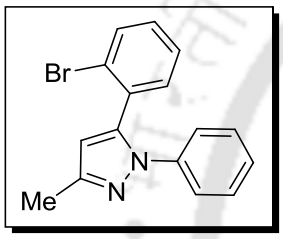

5-(2-Bromophenyl)-3-methyl-1-phenyl-1*H*-pyrazole 3c. Analytical TLC on silica gel, 1:6 ethyl acetate/hexane R_f = 0.63; yellow solid; yield: 45% (140 mg); mp 73-74 ^oC. ^{1}H NMR (600 MHz, $CDCl_3$) δ 7.58 (d, *J* = 8.4 Hz, 1H), 7.27-7.19 (m, 8H), 6.30 (s, 1H), 2.42 (s, 3H); $^{13}C\{^1H\}$ NMR (150 MHz, $CDCl_3$) δ 149.3, 142.0, 140.2, 133.3, 132.9, 132.3, 130.3, 128.9, 127.4, 126.9, 124.2, 124.1, 109.4, 13.8; FT-IR (KBr) 3052, 2961, 2924, 2859, 1598, 1548, 1502, 1430, 1362, 1377, 1261, 1194, 1098, 1026, 970, 783, 756, 689 cm^{-1}; HRMS (APCI) *m/z* $[M+H]^+$ calcd for $C_{16}H_{13}BrN_2$: 313.0335, found: 313.0335.

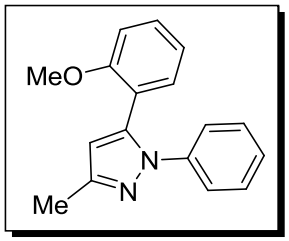

5-(2-Methoxyphenyl)-3-methyl-1-phenyl-1*H*-pyrazole 3d. Analytical TLC on silica gel, 1:9 ethyl acetate/hexane R_f = 0.53; yellow liquid; yield: 66% (174 mg). ^{1}H NMR (600 MHz, $CDCl_3$) δ 7.32 (t, *J* = 7.2 Hz, 1H), 7.27-7.23 (m, 5H), 7.18-7.16 (m, 1H), 6.96 (t, *J* = 7.8 Hz, 1H), 6.79 (d, *J* = 8.4 Hz, 1H), 6.27 (s, 1H), 3.37 (s, 3H), 2.40 (s, 3H); $^{13}C\{^1H\}$ NMR (150 MHz, $CDCl_3$) δ 156.6, 149.3, 141.3, 140.5, 131.3,

130.4, 128.6, 126.6, 123.6, 120.8, 120.5, 111.4, 108.8, 55.1, 13.8; FT-IR (neat) 3052, 2927, 2854, 2837, 1739, 1667, 1600, 1581, 1552, 1504, 1494, 1463, 1377, 1363, 1296, 1264, 1248, 1116, 1026, 970, 757 cm^{-1}; HRMS (APCI) *m/z* $[M+H]^+$ calcd for $C_{17}H_{16}N_2O$: 265.1335, found: 265.1336.

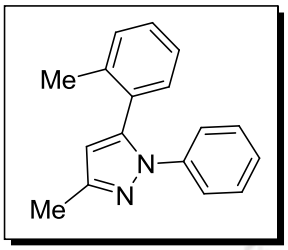

3-Methyl-1-phenyl-5-*o*-tolyl-1*H*-pyrazole[24a] **3e.** Analytical TLC on silica gel, 1:9 ethyl acetate/hexane R_f = 0.73; yellow liquid; yield: 53% (131 mg). ^1H NMR (600 MHz, $CDCl_3$) δ 7.22-7.15 (m, 9H), 6.19 (s, 1H), 2.40 (s, 3H), 2.00 (s, 3H); $^{13}C\{^1H\}$ NMR (150 MHz, $CDCl_3$) δ 149.4, 143.1, 140.5, 137.2, 131.3, 130.7, 130.5, 128.99, 128.90, 126.6, 125.9, 123.6, 108.9, 20.1, 13.8; FT-IR (neat) 3060, 2924, 2859, 1670, 1598, 1552, 1502, 1458, 1416, 1362, 1259, 1175, 1072, 1027, 968, 907, 762, 725 cm^{-1}; HRMS (APCI) *m/z* $[M+H]^+$ calcd for $C_{17}H_{16}N_2$: 249.1386, found: 249.1386.

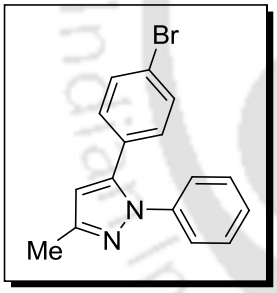

5-(4-Bromophenyl)-3-methyl-1-phenyl-1*H*-pyrazole[27b] **3f**. Analytical TLC on silica gel, 1:9 ethyl acetate/hexane R_f = 0.58; yellow solid; yield: 41% (128 mg); mp 74-75 ^oC. ^1H NMR (600 MHz, $CDCl_3$) δ 7.42 (d, *J* = 7.8 Hz, 2H), 7.33 (t, *J* = 7.2 Hz, 2H), 7.30 (d, *J* = 6.6 Hz, 1H), 7.26-7.24 (m, 2H), 7.08 (d, *J* = 7.8 Hz, 2H), 6.31 (s, 1H), 2.38 (s, 3H); $^{13}C\{^1H\}$ NMR (150 MHz, $CDCl_3$) δ 149.8, 142.6, 140.0, 132.4, 131.8, 130.3, 129.2, 127.5, 125.3, 122.5, 108.3, 13.7; FT-IR (KBr) 2925, 1625, 1503, 1487, 1260, 1072, 1010, 968, 811, 767, 693 cm^{-1}; HRMS (APCI) *m/z* $[M+H]^+$ calcd for $C_{16}H_{13}BrN_2$: 313.0335, found: 313.0335.

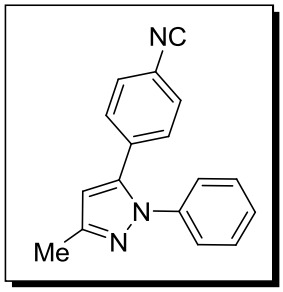

4-(3-Methyl-1-phenyl-1*H*-pyrazol-5-yl)benzonitrile[27b] **3g.**

Analytical TLC on silica gel, 1:6 ethyl acetate/hexane R_f = 0.55; yellow liquid; yield: 38% (98 mg). ^{1}H NMR (600 MHz, $CDCl_3$) δ 7.57 (d, *J* = 7.8 Hz, 2H), 7.35-7.29 (m, 5H), 7.24 (d, *J* = 7.2 Hz, 2H), 6.39 (s, 1H), 2.39 (s, 3H); ^{13}C{^{1}H} NMR (150 MHz, $CDCl_3$) δ 150.0, 141.8, 139.7, 135.2, 132.4, 129.4, 129.1, 128.0, 125.4, 118.6, 111.8, 108.8, 13.6; FT-IR (neat) 3061, 2661, 2625, 2854, 2227, 1717, 1679, 1597, 1562, 1459, 1429, 1363, 1504, 1260, 1177, 1073, 1014, 970, 844, 799, 763, 695 cm^{-1}; HRMS (APCI) *m/z* $[M+H]^+$ calcd for $C_{17}H_{13}N_3$: 260.1182, found: 260.1182.

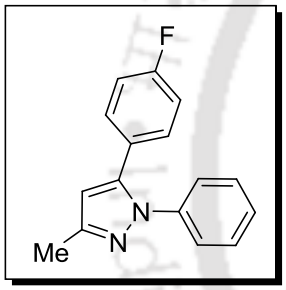

5-(4-Fluorophenyl)-3-methyl-1-phenyl-1*H*-pyrazole[25a] **3h.**

Analytical TLC on silica gel, 1:9 ethyl acetate/hexane R_f = 0.53; yellow liquid; yield: 39% (98 mg). ^{1}H NMR (600 MHz, $CDCl_3$) δ 7.32 (t, *J* = 7.8 Hz, 2H), 7.28-7.24 (m, 3H), 7.19-7.17 (m, 2H), 6.98 (t, *J* = 8.4 Hz, 2H), 6.28 (s, 1H), 2.38 (s, 3H); ^{13}C{^{1}H} NMR (150 MHz, $CDCl_3$) δ 163.5 (J_{C-F} = 246 Hz), 149.6, 142.8, 140.1, 130.6 (J_{C-F} = 7.5 Hz), 129.1, 127.4, 127.0, 125.3, 115.7 (J_{C-F} = 21.0 Hz), 107.9, 13.7; FT-IR (neat) 2924, 2850, 2351, 2073, 1636, 1508, 1427, 1383, 1362, 1225, 1158, 1014, 969, 838, 693 cm^{-1}; HRMS (ESI) *m/z* $[M+H]^+$ calcd for $C_{16}H_{13}FN_2$: 253.1136, found: 253.1137.

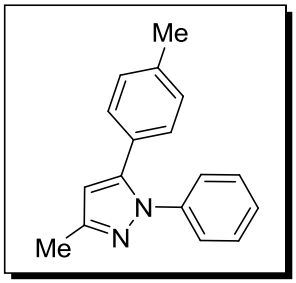

3-Methyl-1-phenyl-5-*p*-tolyl-1*H*-pyrazole[27b] **3i.** Analytical TLC on silica gel, 1:9 ethyl acetate/hexane R_f = 0.56; yellow liquid; yield: 62% (153 mg). ^{1}H NMR (600 MHz, $CDCl_3$) δ 7.31 (d, *J* = 7.2 Hz, 2H), 7.27 (d, *J* = 7.2 Hz, 2H), 7.11-7.08 (m, 5H), 6.27 (s, 1H), 2.37 (s, 3H), 2.33 (s, 3H); ^{13}C{^{1}H} NMR (150 MHz, $CDCl_3$) δ 149.6, 143.9, 140.4, 138.2, 129.3, 129.0, 128.7, 128.0, 127.2, 125.3, 107.7, 21.4, 13.8; FT-IR (neat) 3001, 2957, 2925, 2856, 2836, 1666, 1604, 1517, 1462, 1443, 1377, 1366, 1298, 1249, 1181, 1105, 1033, 971, 833 cm^{-1}; HRMS (APCI) *m/z* $[M+H]^+$ calcd for $C_{17}H_{16}N_2$: 249.1386, found: 249.1388.

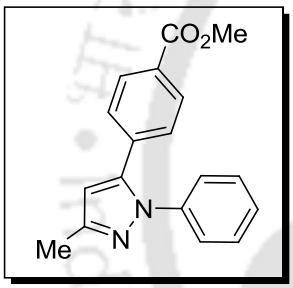

Methyl 4-(3-methyl-1-phenyl-1*H*-pyrazol-5-yl)benzoate 3j. Analytical TLC on silica gel, 1:4 ethyl acetate/hexane R_f = 0.60; yellow liquid; yield: 66% (192 mg). ^{1}H NMR (600 MHz, $CDCl_3$) δ 7.95 (d, *J* = 7.8 Hz, 2H), 7.32 (d, *J* = 6.6 Hz, 2H), 7.30-7.24 (m, 5H), 6.38 (s, 1H), 3.90 (s, 3H), 2.39 (s, 3H); ^{13}C{^{1}H} NMR (150 MHz, $CDCl_3$) δ 166.8, 149.9, 142.7, 140.0, 135.2, 129.8, 129.6, 129.2, 128.6, 127.6, 125.4, 108.5, 52.4, 13.7; FT-IR (neat) 3061, 2951, 2845, 1722, 1611, 1596, 1570, 1509, 1500, 1459, 1434, 1364, 1311, 1278, 1181, 1112, 1018, 970, 860, 827, 771, 695 cm^{-1}; HRMS (APCI) *m/z* $[M+H]^+$ calcd for $C_{18}H_{16}N_2O_2$: 293.1285, found: 293.1285.

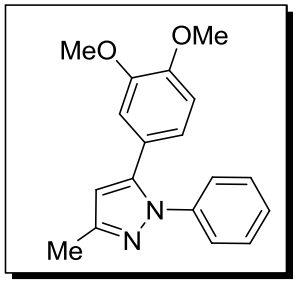

5-(3,4-Dimethoxyphenyl)-3-methyl-1-phenyl-1*H*-pyrazole[27b]

3k. Analytical TLC on silica gel, 1:4 ethyl acetate/hexane R_f = 0.47; yellow liquid; yield: 59% (173 mg). ^{1}H NMR (600 MHz, $CDCl_3$) δ 7.33-7.28 (m, 5H), 6.84 (d, *J* = 8.4 Hz, 1H), 6.80 (d, *J* = 8.4 Hz, 1H), 6.63 (s, 1H), 6.28 (s, 1H), 3.87 (s, 3H), 3.62 (s, 3H), 2.38 (s, 3H); ^{13}C{^{1}H} NMR (150 MHz, $CDCl_3$) δ 149.5, 149.1, 148.7, 143.8, 140.4, 129.0, 127.3, 125.5, 123.5, 121.4, 112.0, 111.1, 107.2, 56.0, 55.8, 13.7; FT-IR (neat) 3062, 2999, 2932, 2835, 1597, 1553, 1513, 1500, 1463, 1436, 1362, 1254, 1235, 1164, 1136, 1073, 1026, 860, 807, 764, 696 cm^{-1}; HRMS (APCI) *m/z* $[M+H]^+$ calcd for $C_{18}H_{18}N_2O_2$: 295.1441, found: 295.1445.

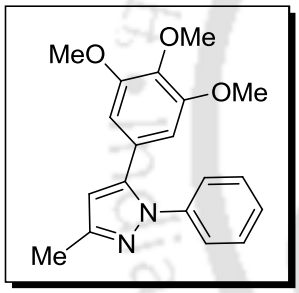

3-Methyl-1-phenyl-5-(3,4,5-trimethoxyphenyl)-1*H*-pyrazole

3l. Analytical TLC on silica gel, 1:4 ethyl acetate/hexane R_f = 0.52; yellow liquid; yield: 68% (220 mg). ^{1}H NMR (600 MHz, $CDCl_3$) δ 7.35-7.33 (m, 2H), 7.30-7.28 (m, 3H), 6.39 (s, 2H), 6.31 (s, 1H), 3.84 (s, 3H), 3.64 (s, 6H), 2.38 (s, 3H); ^{13}C{^{1}H} NMR (150 MHz, $CDCl_3$) δ 153.2, 149.6, 143.8, 140.4, 138.1, 129.0, 127.4, 126.1, 125.6, 107.3, 106.1, 61.1, 56.5, 56.1, 13.7; FT-IR (neat) 2935, 2834, 1691, 1585, 1551, 1500, 1462, 1426, 1362, 1322, 1239, 1126, 1007, 722, 696 cm^{-1}; HRMS (APCI) *m/z* $[M+H]^+$ calcd for $C_{19}H_{20}N_2O_3$: 325.1547 $[M+H]^+$, found: 325.1547.

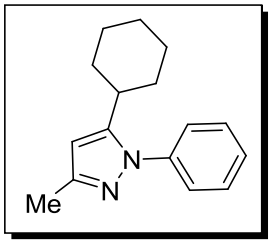

5-Cyclohexyl-3-methyl-1-phenyl-1*H*-pyrazole[27b] **3m**. Analytical TLC on silica gel, 1:9 ethyl acetate/hexane R_f = 0.54; yellow liquid; yield: 62% (148 mg). ^{1}H NMR (600 MHz, $CDCl_3$) δ 7.44-7.43 (m, 4H), 7.34-7.32 (m, 1H), 6.01 (s, 1H), 2.69-2.65 (m, 1H), 2.31 (s, 3H), 2.01-1.99 (m, 2H), 1.82-1.80 (m, 2H), 1.73-1.70 (m, 1H), 1.47-1.35 (m, 5H); ^{13}C{^{1}H} NMR (150 MHz, $CDCl_3$) δ 158.8, 140.2, 139.1, 129.1, 127.3, 124.9, 104.2, 37.8, 33.5, 26.6, 26.3, 12.7; FT-IR (neat) 2925, 2851, 1727, 1599, 1553, 1504, 1447, 1380, 1261, 1072, 1016, 758, 695 cm^{-1}; HRMS (APCI) *m/z* $[M+H]^+$ calcd for $C_{16}H_{20}N_2$: 241.1699, found: 241.1699.

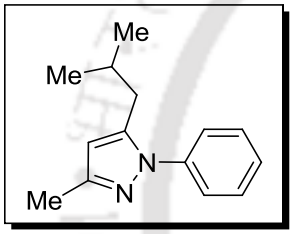

5-Isobutyl-3-methyl-1-phenyl-1*H*-pyrazole[27b] **3n.** Analytical TLC on silica gel, 1:9 ethyl acetate/hexane R_f = 0.62; yellow liquid; yield: 54% (115 mg). ^{1}H NMR (600 MHz, $CDCl_3$) δ 7.44-7.43 (m, 4H), 7.34-7.33 (m, 1H), 5.99 (s, 1H), 2.51 (d, *J* = 7.2 Hz, 2H), 2.31 (s, 3H), 1.97-1.93 (m, 1H), 0.97 (s, 3H), 0.96 (s, 3H); ^{13}C{^{1}H} NMR (150 MHz, $CDCl_3$) δ 153.0, 140.2, 139.2, 129.1, 127.3, 124.9, 106.7, 37.6, 29.1, 22.7, 12.7; FT-IR (neat) 3064, 2955, 2926, 2868, 1730, 1599, 1554, 1503, 1461, 1381, 1261, 1168, 1133, 1018, 759 cm^{-1}; HRMS (APCI) *m/z* $[M+H]^+$ calcd for $C_{14}H_{18}N_2$: 215.1543, found: 215.1542.

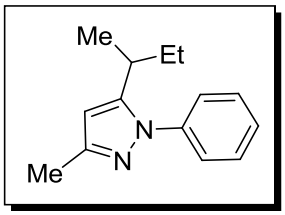

5-Sec-butyl-3-methyl-1-phenyl-1*H*-pyrazole 3o. Analytical TLC on silica gel, 1:9 ethyl acetate/hexane R_f = 0.41; yellow liquid; yield: 58% (124 mg). ^{1}H NMR (600 MHz, $CDCl_3$) δ 7.46-7.43 (m, 2H), 7.39-7.36 (m, 3H), 5.98 (s, 1H), 2.76-2.72 (m, 1H), 2.31 (s, 3H), 1.58-1.54 (m, 1H), 1.50-1.47 (m, 1H), 1.17 (d, *J* = 7.2 Hz, 3H),

0.78 (t, *J* = 7.2 Hz, 3H); $^{13}C\{^{1}H\}$ NMR (150 MHz, $CDCl_3$) δ 150.5, 149.1, 140.2, 129.2, 128.0, 126.4, 103.0, 32.4, 30.5, 21.1, 13.8, 12.0; FT-IR (neat) 3064, 2964, 2929, 2874, 1720, 1598, 1546, 1503, 1455, 1381, 1262, 1104, 1072, 1020, 767 cm^{-1}; HRMS (APCI) *m/z* $[M+H]^+$ calcd for $C_{14}H_{18}N_2$: 215.1543, found: 215.1543.

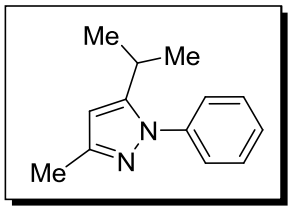

5-Isopropyl-3-methyl-1-phenyl-1*H*-pyrazole[27b] **3p**. Analytical TLC on silica gel, 1:9 ethyl acetate/hexane R_f = 0.59; yellow liquid; yield: 64% (128 mg). ^{1}H NMR (600 MHz, $CDCl_3$) δ 7.44-7.43 (m, 4H), 7.33-7.32 (m, 1H), 6.03 (s, 1H), 3.04-2.99 (m, 1H), 2.31 (s, 3H), 1.29 (s, 3H), 1.28 (s, 3H); $^{13}C\{^{1}H\}$ NMR (150 MHz, $CDCl_3$) δ 159.7, 140.2, 139.2, 129.1, 127.3, 125.0, 103.9, 28.0, 23.1, 12.7; FT-IR (neat) 3064, 2962, 2928, 2869, 1725, 1599, 1552, 1504, 1457, 1380, 1300, 1130, 1071, 1016, 766 cm^{-1}; HRMS (APCI) *m/z* $[M+H]^+$ calcd for $C_{13}H_{16}N_2$: 201.1386, found: 201.1386.

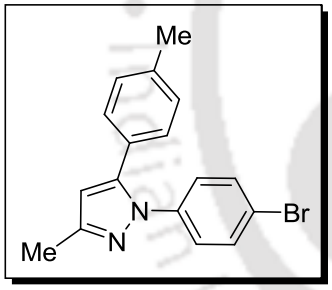

1-(4-Bromophenyl)-3-methyl-5-*p*-tolyl-1*H*-pyrazole 3q. Analytical TLC on silica gel, 1:9 ethyl acetate/hexane R_f = 0.65; yellow solid; yield: 74% (241 mg); mp 75-77 °C. ^{1}H NMR (300 MHz, $CDCl_3$) δ 7.43 (d, *J* = 7.2 Hz, 2H), 7.16-7.08 (m, 6H), 6.27 (s, 1H), 2.36-2.35 (m, 6H); $^{13}C\{^{1}H\}$ NMR (75 MHz, $CDCl_3$) δ 149.5, 143.5, 138.9, 138.0, 131.6, 129.0, 128.3, 127.2, 126.1, 120.2, 107.8, 21.0, 13.3; FT-IR (KBr) 2922, 1634, 1509, 1491, 1400, 1359, 1261, 1097, 1070, 1012, 967, 827, 797 cm^{-1}; HRMS (APCI) *m/z* $[M+H]^+$ calcd for $C_{17}H_{15}BrN_2$: 327.0491, found: 327.0492.

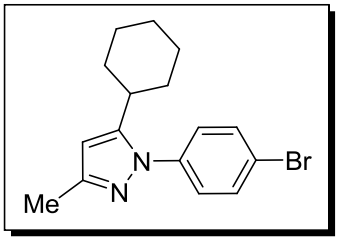

1-(4-Bromophenyl)-5-cyclohexyl-3-methyl-1*H*-pyrazole 3r. Analytical TLC on silica gel, 1:9 ethyl acetate/hexane R_f = 0.57; yellow liquid; yield: 61% (193 mg). ^{1}H NMR (300 MHz, $CDCl_3$) δ 7.59 (d, *J* = 8.7 Hz, 2H), 7.28 (d, *J* = 8.4 Hz, 2H), 5.99 (s, 1H), 2.61-2.54 (m, 1H), 2.28 (s, 3H), 1.84-1.68 (m, 5H), 1.36-1.28 (m, 5H); ^{13}C{^{1}H} NMR (75 MHz, $CDCl_3$) δ 150.1, 149.2, 139.0, 132.1, 127.0, 121.2, 103.6, 35.1, 33.4, 26.2, 25.7, 13.5; FT-IR (neat) 2927, 2852, 1590, 1546, 1493, 1447, 1382, 1363, 1260, 1069, 1013, 989, 830 cm^{-1}; HRMS (APCI) *m/z* $[M+H]^+$ calcd for $C_{16}H_{19}BrN_2$: 319.0804, found: 319.0805.

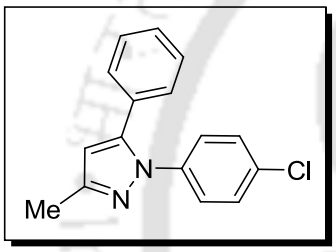

1-(4-Chlorophenyl)-3-methyl-5-phenyl-1*H*-pyrazole[27c] **3s**. Analytical TLC on silica gel, 1:9 ethyl acetate/hexane R_f = 0.64; yellow liquid; yield: 71% (190 mg). ^{1}H NMR (600 MHz, $CDCl_3$) δ 7. 31 (s, 4H), 7.28-7.26 (m, 3H), 7.21 (d, *J* = 7.8 Hz, 2H), 6.30 (s, 1H), 2.37 (s, 3H); ^{13}C{^{1}H} NMR (150 MHz, $CDCl_3$) δ 150.0, 143.9, 138.8, 132.8, 130.6, 129.1, 128.8, 128.7, 128.4, 126.2, 108.3, 13.7; FT-IR (neat) 3060, 2925, 2860, 1892, 1596, 1551, 1493, 1453, 1405, 1377, 1364, 1311, 1267, 1192, 1093, 1015, 968, 831, 757, 697 cm^{-1}; HRMS (APCI) *m/z* $[M+H]^+$ calcd for $C_{16}H_{13}ClN_2$: 269.0840, found: 269.0840.

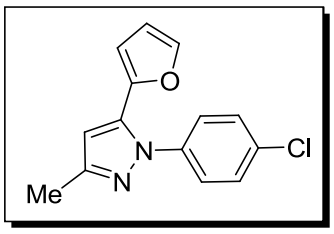

1-(4-Chlorophenyl)-5-(furan-2-yl)-3-methyl-1*H*-pyrazole[27b] **3t.** Analytical TLC on silica gel, 1:9 ethyl acetate/hexane R_f = 0.73; yellow liquid; yield: 60% (154 mg). ^{1}H NMR (600 MHz, $CDCl_3$) δ 7.39 (d, *J* = 8.4 Hz, 3H), 7.33 (d, *J* = 8.4 Hz, 2H), 6.44 (s, 1H), 6.35 (s, 1H), 6.06 (s, 1H), 2.35 (s, 3H); ^{13}C{^{1}H} NMR (150 MHz,

$CDCl_3$) δ 150.0, 144.5, 142.8, 139.0, 135.0, 131.1, 129.3, 126.9, 111.4, 109.2, 106.8, 13.6; FT-IR (neat) 3106, 2961, 2925, 2853, 1726, 1596, 1529, 1502, 1403, 1383, 1261, 1093, 1016, 984, 895, 833, 800, 742 cm^{-1}; HRMS (APCI) *m/z* $[M+H]^+$ calcd for $C_{14}H_{11}ClN_2O$: 259.0633, found: 259.0636.

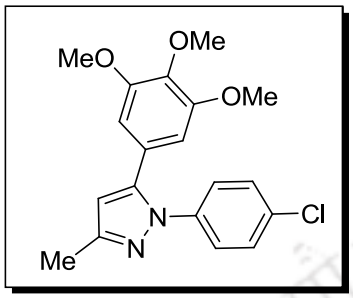

1-(4-Chlorophenyl)-3-methyl-5-(3,4,5-trimethoxyphenyl)-1*H*-pyrazole 3u. Analytical TLC on silica gel, 1:4 ethyl acetate/hexane R_f = 0.69; yellow solid; yield: 48% (171 mg); mp 159-160 °C. ^1H NMR (600 MHz, $CDCl_3$) δ 7.24 (d, *J* = 9.0 Hz, 2H), 7.20 (d, *J* = 8.4 Hz, 2H), 6.76 (s, 1H), 6.42 (s, 1H), 6.24 (s, 1H), 3.90 (s, 3H), 3.78 (s, 3H), 3.38 (s, 3H), 2.37 (s, 3H); $^{13}C\{^1H\}$ NMR (75 MHz, $CDCl_3$) δ 150.7, 150.3, 149.5, 142.8, 140.2, 139.5, 131.8, 128.5, 124.5, 108.6, 97.2, 56.3, 55.9, 55.6, 13.6; FT-IR (KBr) 2959, 2927, 2850, 1666, 1611, 1498, 1465, 1437, 1407, 1384, 1362, 1261, 1219, 1208, 1142, 1092, 1032, 808 cm^{-1}; HRMS (APCI) *m/z* $[M+H]^+$ calcd for $C_{19}H_{19}ClN_2O_3$: 359.1162, found: 359.1162.

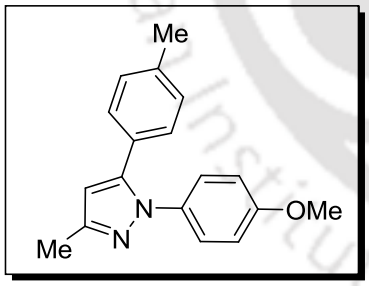

1-(4-Methoxyphenyl)-3-methyl-5-*p*-tolyl-1*H*-pyrazole[27b] **3v**. Analytical TLC on silica gel, 1:4 ethyl acetate/hexane R_f = 0.48; yellow liquid; yield: 68% (189 mg). ^1H NMR (600 MHz, $CDCl_3$) δ 7.19 (d, *J* = 8.4 Hz, 2H), 7.08 (s, 4H), 6.84 (d, *J* = 9.0 Hz, 2H), 6.25 (s, 1H), 3.80 (s, 3H), 2.36 (s, 3H), 2.32 (s, 3H); $^{13}C\{^1H\}$ NMR (150 MHz, $CDCl_3$) δ 158.7, 149.1, 143.9, 138.0, 133.7, 129.2, 128.6, 128.0, 126.8, 114.1, 107.0, 55.6, 21.4, 13.7; FT-IR (neat) 2993, 2924, 2855, 1678, 1607, 1516, 1462, 1443, 1366, 1298, 1249, 1180, 1106, 1032, 971, 833 cm^{-1}; HRMS (APCI) *m/z* $[M+H]^+$ calcd for $C_{18}H_{18}N_2O$: 279.1492, found: 279.1494.

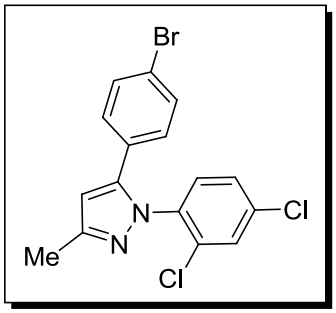

5-(4-Bromophenyl)-1-(2,4-dichlorophenyl)-3-methyl-1*H*-pyrazole 3w. Analytical TLC on silica gel, 1:9 ethyl acetate/hexane R_f = 0.74; yellow solid; yield: 58% (219 mg); mp 66-67 °C. ^{1}H NMR (600 MHz, $CDCl_3$) δ 7.43 (s, 1H), 7.40 (d, *J* = 8.4 Hz, 2H), 7.35 (d, *J* = 8.4 Hz, 1H), 7.32 (d, *J* = 8.4 Hz, 1H), 7.03 (d, *J* = 8.4 Hz, 2H), 6.34 (s, 1H), 2.37 (s, 3H); ^{13}C{^{1}H} NMR (150 MHz, $CDCl_3$) δ 150.6, 144.8, 136.8, 135.6, 133.2, 131.9, 130.8, 130.4, 129.4, 129.1, 128.1, 122.8, 106.8, 13.8; FT-IR (KBr) 2924, 2850, 1622, 1562, 1499, 1484, 1427, 1390, 1362, 1194, 1073, 1010, 967, 812 cm^{-1}; HRMS (APCI) *m/z* $[M+H]^+$ calcd for $C_{16}H_{11}BrCl_2N_2$: 380.9555, found: 380.9556.

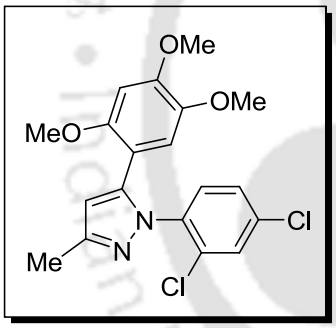

1-(2,4-Dichlorophenyl)-3-methyl-5-(2,4,5-trimethoxyphenyl)-1*H*-pyrazole 3x. Analytical TLC on silica gel, 1:4 ethyl acetate/hexane R_f = 0.41; yellow solid; yield: 63% (246 mg); mp 62-63 °C. ^{1}H NMR (400 MHz, $CDCl_3$) δ 7.33 (s, 1H), 7.12 (s, 2H), 6.59 (s, 1H), 6.31 (s, 1H), 6.21 (s, 1H), 3.78 (s, 3H), 3.62 (s, 3H), 3.48 (s, 3H), 2.30 (s, 3H); ^{13}C{^{1}H} NMR (150 MHz, $CDCl_3$) δ 150.9, 150.3, 149.9, 142.7, 142.2, 137.4, 134.3, 132.8, 130.2, 129.9, 127.1, 114.3, 110.3, 107.6, 97.1, 56.4, 56.0, 55.8, 13.7; FT-IR (KBr) 2998, 2924, 2852, 1614, 1511, 1497, 1464, 1436, 1382, 1266, 1223, 1209, 1151, 1083, 1032, 816 cm^{-1}; HRMS (APCI) *m/z* $[M+H]^+$ calcd for $C_{19}H_{18}Cl_2N_2O_3$: 393.0767, found: 393.0770.

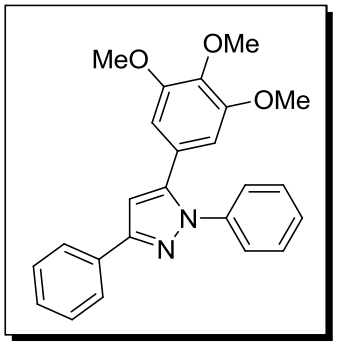

1,3-Diphenyl-5-(3,4,5-trimethoxyphenyl)-1*H*-pyrazole 3y. Analytical TLC on silica gel, 1:4 ethyl acetate/hexane R_f = 0.39; yellow solid; yield: 72% (277 mg); mp 107-108 ^{o}C. ^{1}H NMR (600 MHz, $CDCl_3$) δ 8.02 (d, *J* = 7.8 Hz, 2H), 7.73-7.71 (m, 1H), 7.59 (t, *J* = 7.8 Hz, 1H), 7.51 (t, *J* = 7.2 Hz, 2H), 7.41-7.36 (m, 2H), 7.32 (s, 1H), 7.28-7.27 (m, 1H), 7.14 (s, 1H), 6.86 (s, 2H), 3.92 (s, 6H), 3.90 (s, 3H); ^{13}C{^{1}H} NMR (150 MHz, $CDCl_3$) δ 153.7, 145.2, 140.7, 138.5, 132.9, 130.5, 128.8, 128.6, 127.7, 125.5, 121.7, 105.9, 103.3, 61.2, 56.4; FT-IR (KBr) 2925, 2845, 1660, 1600, 1577, 1503, 1461, 1419, 1319, 1279, 1248, 1215, 1127, 1018, 983, 832, 782, 703, 603 cm^{-1}; HRMS (APCI) *m/z* $[M+H]^+$ calcd for $C_{24}H_{22}N_2O_3$: 387.1703, found: 387.1704.

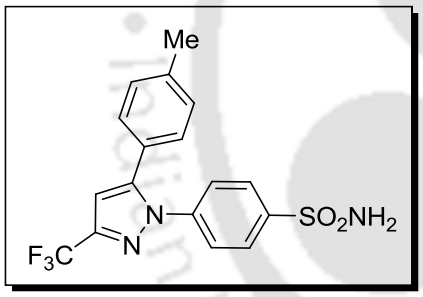

4-(5-*p*-Tolyl-3-(trifluoromethyl)-1H-pyrazol-1-yl)benzenesulfonamide 3z. Analytical TLC on silica gel, 1:4 ethyl acetate/hexane R_f = 0.41; yellow liquid; yield: 45% (171 mg). ^{1}H NMR (600 MHz, $CDCl_3$) δ 7.91(d, *J* = 8.4 Hz, 2H), 7.48 (d, *J* = 8.4 Hz, 2H), 7.18 (d, *J* = 7.8 Hz, 2H), 7.11 (d, *J* = 8.4 Hz, 2H), 6.74 (s, 1H), 4.88 (s, 2H), 2.38 (s, 3H); ^{13}C{^{1}H} NMR (150 MHz, $CDCl_3$) δ145.4, 144.3 (q, J_{C-F} = 39.0 Hz, C), 142.8, 141.4, 140.0, 130.0, 128.9, 127.7, 126.5, 125.9, 122.9 (q, J_{C-F} = 267.0 Hz, C), 106.6, 21.5; FT-IR (neat) 3448, 2961, 2922, 2854, 1746, 1636, 1497, 1468, 1386, 1333, 1272, 1235, 1162, 1129, 1096 cm^{-1}; HRMS (ESI) *m/z* $[M+H]^+$ calcd for $C_{17}H_{14}F_3N_3O_2S$: 382.0832, found: 382.0836.

Crystal Data and Structure Refinement for 3a at 298(2) K.

Identification code	**3a**
Empirical formula	$C_{19}H_{20}N_2O_3$
Formula weight	324.37
Temperature	298(2)
Wavelength	0.71073 Å
Crystal system	Monoclinic
Space group	P 21/c
	Loop xyz
	'x, y, z'
	'-x, y+1/2, -z+1/2'
	'-x, -y, -z'
	'x, -y-1/2, z-1/2'
Unit cell dimensions	*a* = 12.4342(7)Å α(°) = 90.00
	b = 16.3750(11)Å β(°) = 106.914(4)
	c = 8.6369(5)Å γ(°) = 90.00
Volume	1682.49(18) $Å^3$
Z	4
Density (calculated)	1.281Mg/m^3
Absorption coefficient	0.087mm^{-1}
F(000)	688.0
Crystal size	0.24 x 0.22 x 0.21 mm
Theta range for data collection	2.49 to 25.40 °
Index ranges	-16<=h<=16, -22<=k<=22, -11<=l<=11
Reflections collected	4492
Independent reflections	3982 [R (int) = 0.0499]
Completeness to theta = 29.07°	99.7 %
Absorption correction	Multi-scan
Refinement method	Full-matrix least-squares on F^2
Data / restraints / parameters	4492/ 0 /221
Goodness-of-fit on F^2	1.042

2.5 References

1. (a) Webb, M. E.; Marquet, A.; Mendel, R. R.; Rebeille, F.; Smith, A. G. *Nat. Prod. Rep.* **2007**, *24*, 988. (b) Quin, L. D.; Tyrell, J. *Fundamentals of Heterocyclic Chemistry: Importance in Nature and in the Synthesis of Pharmaceuticals*; John Wiley & Sons Inc.: New York, 2010.
2. (a) Bagley, M. C.; Dale, J. W.; Merritt, E. A.; Xiong, X. *Chem. Rev.* **2005**, *105*, 685. (b) Dua, R.; Shrivastava, S.; Sonwane, S. K.; Srivastava, S. K. *Advan. Biol. Res*. **2011**, *5*, 120. (c) Beno, B. R.; Yeung, K.-S.; Bartberger, M. D.; Pennington, L. D.; Meanwell, N. A. *J. Med. Chem.* **2015**, *58*, 4383. (d) Zhang, F.; Li, C.; Kelly, W. L. *ACS Chem. Biol*. **2016**, *11*, 415
3. (a) Wang, C.; Dong, H.; Hu, W.; Liu, Y.; Zhu, D. *Chem. Rev*. **2012**, *112*, 2208. (b) Melkonyan, F. S.; Zhao, W.; Drees, M.; Eastham, N. D.; Leonardi, M. J.; Butler, M. R.; Chen, Z.; Yu, X.; Chang, R. P. H.; Ratner, M. A.; Facchetti, A. F.; Marks, T. J. *J. Am. Chem. Soc.* **2016**, *138*, 6944. (c) Han, A.-R.; Lee, J.; Lee, H. R.; Lee, J.; Kang, S.-H.; Ahn, H.; Shin, T. J.; Oh, J. H.; Yang, C. *Macromolecules* **2016**, 49, 3739.
4. For some examples on *C–C* bond formation, see: (a) Iwai, T.; Fujihara, T.; Terao, J.; Tsuji, Y. *J. Am. Chem. Soc.* **2010**, *132*, 9602. (b) Yang, X.-F.; Hu, X.-H.; Loh, T.-P. *Org. Lett.* **2015**, *17*, 1481. (c) Zhao, S.; Yu, R.; Chen, W.; Liu, M.; Wu, H. *Org. Lett.* **2015**, *17*, 2828. (d) Li, X.; Li, X.; Jiao, N. *J. Am. Chem. Soc.* **2015**, *137*, 9246. (e) Xie, Z.; Jia, J.; Liu, X.; Liu, L. *Adv. Synth. Catal.* **2016**, *358*, 919. (f) Sarkar, R.; Mukhopadhyay, C. *Org. Biomol. Chem.* **2016**, *14*, 2706. (g) Kong, L.; Yu, S.; Zhou, X.; Li, X. *Org. Lett.* **2016**, *18*, 588.
5. For examples on *C–N* bond formation, see: (a) Tsang, W. C. P.; Zheng, N.; Buchwald, S. L. *J. Am. Chem. Soc.* **2005**, *127*, 14560. (b) Guru, M. M.; Punniyamurthy, T. *J. Org. Chem.* **2012**, *77*, 5063. (c) Alla, S. K.; Kumar, R. K.; Sadhu, P.; Punniyamurthy, T. *Org. Lett.* **2013**, *15*, 1334. (d) Senadi, G. C.; Hu, W.-P.; Garkhedkar, A. M.; Boominathan, S. S. K.; Wang, J.-J. *Chem. Commun*. **2015**, *51*, 13795. (e) Huang, H.; Guo, W.; Wu, W.; Li, C.-J.; Jiang, H. *Org. Lett.* **2015**, *17*, 2894. (f) Chen, Z.; Li, H.; Dong, W.; Miao, M.; Ren, H. *Org. Lett.* **2016**, *18*, 1334. (g) Yedage, S. L.; Bhanage, B. M. *J. Org. Chem.* **2016**, *81*, 4103.
6. For some examples on *C–O* bond formation, see: (a) Zhao, J.; Zhang, Q.; Liu, L.; He, Y.; Li, J.; Li, J.; Zhu, Q. *Org. Lett.* **2012**, *14*, 5362. (b) Cheung, C. W.; Buchwald, S. L. *J. Org. Chem.* **2012**, *77*, 7526. (c) Alla, S. K.; Sadhu, P.; Punniyamurthy, T. *J.*

Org. Chem. **2014**, *79*, 7502. (d) Oonishi, Y.; Suárez, A. G.; Martin, A. R.; Makida, Y.; Slawin, A. M. Z.; Nolan, S. P. *Chem.–Eur. J*. **2014**, *20*, 13507. (e) Cai, Z.-J.; Yang, C.; Wang, S.-Y.; Ji, S.-J. *Chem. Commun*. **2015**, *51*, 14267.

7. For some examples, see: (a) Nakamura, I.; Yamamoto, Y. *Chem. Rev*. **2004**, *104*, 2127. (b) D'Souza, D. M.; Rominger, F.; Muller, T. J. J. *Angew. Chem., Int. Ed*. **2005**, *44*, 153. (c) Crawley, M. L.; Goljer, I.; Jenkins, D. J.; Mehlmann, J. F.; Nogle, L.; Dooley, R.; Mahaney, P. E. *Org. Lett*. **2006**, *8*, 5837. (d) Carvalho, L. C. R.; Fernandes, E.; Marques, M. M. B. *Chem.–Eur. J*. **2011**, *17*, 12544. (e) Greenaway, R. L.; Campbell, C. D.; Holton, O. T.; Rusell, C. A.; Anderson, E. A. *Chem.–Eur. J*. **2011**, *17*, 14366. (f) Platon, M.; Amardeil, R.; Djakovitch, L.; Hierso, J.-C. *Chem. Soc. Rev*. **2012**, *41*, 3929. (g) Too, P. C.; Chiba, S. *Chem. Commun*. **2012**, *48*, 7634. (h) Gulevich, A. V.; Dudnik, A. S.; Chernyak, N.; Gevorgyan, V. *Chem. Rev.* **2013**, *113*, 3084. (i) Li, R.; Hu, Y.; Liu, R.; Hu, R.; Li, B.; Wang, B. *Adv.Synth. Catal.* **2015**, *357*, 3885. (j) Wu, J.; Xu, W.; Yu, Z.-X.; Wang, J. *J. Am. Chem. Soc.* **2015**, *137*, 9489. (k) Ling, F.; Wan, Y.; Wang, D.; Ma, C. *J. Org. Chem.* **2016**, *81*, 2770. (l) Zheng, X.-X.; Du, C.; Zhao, X.-M.; Zhu, X.; Suo, J.-F.; Hao, X.-Q.; Niu, J.-L.; Song, M.-P. *J. Org. Chem.* **2016**, **81**, 4002. (m) Zhao, M.-N.; Yu, L.; Hui, R.-R.; Ren, Z.-H.; Wang, Y.-Y.; Guan, Z.-H. *ACS Catal.* **2016**, *6*, 3473. (n) Wang, J.; Zha, S.; Chen, K.; Zhang, F.; Song, C.; Zhu, J. *Org. Lett.* **2016**, *18*, 2062. (o) Saunthwal, R. K.; Patel, M.; Verma, A. K. *Org. Lett.* **2016**, *18*, 2200. (p) Barday, M.; Ho, K. Y. T.; Halsall, C. T.; Aïssa, C. *Org. Lett.* **2016**, *18*, 1756.

8. For examples, see: (a) Cho, S. H.; Kim, J. Y.; Kwak, J.; Chang, S. *Chem. Soc. Rev.* **2011**, *40*, 5068. (b) Arockiam, P. B.; Bruneau, C.; Dixneuf, P. H. *Chem. Rev.* **2012**, *112*, 5879. (c) Kim, J. Y.; Park, S. H.; Ryu, J.; Cho, S. H.; Kim, S. H.; Chang, S. *J. Am. Chem. Soc.* **2012**, *134*, 9110. (d) Zhang, X.-G.; Dai, H.-X.; Wasa, M.; Yu, J.-Q. *J. Am. Chem. Soc.* **2012**, *134*, 11948. (e) Schröder, N.; Wencel-Delord, J.; Glorius, F. *J. Am. Chem. Soc.* **2012**, *134*, 8298. (f) Rosen, B. R.; Simke, L. R.; Thuy-Boun, P. S.; Dixon, D. D.; Yu, J.-Q.; Baran, P. S. *Angew. Chem., Int. Ed.* **2013**, *52*, 7317. (g) Sadhu. P.; Alla. S. K.; Punniyamurthy, T. *J. Org. Chem.* **2013**, *78*, 6104. (h) Thirunavukkarasu, V. S.; Kozhushkov, S. I.; Ackermann, L. *Chem. Commun.* **2014**, *50*, 29. (i) Becker, P.; Priebbenow, D. L.; Pirwerdjan, R.; Bolm, C. *Angew. Chem., Int. Ed.* **2014**, *53*, 269. (j) Parthasarathy, K.; Bolm, C. *Chem.-Eur. J.* **2014**, *20*, 4896. (k) Zhao, D.; Lied, F.; Glorius, F. *Chem. Sci.* **2014**, *5*, 2869. (l) Yokoyama, Y.; Unoh,

Y.; Hirano, K.; Satoh, T.; Miura, M. *J. Org. Chem.* **2014**, *7 9*, 7649. (m) Wu, Y.; Jiang, C.; Wu, D.; Gu, Q.; Luo, Z.-Y.; Luo, H.-B. *Chem. Commun.* **2016**, *52*, 1286. (n) Zhou, X.; Yu, S.; Qi, Z.; Kong, L.; Li, X. *J. Org. Chem.* **2016**, *81*, 4869. (o) Zhang, L.-B.; Zhang, S.-K.; Wei, D.; Zhu, X.; Hao, X.-Q.; Su, J.-H.; Niu, J.-L.; Song, M.-P. *Org. Lett.* **2016**, *18*, 1318. (p) Okada, T.; Nobushige, K.; Satoh, T.; Miura, M. *Org. Lett.* **2016**, *18*, 1150.

9. For examples, see: (a) Hirao, T. *Chem. Rev.* **1997**, *97*, 2707. (b) Taniguchi, Y.; Hayashida, T.; Shibasaki, H.; Piao, D.; Kitamura, T.; Yamaji, T.; Fujiwara, Y. *Org. Lett.* **1999**, *1*, 557. (c) Lorber, C.; Choukroun, R.; Vendier, L. *Organometallics* **2004**, *23*, 1845. (d) Velusamy, S.; Punniyamurthy, T. *Org. Lett.* **2004**, *6*, 217. (e) Radosevich, A. T.; Musich, C.; Toste, F. D.; *J. Am. Chem. Soc.* **2005**, *127*, 1090. (f) Zhang, S.; Nomura, K. *J. Am. Chem. Soc.* **2010**, *132*, 4960. (g) Ramos-Luna, M. A.; Cedeno-Caero, L. *Ind. Eng. Chem. Res.* **2011**, *50*, 2641. (h) Nomura, K.; Matsumoto, Y. *Organometallics* **2011**, *30*, 3610. (i) McLauchlan, C. C.; Crans, D. C. *Dalton Trans* **2013**, *42*, 11744. (j) Strassberger, Z.; Ramos-Fernandez, E. V.; Boonstra, A.; Jorna, R.; Tanase, S.; Rothenberg, G. *Dalton Trans* **2013**, *42*, 5546. (k) Liu, L.; Carroll, P. J.; Kozlowski, M. C. *Org. Lett.* **2015**, *17*, 508.

10. For some recent examples, see: (a) Girard, S. A.; Knauber, T.; Li, C.-J. *Angew. Chem., Int. Ed.* **2014**, *53*, 74. (b) Tran, B. L.; Driess, M.; Hartwig, J. F. *J. Am. Chem. Soc.* **2014**, *136*, 17292. (c) Zhao, J.; Fang, H.; Zhou, W.; Han, J.; Pan, Y. *J. Org. Chem.* **2014**, *79*, 3847. (d) Cheng, Y.; Dong, W.; Wang, L.; Parthasarathy, K.; Bolm, C. *Org. Lett.* **2014**, *16*, 2000.

11. For examples, see: (a) Ishii, Y.; Matsunaka, K.; Sakaguchi, S. *J. Am. Chem. Soc.* **2000**, *122*, 7390. (b) Hirao, T.; Morimoto, C.; Takada, T.; Sakurai, H. *Tetrahedron* **2001**, *57*, 5073. (c) Punniyamurthy, T.; Velusamy, S.; Iqbal, J. *Chem. Rev.* **2005**, *105*, 2329.

12. For examples, see: (a) Narayan, S.; Muldoon, J.; Finn, M. G.; Fokin, V. V.; Kolb, H. C.; Sharpless, K. B. *Angew. Chem., Int. Ed.* **2005**, *44*, 3275. (b) Shapiro, N.; Vigalok, A. *Angew. Chem., Int. Ed.* **2008**, *47*, 2849. (c) Jammi, S.; Ali, M. A.; Sakthivel, S.; Rout, L.; Punniyamurthy, T. *Chem. Asian J.* **2009**, *4*, 314. (d) Mellouli, S.; Bousekkine, L.; Theberge, A. B.; Huck, W. T. S. *Angew. Chem., Int. Ed.* **2012**, *51*, 7981. (e) Sengoden, M.; Punniyamurthy, T. *Angew. Chem., Int. Ed.* **2013**, *52*, 572.

13. (a) Sui, Z.; Guan, J.; Ferro, M. P.; McCoy, K.; Wachter, M. P.; Murray, W. V.; Singer, M.; Steber, M.; Ritchie, D. M.; Argentieri, D. C. *Bioorg. Med. Chem. Lett*. **2000**, *10*, 601. (b) Katoch-Rouse, R.; Pavlova, L. A.; Caulder, T.; Hoffman, A. F.; Mukhin, A. G.; Horti, A. G. *J. Med. Chem.* **2003**, *46*, 642. (c) Sridhar, R.; Perumal, P. T.; Etti, S.; Shanmugam, G.; Ponnuswamy, M. N.; Prabavathyc, V. R.; Mathivanan, N. *Bioorg. Med. Chem. Lett.* **2004**, *14*, 6035. (d) Selvam, C.; Jachak, S. M.; Thilagavathi, R.; Chakraborti, A. K. *Bioorg. Med. Chem. Lett*. **2005**, *15*, 1793. (e) Lee, E.; Choi, M. K.; Youk, H. J.; Kim, C. H.; Han, I. C.;Yoo, B. C.; Lee, M. K.; Lim, S. J. *J. Cancer Res. Clin. Oncol.* **2006**, *132*, 223. (f) Gilbert, A. M.; Failli, A.; Shumsky, J.; Yang, Y.; Severin, A.; Singh, G.; Hu, W.; Keeney, D.; Petersen, P. J.; Katz, A. H. *J. Med. Chem*. **2006**, *49*, 6027. (g) Magedov, I. V.; Manpadi, M.; Slambrouck, S. V.; W.F.A. Steelant, W. F. A.; Rozhkova, E.; Przheval'skii, N. M.; Rogelj, S.; Kornienko, A. *J. Med. Chem*. **2007**, *50*, 5183. (h) Sun, A.; Yoon, J. J.; Yin, Y.; Prussia, A.; Yang, Y.; Min, J.; Plemper, R. K.; Snyder, J. P. *J. Med. Chem.* **2008**, *51*, 3731. (i) Tewari, A. K.; Singh, V. P.; Yadav, P.; Gupta, G.; Singh, A.; Goel, R. K.; Shinde, P.; Mohan, C. G. *Bioorg. Chem.* **2014**, *56*, 8.

14. (a) Terrett, N. K.; Bell, A. S.; Brown, D.; Ellis, P. *Bioorg. Med. Chem. Lett.* **1996**, *6*, 1819. (b) Hainzl, D.; Casida, J. E. *Proc. Natl. Acad. Sci. USA* **1996**, *93*, 12764. (c) Penning, T. D.; Talley, J. J.; Bertenshaw, S. R.; Carter, J. S.; Collins, P. W.; Docter, S.; Graneto, M. J.; Lee, L. F.; Malecha, J. W.; Miyashiro, J. M.; Rogers, R. S.; Rogier, D. J.; Yu, S. S.; Anderson, G. D.; Burton, E. G.; Cogburn, J. N.; Gregory, S. A.; Koboldt, C. M.; Perkins, W. E.; Seibert, K.; Veenhuizen, A. W.; Zhang, Y. Y.; Isakson, P. C. *J. Med. Chem.* **1997**, *40*, 1347.

15. (a) Mukherjee, R. *Coord. Chem.Rev.* **2000**, *203*, 151. (b) Dolars, A.; Schellhammer, C.-W.; Schroeder, J. *Angew. Chem., Int. Ed. Engl.* **1975**, *14*, 665. (c) Catalan, J.; Fabero, F.; Claramunt, R. M.; Santa Maria, M. D.; Foces-Foces, M. C.; Hernandez Cano, F.; Martinez-Ripoll, M.; Elguero, J.; Sastre, R. *J. Am. Chem. Soc.* **1992**, *114*, 5039.

16. For synthesis of pyrazoles, see: (a) Landge, S. M.; Schmidt, A.; Outerbridge, V.; Török, B. *Synlett* **2007**, 1600. (b) Neumann, J. J.; Suri, M.; Glorius, F. *Angew. Chem., Int. Ed.* **2010**, *49*, 7790. (c) Fustero, S.; Sanchez-Rosello, M.; Barrio, P.; Simon-Fuentes, A. *Chem. Rev.* **2011**, *111*, 6984. (d) Zhang, T.; Bao, W. *J. Org.*

Chem. **2013**, *78*, 1317. (e) Ananthnag, G. S.; Adhikari, A. Balakrishna, M. S. *Catal. Commun.* **2014**, *43*, 240.

17. Knorr, L. *Ber. Dtsch. Chem. Ges.* **1883**, *16*, 2597.
18. (a) Aggarwal, V. K.; de Vicente, J.; Bonnert, R. V. *J. Org. Chem.* **2003**, *68*, 5381. (b) Jianga, N.; Li, C.-J. *Chem. Commun.* **2004**, 394. (c) Muruganantham, R.; Mobin, S. M.; Namboothiri, I. N. N. *Org. Lett.* **2007**, *9*, 1125. (d) Qi, X.; Ready, J. M. *Angew. Chem., Int. Ed.* **2007**, *46*, 3242. (e) Vuluga, D.; Legros, J.; Crousse, B.; Bonnet-Delpon, D. *Green Chem.* **2009**, *11*, 156. (f) Xie, J.-W.; Wang, Z.; Yang, W.-J.; Kong, L.-C.; Xu, D.-C. *Org. Biomol. Chem.* **2009**, *7*, 4352.
19. (a) Donohue, A. C.; Pallich, S.; McCarthy, T. D. *J. Chem. Soc., Perkin Trans. 1.* **2001**, 2817. (b) Conti, P.; Pinto, A.; Tamborini, L.; Rizzo, V.; De Micheli, C. *Tetrahedron* **2007**, *63*, 5554. (c) Abunada, N. M.; Hassaneen, H. M.; Kandile, N. G.; Miqdad, O. A. *Molecules* **2008**, *13*, 1501. (d) Sun, A.; Ye, J.-H.; Yu, H.; Zhang, W.; Wang, X. *Tetrahedron Lett.* **2014**, *55*, 889.
20. (a) Rai, G.; Puranik, V. G.; Kalluraya, B.; Hegde, J. C. *Synth. Commun.* **2006**, *36*, 1285. (b) Foster, R. S.; Jakobi, H.; Harrity, J. P. A. *Org. Lett.* **2012**, *14*, 4858.
21. (a) Zora, M.; Kivrak, A. *J. Org. Chem.* **2011**, *76*, 9379. (b) Qian, J.; Liu, Y.; Zhu, J.; Jiang, B.; Xu, Z. *Org. Lett.* **2011**, *13*, 4220. (c) Bharathiraja, G.; Sengoden, M.; Kannan, M.; Punniyamurthy, T. *Org. Biomol. Chem.* **2015**, *13*, 2786. (d) Jeyaveeran, J. C.; Praveen, C.; Arun, Y.; Prince, A. A. M.; Perumal, P. T. *J. Chem. Sci.* **2016**, *128*, 73.
22. (a) Mohamed Ahmed, M. S.; Kobayashi, K.; Mori, A. *Org. Lett.* **2005**, *7*, 4487. (b) Chen, B.; Zhu, C.; Tang. Y.; Ma.; S. *Chem. Commun.* **2014**, *50*, 7677.
23. (a) Antilla, J. C.; Baskin, J. M.; Barder, T. E.; Buchwald, S. L. *J. Org. Chem.* **2004**, *69*, 5578. (b) Kumar, S.; Ila, H.; Junjappa, H. *J. Org. Chem.* **2009**, *74*, 7046.
24. (a) Dvorak, C. A.; Rudolph, D. A.; Ma, S.; Carruthers, N. I. *J. Org. Chem.* **2005**, *70*, 4188. (b) Jeon, S. L.; Choi, J. H.; Kim, B. T.; Jeong, I. H. *J. Fluorine. Chem.* **2007**, *128*, 1191.
25. (a) Hu, J.; Chen, S.; Sun, Y.; Yang, J.; Rao, Y. *Org. Lett.* **2012**, *14*, 5030. (b) Li, X.; He, L.; Chen, H.; Wu, W.; Jiang, H. *J. Org. Chem.* **2013**, *78*, 3636.

26. Conn, R. S. E.; Douglas, A. W.; Karady, S.; Corley, E. G.; Lovell, A. V.; Shinkai, I. *J. Org. Chem.* **1990**, *55*, 2908.

27. (a) Kim, B. R.; Sung, G. H.; Ryu, K. E.; Lee, S.-G.; Yoon, H. J.; Shin, D.-S.; Yoon, Y.-J. *Chem. Commun.* **2015**, *51*, 9201. (b) Sar, D.; Paul, R.; Sengoden, M.; Punniyamurthy, T. *Asian J. Org. Chem*. **2014**, *3*, 638. (c) Liang, D.; Zhu, Q. *Asian J. Org. Chem*. **2015**, *4*, 42.

2.6 Selected Spectra

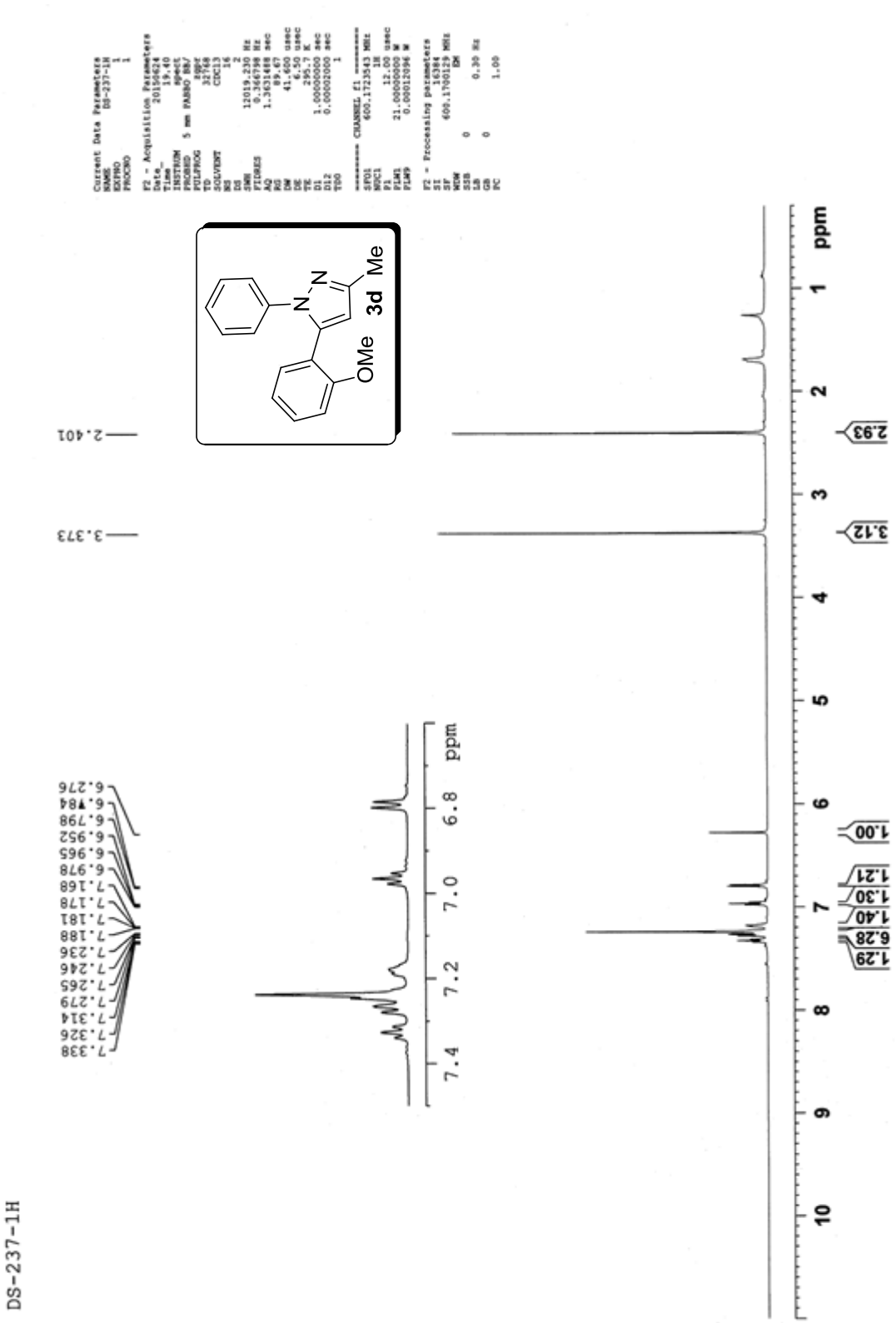

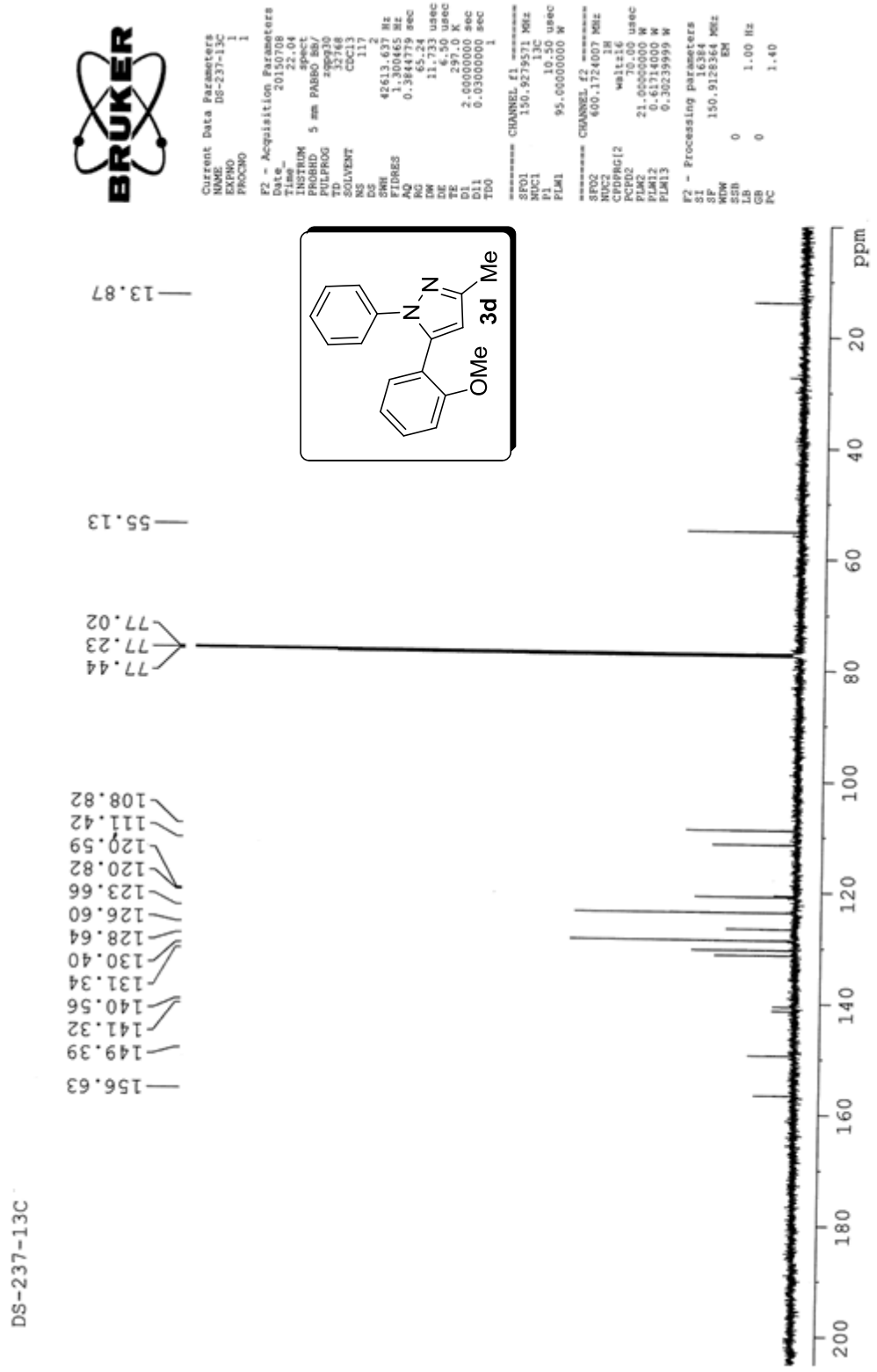
BRUKER
Current Data Parameters
NAME DS-237-13C
EXPNO 1
PROCNO 1
F2 - Acquisition Parameters
Date_ 20151008
Time 22.04
INSTRUM spect
PROBHD 5 mm PABBO BB/
PULPROG zgpg30
TD 32768
SOLVENT CDCl3
NS 117
DS 2
SWH 42613.637 Hz
FIDRES 1.300465 Hz
AQ 0.3844779 sec
RG 65.24
DW 11.733 usec
DE 6.50 usec
TE 297.0 K
D1 2.00000000 sec
D11 0.03000000 sec
TD0 1
======== CHANNEL f1 ========
SFO1 150.9279571 MHz
NUC1 13C
P1 10.50 usec
PLW1 95.00000000 W
======== CHANNEL f2 ========
SFO2 600.1724007 MHz
NUC2 1H
CPDPRG[2 waltz16
PCPD2 70.00 usec
PLW2 21.00000000 W
PLW12 0.61714000 W
PLW13 0.30239999 W
F2 - Processing parameters
SI 16384
SF 150.9128364 MHz
WDW EM
SSB 0
LB 1.00 Hz
GB 0
PC 1.40
OMe
3d
Me
13.87
55.13
77.02
77.23
77.44
108.82
111.42
120.59
120.82
123.66
126.60
128.64
130.40
131.34
140.56
141.32
149.39
156.63
ppm
20
40
60
80
100
120
140
160
180
200
DS-237-13C

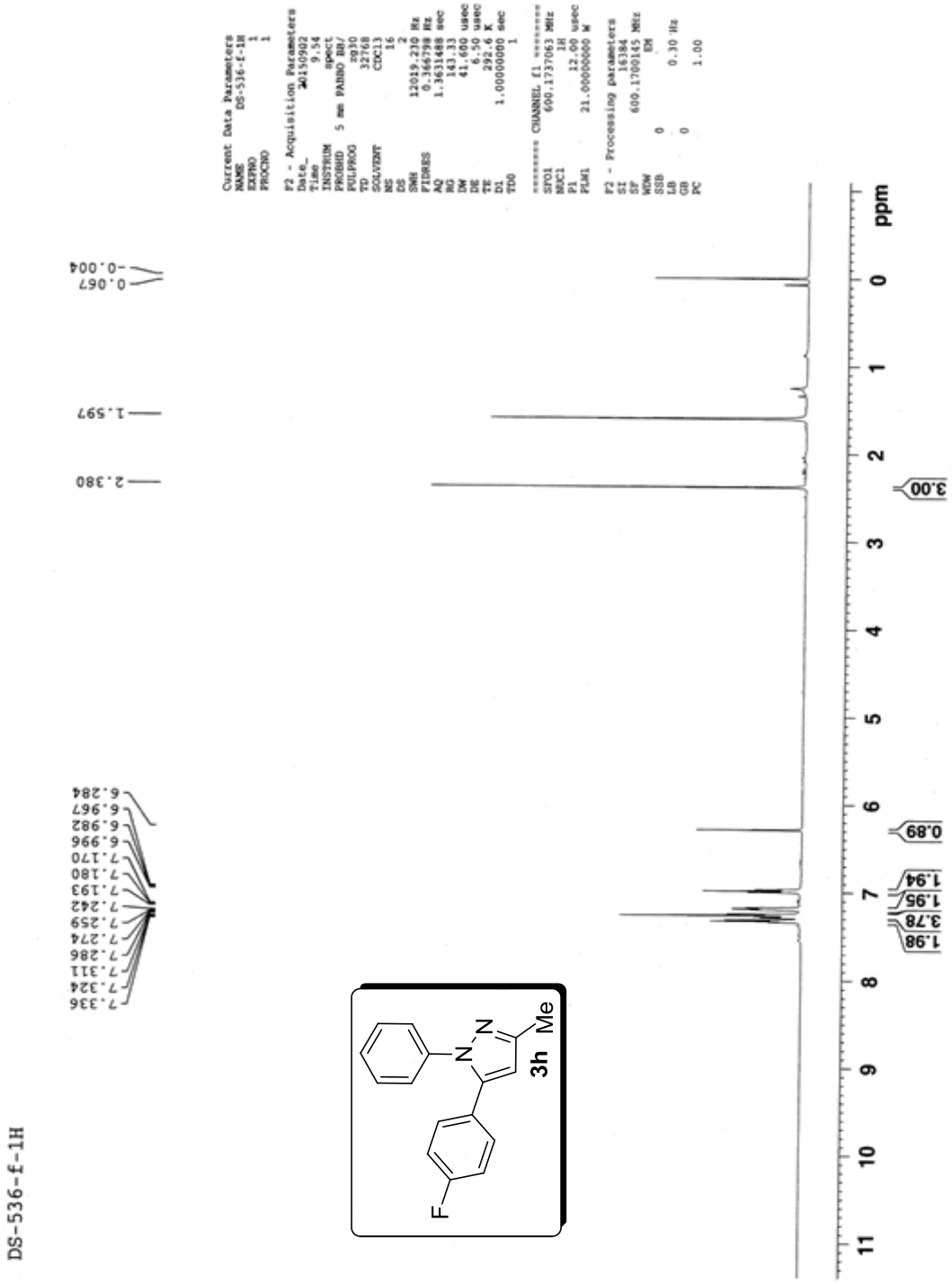
DS-536-f-1H
Current Data Parameters
NAME DS-536-f-1H
EXPNO 1
PROCNO 1
F2 - Acquisition Parameters
Date_ 20150902
Time 9.54
INSTRUM spect
PROBHD 5 mm PABBO BB/
PULPROG zg30
TD 32768
SOLVENT CDCl3
NS 16
DS 2
SWH 12019.230 Hz
FIDRES 0.366798 Hz
AQ 1.36311488 sec
RG 143.33
DW 41.600 usec
DE 6.50 usec
TE 292.6 K
D1 1.00000000 sec
TD0 1
======== CHANNEL f1 ========
SFO1 600.1737063 MHz
NUC1 1H
P1 12.00 usec
PLW1 21.00000000 W
F2 - Processing parameters
SI 16384
SF 600.1700145 MHz
WDW EM
SSB 0
LB 0.30 Hz
GB 0
PC 1.00
0.067
-0.004
1.597
2.380
6.284
6.967
6.982
6.996
7.170
7.180
7.193
7.242
7.259
7.274
7.286
7.311
7.324
7.336
3h
Me
F
3.00
0.89
1.94
1.95
3.78
1.98
ppm

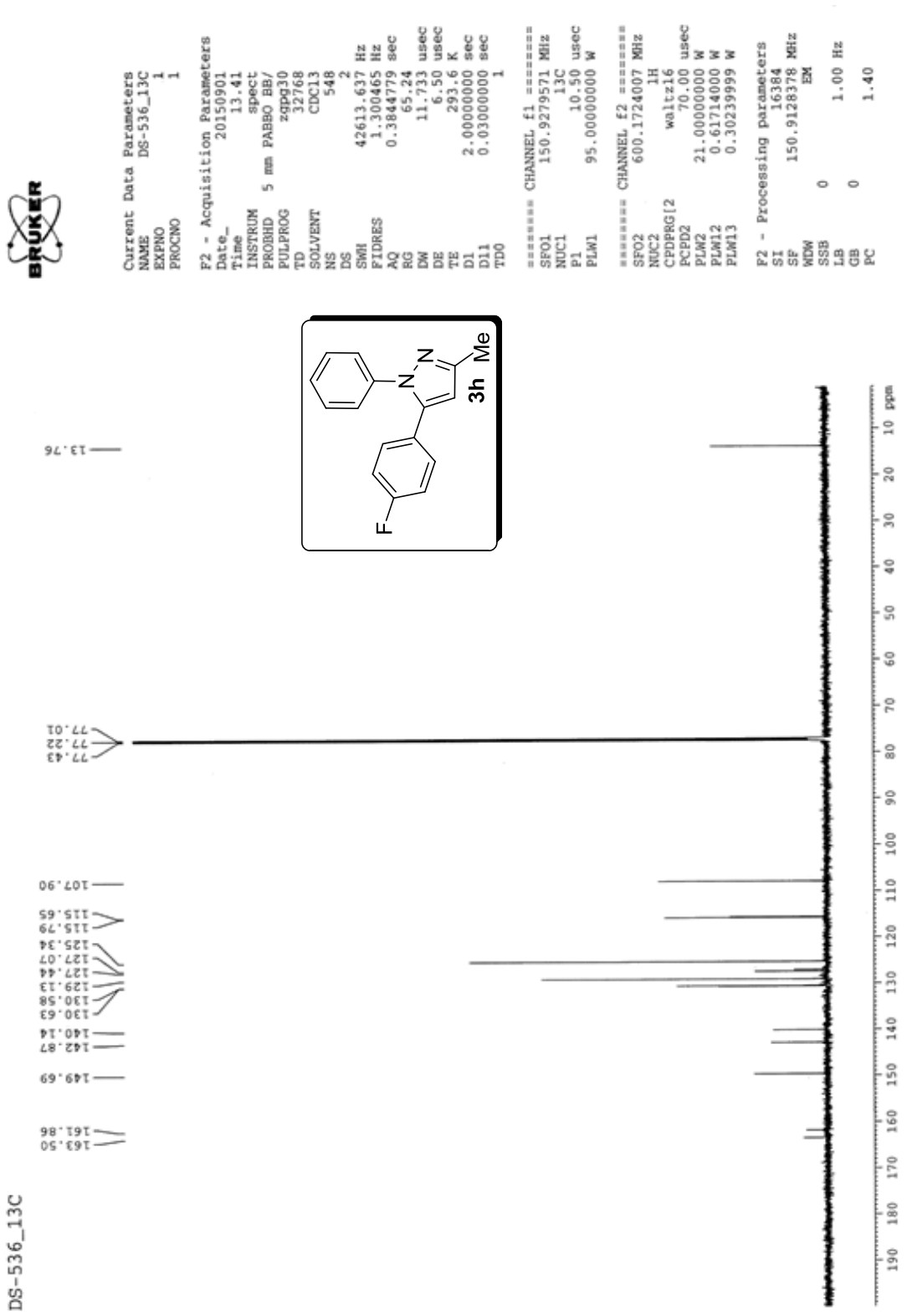
BRUKER
Current Data Parameters
NAME DS-536_13C
EXPNO 1
PROCNO 1
F2 - Acquisition Parameters
Date_ 20150901
Time 13.41
INSTRUM spect
PROBHD 5 mm PABBO BB/
PULPROG zgpg30
TD 32768
SOLVENT CDCl3
NS 548
DS 2
SWH 42613.637 Hz
FIDRES 1.300465 Hz
AQ 0.3844779 sec
RG 65.24
DW 11.733 usec
DE 6.50 usec
TE 293.6 K
D1 2.00000000 sec
D11 0.03000000 sec
TD0 1
======== CHANNEL f1 ========
SFO1 150.9279571 MHz
NUC1 13C
P1 10.50 usec
PLW1 95.00000000 W
======== CHANNEL f2 ========
SFO2 600.1724007 MHz
NUC2 1H
CPDPRG[2 waltz16
PCPD2 70.00 usec
PLW2 21.00000000 W
PLW12 0.61714000 W
PLW13 0.30239999 W
F2 - Processing parameters
SI 16384
SF 150.9128378 MHz
WDW EM
SSB 0
LB 1.00 Hz
GB 0
PC 1.40
3h
Me
N
N
F
13.76
77.01
77.22
77.43
107.90
115.65
115.79
125.34
127.07
127.44
129.13
130.58
130.63
140.14
142.87
149.69
161.86
163.50
DS-536_13C
ppm

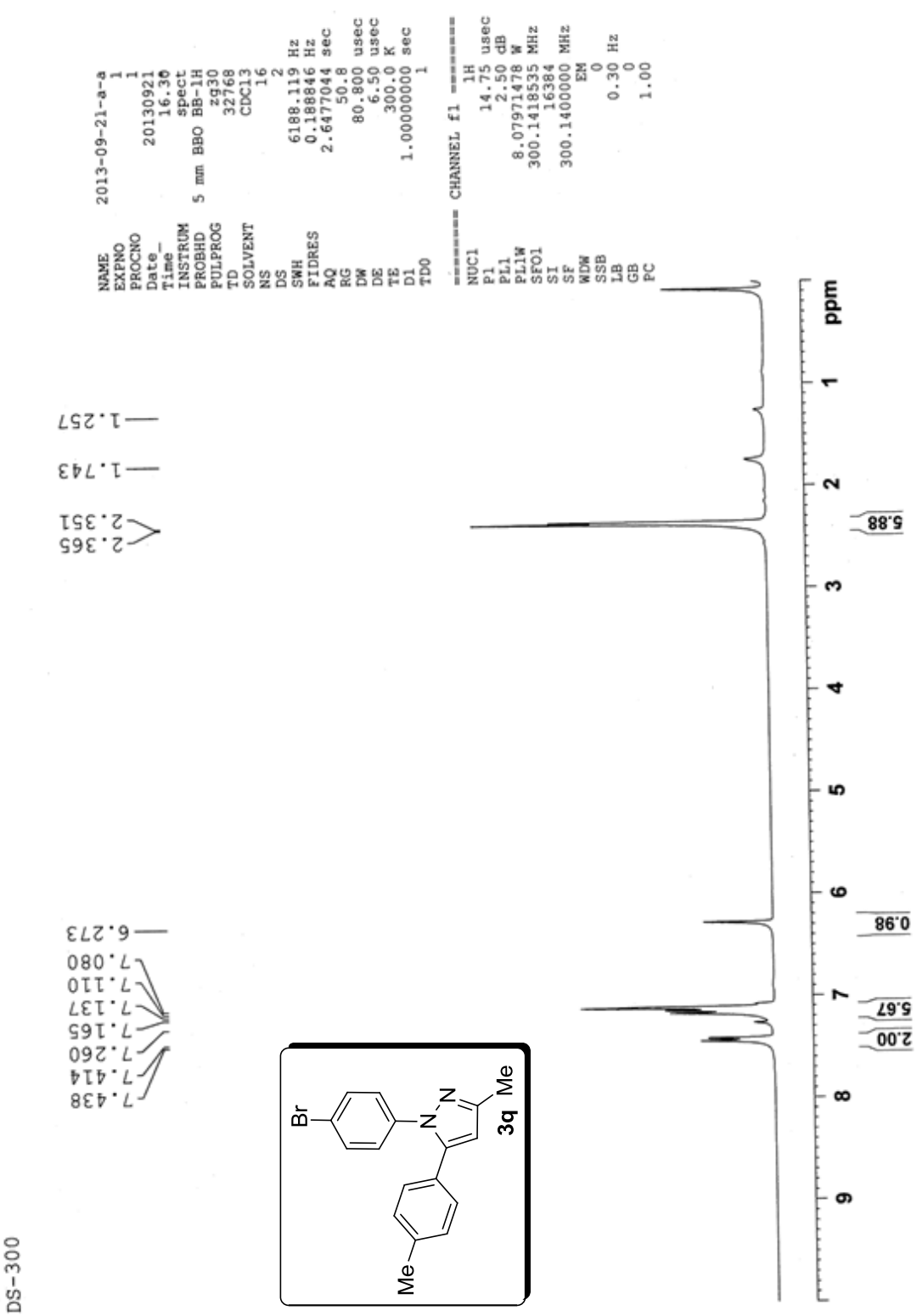
DS-300
NAME 2013-09-21-a-a
EXPNO 1
PROCNO 1
Date_ 20130921
Time_ 16.36
INSTRUM spect
PROBHD 5 mm BBO BB-1H
PULPROG zg30
TD 32768
SOLVENT CDC13
NS 16
DS 2
SWH 6188.119 Hz
FIDRES 0.188846 Hz
AQ 2.6477044 sec
RG 50.8
DW 80.800 usec
DE 6.50 usec
TE 300.0 K
D1 1.00000000 sec
TD0 1
======== CHANNEL f1 ========
NUC1 1H
P1 14.75 usec
PL1 2.50 dB
PL1W 8.07971478 W
SFO1 300.1418535 MHz
SI 16384
SF 300.1400000 MHz
WDW EM
SSB 0
LB 0.30 Hz
GB 0
PC 1.00
1.257
1.743
2.351
2.365
6.273
7.080
7.110
7.137
7.165
7.260
7.414
7.438
5.88
0.98
5.67
2.00
ppm
Br
Me
Me
3q

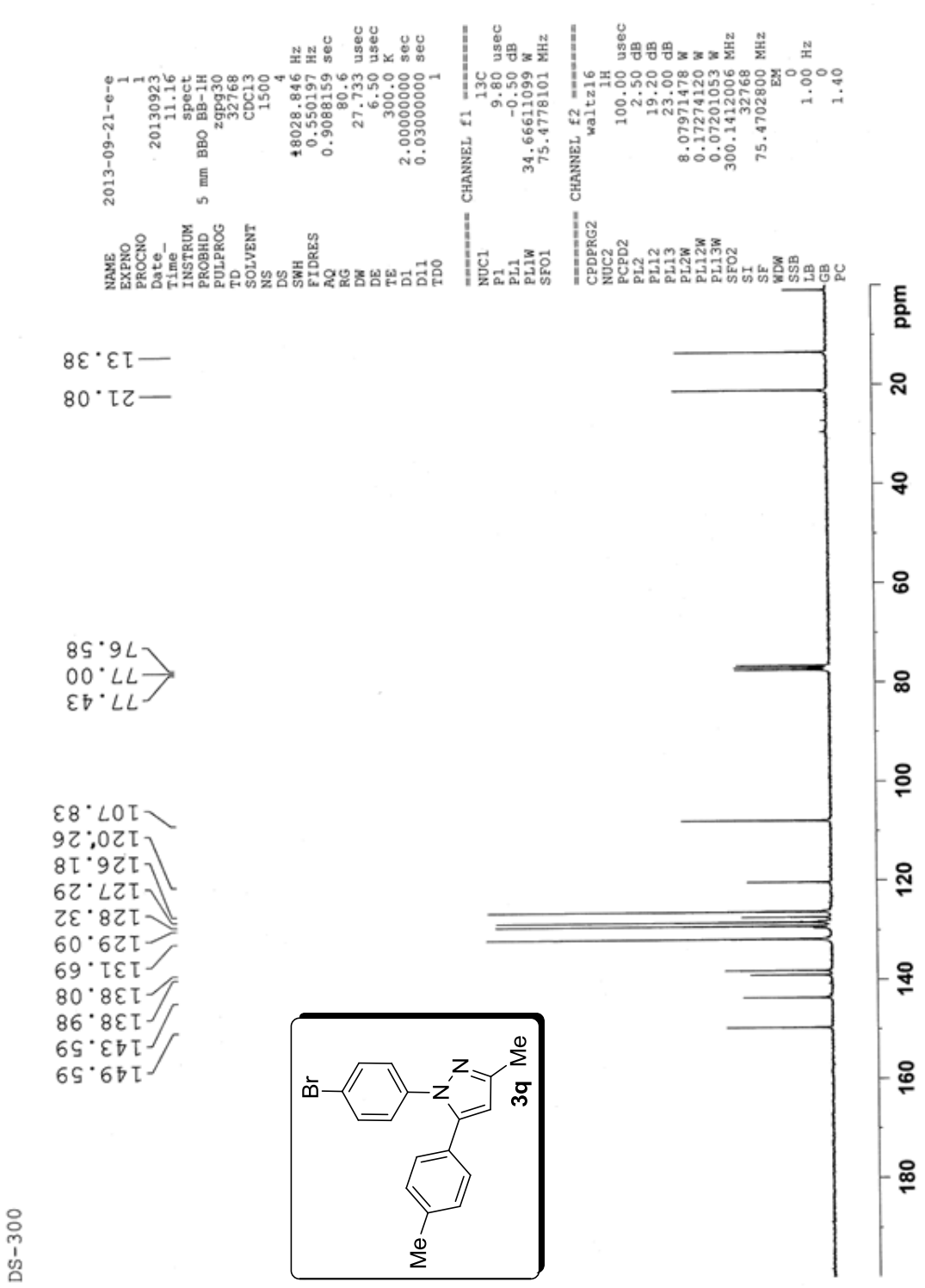
NAME 2013-09-21-e-e
EXPNO 1
PROCNO 1
Date_ 20130923
Time 11.16
INSTRUM spect
PROBHD 5 mm BBO BB-1H
PULPROG zgpg30
TD 32768
SOLVENT CDCl3
NS 1500
DS 4
SWH 18028.846 Hz
FIDRES 0.550197 Hz
AQ 0.9088159 sec
RG 80.6
DW 27.733 usec
DE 6.50 usec
TE 300.0 K
D1 2.00000000 sec
D11 0.03000000 sec
TD0 1
======== CHANNEL f1 ========
NUC1 13C
P1 9.80 usec
PL1 -0.50 dB
PL1W 34.66611099 W
SFO1 75.4778101 MHz
======== CHANNEL f2 ========
CPDPRG2 waltz16
NUC2 1H
PCPD2 100.00 usec
PL2 2.50 dB
PL12 19.20 dB
PL13 23.00 dB
PL2W 8.07971478 W
PL12W 0.17274120 W
PL13W 0.07201053 W
SFO2 300.1412006 MHz
SI 32768
SF 75.4702800 MHz
WDW EM
SSB 0
LB 1.00 Hz
GB 0
PC 1.40
13.38
21.08
77.43
77.00
76.58
107.83
120.26
126.18
127.29
128.32
129.09
131.69
138.08
138.98
143.59
149.59
Br
N
N
Me
Me
3q
ppm
180
160
140
120
100
80
60
40
20
DS-300

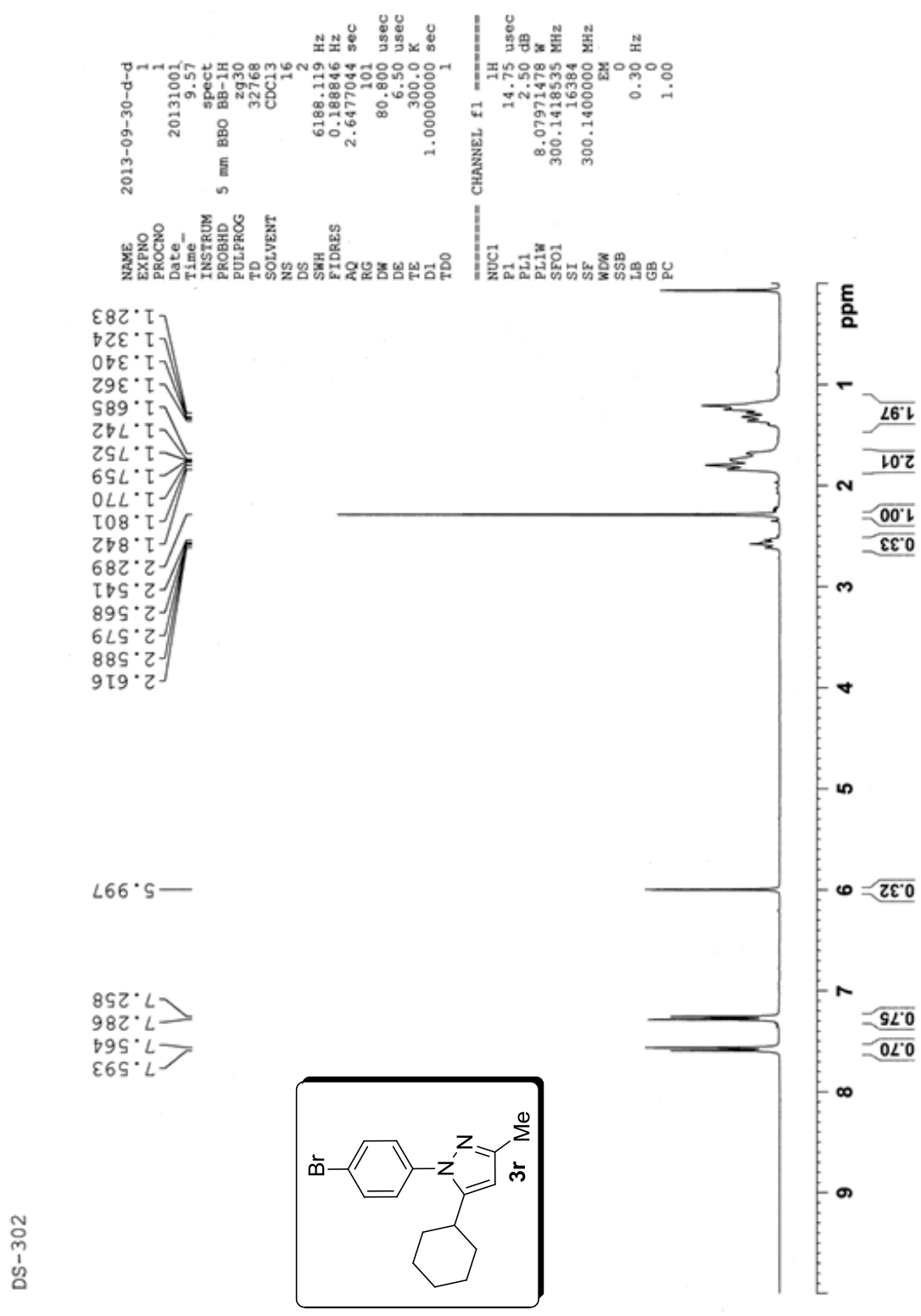
DS-302
3r
Br
Me
N
N
ppm
1.97
2.01
1.00
0.33
0.32
0.75
0.70
7.593
7.564
7.286
7.258
5.997
2.616
2.588
2.579
2.568
2.541
2.289
1.842
1.801
1.770
1.759
1.752
1.742
1.685
1.362
1.340
1.324
1.283
NAME
EXPNO
PROCNO
Date_
Time
INSTRUM
PROBHD
PULPROG
TD
SOLVENT
NS
DS
SWH
FIDRES
AQ
RG
DW
DE
TE
D1
TD0
CHANNEL f1
NUC1
P1
PL1
PLIW
SFO1
SI
SF
WDW
SSB
LB
GB
PC

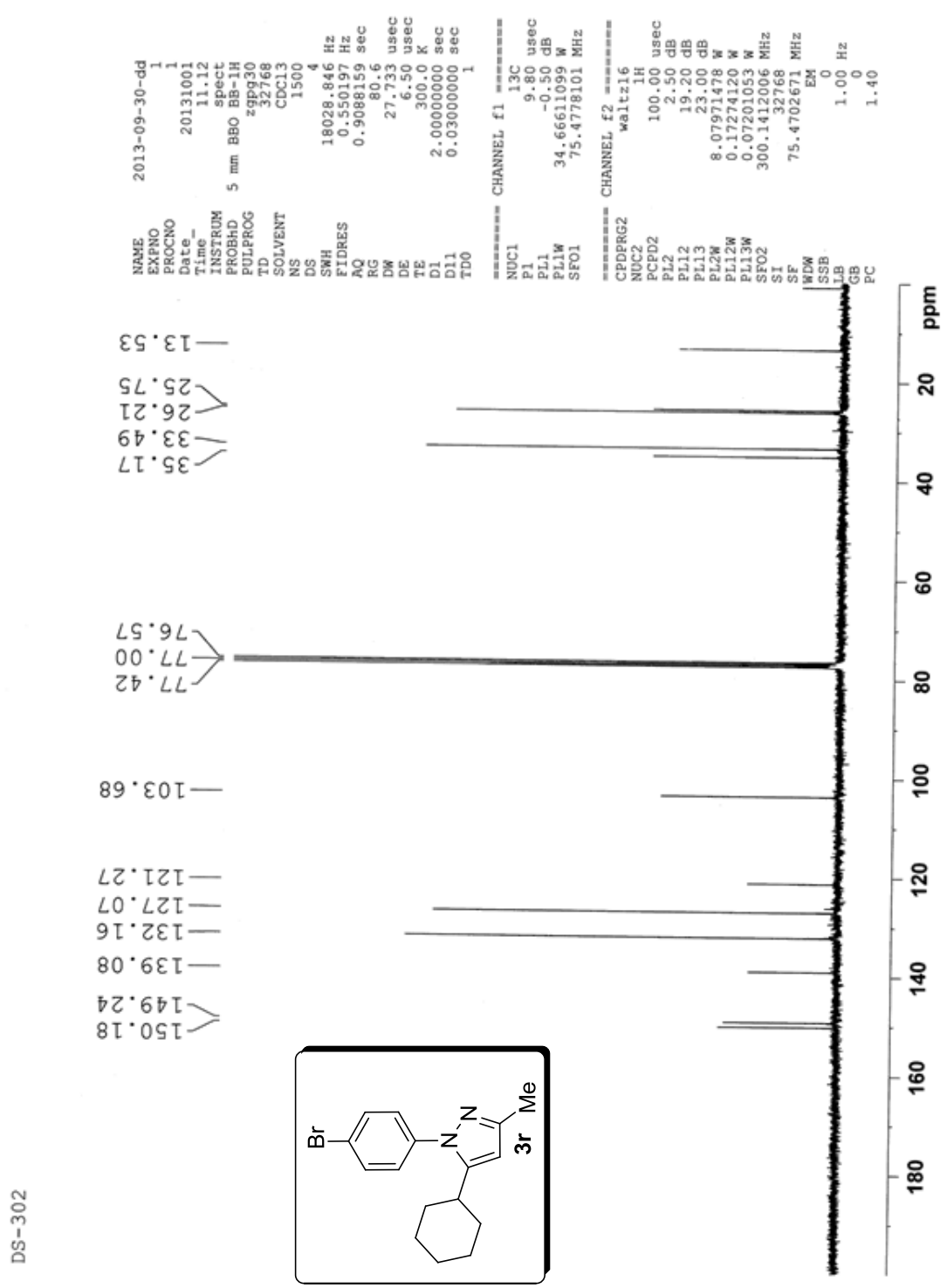
DS-302
NAME
EXPNO
PROCNO
Date_
Time_
INSTRUM
PROBHD
PULPROG
TD
SOLVENT
NS
DS
SWH
FIDRES
AQ
RG
DW
DE
TE
D1
D11
TD0
CHANNEL f1
NUC1
P1
PL1
PL1W
SFO1
CHANNEL f2
CPDPRG2
NUC2
PCPD2
PL2
PL12
PL13
PL2W
PL12W
PL13W
SFO2
SI
SF
WDW
SSB
LB
GB
PC
13.53
25.75
26.21
33.49
35.17
76.57
77.00
77.42
103.68
121.27
127.07
132.16
139.08
149.24
150.18
Br
N
N
Me
3r
ppm

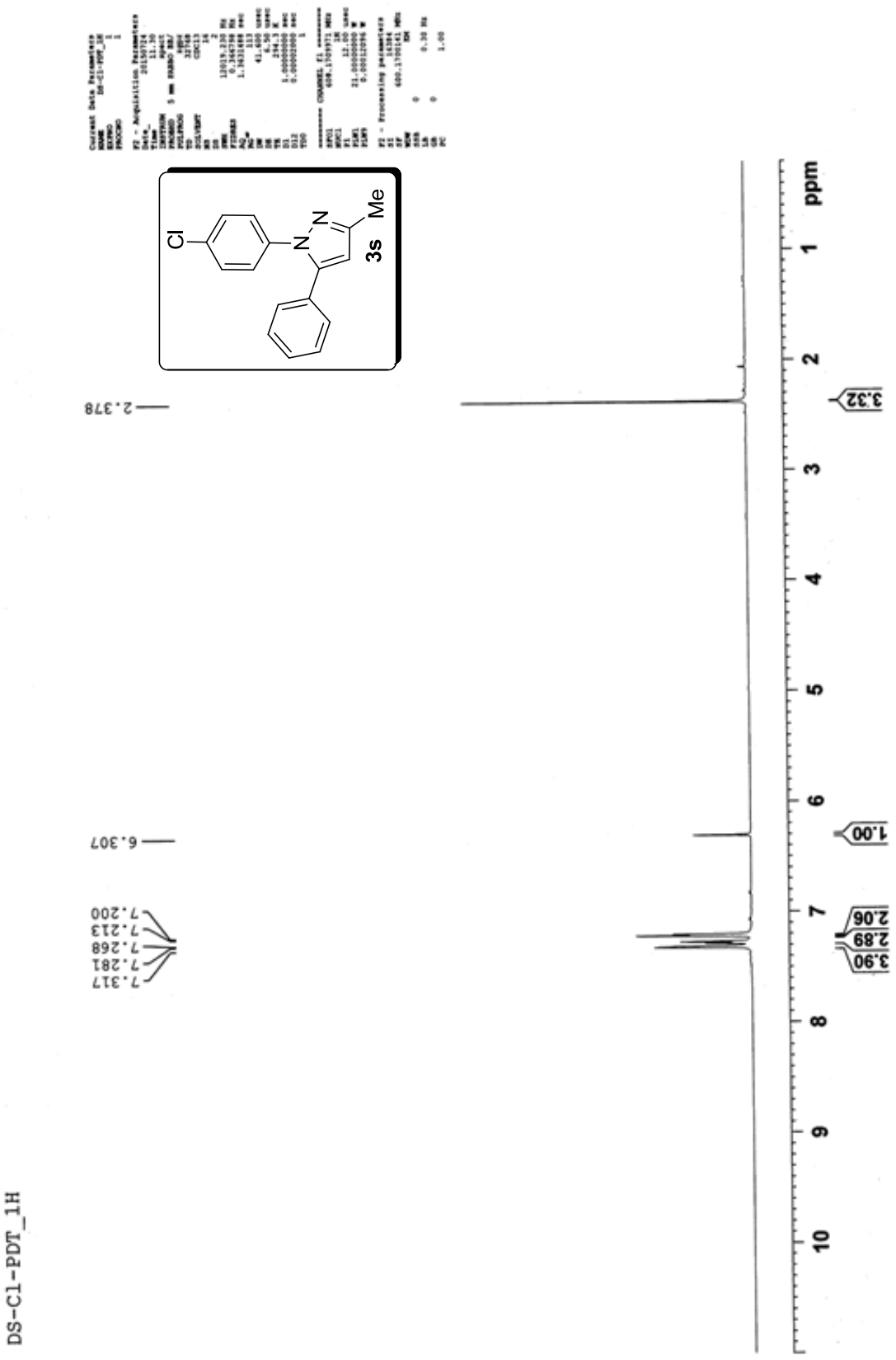
DS-Cl-PDT_1H
Cl
N
N
Me
3s
ppm
1
2
3
4
5
6
7
8
9
10
3.32
1.00
2.06
2.89
3.90
2.378
6.307
7.200
7.213
7.268
7.281
7.317

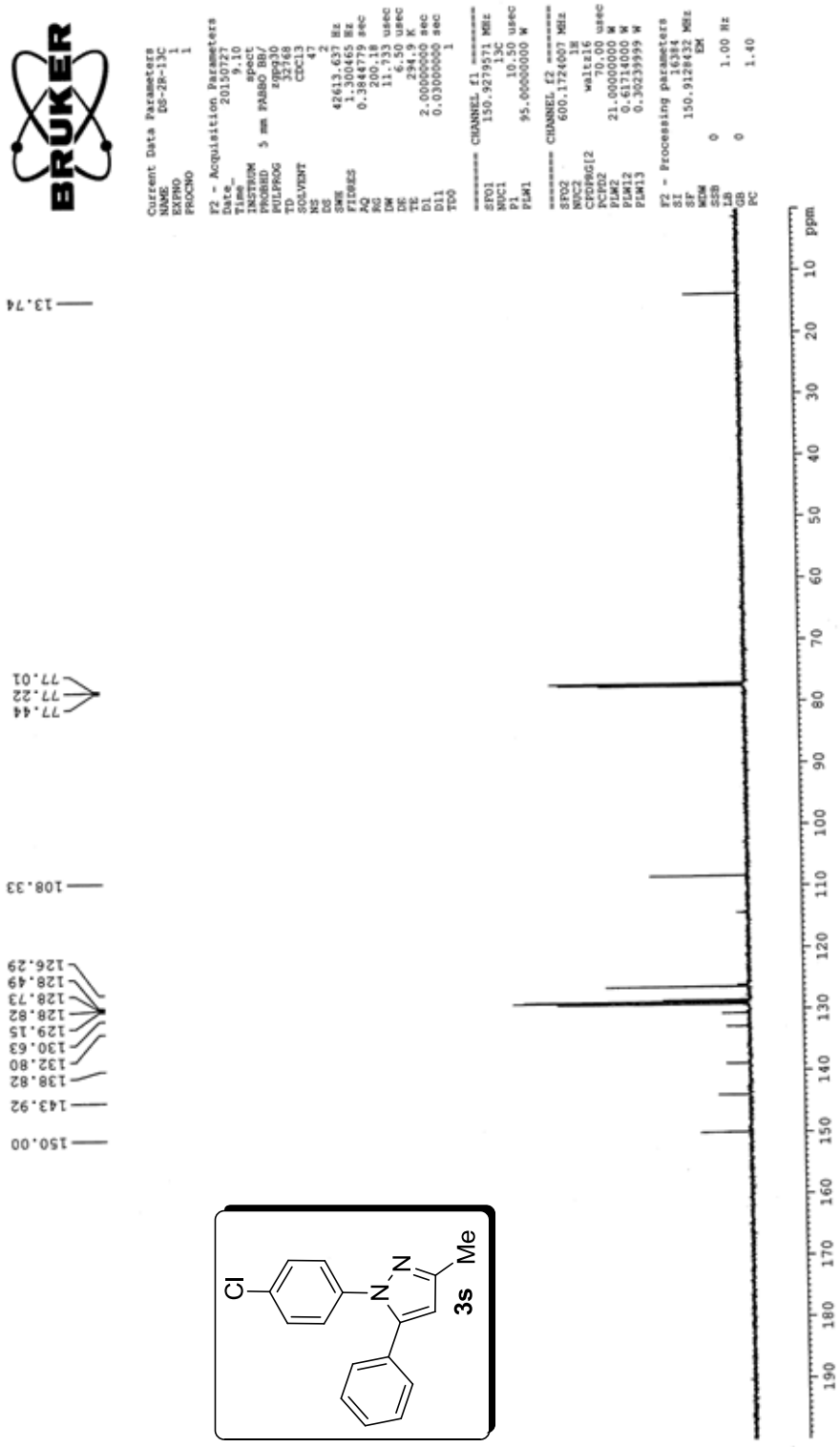
BRUKER
Current Data Parameters
NAME DS-2R-13C
EXPNO 1
PROCNO 1
F2 - Acquisition Parameters
Date_ 20150727
Time_ 9.10
INSTRUM spect
PROBHD 5 mm PABBO BB/
PULPROG zgpg30
TD 32768
SOLVENT CDCl3
NS 47
DS 2
SWH 42613.633 Hz
FIDRES 1.300465 Hz
AQ 0.3844779 sec
RG 200.18
DW 11.733 usec
DE 6.50 usec
TE 294.9 K
D1 2.00000000 sec
D11 0.03000000 sec
TD0 1
======== CHANNEL f1 ========
SFO1 150.9279571 MHz
NUC1 13C
P1 10.50 usec
PLW1 95.00000000 W
======== CHANNEL f2 ========
SFO2 600.1724007 MHz
NUC2 1H
CPDPRG[2 waltz16
PCPD2 70.00 usec
PLW2 21.00000000 W
PLW12 0.61714000 W
PLW13 0.30239999 W
F2 - Processing parameters
SI 16384
SF 150.9128432 MHz
WDW EM
SSB 0
LB 1.00 Hz
GB 0
PC 1.40
13.74
77.44
77.22
77.01
108.33
126.29
128.49
128.73
128.82
129.15
130.63
132.80
138.82
143.92
150.00
ppm
Cl
N
N
Me
3s

Chapter III

TEMPO/NBS Mediated C-H Oxidative Cyclization of Vinylhydrazones: Synthesis of Substituted Pyrazoles

Functionalized nitrogen and oxygen containing heterocyclic compounds are of incredible importance as they form the core of many biologically active molecules.[1] Among them, pyrazole is one of the important heterocyclic compounds, which have been attracted recent research interests.[2,3] Several transition metals, such as Cu, Fe, Rh, Ru, Pd, catalyzed methodologies have been explored for the synthesis of pyrazole.[4] In addition, few reports are focused on the metal-free synthesis of substituted pyrazoles.[5] However, these methodologies suffer from disadvantages such as, use of strong acid/base with elevated temperature, difficulties of preparation of starting materials and longer reaction time. Therefore, there is need to develop new metal-free protocols for the construction of medicinally important pyrazoles under mild reaction conditions. In this chapter, we report 2,2,6,6-tetramethylpiperidine-1-oxyl (TEMPO)[6]/*N*-bromosuccinimide (NBS)[7] mediated synthesis of pyrazoles from vinylhydrazones via bromoamination and hydroamination processes. These protocols involve room temperature C-H functionalization followed by *C-N* bond formation to give the target heterocycles in moderate to good yields.

3.1 Strategies for the Synthesis of Pyrazoles

3.1.1 Metal-Free Synthesis of Pyrazoles

Metal-free 1,3-dipolar cycloaddition, electrophilic cyclization, multi component reactions and other procedures are convenient routes for the synthesis of substituted pyrazoles. In addition, oxidative C-H functionalization also offers a straightforward and greener approach towards the synthesis of substituted pyrazoles. For examples, Larock and co-workers reported the synthesis of 3,5-disubstituted-1-acyl-4-iodo-1*H*-pyrazoles via dehydration/iodination of 1-acetyl-5-hydroxy-4,5-dihydro-1*H*-pyrazoles using ICl in the presence of Li_2CO_3 (Scheme 1).[5b]

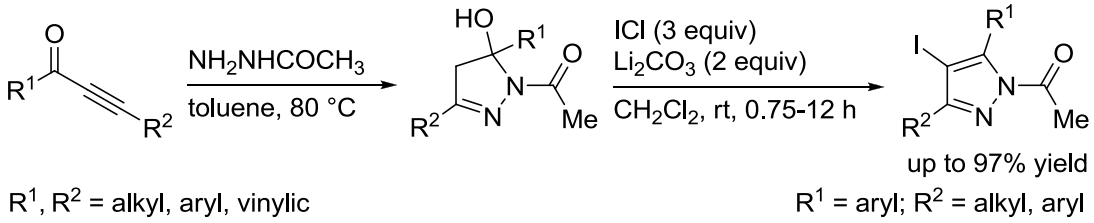

Scheme 1. Synthesis of 3,5-Disubstituted-1-acyl-4-iodo-1*H*-pyrazoles

Zora and co-workers disclosed I_2-mediated synthesis of 4-iodopyrazoles via electrophilic cyclizations of *α,β*-alkynic hydrazones (Scheme 2).[5c] Condensation reaction of hydrazines with acetylinic aldehydes and ketones affords corresponding *α,β*-alkynic hydrazones.

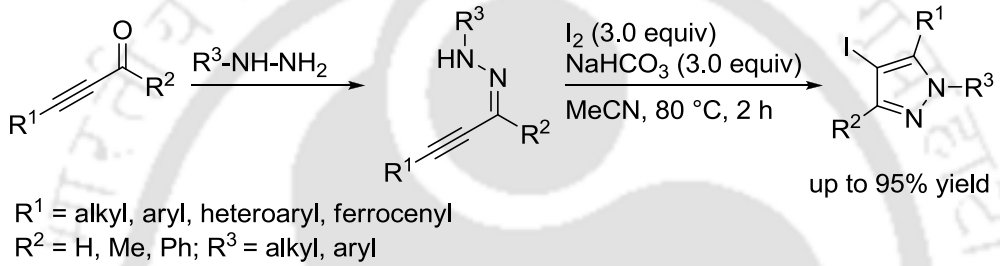

Scheme 2. Electrophilic Cyclizations of *α,β*-Alkynic Hydrazones

The *α,β*-unsaturated carbonyl compounds and hydrazine salts have also been utilized as starting precursors for the construction of tri-, and tetrasubstituted pyrazoles in one-pot through intramolecular oxidative *C-N* bond formation under I_2-mediated metal-free condition (Scheme 3).[5d]

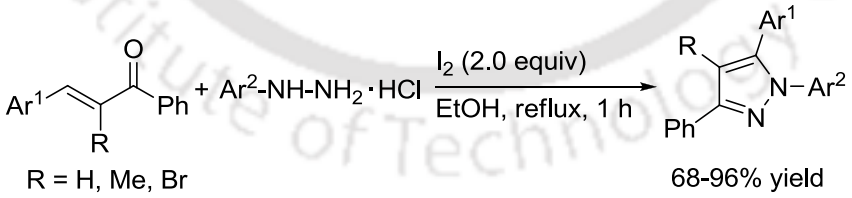

Scheme 3. I_2 Mediated One-Pot Synthesis of Substituted Pyrazoles

DIB mediated synthesis of 1,3,5-trisubstituted pyrazoles has been achieved from *N*-substituted hydrazones of chalcones (Scheme 4).[5e] *N*-Substituted hydrazones of chalcones were synthesized via the condensation of *α,β*-unsaturated ketones with hydrazines. Mild reaction condition and moderate yields of the products are the significant features of this protocol.

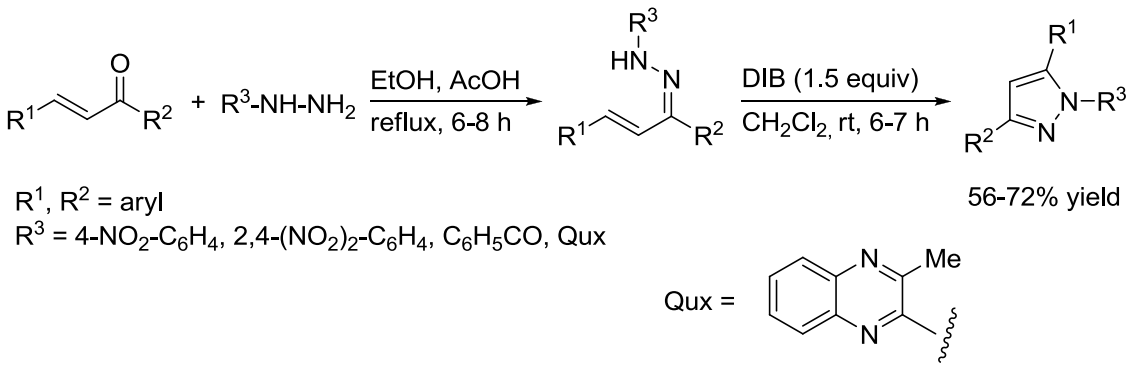

Scheme 4. DIB Mediated Synthesis of 1,3,5-Trisubstituted Pyrazoles

The synthesis of trisubstituted pyrazoles is reported from hydrazones using DDQ as an oxidising agent at ambient temperature (Scheme 5).[5f] This reaction proceeds through oxidative cyclization of hydrazones via formation of dihydropyrazoles to produce pyrazoles. Recrystallization of the crude pyrazoles from ethanol to produced pure pyrazole products.

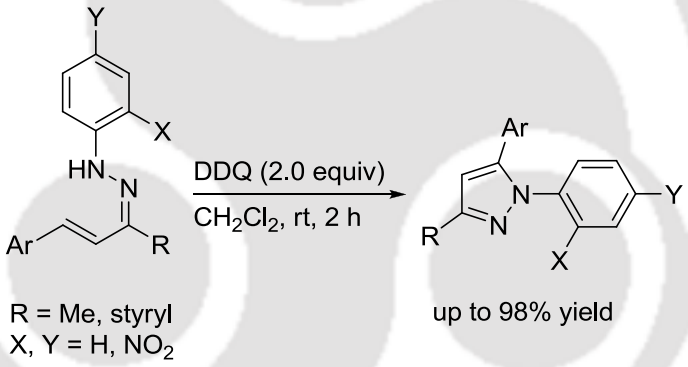

Scheme 5. DDQ Mediated synthesis of 1,3,5-Trisubstituted Pyrazoles

The Huisgen cyclization of nitrilimines with a trisubstituted bromoalkene afforded tetra substituted pyrazoles in high yield (Scheme 6).[5g] The substituted bromoalkene acts as an alkyne surrogate reacts with nitrilimines to provide pyrazoles via 5,5-disubstituted bromopyrazoline intermediate.

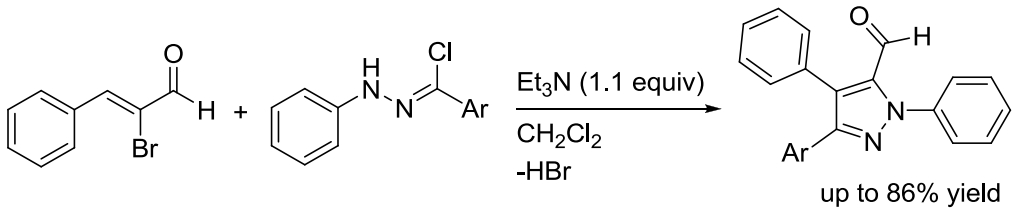

Scheme 6. Synthesis of Tetrasubstituted Pyrazoles

Yu and co-workers reported metal-free synthesis of multisubstituted pyrazoles from *β*-thioalkyl-*α,β*-unsaturated ketones and hydrazines via cyclocondensation (Scheme 7).[5h]

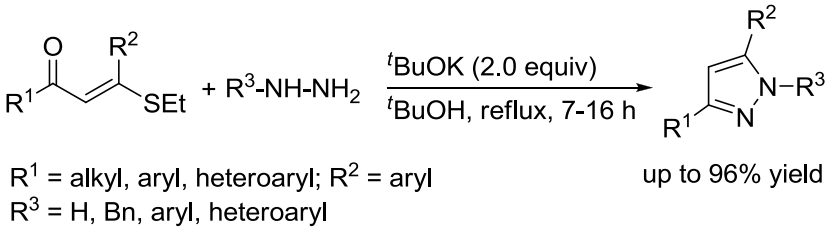

Scheme 7. Synthesis of Substituted Pyrazoles from *β*-Thioalkyl-*α,β*-unsaturated Ketones and Hydrazines

The synthesis of 3-trifluoromethylpyrazole have been demonstrated from *α,β*-alkynyl hydrazones using hypervalent iodine (Scheme 8).[5i] The reaction takes place via trifluoromethylation/cyclization and the presence of small amount of water increases the yield of the products.

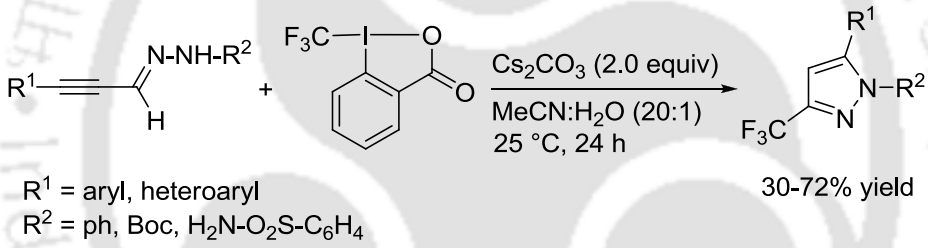

Scheme 8. Synthesis of 3-Trifluoromethylpyrazoles using Hypervalent Iodine Reagent

The use of three-component coupling of aldehydes, 1,3-dicarbonyls and diazo compounds/tosyl hydrazones is demonstrated under metal-free condition via sequential knoevenagel condensation, 1,3-dipolar cycloaddition and oxidative aromatization reaction using molecular oxygen (Scheme 9).[5j] The reaction produces the pyrazole derivatives in excellent yields.

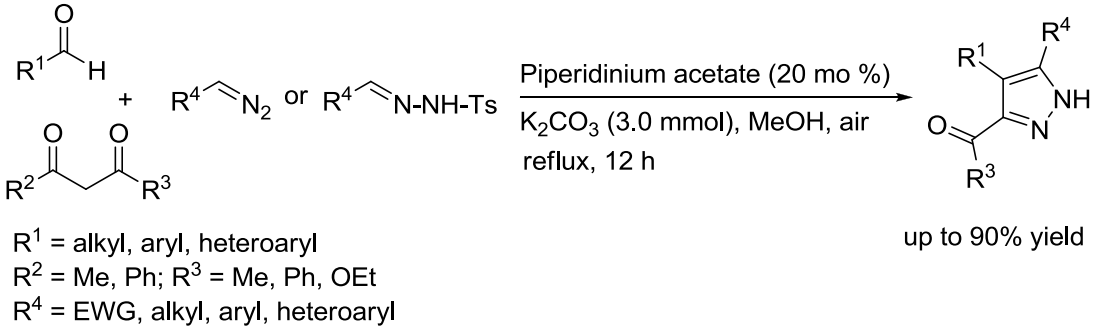

Scheme 9. Three-Component Synthesis of 3,4,5-Trisubstituted Pyrazoles

The synthesis of 3,5-disubstituted 1*H*- and 1-aryl-1*H*-pyrazoles is reported from 1,3-diyne-indoles and hydrazines in PEG-400 via successive hydroaminations (Scheme 10).[5k] The construction of a number of pyrazole derivatives bearing different functional groups is demonstrated.

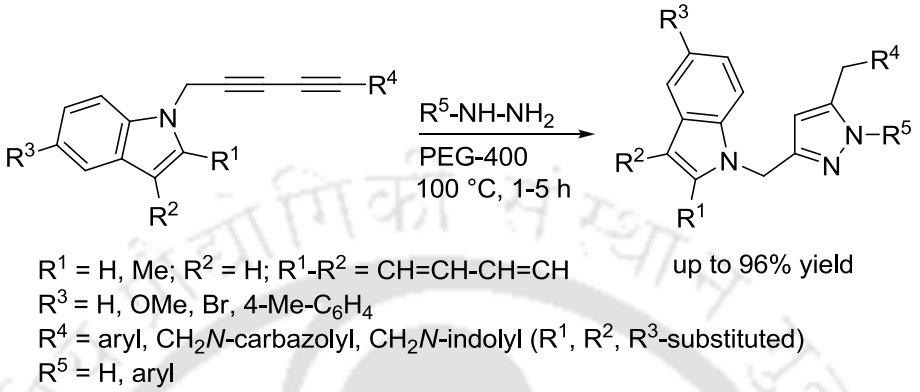

Scheme 10. Synthesis of Substituted Pyrazoles from *N*-(1,3-Diynylpentyl) substituted Indole Derivatives

3.2 Present Study

Herein we present an oxidative C-H amination route for the synthesis of pyrazoles. The use of the combination of TEMPO and NBS as well as NBS is described for the synthesis of substituted pyrazoles and bromopyrazoles, respectively.

Synthesis of (*Z*)-1-Allylidine-2-arylhydrazines. Scheme 11 shows the preparation of (*Z*)-1-allylidine-2-arylhydrazines.[8] The condensation of aryl hydrazines[9] with *α,β*-unsaturated ketones provided the titled compounds.

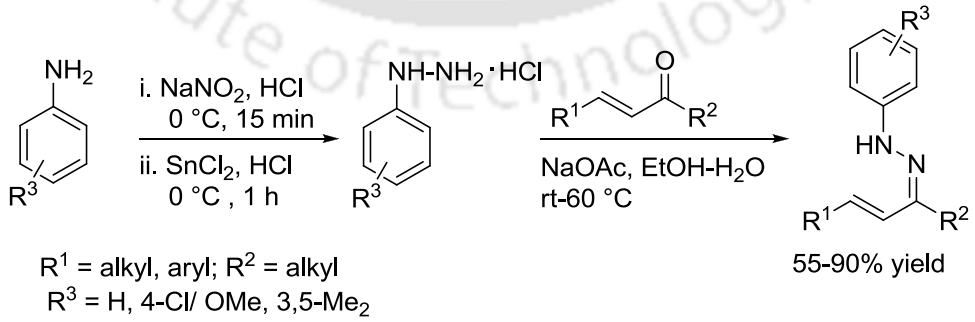

Scheme 11. Synthesis of (*Z*)-1-allylidine-2-arylhydrazines

Synthesis of Pyrazoles

Initially, the reaction condition was optimized using (*Z*)-1-(4-chlorophenyl)-2-((*E*)-3-phenylallylidene)hydrazine **1f** as a standard substrate with different solvents and varied amounts of TEMPO and NBS (Table 1). To our delight, the reaction proceeded to afford the desired substituted pyrazole **2f** in 80% yield when the substrate **1f** was stirred for 0.5 h with 10 mol % TEMPO and one equivalent of NBS in CH_3CN at room temperature under nitrogen atmosphere (entry 4). Among the screened solvents, CH_2Cl_2, THF, DMF, CH_3CN, toluene and 1,4-dioxane, CH_3CN produced best results. While the reactions using toluene and 1,4-dioxane gave **2f** in 50% and 40% yields, respectively (entries 5 and 6). In contrast, CH_2Cl_2, THF and DMF yielded inferior results (entries 1-3). The use of *N*-chlorosuccinimide (NCS) or *N*-iodosuccinimide (NIS) showed no reaction (entries 7 and 8). Decrease in the amount of TEMPO to 5 mol % had a detrimental effect on the yield of the product (41% yield, entry 9). Similar result was observed with the reaction using oxygen or air (entries 10 and 11). A control experiment without TEMPO and NBS gave no desired product and the starting material was recovered intact (entry 12).

With the optimized condition, we evaluated the scope of the procedure for the reactions of substituted hydrazones (Table 2). Alkyl hydrazones **1a-d** were converted into the corresponding alkyl pyrazoles **2a-d** in 55-60% yield. Similarly, (*Z*)-1-phenyl-2-((*E*)-3-phenylallylidene) hydrazine (**1e)** was transformed into pyrazole **2e** in 65% yield. Both the substrates bearing electron-donating and -withdrawing substituents are compatible. For examples, the substrates **1f** and **1g** with 1-(4-chlorophenyl) and 1-(4-methoxyphenyl) substituents underwent reaction to afford **2f** and **2g** in 80% and 75% yields, respectively. The reactions of (*Z*)-1-phenyl-2-((*E*)-4-substituted but-3-en-2-ylidene)-hydrazines **1h-l** afforded pyrazoles **2h-l** in 40-65% yields. Furthermore, (*Z*)-1-(4-methoxyphenyl)-2-((*E*)-4-*p*-tolylbut-3-en-2-ylidene)hydrazine (**1k)** and (*Z*)-1-((*E*)-4-(3,4-dimethoxyphenyl)but-3-en-2-ylidene)-2-(3,5-dimethylphenyl)-hydrazine (**1m)** were transformed into pyrazoles **2k** and **2m** in 73% and 62% yields, respectively. In addition, (*Z*)-1-substituted ((*E*)-4-(furan-2-yl)but-3-en-2-ylidene)-2-phenyl-hydrazines **1n** and **1o** cyclized to give pyrazoles **2n** and **2o** in 60% and 70% yields, respectively.

Table 1. Optimization of the Reaction Conditions[a]

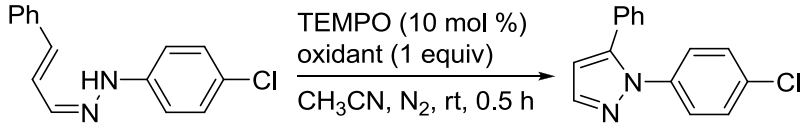

1f **2f**

Entry	TEMPO (mol %)	Oxidant	Solvent	Yield (%)[b]
1	10	NBS	CH_2Cl_2	5
2	10	NBS	THF	4
3	10	NBS	DMF	n.o.
4	**10**	**NBS**	**CH_3CN**	**80**
5	10	NBS	toluene	50
6	10	NBS	1,4-dioxane	40
7	10	NCS	CH_3CN	n.o.
8	10	NIS	CH_3CN	n.o.
9	5	NBS	CH_3CN	41
10	10	NBS	CH_3CN	70[c]
11	10	NBS	CH_3CN	60[d]
12	-	-	CH_3CN	n.o.

[a] Reaction conditions: Substrate **1f** (1 mmol), TEMPO (0.1 mmol) and oxidant (1mmol) were stirred in CH_3CN (4 mL) at room temperature for 0.5 h under N_2 balloon. [b] Isolated yield. [c] Under O_2 balloon. [d] In air. n.o. = not observed.

Table 2. TEMPO-Catalyzed Synthesis of *N*-Arylpyrazoles[a,b]

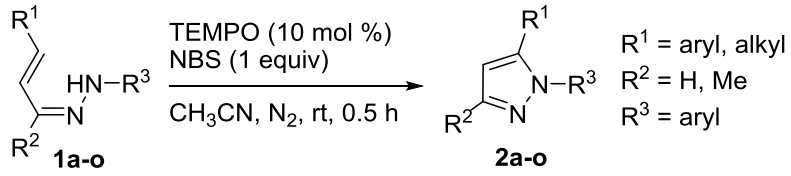

Entry	Substrate	Product	Yield (%)[b]
1	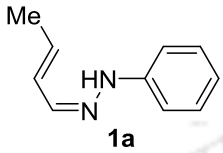 **1a**	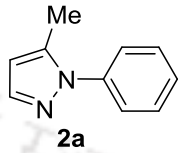 **2a**	55
2	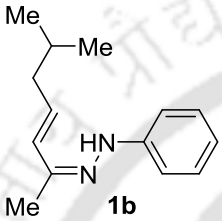 **1b**	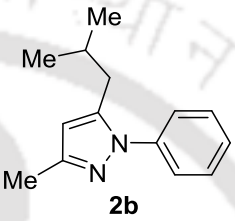 **2b**	60
3	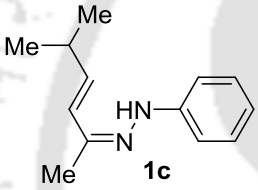 **1c**	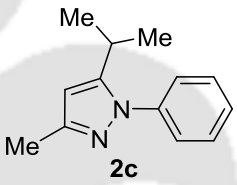 **2c**	55
4	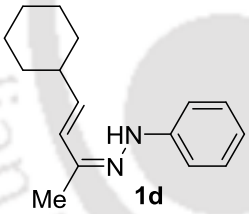 **1d**	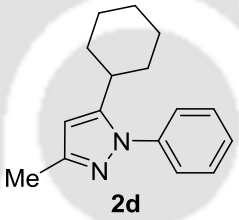 **2d**	55
5	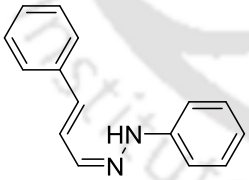 **1e**	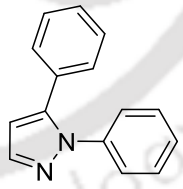 **2e**	65
6	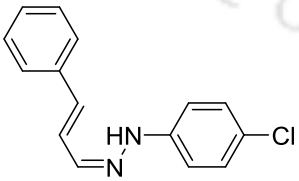 **1f**	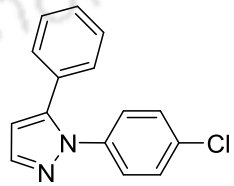 **2f**	80
7	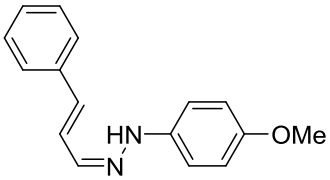 **1g**	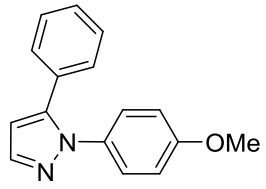 **2g**	75

Table 2 continues.....

8	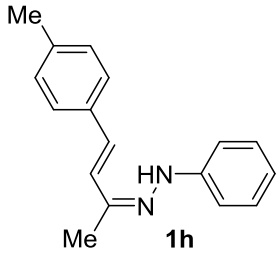 **1h**	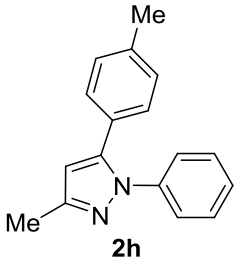 **2h**	58
9	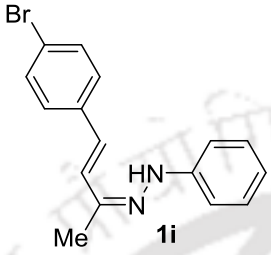 **1i**	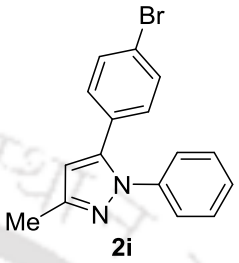 **2i**	60
10	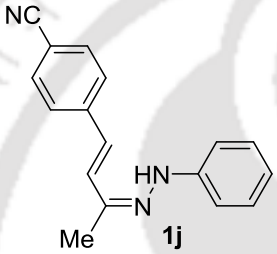 **1j**	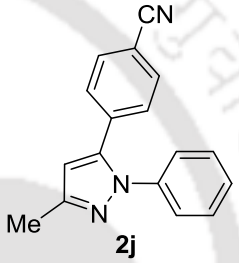 **2j**	40
11	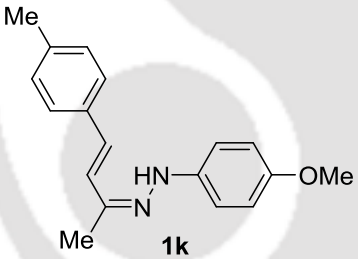 **1k**	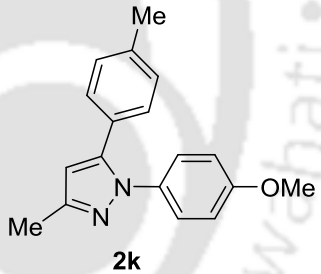 **2k**	73
12	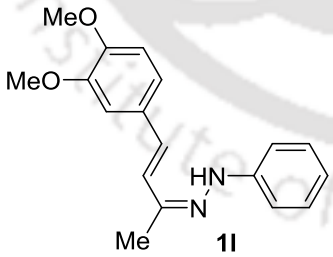 **1l**	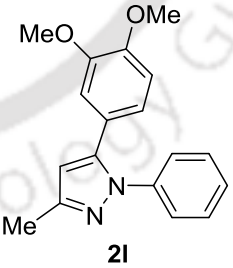 **2l**	65
13	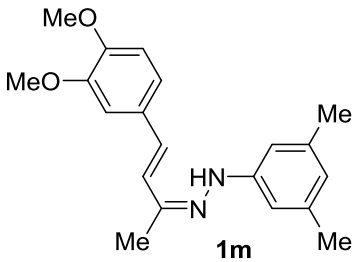 **1m**	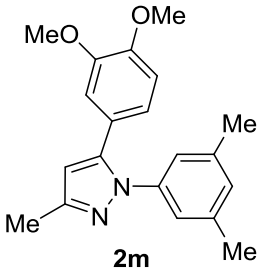 **2m**	62

Table 2 continues.....

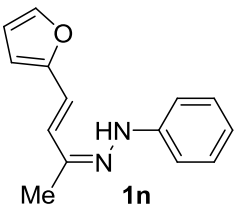

1n

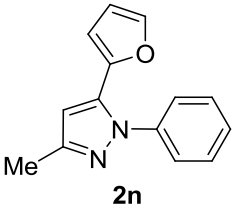

2n

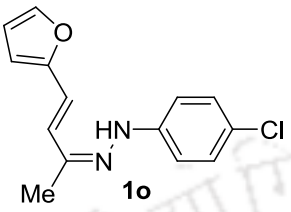

1o

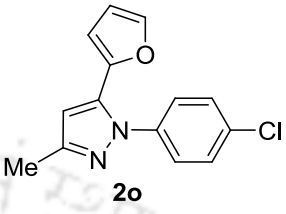

2o

[a] Substrate (1.0 mmol), TEMPO (0.1 mmol) and NBS (1.0 mmol) were stirred in CH_3CN (4 mL) for 0.5 h at room temperature under N_2 balloon. [b] Isolated yield.

Synthesis of 4-Bromopyrazoles. To reveal the reaction pathway, the reaction of **1h** was carried out using NBS as sole reagent (Scheme 12). The reaction occurred to afford a mixture of 4-bromo-3-methyl-1-phenyl-5-*p*-tolyl-1*H*-pyrazole[10a] **3e** and dimer **A** in 41% and 24% yields, respectively. These results suggest that the formation of **A** may occur by the dimerization of 3-methyl-1-phenyl-5-p-tolyl-1*H*-pyrazolyl radical **II**. As the 4-bromopyrazole **3e** is a valuable structural motif in medicinal chemistry, we further optimized the reaction condition for its selective formation.[10b] Interestingly, the use of 2 equivalent of NBS promoted the selective formation of the substituted 4-bromopyrazoles in good yields (Table 3). For example, the substituted alkyl hydrazones **1b-d** underwent reaction to give the corresponding 4-bromo-1,3,5-trisubstituted-1*H*-pyrazoles **3a-c** in 68-75% yields. Likewise, the reactions of substrates with electron-donating and electron-withdrawing substituents at various positions on the hydrazones **1f**, **1h,** and **1k** proceeded reaction to give the target products **3d-f** in 72-90% yields. Furthermore, the substituted hydrazones **1l** and **1m** cyclized to give the pyrazoles **3g** and **3h** in 77% and 75% yields, respectively. These studies suggest that the C-H oxidative cyclization of hydrazones can be performed at ambient conditions to give substituted pyrazoles and 4-bromopyrzoles. Recrystallization of **3d** in CH_3CN gave a single crystal whose structure was determined by a single crystal X-ray analysis (Figure 1).

Table 3. NBS-Mediated Synthesis of 4-bromosubstituted Pyrazoles[a,b]

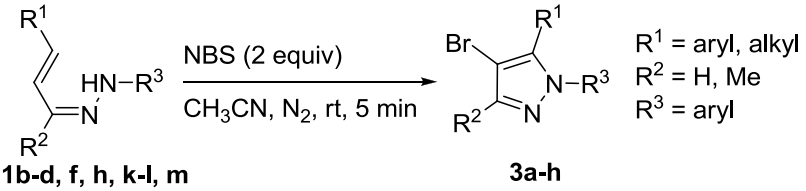

1b-d, f, h, k-l, m **3a-h**

Entry	Substrate	Product	Yield (%)[b]
1	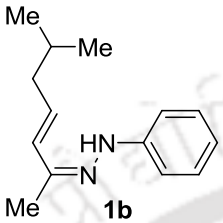 **1b**	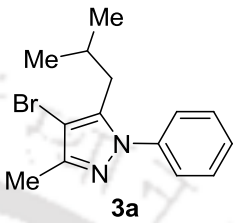 **3a**	68
2	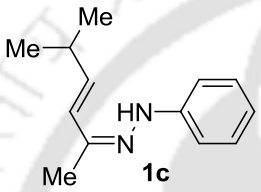 **1c**	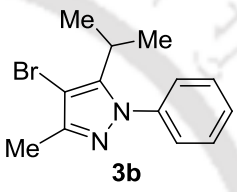 **3b**	70
3	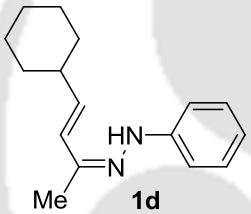 **1d**	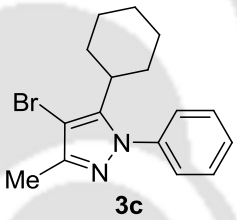 **3c**	75
4	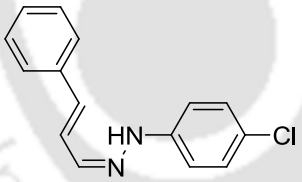 **1f**	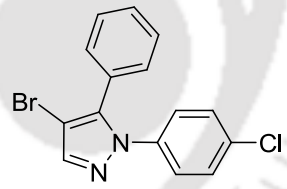 **3d**	90
5	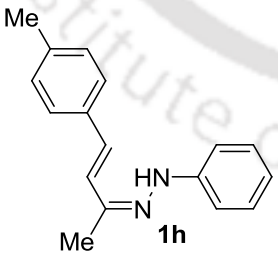 **1h**	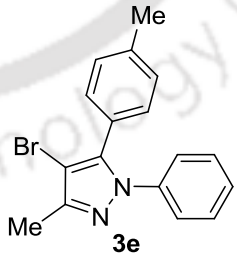 **3e**	80
6	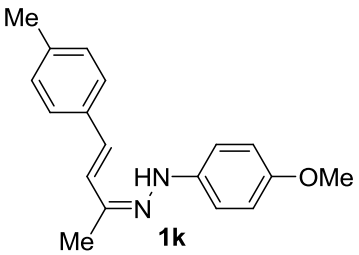 **1k**	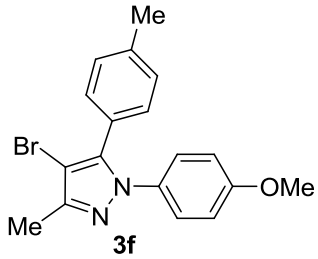 **3f**	72

Table 3 continues.....

7	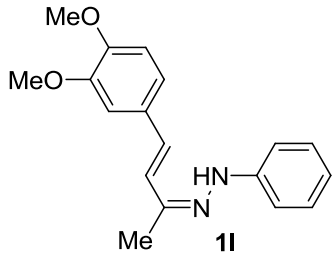 **1l**	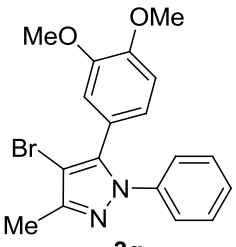 **3g**	77
8	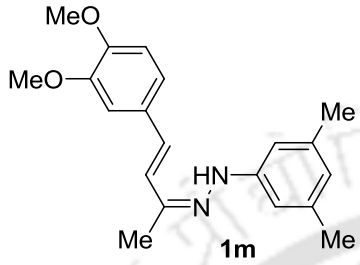 **1m**	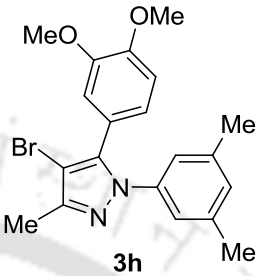 **3h**	75

[a] Reaction conditions: Substrate (1.0 mmol) and NBS (2.0 mmol) were stirred in CH_3CN (4 mL) at room temperature for 5 min under N_2 balloon. [b] Isolated yield.

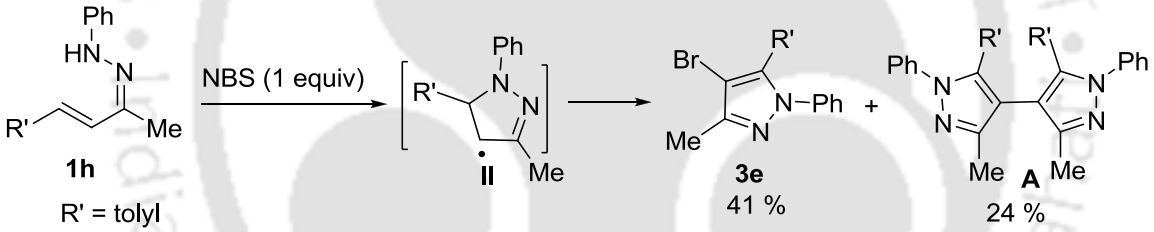

Scheme 12. Reaction of **1h** with NBS in the Absence of TEMPO

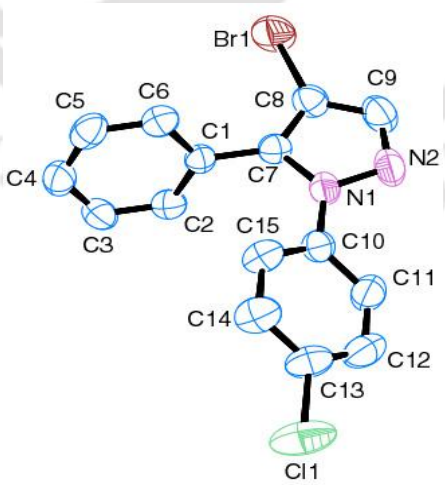

Figure 1. ORTEP diagram of 4-bromo-1-(4-chlorophenyl)-5-phenyl-1*H*-pyrazole **3d** with 50% ellipsoid. *H*-Atoms are omitted for clarity (CCDC 938512).

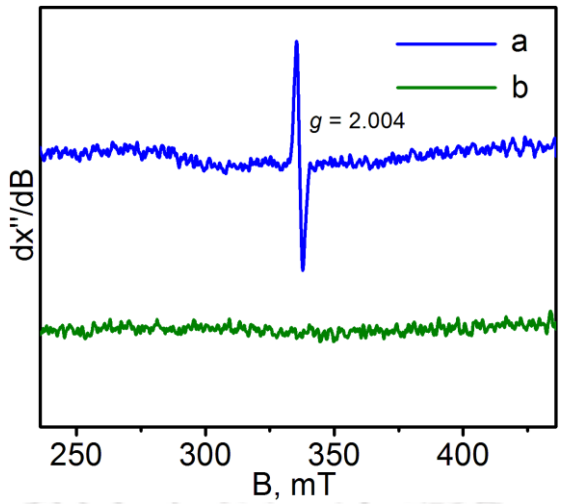

Figure 2. EPR spectra of (a) NBS with **1h** in CH_3CN and (b) NBS without **1h** in CH_3CN

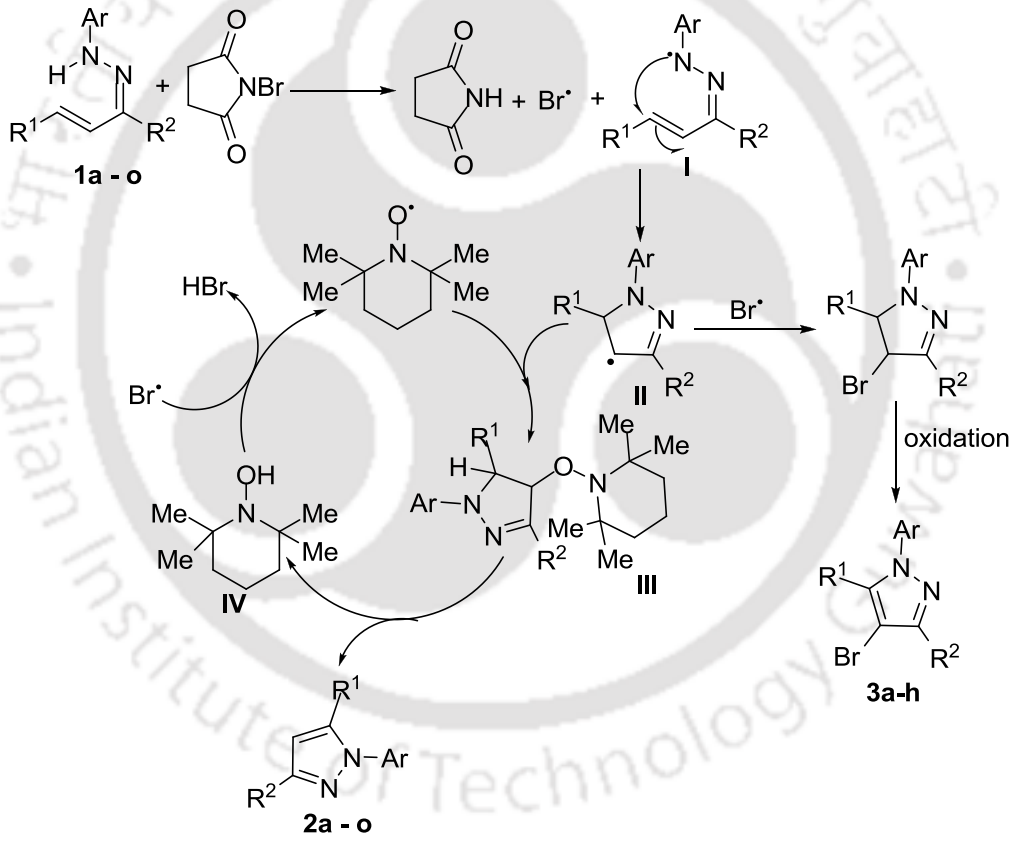

Scheme 13. Proposed Reaction Pathway

The EPR of the reaction of **1h** using NBS gave a signal whose g_{iso} is found to be 2.004 (Figure 2a). The control experiment using NBS without **1h** showed no EPR signal (Figure 2b). These results reveal that the reaction with NBS involves a radical intermediate. Thus, the observed results suggested that the substrates **1a-o** might react with NBS to give the

intermediate **I** that could cyclize to form species **II**.[7] The latter **II** may react with TEMPO to form **III** which may lead to the formation of **2a-o**[6] via elimination of the intermediate **IV**. The intermediate **IV** could be oxidized by the bromonium radical to regenerate the catalyst (Scheme 13). In the absence of TEMPO, the radical species **II** might either dimerize to generate **A** or react with NBS to afford 4-bromo-1,3,5-trisubstituted-1*H*-pyrazoles **3e**.

In conclusion, the synthesis of a series of substituted pyrazoles is described via C-H amination of vinylhydrazones using TEMPO as the catalyst and NBS as an oxidant in CH_3CN at ambient condition. The synthesis of substituted 4-bromopyrazole is also demonstrated using NBS in moderate to high yields at room temperature. These protocols provide potential route for the synthesis of pyrazoles and 4-bromopyrazoles.

3.3 Experimental Section

General Information: All solvents were distilled and dried prior to use. Aryl amine, TEMPO, NCS and cinnamaldehyde were obtained from Aldrich and were used as received. NBS and NIS were purchased from Aldrich and recrystallized from hot water prior to use. Acetone and sodium nitrite ($NaNO_2$) were purchased from Rankem. Stannous chloride ($SnCl_2$) was purchased from Merck. The progress of the reaction was monitored by analytical TLC on Merck silica gel G/GF 254 plates. Rankem silica gel (60-120 mesh) was used for column chromatography. NMR (^1H and ^{13}C) spectra were recorded on DRX-400 Varian spectrometer, Bruker Ultrashield TM 300 and BRUKER-AC 400 MHz using $CDCl_3$ as a solvent and Me_4Si as an internal standard. Chemical shifts (δ) are reported in ppm downfield of TMS in all ^1H NMR and ^{13}C NMR spectra and other data are reported as follows: s = singlet, d = doublet, m = multiplet and *J* = spin-spin coupling constant (Hz). Melting points were determined with a Büchi B-540 apparatus and are uncorrected. FT-IR spectra were recorded by Perkin Elmer IR spectrometer. Mass spectra were recorded on a Q-Tof ESI-MS Instrument (model HAB 273). EPR spectra were measured on X-Band Microwave Unit, JES-FA200 ESR spectrometer. Single crystal X-ray data were collected using Bruker SMART APEX-II CCD diffractometer, which is equipped with 1.75 kW sealed-tube Mo-Kα irradiation (λ = 0.71073 Å) at 298(2) K. The crystal structures were solved by direct methods using SHELXL-97 (Göttingen, Germany) and refined with full-matrix least squares on F2 using SHELXL-97.

General Procedure for TEMPO-Catalyzed Synthesis of Pyrazoles 2a-o. To a solution of hydrazones **1** (1 mmol) in CH_3CN (4 mL), TEMPO (10 mol %) and NBS (1 mmol) were added. The reaction mixture was stirred for 0.5 h at room temperature under N_2 balloon. The solvent was evaporated and the residue was extracted with ethyl acetate (3 x 15 mL) and washed with brine (1 x 10 mL) and water (1 x 10 mL). Drying (Na_2SO_4) and evaporation of the solvent gave a residue that was purified on silica gel by column chromatography using hexane and ethyl acetate as eluent.

General Procedure for NBS-Mediated Synthesis of 4-Bromopyrazoles 3a-h. To a solution of hydrazones **1** (1 mmol) in CH_3CN (4 mL), NBS (2 mmol) was added. The resultant mixture was stirred for 5 min at room temperature under N_2 balloon. The solvent was then evaporated and the residue was extracted with ethyl acetate (3 x 15 mL) and washed with brine (1 x 10 mL) and water (1 x 10 mL). Drying (Na_2SO_4) and evaporation of the solvent gave a residue which was purified on silica gel column chromatography using hexane and ethyl acetate as eluent.

3.4 Characterization Data of Products

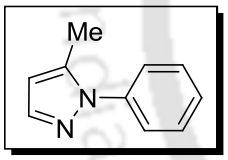

5-Methyl-1-phenyl-1*H*-pyrazole[11a] **2a.** Analytical TLC on silica gel, 1:9 ethyl acetate/hexane R_f = 0.68; reddish yellow liquid; yield: 55% (88 mg). ^{1}H NMR (400 MHz, $CDCl_3$) δ 7.82 (d, *J* = 2.0 Hz, 1H), 7.66 (d, *J* = 8.4 Hz, 2H), 7.45 (t, *J* = 7.6 Hz, 3H), 6.25 (d, *J* = 2.0 Hz, 1H), 2.38 (s, 3H); ^{13}C{^{1}H} NMR (75 MHz, $CDCl_3$) δ 140.1, 139.6, 129.3, 127.4, 125.9, 118.8, 107.5, 13.8; FT-IR (neat) 2960, 2928, 1598, 1533, 1504, 1364, 1044 cm^{-1}; HRMS (ESI) *m/z* $[M+H]^+$ calcd for $C_{10}H_{10}N_2$: 159.0917, found: 159.0921.

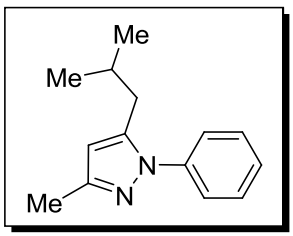

5-Isobutyl-3-methyl-1-phenyl-1*H*-pyrazole 2b. Analytical TLC on silica gel, 1:9 ethyl acetate/hexane R_f = 0.62; yellow liquid; yield: 60% (130 mg). ^{1}H

NMR (400 MHz, $CDCl_3$) δ 7.45-7.38 (m, 5H), 5.97 (s, 1H), 2.50 (d, *J* = 7.2 Hz, 2H), 2.29 (s, 3H), 1.95-1.91 (m, 1H), 0.96 (d, *J* = 6.8 Hz, 6H); $^{13}C\{^1H\}$ NMR (75 MHz, $CDCl_3$) δ 152.7, 140.0, 139.0, 129.0, 127.1, 124.7, 106.4, 37.4, 29.0, 22.6, 12.5; FT-IR (neat) 3065, 2955, 2927, 2868, 1599, 1555, 1504, 1462, 1381, 1134, 1018 cm^{-1}; HRMS (ESI) *m/z* $[M+H]^+$ calcd for $C_{14}H_{18}N_2$: 215.1543, found: 215.1550.

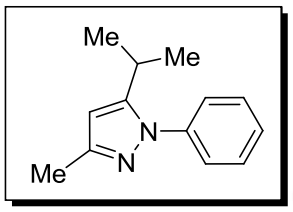

5-Isopropyl-3-methyl-1-phenyl-1*H*-pyrazole 2c. Analytical TLC on silica gel, 1:9 ethyl acetate/hexane R_f = 0.59; yellow liquid; yield: 55% (111 mg). ^1H NMR (400 MHz, $CDCl_3$) δ 7.44-7.43 (m, 4H), 7.35-7.32 (m, 1H), 6.03 (s, 1H), 3.03-3.00 (m, 1H), 2.31 (s, 3H), 1.30 (s, 3H), 1.28 (s, 3H); $^{13}C\{^1H\}$ NMR (100 MHz, $CDCl_3$) δ 159.5, 140.1, 139.1, 129.0, 127.2, 124.9, 103.9, 27.9, 23.0, 12.6; FT-IR (neat) 3064, 2962, 2928, 2869, 1726, 1599, 1553, 1503, 1456, 1380, 1300, 1130, 1071 cm^{-1}; HRMS (ESI) *m/z* $[M+H]^+$ calcd for $C_{13}H_{16}N_2$: 201.1386, found: 201.1389.

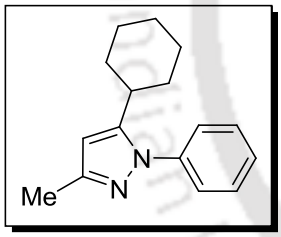

5-Cyclohexyl-3-methyl-1-phenyl-1*H*-pyrazole 2d. Analytical TLC on silica gel, 1:9 ethyl acetate/hexane R_f = 0.54; yellow liquid; yield: 55% (178 mg). ^1H NMR (400 MHz, $CDCl_3$) δ 7.48-7.40 (m, 4H), 7.36-7.30 (m, 1H), 6.02 (s, 1H), 2.70-2.65 (m, 1H), 2.31 (s, 3H), 2.02-2.00 (m, 2H), 1.83-1.70 (m, 3H), 1.49-1.26 (m, 5H); $^{13}C\{^1H\}$ NMR (75 MHz, $CDCl_3$) δ 158.8, 140.1, 139.0, 129.0, 127.2, 124.9, 104.2, 37.6, 33.4, 26.4, 26.1, 12.5; FT-IR (neat) 2925, 2851, 1599, 1553, 1504, 1447, 1380, 1072 cm^{-1}; HRMS (ESI) *m/z* $[M+H]^+$ calcd for $C_{16}H_{20}N_2$: 241.1699, found: 241.1693.

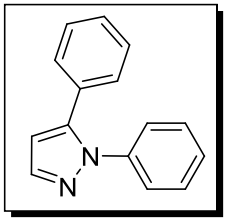

1,5-Diphenyl-1*H*-pyrazole[11b] **2e.** Analytical TLC on silica gel, 1:9 ethyl acetate/hexane R_f = 0.52; yellow liquid; yield: 65% (144 mg). ^{1}H NMR (400 MHz, $CDCl_3$) δ 7.73 (d, *J* = 1.6 Hz, 1H), 7.33-7.22 (m, 10H), 6.51 (d, *J* = 1.6 Hz, 1H); $^{13}C\{^1H\}$ NMR (100 MHz, $CDCl_3$) δ 143.2, 140.4, 140.3, 130.8, 129.0, 128.9, 128.6, 128.4, 127.6, 125.4, 108.0; FT-IR (neat) 3058, 2963, 1596, 1501, 1450, 1386, 1261, 1068 cm^{-1}; HRMS (ESI) *m/z* $[M+H]^+$ calcd for $C_{15}H_{12}N_2$: 221.1073, found: 221.1069.

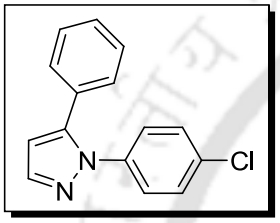

1-(4-Chlorophenyl)-5-phenyl-1*H*-pyrazole[11b] **2f.** Analytical TLC on silica gel, 1:9 ethyl acetate/hexane R_f = 0.63; yellow liquid; yield: 80% (205 mg). ^{1}H NMR (400 MHz, $CDCl_3$) δ 7.73 (d, *J* = 1.6 Hz, 1H), 7.34-7.29 (m, 5H), 7.26-7.22 (m, 4H), 6.51 (d, *J* = 1.6 Hz, 1H); $^{13}C\{^1H\}$ NMR (100 MHz, $CDCl_3$) δ 143.3, 140.8, 138.8, 131.4, 130.5, 129.4, 129.2, 128.7, 128.1, 126.4, 108.4; FT-IR (neat) 3058, 2925, 1497, 1410, 1384, 1093 cm^{-1}; HRMS (ESI) *m/z* $[M+H]^+$ calcd for $C_{15}H_{11}ClN_2$: 255.0684, found: 255.0689.

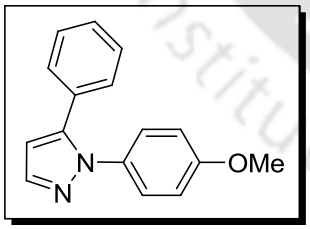

1-(4-Methoxyphenyl)-5-phenyl-1*H*-pyrazole[11c] **2g.** Analytical TLC on silica gel, 1:9 ethyl acetate/hexane R_f = 0.48; yellow liquid; yield: 75% (189 mg). ^{1}H NMR (400 MHz, $CDCl_3$) δ 7.69 (d, *J* = 1.6 Hz, 1H), 7.30-7.20 (m, 7H), 6.86 (d, *J* = 8.8 Hz, 2H), 6.50 (d, *J* = 2.0 Hz, 1H), 3.80 (s, 3H); $^{13}C\{^1H\}$ NMR (75 MHz, $CDCl_3$) δ 158.7, 142.9, 139.9, 133.3, 130.6, 128.7, 128.4, 128.1, 126.6, 114.0, 107.3, 55.1; FT-IR (neat) 2925, 2853, 1514, 1457, 1249, 1026 cm^{-1}; HRMS (ESI) *m/z* $[M+H]^+$ calcd for $C_{16}H_{14}N_2O$: 251.1179, found: 251.1182.

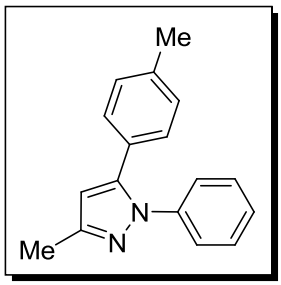

3-Methyl-1-phenyl-5-*p*-tolyl-1*H*-pyrazole 2h. Analytical TLC on silica gel, 1:9 ethyl acetate/hexane R_f = 0.56; yellow liquid; yield: 58% (145 mg). ^{1}H NMR (400 MHz, $CDCl_3$) δ 7.33-7.26 (m, 6H), 7.13-7.06 (m, 3H), 6.28 (s, 1H), 2.38 (s, 3H), 2.33 (s, 3H); $^{13}C\{^1H\}$ NMR (100 MHz, $CDCl_3$) δ 149.5, 143.9, 140.4, 138.1, 129.3, 129.0, 128.6, 128.0, 127.2, 125.3, 107.6, 21.4, 13.7; FT-IR (neat) 2922, 1598, 1500, 1427, 1363, 1071 cm^{-1}; HRMS (ESI) *m/z* $[M+H]^+$ calcd for $C_{17}H_{16}N_2$: 249.1386, found: 249.1380.

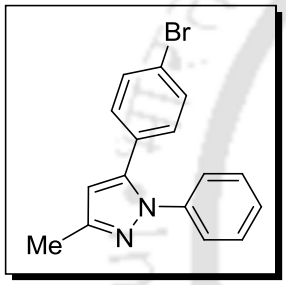

5-(4-Bromophenyl)-3-methyl-1-phenyl-1*H*-pyrazole[4g] **2i.** Analytical TLC on silica gel, 1:9 ethyl acetate/hexane R_f = 0.58; yellow liquid; yield: 60% (181 mg). ^{1}H NMR (400 MHz, $CDCl_3$) δ 7.43 (d, *J* = 8.0 Hz, 2H), 7.34-7.24 (m, 5H), 7.09 (d, *J* = 8.8 Hz, 2H), 6.31(s, 1H), 2.38 (s, 3H); $^{13}C\{^1H\}$ NMR (75 MHz, $CDCl_3$) δ 149.7, 142.5, 139.8, 132.2, 131.6, 130.1, 129.0, 127.4, 125.1, 122.4, 107.9, 14.0; FT-IR (neat) 3048, 2959, 2920, 2850, 1597, 1504, 1487, 1260, 1073, 1010 cm^{-1}; HRMS (ESI) *m/z* $[M+H]^+$ calcd for $C_{16}H_{13}BrN_2$: 313.0335, found: 313.0332.

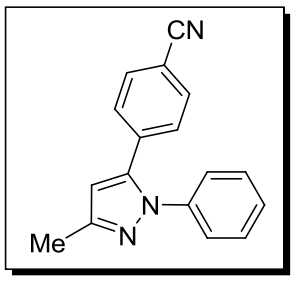

4-(3-Methyl-1-phenyl-1*H*-pyrazol-5-yl)benzonitrile 2j. Analytical TLC on silica gel, 1:6 ethyl acetate/hexane R_f = 0.55; reddish yellow liquid; yield: 40% (104 mg). ^{1}H NMR (400 MHz, $CDCl_3$) δ 7.58 (d, *J* = 8.4 Hz, 2H), 7.38-7.23

(m, 7H), 6.40 (s, 1H), 2.40 (s, 3H); $^{13}C\{^{1}H\}$ NMR (75 MHz, $CDCl_3$) δ 149.9, 141.7, 139.5, 135.0, 132.2, 129.2, 128.9, 127.8, 125.2, 118.5, 113.0, 108.6, 13.7; FT-IR (neat) 3057, 2924, 2852, 2227, 1597, 1499, 1363, 1261 cm^{-1}; HRMS (ESI) *m/z* $[M+H]^+$ calcd for $C_{17}H_{13}N_3$: 260.1182, found: 260.1186.

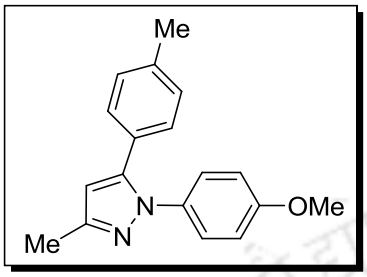

1-(4-Methoxyphenyl)-3-methyl-5-*p*-tolyl-1*H*-pyrazole[4e]

2k. Analytical TLC on silica gel, 1:4 ethyl acetate/hexane R_f = 0.48; yellow liquid; yield: 73% (205 mg). ^{1}H NMR (400 MHz, $CDCl_3$) δ 7.20 (d, *J* = 8.8 Hz, 2H), 7.13-7.09 (m, 4H), 6.85 (d, *J* = 8.8 Hz, 2H), 6.26 (s, 1H), 3.80 (s, 3H), 2.37 (s, 3H), 2.33 (s, 3H); $^{13}C\{^{1}H\}$ NMR (100 MHz, CDCl3) δ 158.7, 149.1, 143.9, 138.0, 133.7, 129.2, 128.6, 128.0, 126.7, 114.1, 107.0, 55.6, 21.4, 13.7; FT-IR (neat) 2925, 2857, 1518, 1462, 1299, 1249, 1033 cm^{-1}; HRMS (ESI) *m/z* $[M+H]^+$ calcd for $C_{18}H_{18}N_2O$: 279.1492, found: 279.1488.

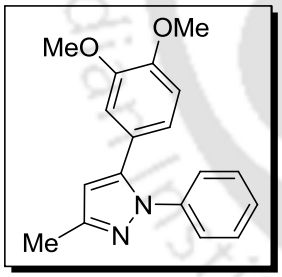

5-(3,4-Dimethoxyphenyl)-3-methyl-1-phenyl-1*H*-pyrazole 2l.

Analytical TLC on silica gel, 1:4 ethyl acetate/hexane R_f = 0.47; yellow liquid; yield: 65% (192 mg). ^{1}H NMR (400 MHz, $CDCl_3$) δ 7.28-7.25 (m, 5H), 6.80 (d, *J* = 8.8 Hz, 2H), 6.60 (s, 1H), 6.26 (s, 1H), 3.84 (s, 3H), 3.60 (s, 3H), 2.36 (s, 3H); $^{13}C\{^{1}H\}$ NMR (75 MHz, $CDCl_3$) δ 149.1, 148.7, 148.3, 143.4, 140.1, 128.7, 127.0, 125.1, 123.0, 121.1, 111.6, 110.8, 106.9, 55.6, 55.4, 13.4; FT-IR (neat) 2931, 2834, 1597, 1514, 1500, 1463, 1254, 1234, 1064, 1026 cm^{-1}; HRMS (ESI) *m/z* $[M+H]^+$ calcd for $C_{18}H_{18}N_2O_2$: 295.1441, found: 295.1447.

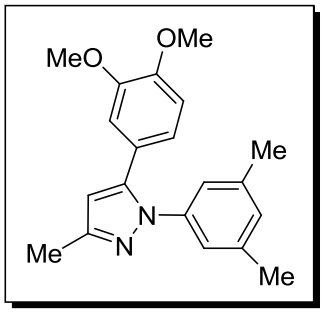

5-(3,4-Dimethoxyphenyl)-1-(3,5-dimethylphenyl)-3-methyl-1*H*-pyrazole 2m. Analytical TLC on silica gel, 3:7 ethyl acetate/hexane R_f = 0.52; yellow liquid; yield: 62% (201 mg). ^{1}H NMR (400 MHz, $CDCl_3$) δ 6.91 (s, 2H), 6.88-6.78 (m, 3H), 6.69-6.68 (m, 1H), 6.27 (s, 1H), 3.88 (s, 3H), 3.66 (s, 3H), 2.37 (s, 3H), 2.25 (s, 6H); ^{13}C{^{1}H} NMR (75 MHz, $CDCl_3$) δ 149.0, 148.7, 148.3, 143.4, 140.0, 138.5, 128.8, 123.3, 123.1, 121.1, 111.6, 110.8, 106.7, 55.7, 55.6, 21.2, 13.5; FT-IR (neat) 3011, 2919, 2835, 1601, 1512, 1464, 1257, 1241, 1145, 1026 cm^{-1}; HRMS (ESI) *m/z* $[M+H]^+$ calcd for $C_{20}H_{22}N_2O_2$: 323.1754, found: 323.1751.

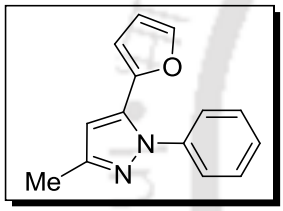

5-(Furan-2-yl)-3-methyl-1-phenyl-1*H*-pyrazole 2n. Analytical TLC on silica gel, 1:9 ethyl acetate/hexane R_f = 0.68; yellow liquid; yield: 60% (136 mg). ^{1}H NMR (400 MHz, $CDCl_3$) δ 7.43-7.38 (m, 6H), 6.46 (s, 1H), 6.32-6.31 (m, 1H), 5.95 (d, *J* = 3.2 Hz, 1H), 2.36 (s, 3H); ^{13}C{^{1}H} NMR (75 MHz, $CDCl_3$) δ 151.4, 149.4, 142.4, 140.3, 129.0, 128.2, 125.8, 123.1, 111.1, 108.6, 106.0, 13.7; FT-IR (neat) 2925, 1597, 1504, 1458, 1363, 1015 cm^{-1}; HRMS (ESI) *m/z* $[M+H]^+$ calcd for $C_{14}H_{12}N_2O$: 225.1022, found: 225.1026.

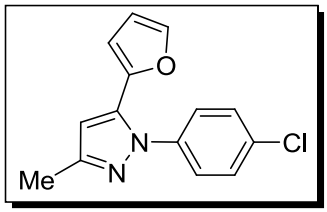

1-(4-Chlorophenyl)-5-(furan-2-yl)-3-methyl-1*H*-pyrazole 2o. Analytical TLC on silica gel, 1:9 ethyl acetate/hexane R_f = 0.73; yellow liquid; yield: 70% (182 mg). ^{1}H NMR (400 MHz, $CDCl_3$) δ 7.39-7.30 (m, 5H), 6.43 (s, 1H), 6.35-6.34 (m, 1H), 6.05 (d, *J* = 3.6 Hz, 1H), 2.34 (s, 3H); ^{13}C{^{1}H} NMR (75 MHz, $CDCl_3$) δ 153.6,

150.0, 142.8, 138.9, 131.1, 129.3, 126.9, 111.3, 109.1, 106.7, 13.6; FT-IR (neat) 3107, 2925, 1503, 1364, 1272, 1093 cm^{-1}; HRMS (ESI) *m/z* $[M+H]^+$ calcd for $C_{14}H_{11}N_2OCl$: 259.0633, found: 259.0630.

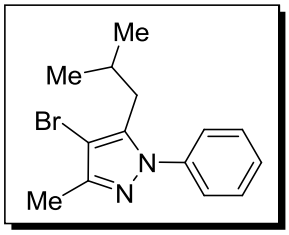

4-Bromo-5-isobutyl-3-methyl-1-phenyl-1*H*-pyrazole 3a.

Analytical TLC on silica gel, 1:9 ethyl acetate/hexane R_f = 0.67; yellow liquid; yield: 68% (147 mg). ^1H NMR (400 MHz, $CDCl_3$) δ 7.44-7.39 (m, 5H), 2.53 (d, *J* =7.2 Hz, 2H), 2.29 (s, 3H), 2.13-2.02 (m, 1H), 0.97 (d, *J* = 6.8 Hz, 6H); $^{13}C\{^1H\}$ NMR (100 MHz, $CDCl_3$) δ 150.8, 140.1, 137.5, 129.4, 128.0, 125.0, 96.6, 36.0, 28.5, 27.7, 12.0; FT-IR (neat) 3058, 2958, 2868, 1598, 1504, 1464, 1380, 1261, 1078 cm^{-1}; HRMS (ESI) *m/z* $[M+H]^+$ calcd for $C_{14}H_{17}BrN_2$: 293.0648, found: 293.0650.

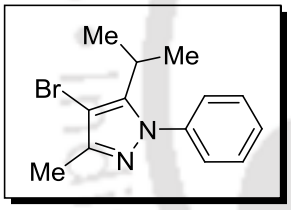

4-Bromo-5-isopropyl-3-methyl-1-phenyl-1*H*-pyrazole 3b.

Analytical TLC on silica gel, 1:9 ethyl acetate/hexane R_f = 0.59; yellow liquid; yield: 70% (141 mg). ^1H NMR (400 MHz, $CDCl_3$) δ 7.46-7.34 (m, 5H), 3.09-3.05 (m, 1H), 2.28 (s, 3H), 1.33 (s, 3H), 1.31 (s, 3H); $^{13}C\{^1H\}$ NMR (75 MHz, $CDCl_3$) δ 155.7, 139.9, 137.4, 129.1, 127.6, 124.7, 94.6, 27.1, 21.3, 11.5; FT-IR (neat) 2964, 2918, 1851, 1598, 1504, 1385, 1261, 1090 cm^{-1}; HRMS (ESI) *m/z* $[M+H]^+$ calcd for $C_{13}H_{15}BrN_2$: 279.0491, found: 279.0495.

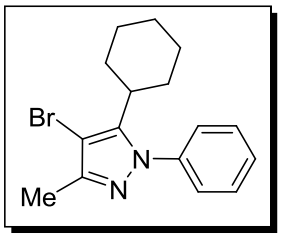

4-Bromo-5-cyclohexyl-3-methyl-1-phenyl-1*H*-pyrazole 3c.

Analytical TLC on silica gel, 1:9 ethyl acetate/hexane R_f = 0.72; yellow liquid; yield: 75% (170 mg). ^1H NMR (400 MHz, $CDCl_3$) δ 7.43-7.33 (m, 5H), 2.75-2.67 (m, 1H),

2.28 (s, 3H), 1.95-1.92 (m, 2H), 1.83-1.82 (m, 2H), 1.80-1.58 (m, 3H), 1.39-1.24 (m, 3H); $^{13}C\{^{1}H\}$ NMR (75 MHz, $CDCl_3$) δ 155.0, 139.9, 137.2, 129.0, 127.6, 124.7, 94.8, 36.8, 31.5, 26.5, 26.0, 11.5; FT-IR (neat) 3068, 2928, 2852, 1598, 1505, 1448, 1385, 1081 cm^{-1}; HRMS (ESI) *m/z* $[M+H]^+$ calcd for $C_{16}H_{19}BrN_2$: 319.0804, found: 319.0801.

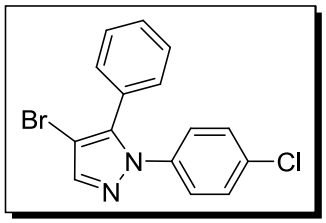

4-Bromo-1-(4-chlorophenyl)-5-phenyl-1*H*-pyrazole 3d.

Analytical TLC on silica gel, 1:9 ethyl acetate/hexane R_f = 0.73; colourless solid; yield: 90% (231 mg); mp 84-85 °C. ^{1}H NMR (400 MHz, $CDCl_3$) δ 7.76 (s, 1H), 7.40-7.38 (m, 4H), 7.28-7.26 (m, 3H), 7.17 (d, *J* = 8.8 Hz, 2H); $^{13}C\{^{1}H\}$ NMR (75 MHz, $CDCl_3$) δ 141.3, 140.4, 138.3, 133.3, 129.9, 129.1, 129.0, 128.6, 128.2, 125.8, 96.2; FT-IR (KBr) 2963, 2919, 2852, 1497, 1262, 1093, 1018 cm^{-1}; HRMS (ESI) *m/z* $[M+H]^+$ calcd for $C_{15}H_{10}ClBrN_2$: 332.9789, found: 332.9781.

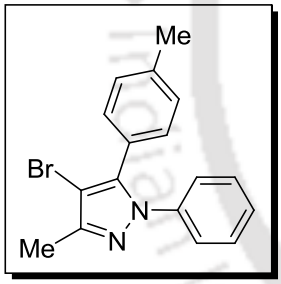

4-Bromo-3-methyl-1-phenyl-5-*p*-tolyl-1*H*-pyrazole 3e.

Analytical TLC on silica gel, 1:9 ethyl acetate/hexane R_f = 0.68; yellow liquid; yield: 80% (200 mg). ^{1}H NMR (400 MHz, $CDCl_3$) δ 7.39 (d, *J* = 8.8 Hz, 2H), 7.18-7.10 (m, 5H), 7.07 (d, *J* = 8.8 Hz, 2H), 2.36-2.35 (m, 6H); $^{13}C\{^{1}H\}$ NMR (100 MHz, $CDCl_3$) δ 149.0, 141.0, 139.3, 139.1, 132.1, 129.8, 129.6, 126.1, 126.0, 120.9, 97.5, 21.6, 12.7; FT-IR (neat) 2918, 1492, 1362, 1262, 1060 cm^{-1}; HRMS (ESI) *m/z* $[M+H]^+$ calcd for $C_{17}H_{15}BrN_2$: 327.0491, found: 327.0497.

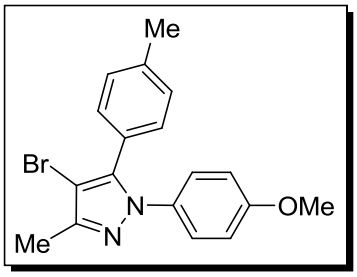

4-Bromo-1-(4-methoxyphenyl)-3-methyl-5-*p*-tolyl-1*H*-pyrazole 3f. Analytical TLC on silica gel, 1:4 ethyl acetate/hexane R_f = 0.55; yellow liquid; yield: 72% (202 mg). ^{1}H NMR (400 MHz, $CDCl_3$) δ 7.13-7.08 (m, 6H), 6.79 (d, *J* = 8.8 Hz, 2H), 3.76 (s, 3H), 2.35 (s, 3H), 2.33 (s, 3H); ^{13}C{^{1}H} NMR (75 MHz, $CDCl_3$) δ 158.6, 148.0, 140.7, 138.7, 133.4, 129.7, 129.1, 128.2, 126.1, 114.0, 96.1, 55.4, 21.4, 12.5; FT-IR (neat) 2927, 2851, 1508, 1493, 1462, 1360, 1254, 1232, 1139, 1060, 1025 cm^{-1}; HRMS (ESI) *m/z* $[M+H]^+$ calcd for $C_{18}H_{17}BrN_2O$: 357.0597, found: 357.0599.

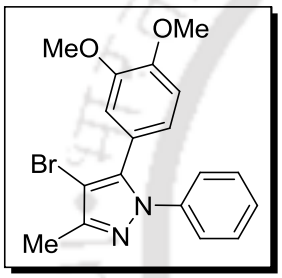

4-Bromo-5-(3,4-dimethoxyphenyl)-3-methyl-1-phenyl-1*H*-pyrazole 3g. Analytical TLC on silica gel, 1:4 ethyl acetate/hexane R_f = 0.53; yellow liquid; yield: 77% (227 mg). ^{1}H NMR (400 MHz, $CDCl_3$) δ 7.43 (d, *J* = 8.4 Hz, 2H), 7.11 (d, *J* = 8.4 Hz, 2H), 6.88-6.81 (m, 3H), 6.76 (s, 1H), 3.91 (s, 3H), 3.75 (s, 3H), 2.37 (s, 3H); ^{13}C{^{1}H} NMR (75 MHz, $CDCl_3$) δ 149.6, 148.97, 148.93, 140.7, 139.1, 132.1, 126.1, 124.8, 122.9, 120.9, 112.8, 111.2, 97.3, 56.4, 13.3; FT-IR (neat) 2918, 2845, 1515, 1250, 1177, 1166, 1060, 1032 cm^{-1}; HRMS (ESI) *m/z* $[M+H]^+$ calcd for $C_{18}H_{17}BrN_2O_2$: 373.0546, found: 373.0540 ($[M+H]^+$).

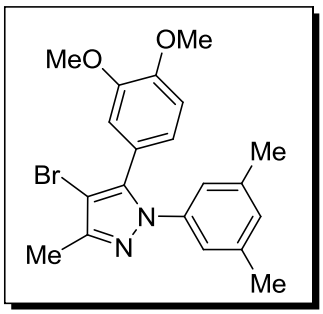

4-Bromo-5-(3,4-dimethoxyphenyl)-1-(3,5-dimethylphenyl)-3-methyl-1*H*-pyrazole 3h. Analytical TLC on silica gel, 1:4 ethyl acetate/hexane R_f =

0.57; yellow liquid; yield: 75% (243 mg). ^{1}H NMR (400 MHz, $CDCl_3$) δ 6.92 (s, 2H), 6.82-6.79 (m, 4H), 3.88 (s, 3H), 3.74 (s, 3H), 2.34 (s, 3H), 2.29 (s, 6H); $^{13}C\{^{1}H\}$ NMR (100 MHz, $CDCl_3$) δ 149.7, 148.9, 148.7, 140.8, 139.2, 138.6, 126.3, 124.3, 123.1, 121.5, 113.1, 111.2, 96.9, 56.5, 56.4, 24.1, 12.7; FT-IR (neat) 2926, 2853, 2835, 1588, 1508, 1464, 1258, 1240, 1027 cm^{-1}; HRMS (ESI) *m/z* $[M+H]^+$ calcd for $C_{20}H_{21}BrN_2O_2$: 401.0859, found: 401.0865.

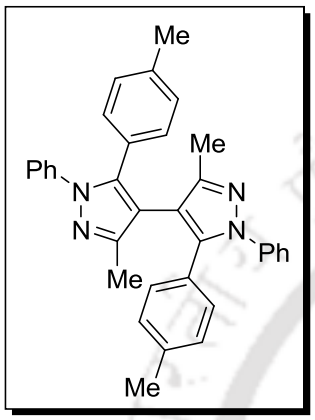

3,3'-Dimethyl-1,1'-diphenyl-5,5'-di-*p*-tolyl-1*H*,1'*H*-4,4'-bipyrazole A. Analytical TLC on silica gel, 1:9 ethyl acetate/hexane R_f = 0.59; yellow liquid; yield: 24% (73 mg). ^{1}H NMR (400 MHz, $CDCl_3$) δ 7.26-7.16 (m, 9H), 2.38 (s, 3H), 2.36 (s, 3H); $^{13}C\{^{1}H\}$ NMR (75 MHz, $CDCl_3$) δ 150.0, 144.0, 140.1, 138.5, 129.9, 129.3, 129.0, 127.7, 126.3, 124.9, 108.2, 21.5, 12.7; FT-IR (neat) 3032, 2924, 2855, 1597, 1507, 1453, 1376, 1362, 1064 cm^{-1}; HRMS (ESI) *m/z* $[M+H]^+$ calcd for $C_{34}H_{30}N_4$: 495.2544, found: 495.2541.

Crystal Data and Structure Refinement for 3d at 298(2) K.

Identification code	**3d**
Empirical formula	$C_{15}H_{10}ClBrN_2$
Formula weight	333.60
Temperature	298(2)
Wavelength	0.71073 Å
Crystal system	Triclinic
Space group	P-1
	Loop xyz
	'x, y, z'
	'-x, -y, -z'
Unit cell dimensions	*a* = 5.7832(5)Å α(°) = 92.707(5)
	b = 9.2597(8) Å β(°) = 95.546(5)
	c = 13.1413(10) Å γ(°) = 95.186(5)
Volume	696.45(10) $Å^3$
Z	2
Density (calculated)	1.596 Mg/m^3
Absorption coefficient	3.129 mm^{-1}
F(000)	332.0
Crystal size	0.28 x 0.23 x 0.21 mm
Theta range for data collection	2.63 to 23.36 °
Index ranges	-7<=h<=6, -10<=k<=11, -16<=l<=17
Reflections collected	3356
Independent reflections	1931 [R (int) = 0.0308]
Completeness to theta = 28.26°	97.2 %
Absorption correction	Multi-scan
Refinement method	Full-matrix least-squares on F^2
Data / restraints / parameters	3356/ 0 /172
Goodness-of-fit on F^2	1.015
Final R indices [I>2sigma (I)]	*R1* = 0.0398, *wR2* = 0.0952
R indices (all data)	*R1* = 0.0744, *wR2* = 0.1076

3.5 References

1. (a) Sun, L.-Q.; Chen, J.; Bruce, M.; Deskus, J. A.; Epperson, J. R.; Takaki, K.; Johnson, G.; Iben, L.; Malhe, C. D.; Ryan, E.; Xu, C. *Bioorg. Med. Chem. Lett.* **2004**, *14*, 3799. (b) Semple, G.; Skinner, P. J.; Cherrier, M. C.; Webb, P. J.; Sage, C. R.; Tamura, S. Y.; Chen, R.; Richman, J. G.; Connolly, D. T. *J. Med. Chem.* **2006**, *49*, 1227. (c) Jung, J.-K.; Johnson, B. R.; Duong, T.; Decaire, M.; Uy, J.; Gharbaoui, T.; Boatman, P. D.; Sage, C. R.; Chen, R.; Richman, J. G.; Connolly, D. T.; Semple, G. *J. Med. Chem.* **2007**, *50*, 1445. (d) Skinner, P. J.; Cherrier, M. C.; Webb, P. J.; Shin, Y.-J.; Gharbaoui, T.; Lindstrom, A.; Hong, V.; Tamura, S. Y.; Dang, H. T.; Pride, C. C.; Chen, R.; Richman, J. G.; Connolly, D. T.; Semple, G. *Bioorg. Med. Chem. Lett.* **2007**, *17*, 5620. (e) Skinner, P. J.; Webb, P. J.; Sage, C. R.; Dang, H. T.; Pride, C. C.; Chen, R.; Tamura, S. Y.; Richman, J. G.; Connolly, D. T.; Semple, G. *Bioorg. Med. Chem. Lett.* **2009**, *19*, 4207. (f) Luo, Y.; Yao, J.-P.; Yang, L.; Feng, C.-L.; Tang, W.; Wang, G.-F.; Zuo, J.-P.; Lu, W. *Bioorg. Med. Chem.* **2010**, *18*, 5048. (g) Bobileva, O.; Bokaldere, R.; Gailite, V.; Kaula, I.; Ikaunieks, M.; Duburs, G.; Petrovska, R.; Mandrika, I.; Klovins, J.; Loza, E. *Bioorg. Med. Chem.* **2014**, *22*, 3654. (h) Ellard, J. M.; Madin, A.; Philps, O.; Hopkin, M.; Henderson, S.; Birch, L.; O'Connor, D.; Arai, T.; Takase, K.; Morgan, L.; Reynolds, D.; Talma, S.; Howley, E.; Powney, B.; Payne, A. H.; Hall, A.; Gartlon, J. E.; Dawson, L. A.; Castro, L.; Atkinson, P. J. *Bioorg. Med. Chem. Lett.* **2015**, *25*, 5792.
2. For examples, see: (a) Eicher, T.; Hauptmann, S.; Speicher, A. *The Chemistry of Heterocycles*, *2nd ed.*; Wiley & Sons: New York, 2004; pp. 179. (b) Stanovnik, B.; Svete, J.; In *Pyrazoles*, Neier, R., Ed.; Science of Synthesis, Houben-Weyl, *Methods of Organic Transformations*, Vol. 12, Georg Thieme, Stuttgart, Germany, 2002; pp.15. (c) Elguero, J. In *Comprehensive Heterocyclic Chemistry*, Katritzky, A. R., Rees, C. W., Eds.; Pergamon Press: Oxford, UK, 1984; Vol. 5; pp. 167.
3. (a) Bekhit, A. A.; Abdel-Aziem, T. *Bioorg. Med. Chem*. **2004**, *12*, 1935. (b) Sperandeo, N. R.; Brun, R. *Chem. BioChem*. **2003**, *4*, 69. (c) Mukherjee, R. *Coord. Chem. Rev*. **2000**, *203*, 151.
4. For transition-metal-catalyzed synthesis of pyrazoles, see: (a) Cristau, H.-J.; Cellier, P. P.; Spindler, J.-F.; Taillefer, M. *Eur. J. Org. Chem*. **2004**, 695. (b) Martin, R.; Rivero, M. R.; Buchwald, S. L. *Angew. Chem., Int. Ed*. **2006**, *45*, 7079. (c) Hu, J.;

Cheng, Y.; Yang, Y.; Rao, Y. *Chem. Commun*. **2011**, *47*, 10133. (d) Suri, M.; Jousseaume, T.; Neumann, J. J. Glorius, F. *Green Chem*. **2012**, *14*, 2193. (e) Hu, J.; Chen, S.; Sun, Y.; Yang, J.; Rao, Y. *Org. Lett.* **2012**, *14*, 5030. (f) Panda, N.; Jena, A. K. *J. Org. Chem.* **2012**, *77*, 9401. (g) Zhang, T.; Bao, W. *J. Org. Chem.* **2013**, *78*, 1317. (h) Li, D. Y.; Mao, X. F.; Chen, H. J.; Chen, G. R.; Liu, P. N. *Org. Lett.* **2014**, *16*, 3476. (i) Schmitt, D. C.; Taylor, A. P.; Flick, A. C.; Kyne, R. E., Jr.; *Org. Lett.* **2015**, *17*, 1405. (j) Chen, Q.; Yao, F.; Yin, L.; Cai, M. *J. Organomet. Chem.* **2016**, *804*, 108.

5. (a) Bagley, M. C.; Lubinu, M. C.; Mason, C. *Synlett* **2007**, *5*, 0704. (b) Waldo, J. P.; Mehta, S.; Larock, R. C. *J. Org. Chem.* **2008**, *73*, 6666. (c) Zora, M.; Kivrak, A.; Yazici, C. *J. Org. Chem.* **2011**, *76*, 6726. (d) Zhang, X.; Kang, J.; Niu, P.; Wu, J.; Yu, W.; and Chang, J. *J. Org. Chem.* **2014**, *79*, 10170. (e) Aggarwal, R.; Kumar, R. *Synth. Commun*. **2009**, *39*, 2169. (f) Desai, V. G.; Satardekar, P. C.; Polo, S.; Dhumaskar, K. *Synth. Commun.* **2012**, *42*, 836. (g) Dadiboyena, S.; Valente, E. J.; Hamme, A. T., II *Tetrahedron Lett.* **2010**, *51*, 1341. (h) Jin, W.; Yu, H.; Yu, Z. *Tetrahedron, Lett.* **2011**, *52*, 5884. (i) Ji, G.; Wang, X.; Zhang, S.; Xu, Y.; Ye, Y.; Li, M.; Zhang, Y.; Wang, J. *Chem. Commun.* **2014**, *50*, 4361. (j) Kamal, A.; Visweswara Sastry, K. N.; Chandrasekhar, D.; Mani, G. S.; Adiyala, P. R.; Nanubolu, J. B.; Singarapu, K. K.; Maurya, R. A. *J. Org. Chem.* **2015**, *80*, 4325. (k) Bassaco, M. M.; Fortes, M. P.; Kaufman, T. S.; Silveira, C. C. *RSC, Adv.* **2015**, *5*, 21112. (l) Fuchibe, k.; Takahashi, M.; Ichikawa, J. *Angew. Chem., Int. Ed.* **2012**, *51*, 12059. (m) Kirkham, J. D.; Edeson, S. J.; Stokes, S.; Harrity, J. P. A. *Org. Lett.* **2012**, *14*, 5354. (n) Zhang, G.; Ni, H.; Chen, W.; Shao, J.; Liu, H.; Chen, B.; Yu, Y. *Org. Lett.* **2013**, *15*, 5967. (o) Zhang, J.; Shao, Y.; Wang, H.; Luo, Q.; Chen, J.; Xu, D.; Wan, X. *Org. Lett.* **2014**, *16*, 3312. (p) Kong, Y.; Tang, M.; Wang, Y. *Org. Lett.* **2014**, *16*, 576.

6. For some examples on the use of TEMPO, see: (a) Wencel-Delord, J.; Glorius, F. *Nature Chem*. **2013**, *5*, 369. (b) Hoover, J. M.; Stahl, S. S. *J. Am. Chem. Soc*. **2011**, *133*, 16901. (c) Guérin, C.; Bellosta, V.; Guillamot, G.; Cossy, J. *Org. Lett*. **2011**, *13*, 3534. (d) Tebben, L.; Studer, A. *Angew. Chem., Int. Ed*. **2011**, *50*, 5034. (e) Maji, M. S.; Murarka, S.; Studer, A. *Org. Lett*. **2010**, *12*, 3878. (f) Pradhan, P. P.; Bobbitt, J. M.; Bailey, W. F. *J. Org. Chem*. **2009**, *74*, 9524. (g) Vogler, T.; Studer, A. *Synthesis* **2008**, *13*, 1979. (h) Shibuya, M.; Tomizawa, M.; Iwabuchi, Y. *J. Org. Chem*. **2008**, *73*, 4750. (i) Bailey, W. F.; Bobbitt, J. M.; Wiberg, K. B. *J. Org. Chem*. **2007**, *72*,

4504. (j) Jiang, N.; Ragauskas, A. J. *J. Org. Chem*. **2006**, *71*, 7087. (k) Punniyamurthy, T.; Velusamy, S.; Iqbal, J. *Chem. Rev*. **2005**, *105*, 2329. (l) Ansari, I. A.; Gree, R. *Org. Lett*. **2002**, *4*, 1507. (m) Bolm, C.; Magnus, A. S.; Hildebrand, J. P. *Org. Lett*. **2000**, *2*, 1173.

7. For the use of NBS, see: (a) Sadhu, P.; Alla, S. K.; Punniyamurthy, T. *J. Org. Chem*. **2013**, *78*, 6104. (b) Schröder, N.; Wencel-Delord, J.; Glorius, F. *J. Am. Chem. Soc*. **2012**, *134*, 8298. (c) Gao, F.; Hoveyda, A. H. *J. Am. Chem. Soc*. **2010**, *132*, 10961. (d) Murai, K.; Takahara, Y.; Matsushita, T.; Komatsu, H.; Fujioka, H. *Org. Lett*. **2010**, *12*, 3456. (e) Mundal, D. A.; Lutz, K. E.; Thomson, R. J. *Org. Lett*. **2009**, *11*, 465. (f) García Mancheño, O.; Bistri, O.; Bolm, C. *Org. Lett*. **2007**, *9*, 3809. (g) Prakash, G. K. S.; Mathew, T.; Hoole, D.; Esteves, P. M.; Wang, Q.; Rasul, G.; Olah, G. A. *J. Am. Chem. Soc*. **2004**, *126*, 15770. (h) Thakur, V. V.; Talluri, S. K.; Sudalai, A. *Org. Lett*. **2003**, *5*, 861.
8. (a) Guru, M. M.; Ali, M. A.; Punniyamurthy, T. *J. Org. Chem.* **2011**, *76*, 5295.
9. Conn, R. S. E.; Douglas, A. W.; Karady, S.; Corley, E. G.; Lovell, A. V.; Shinkai, I. *J. Org. Chem.* **1990**, *55*, 2908.
10. (a) Li, G.; Kakarla, R. S.; Gerritz, W. *Tetrahedron Lett*. **2007**, *48*, 4595. (b) Jeon, S. L.; Choi, J. H.; Kim, B. T.; Jeong, I. H.; *J. Fluorine Chem.* **2007**, *128*, 1191.
11. (a) Peruncheralathan, S.; Khan, T. A.; Ila, H.; Junjappa, H. *J. Org. Chem*. **2005**, *70*, 10030. (b) Kirkham, J. D.; Edeson, S. J.; Stokes, S.; Harrity, J. P. A. *Org. Lett*. **2012**, *14*, 5354. (c) Spivey, A. C.; Diaper, C. M.; Adams, H.; Rudge, A. J. *J. Org. Chem*. **2000**, *65*, 5253.

3.6 Selected Spectra

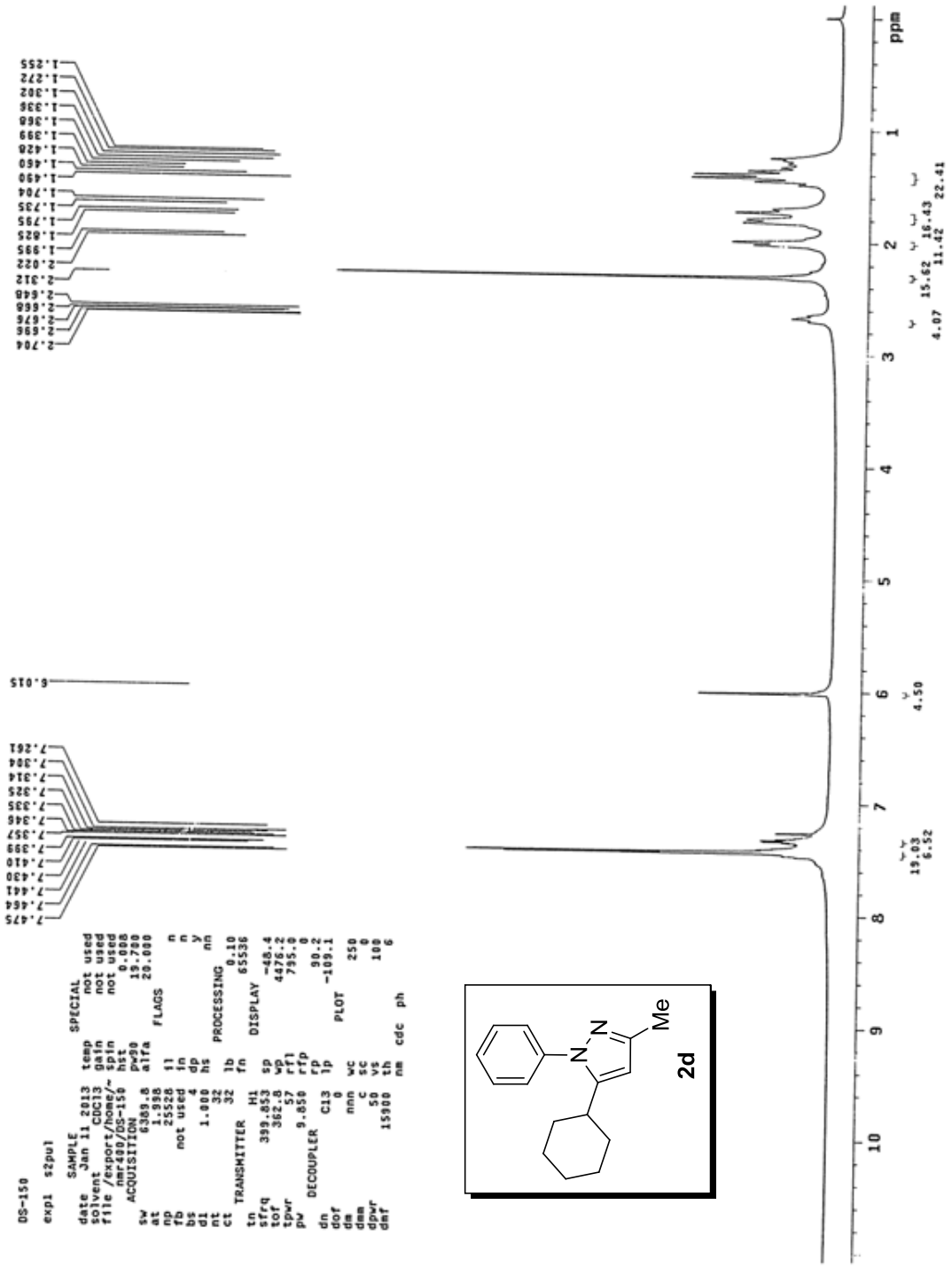

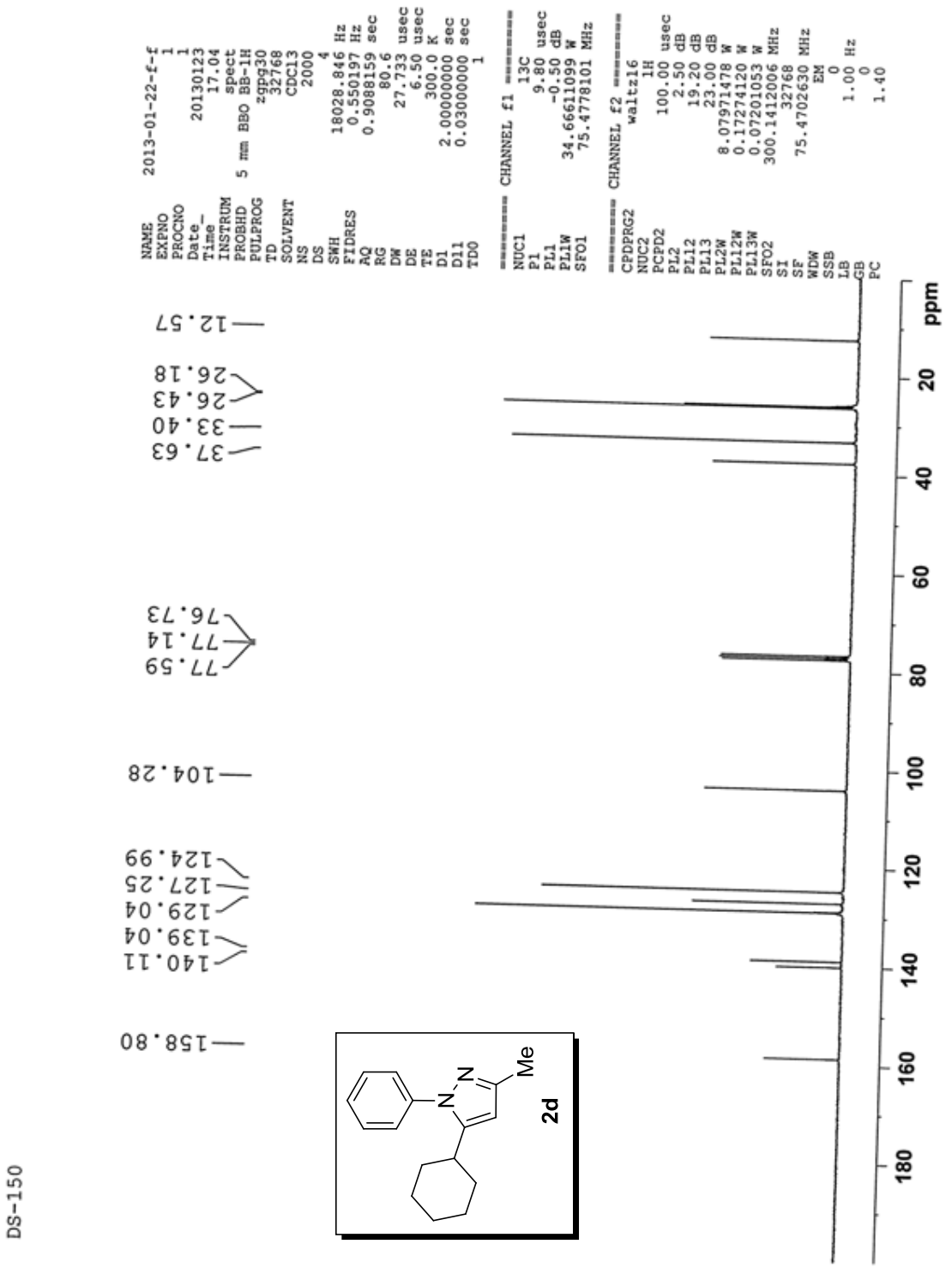
DS-150
NAME 2013-01-22-f-f
EXPNO 1
PROCNO 1
Date_ 20130123
Time_ 17.04
INSTRUM spect
PROBHD 5 mm BBO BB-1H
PULPROG zgpg30
TD 32768
SOLVENT CDCl3
NS 2000
DS 4
SWH 18028.846 Hz
FIDRES 0.550197 Hz
AQ 0.9088159 sec
RG 80.6
DW 27.733 usec
DE 6.50 usec
TE 300.0 K
D1 2.00000000 sec
D11 0.03000000 sec
TD0 1
======== CHANNEL f1 ========
NUC1 13C
P1 9.80 usec
PL1 -0.50 dB
PL1W 34.66611099 W
SFO1 75.4778101 MHz
======== CHANNEL f2 ========
CPDPRG2 waltz16
NUC2 1H
PCPD2 100.00 usec
PL2 2.50 dB
PL12 19.20 dB
PL13 23.00 dB
PL2W 8.07971478 W
PL12W 0.17274120 W
PL13W 0.07201053 W
SFO2 300.1412006 MHz
SI 32768
SF 75.4702630 MHz
WDW EM
SSB 0
LB 1.00 Hz
GB 0
PC 1.40
12.57
26.18
26.43
33.40
37.63
76.73
77.14
77.59
104.28
124.99
127.25
129.04
139.04
140.11
158.80
Me
2d
ppm
20
40
60
80
100
120
140
160
180

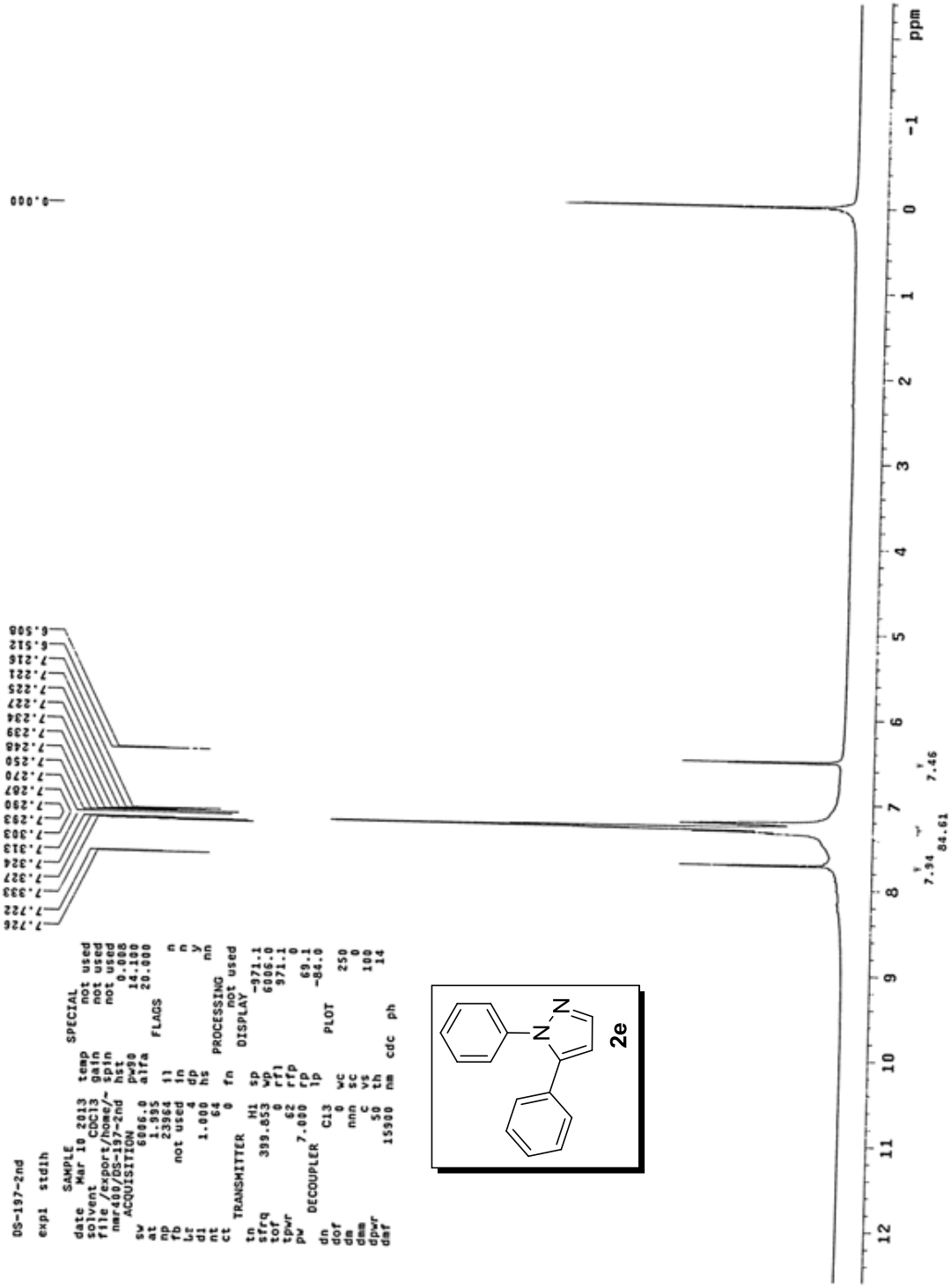
DS-197-2nd
expl stdih
SAMPLE
date Mar 10 2013
solvent CDCl3
file /export/home/~
nmr400/DS-197-2nd
ACQUISITION
sw 6006.0
at 1.995
np 23964
fb not used
bs 4
d1 1.000
nt 64
ct 0
TRANSMITTER
tn H1
sfrq 399.853
tof 0
tpwr 62
pw 7.000
DECOUPLER
dn C13
dof 0
dm nnn
dmm c
dpwr 50
dmf 15900
SPECIAL
temp not used
gain not used
spin not used
hst 0.008
pw90 14.100
alfa 20.000
FLAGS
il n
in n
dp y
hs nn
PROCESSING
fn not used
DISPLAY
sp -971.1
wp 6006.0
rfl 971.1
rfp 0
rp 69.1
lp -84.0
PLOT
wc 250
sc 0
vs 100
th 14
cdc ph
nm
2e
7.726
7.722
7.333
7.327
7.324
7.313
7.303
7.293
7.290
7.287
7.270
7.250
7.248
7.239
7.234
7.227
7.225
7.221
7.216
6.512
6.508
0.000
ppm
7.94
7.46
84.61

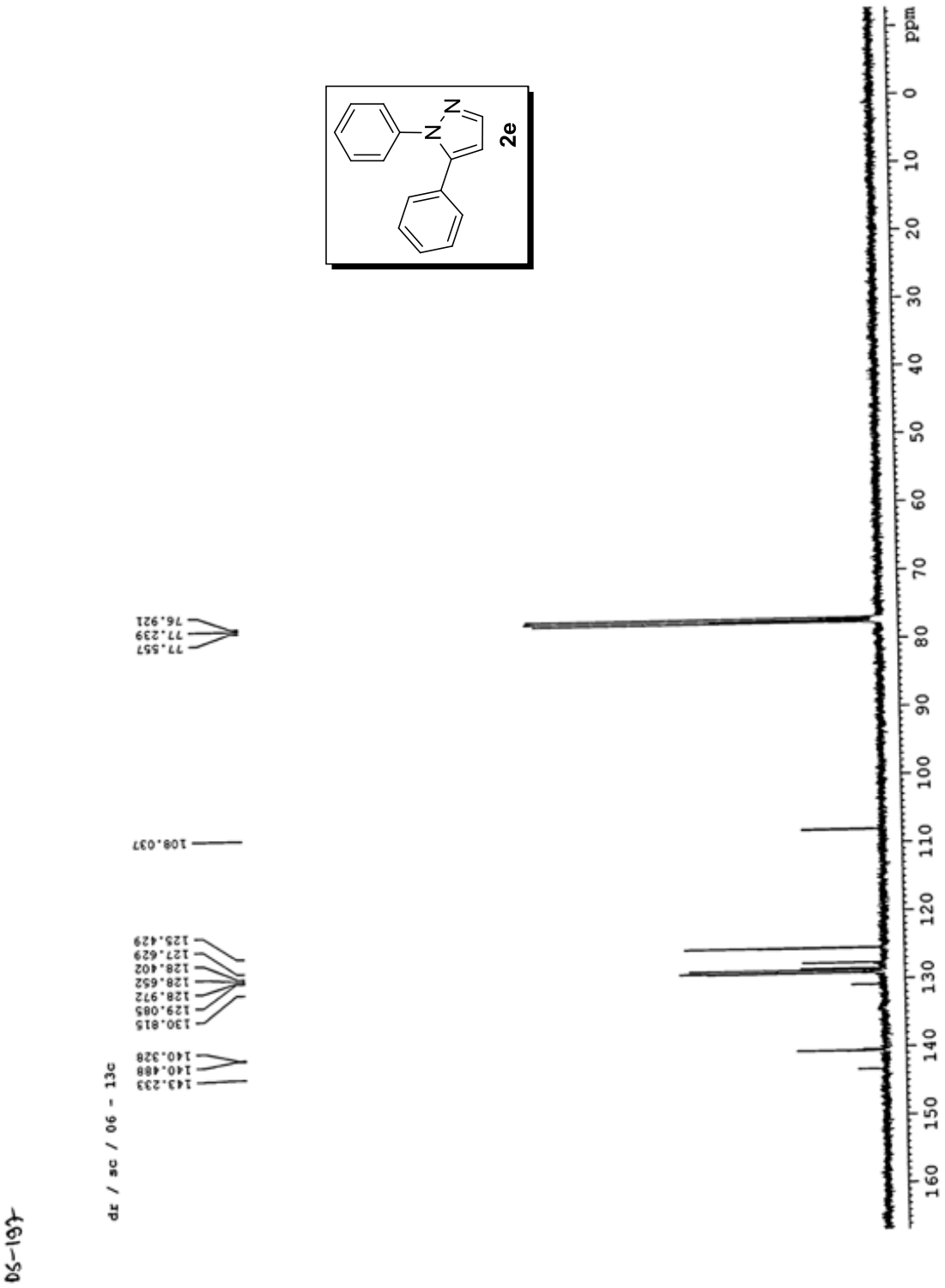
2e
ppm
0
10
20
30
40
50
60
70
80
90
100
110
120
130
140
150
160
76.921
77.239
77.557
108.037
125.429
127.629
128.402
128.652
128.972
129.085
130.815
140.328
140.488
143.233
dz / sc / 06 - 13c
DS-197

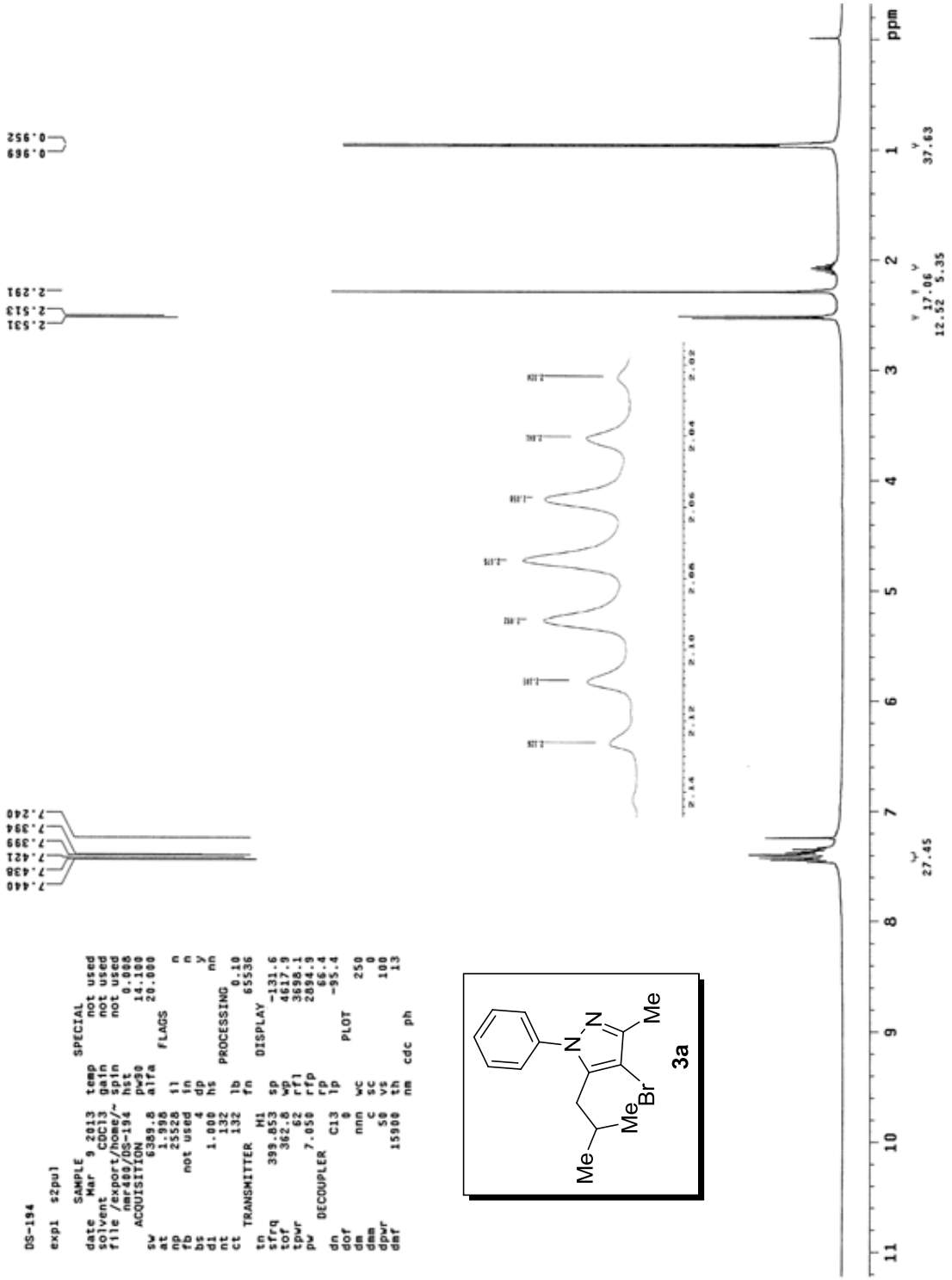
DS-194
expl szpul
SAMPLE
date Mar 9 2013
solvent CDCl3
file /export/home/~
nmr400/DS-194
ACQUISITION
sw 6389.8
at 1.998
np 25528
fb not used
bs 4
d1 1.000
nt 132
ct 132
TRANSMITTER
tn H1
sfrq 399.853
tof 362.8
tpwr 62
pw 7.050
DECOUPLER
dn C13
dof 0
dm nnn
dmm c
dpwr 50
dmf 15900
SPECIAL
temp not used
gain not used
spin not used
hst 0.008
pw90 14.100
alfa 20.000
FLAGS
il n
in n
dp y
hs nn
PROCESSING
lb 0.10
fn 65536
DISPLAY
sp -131.6
wp 4617.9
rfl 3698.1
rfp 2894.9
rp 66.4
lp -95.4
PLOT
wc 250
sc 0
vs 100
th 13
cdc ph
nm
7.460
7.438
7.421
7.399
7.394
7.240
2.531
2.513
2.291
0.969
0.952
Me
Me
Br
Me
3a
ppm
27.45
17.06
12.52
5.35
37.63

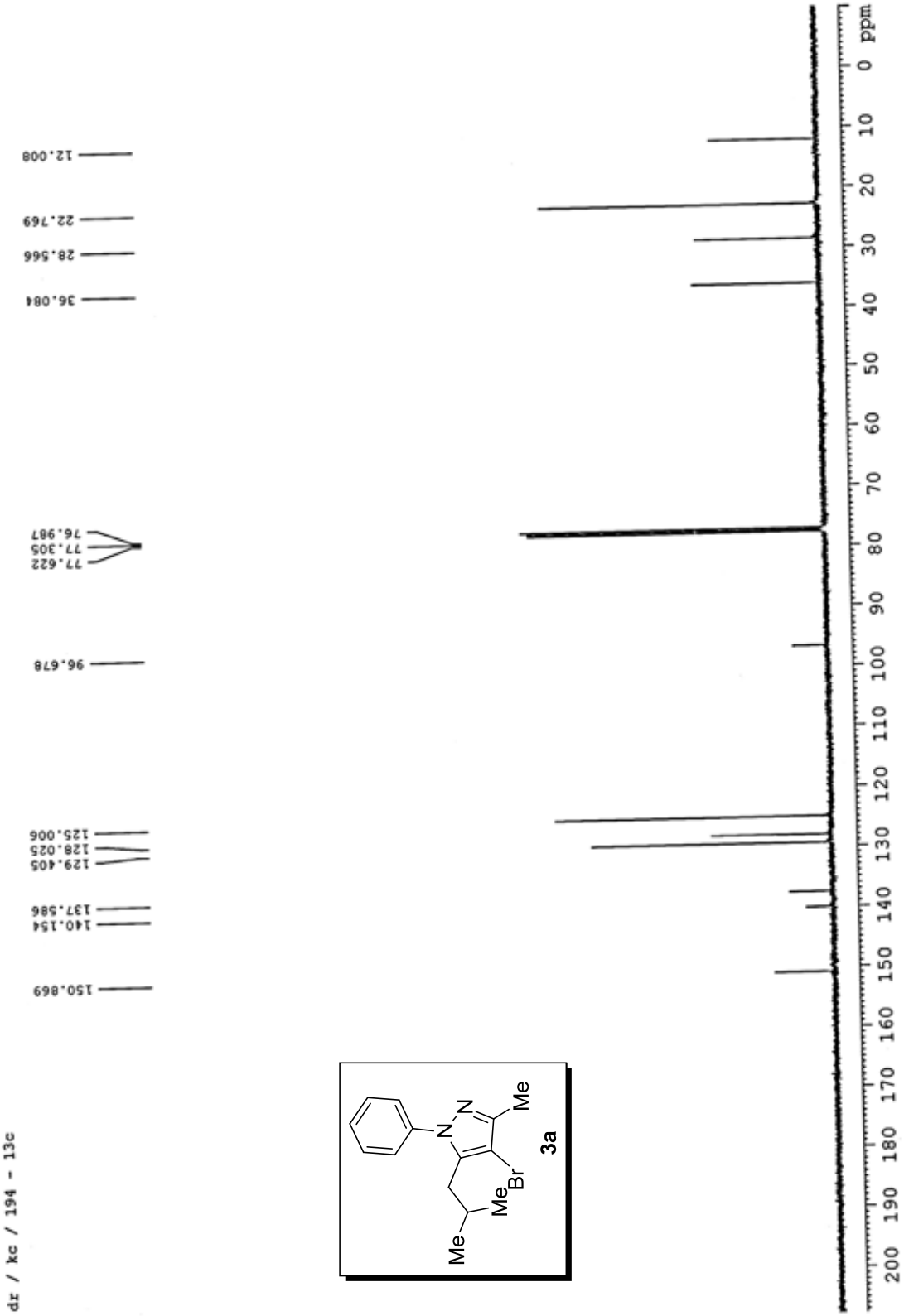
dr / kc / 194 - 13c
12.008
22.769
28.566
36.084
76.987
77.305
77.622
96.678
125.006
128.025
129.405
137.586
140.154
150.869
0 ppm
10
20
30
40
50
60
70
80
90
100
110
120
130
140
150
160
170
180
190
200
Me
N
N
Me
Br
Me
3a

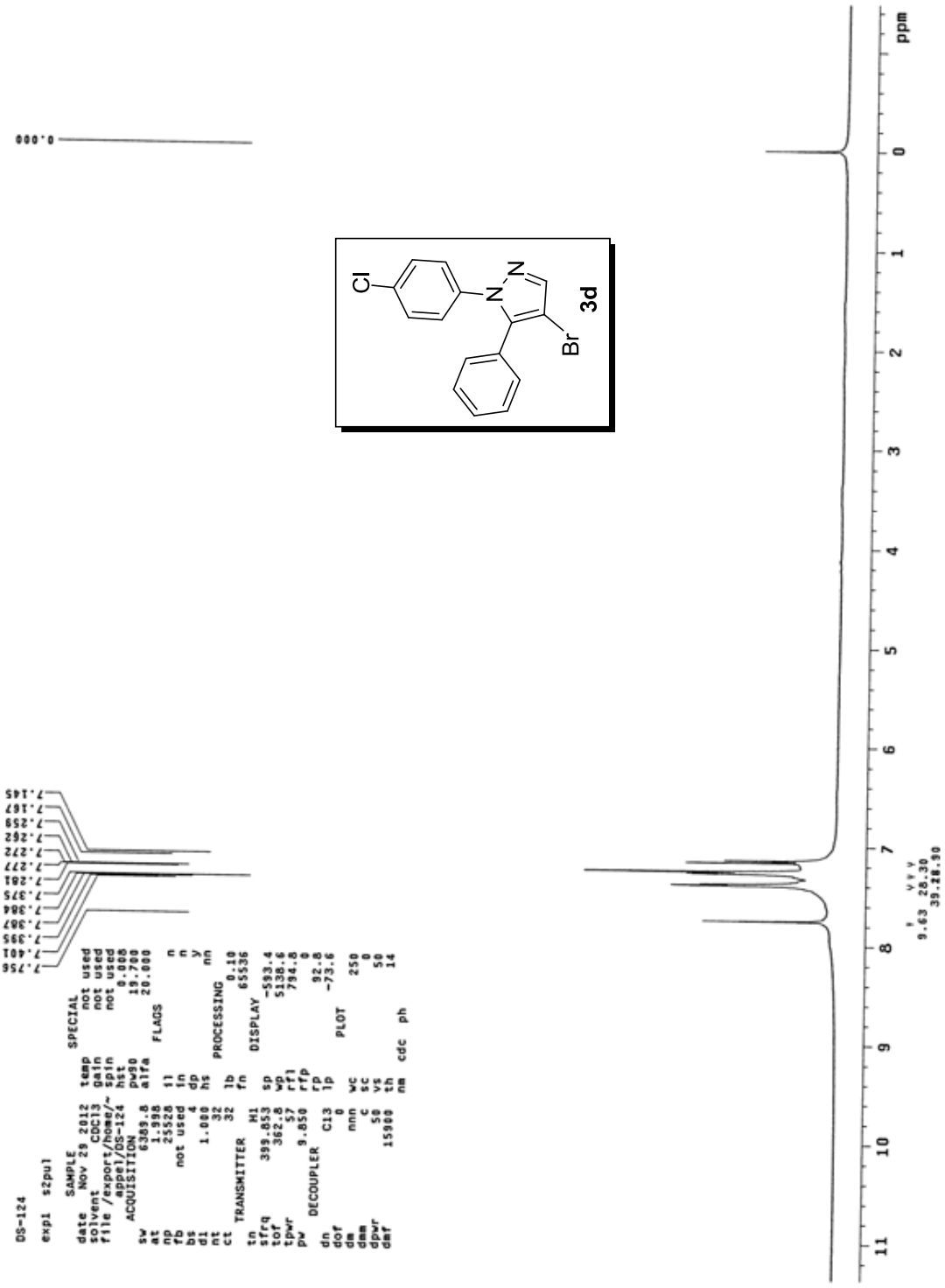
Cl
N
N
Br
3d
ppm
0
1
2
3
4
5
6
7
8
9
10
11
9.63
28.30
39.28.90

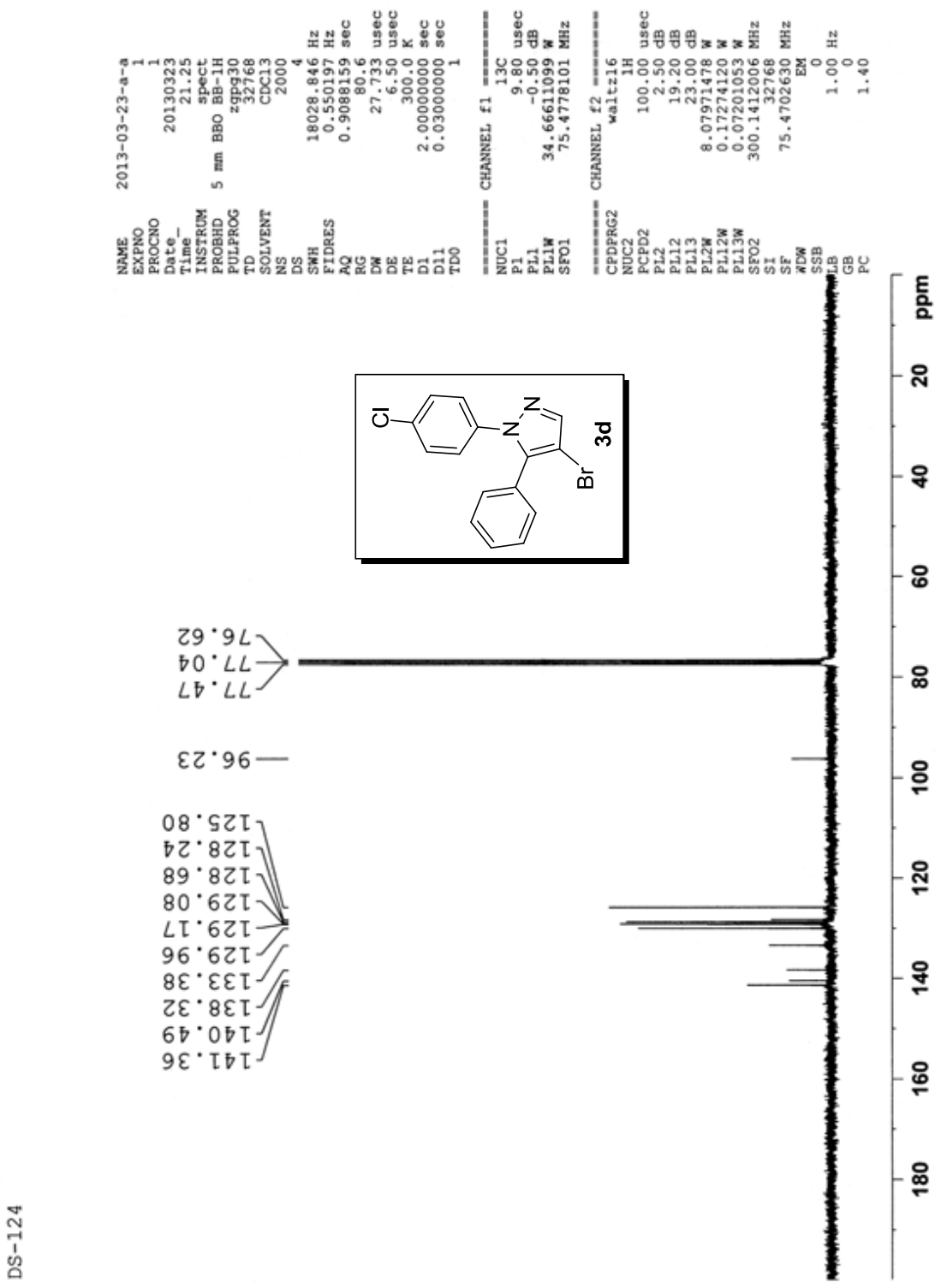
DS-124
NAME 2013-03-23-a-a
EXPNO 1
PROCNO 1
Date_ 20130323
Time 21.25
INSTRUM spect
PROBHD 5 mm BBO BB-1H
PULPROG zgpg30
TD 32768
SOLVENT CDCl3
NS 2000
DS 4
SWH 18028.846 Hz
FIDRES 0.550197 Hz
AQ 0.9088159 sec
RG 80.6
DW 27.733 usec
DE 6.50 usec
TE 300.0 K
D1 2.00000000 sec
D11 0.03000000 sec
TD0 1
CHANNEL f1
NUC1 13C
P1 9.80 usec
PL1 -0.50 dB
PL1W 34.66611099 W
SFO1 75.4778101 MHz
CHANNEL f2
CPDPRG2 waltz16
NUC2 1H
PCPD2 100.00 usec
PL2 2.50 dB
PL12 19.20 dB
PL13 23.00 dB
PL2W 8.07971478 W
PL12W 0.17274120 W
PL13W 0.07201053 W
SFO2 300.1412006 MHz
SI 32768
SF 75.4702630 MHz
WDW EM
SSB 0
LB 1.00 Hz
GB 0
PC 1.40
Cl
N
N
Br
3d
77.47
77.04
76.62
96.23
125.80
128.24
128.68
129.08
129.17
129.96
133.38
138.32
140.49
141.36
180
160
140
120
100
80
60
40
20
ppm

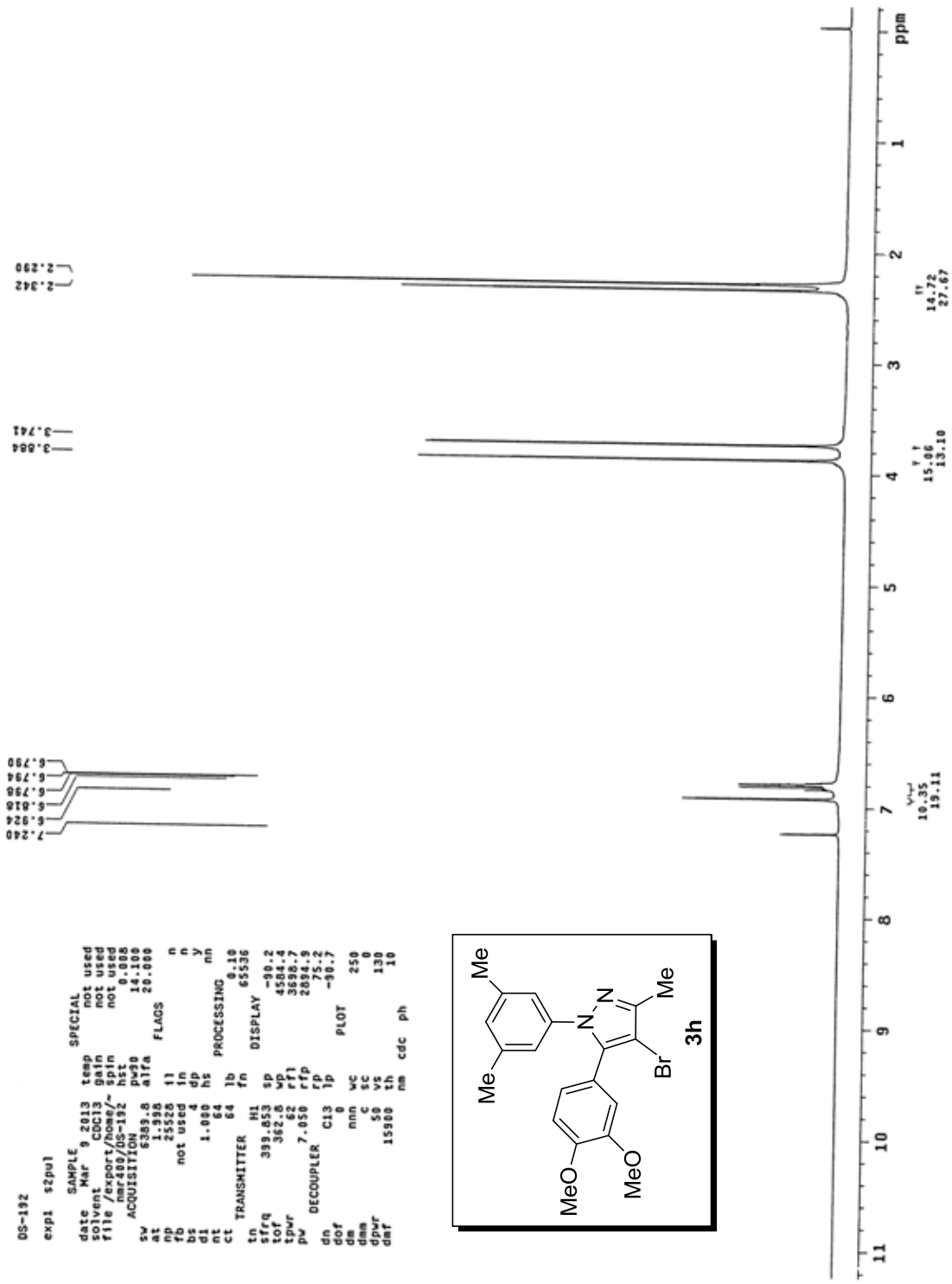
DS-192
expl s2pul
SAMPLE
date Mar 9 2013
solvent CDCl3
file /export/home/~
nmr400/DS-192
ACQUISITION
sw 6389.8
at 1.998
np 25528
fb
bs 4
d1 1.000
nt 64
ct 64
TRANSMITTER
tn H1
sfrq 399.853
tof 362.8
tpwr 62
pw 7.050
DECOUPLER
dn C13
dof 0
dm nnn
dmm c
dpwr 50
dmf 15900
SPECIAL
temp not used
gain not used
spin not used
hst 0.008
pw90 14.100
alfa 20.000
FLAGS
ll n
in n
dp y
hs nn
PROCESSING
lb 0.10
fn 65536
DISPLAY
sp -90.2
wp 4584.4
rfl 3698.7
rfp 2894.9
rp 75.2
lp -90.7
PLOT
wc 250
sc 0
vs 130
th 10
nm cdc ph
7.240
6.824
6.818
6.798
6.794
6.780
3.864
3.741
2.342
2.290
Me
Me
N
N
Me
Br
MeO
MeO
3h
ppm
1
2
3
4
5
6
7
8
9
10
11
14.72
27.67
15.06
13.10
10.35
19.11

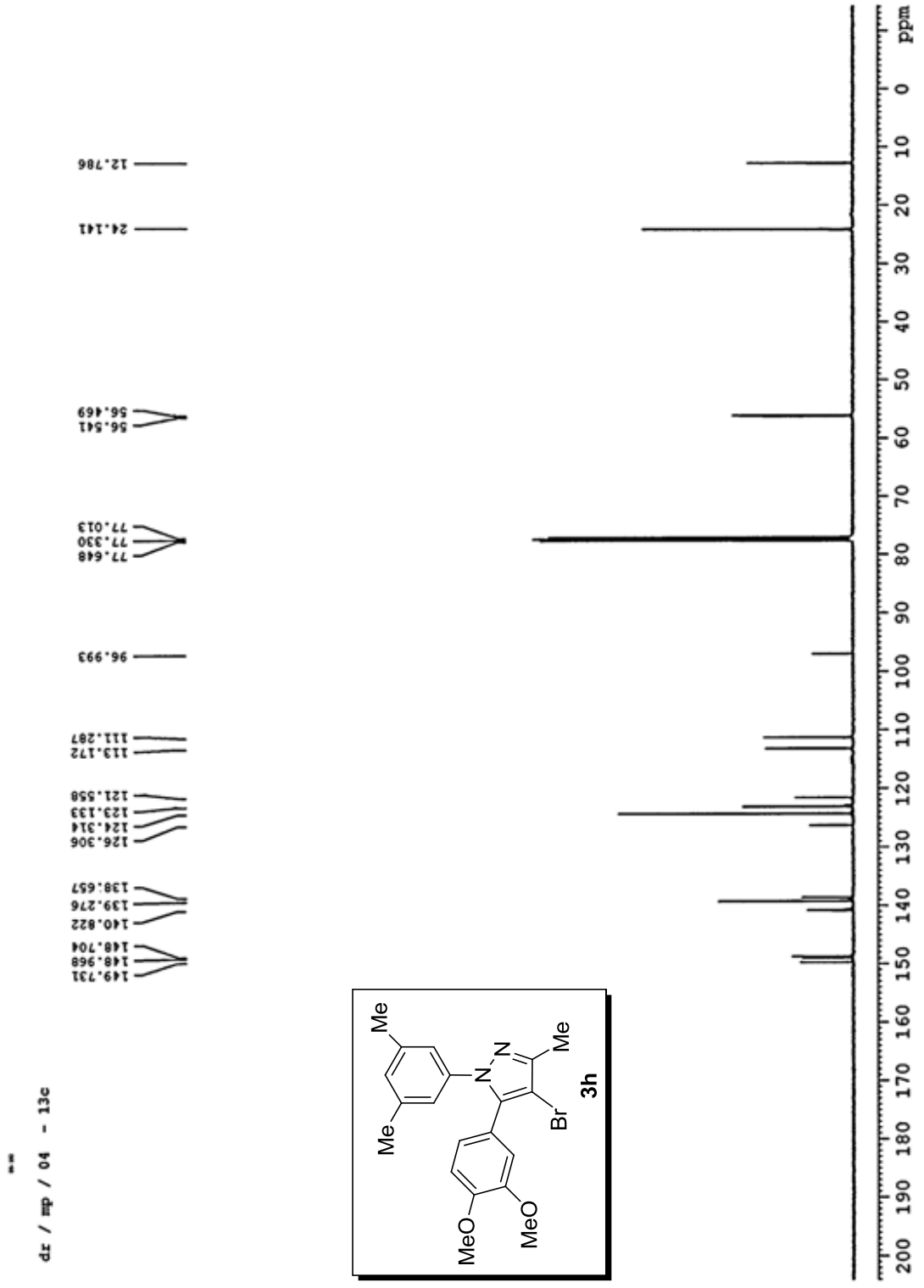
dr / mp / 04 - 13c
12.786
24.141
56.469
56.541
77.013
77.330
77.648
96.993
111.287
113.172
121.558
123.133
124.314
126.306
138.657
139.276
140.822
148.704
148.968
149.731
Me
Me
N
N
Me
Br
MeO
MeO
3h
ppm
0
10
20
30
40
50
60
70
80
90
100
110
120
130
140
150
160
170
180
190
200

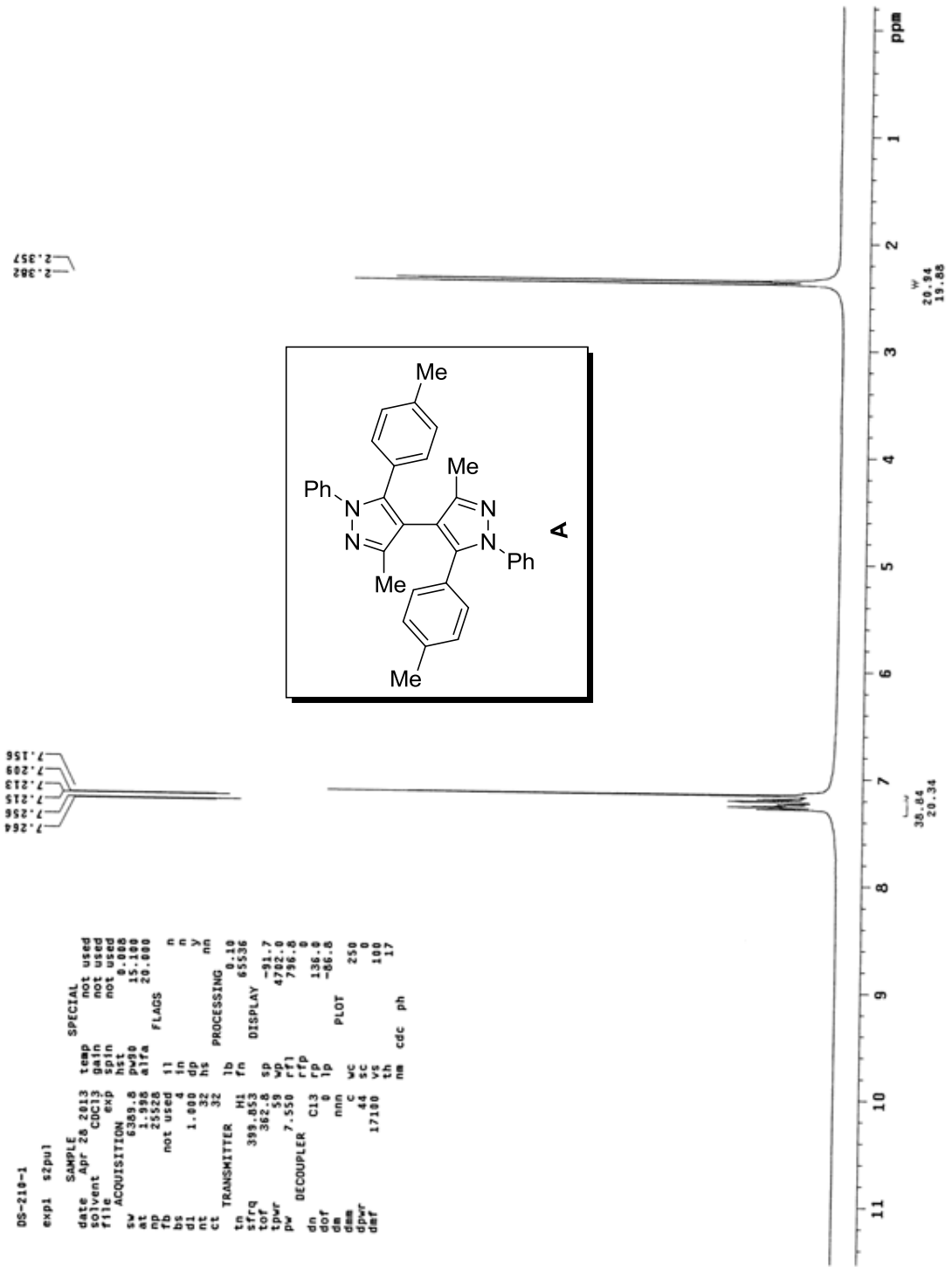
Me
Ph
N
N
Me
Me
N
N
Ph
Me
A
ppm

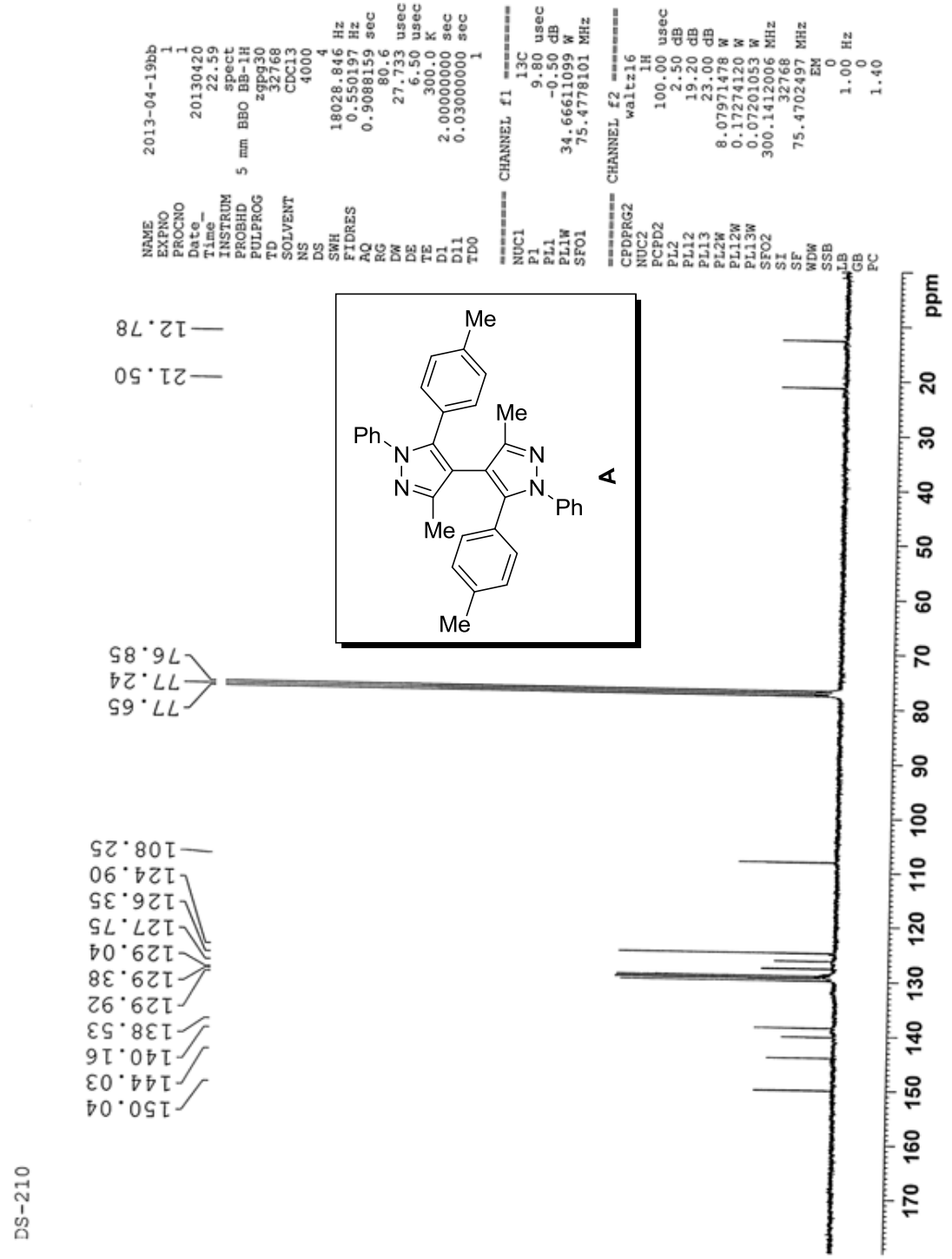
DS-210
12.78
21.50
76.85
77.24
77.65
108.25
124.90
126.35
127.75
129.04
129.38
129.92
138.53
140.16
144.03
150.04
Me
Ph
N
N
Me
Me
N
N
Ph
Me
A
ppm

Chapter IV

Photophysical Properties and Application of Pyrazoles: Fluorescence Switch-On Sensing of BSA Protein

Protein-drug interaction has made tremendous research interest as they play important role in pharmacology.[1] Study of interaction of proteins with drugs and interbiomolecular interactions is of pivotal impact in development of chemotherapeutics and in chemical biology. Many drugs bind to serum albumin such as bovine serum albumin proteins (BSA) and human serum albumin protein (HSA) in plasma, as BSA and HSA are extensively present in plasma and play biological roles.[2] As a result, protein structure, function, and small molecule-protein/interbiomolecular interaction can be understood.

Protein-ligand interactions are a complex array of intermolecular interactions and play a crucial role in all the living organisms.[3] These may involve specific interactions on the binding site of the protein as well as non-specific forces outside the protein binding site. The interaction between proteins and flexible target molecules including nucleic acids and small molecules changes the conformation of proteins. A complex so formed between the protein and a small molecule involves a complex equilibrium process (Scheme 1).

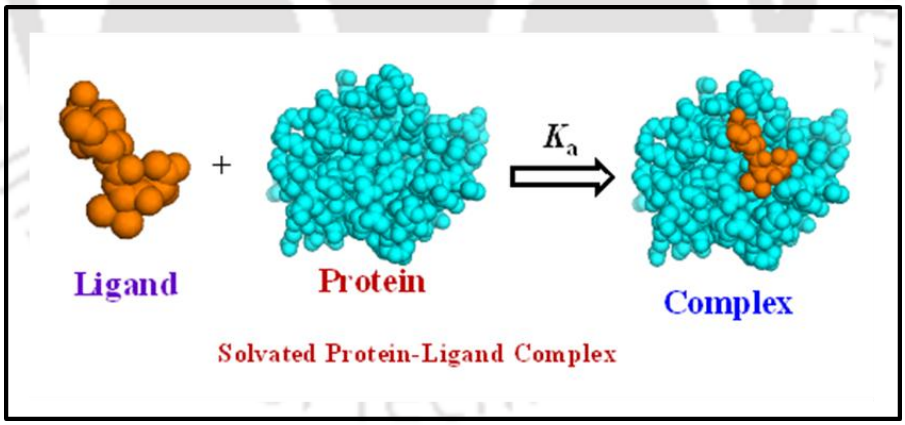

Scheme 1. Protein-Ligand Complex Equilibrium Process

4.1 Bovine Serum Albumin (BSA).

Serum albumins, widely present in blood plasma are the best known as transport protein[4] due to its ability of binding and transporting of wide range of important compounds in the blood stream to the target organs.[5] The compound such as fatty acids, surfactants, certain metal ions, hormones, enzymes and many therapeutic drugs are transported via serum

albumins proteins.[6] A large number of studies have been devoted to investigate the actual interaction behaviour of serum albumins with other proteins, drugs and fluorescent probes as well as actual structure and properties of serum albumins in these events. Bovine serum albumin (BSA) is one of the most commonly studied serum albumin, among the several serum albumins that are present in circulatory system, due to its abundance and structural similarity with well-established crystal structure of human serum albumin (HSA).[7] About 75% identity and 87% similarity are exhibited between BSA and HSA sequence. BSA contains three homologous domains I, II and III, and each domain is shared by two sub domains such as IA, IB; IIA, IIB; and IIIA, IIIB.[8] BSA contains two tryptophan residues, which are Trp-134 and Trp-212, located in IB and IIA sub domains, respectively.[9] The protein also has two structurally selective binding sites, such as site-I, which is located in IIA sub domain and binds mostly neutral bulky heterocyclic compounds by strong hydrophobic interaction and site-II, is located in IIIA and binds aromatic carboxylic acids by the combination of both hydrophobic, hydrogen bonding and electrostatic interactions.[10] The structure and position of various homologous domain and sub domain of BSA and HSA are shown in figure 1.

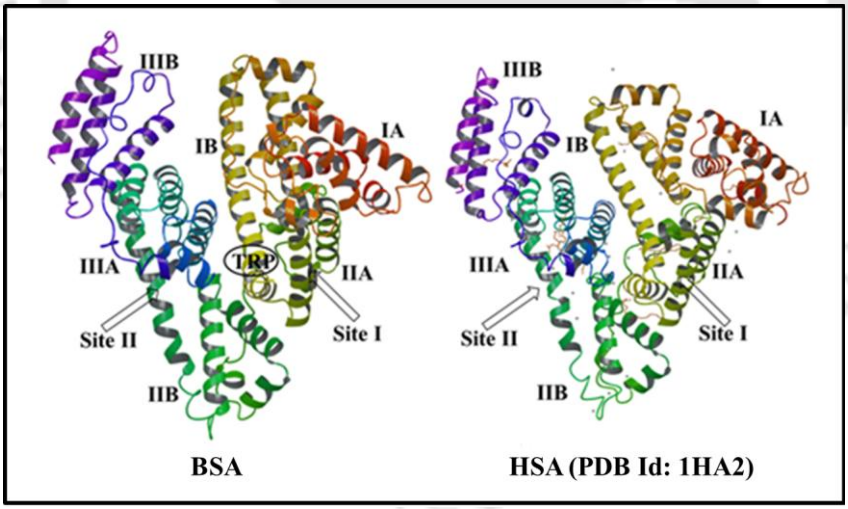

Figure 1. Structure and Various Homologous Domain and Sub Domain of BSA and HSA

Functionalized pyrazoles are the subject of recent research interest due to their widespread potential biological applications.[11] Furthermore, pyrazoles are known to bind strongly with biomolecules.[12] Therefore, study the interaction behaviour of synthesized

pyrazoles with biomolecules such as bovine serum albumin (BSA) which is described in this chapter, could find useful application in synthetic and medicinal sciences.[13]

4.2 Some Reported Small Molecule Probes of BSA

Fluorescence based studies have been widely utilized for the study of structure and binding event of BSA with drugs and small molecules. Thus, the photophysical properties are methods for studying the binding ability of proteins with drugs and small molecules via distinct fluorescence signal generation.[14] For example, Liu and co-workers reported the interaction behaviour of colchicine and BSA by fluorescence quenching method (Figure 2).[15a] They demonstrated that fluorescence of BSA is quenched due to the formation of the complex between BSA and colchicine, which is stabilized by van der Wall interaction and hydrogen bonds.

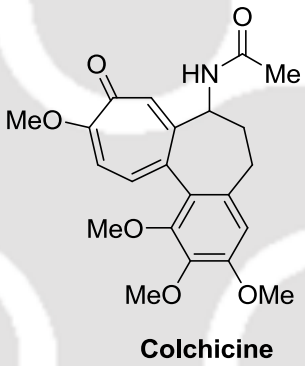

Figure 2. The chemical structure of Colchicine used in studying interaction with BSA

Das and co-workers synthesized amphiphilic fluorescent probe for selective detection of BSA protein (Figure 3).[15b] The fluorescence intensity of synthesized amphiphilic fluorescent probe increased upon addition of BSA due to non-covalent interaction with the probe.

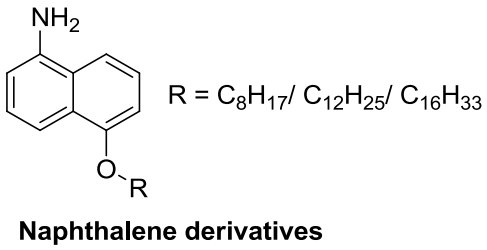

Figure 3. Naphthalene Derivatives as Amphiphilic Fluorescent Probe for BSA

Spectroscopic and theoretical studies are utilized to analyse the binding interaction of BSA and polarity sensitive flexible charge transfer fluorescent probe 5-(4-dimethylamino-phenyl)-penta-2,4-dienenitrile (DMAPPDN, Figure 4).[15c] A strong blue shifted emission (78 nm) with increased in intensity of fluorescence is observed for DMAPPDN in presence of increasing amount of BSA in aqueous buffer solution.

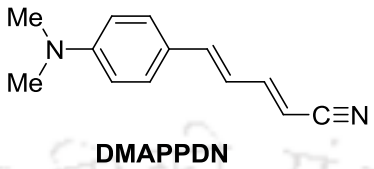

Figure 4. Example of Flexible Charge Transfer Fluorescence Probe for BSA

Campo and co-workers reported the synthesis of water-insoluble squaraine dyes with *N*-octyl pendent groups and studied their photophysical properties in organic solvents or in phosphate buffer solution in presence and absence of BSA (Figure 5).[15d] Squaraine dyes did not aggregate in organic solvents but a *J*-type aggregation could be formed in phosphate buffer solution. The fluorescence intensity of squaraine increased upon addition of BSA but in absence of BSA it showed almost no fluorescence.

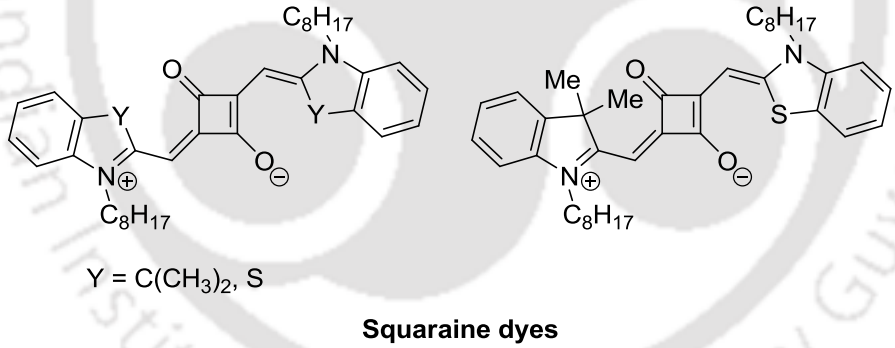

Figure 5. Chemical Structure of Squaraine Dyes

Lu and co-workers studied the interaction behaviour of BSA with 2,2-diphenyl-1-picrylhydrazyl (DPPH) radical by fluorescence technique and circular dichroism (CD) spectroscopy in absence and presence of eight antioxidant (Figure 6).[15e] The fluorescence intensity of BSA is quenched in presence of DPPH radical via a static mechanism. BSA scavenges DPPH radical as has been reflected from the UV-visible absorption study.

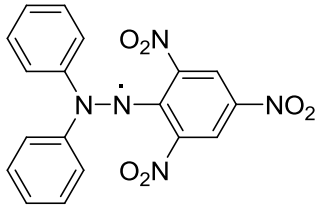

DPPH radical

Figure 6. DPPH Radical Used to Study Interaction Behaviour of BSA

The interaction behaviour of lysionotin and BSA has been shown at physiological pH by spectroscopic technique (Figure 7).[15f] The fluorescence quenching of BSA has been observed in presence of lysionotin. There was high interaction between lysionotin and BSA as was revealed from the binding constant value in the order of 10^5 L mol^{-1}.

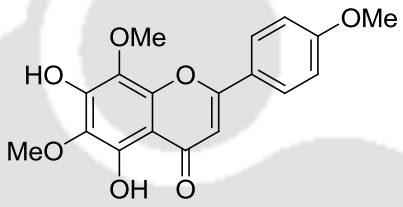

Lysionotin

Figure 7. Lysionotin Used as a Fluorescent Probe for BSA

The quantitation of BSA has been determined by a water soluble "turn-on" fluorescent probe sodium4,4′4″-(3,4-diphenyl-1*H*-pyrrole-1,2,5-triyl)tribenzoate (DP-TPPNa, Figure 8).[15g] The observed fluorescence turn-on behaviour is due to binding of BSA and DP-TPPNa via hydrophobic and hydrogen bonding interactions resulting restriction of intermolecular rotation.

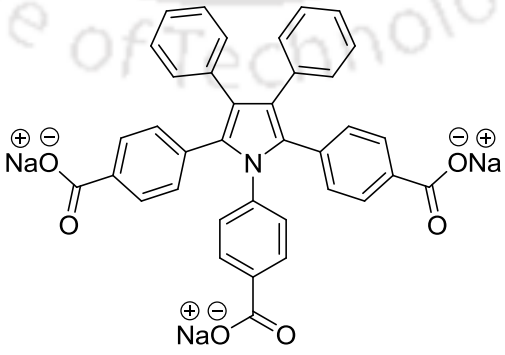

DP-TPPNa

Figure 8. Example of a Water Soluble "turn-on" Fluorescent Probe for BSA

4.3 Present Study

Herein we present the photophysical properties of the pyrazoles described in figure 9. We also describe the binding studies of the pyrazoles **3a** and **3y** towards BSA protein.

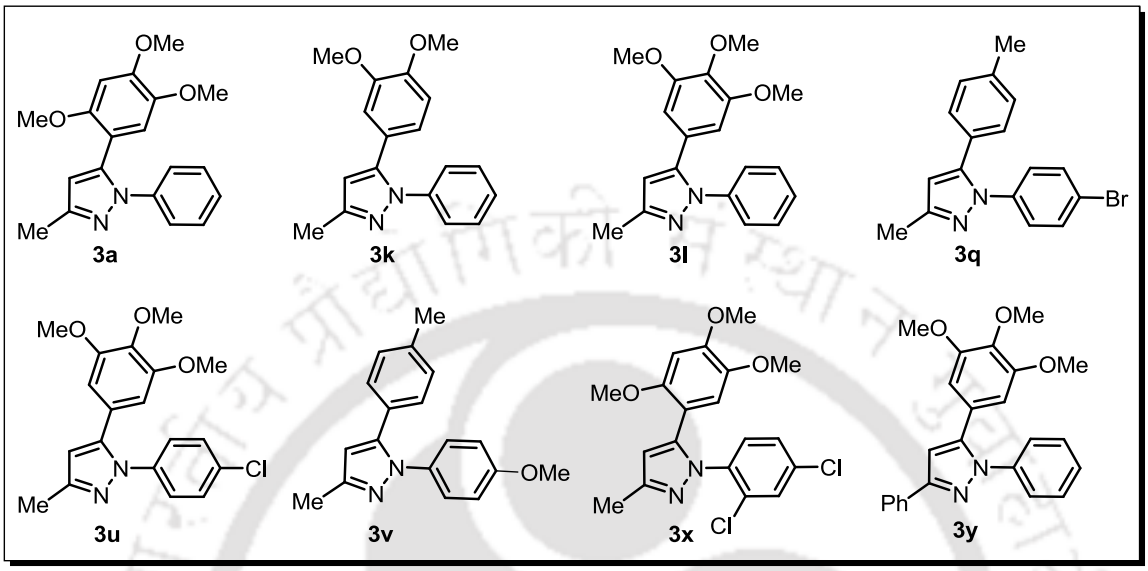

Figure 9. Synthesized Pyrazole Derivatives

4.3.1 UV-Visible and Fluorescence Study

All UV-visible and Fluorescence spectra of the compounds (10 μM) was measured in different solvents of varying dielectric constant by UV-visible spectrophotometer and fluorescence spectrophotometer using 1 cm path length cell at 298 K. Pyrazole **3a** exhibited strong absorption bands at 260 and 302 nm as was revealed from UV-visible spectra. When excited at 302 nm it showed strong red shifted emission (31 nm) at around 363-394 nm (Figure 10, Table 1). On the contrary, **3u**, in which the *N*-1 of pyrazole was substituted by the electron withdrawing group, chlorophenyl, showed red shifted (24 nm) emission at around 367-391 nm with decreased intensity as the solvent polarity increased when excited at its strong charge transfer absorption band at 301 nm. The emission was characterized as ICT emission (Figure 11, Table 2).

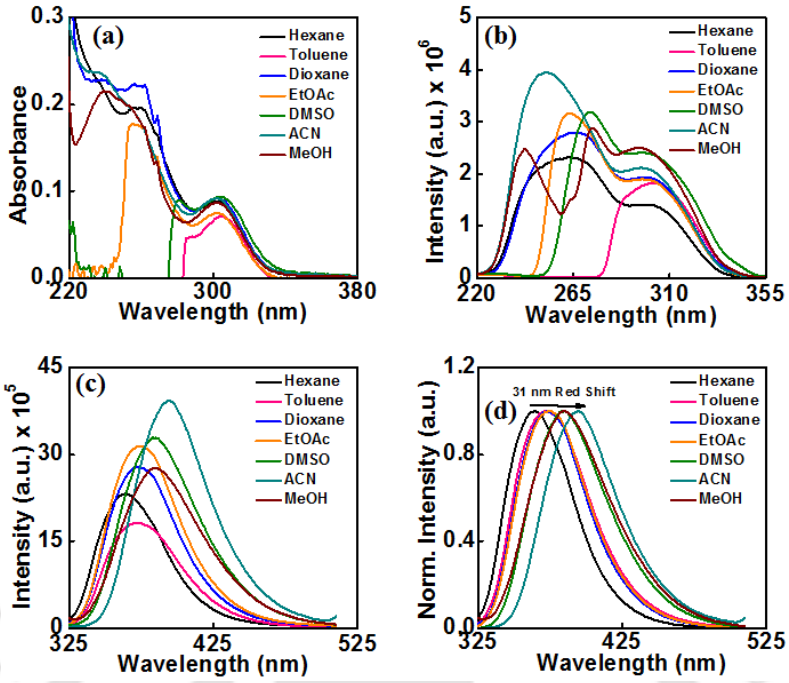

Figure 10. UV-visible (a), excitation (b), fluorescence emission spectra (c), and normalized fluorescence emission spectra (d) of **3a** in different solvents [10 μM, r.t.; $\lambda_{ex} = \lambda_{max} \approx$ 300-305 nm in each solvent].

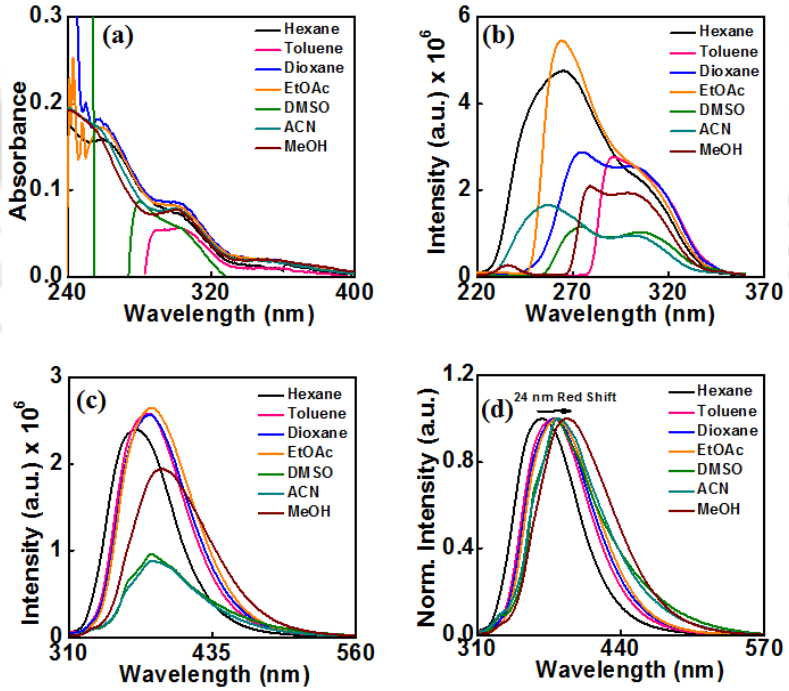

Figure 11. UV-Visible (a), excitation (b), fluorescence emission spectra (c), and normalized fluorescence emission spectra (d) of **3u** in different solvents [10 μM, r.t.; $\lambda_{ex} = \lambda_{max} \approx$ 300-305 nm in each solvent].

Table 1. Summary of Photophysical Properties of **3a**

Entry	Solvents	Δf	UV-Vis & Fluorescence		
			λ_{max}^{abs} (nm)	λ_{max}^{fl} (nm)	Φ_s
3a	Hexane	0.001	257, 302	363	0.105
	Toluene	0.013	305	372	0.106
	Dioxane	0.021	258, 303	373	0.132
	EtOAc	0.201	256, 302	374	0.183
	DMSO	0.265	281, 303	384	0.162
	ACN	0.307	235, 302	394	0.184
	MeOH	0.309	240, 301	384	0.158

Table 2. Summary of Photophysical Properties of **3u**

Entry	Solvents	Δf	UV-Vis & Fluorescence	
			λ_{max}^{abs} (nm)	λ_{max}^{fl} (nm)
3u	Hexane	0.001	258, 300	367
	Toluene	0.013	303	380
	Dioxane	0.021	257, 301	380
	EtOAc	0.201	259, 301	383
	DMSO	0.265	302	382
	ACN	0.307	256, 300	382
	MeOH	0.309	254, 302	391

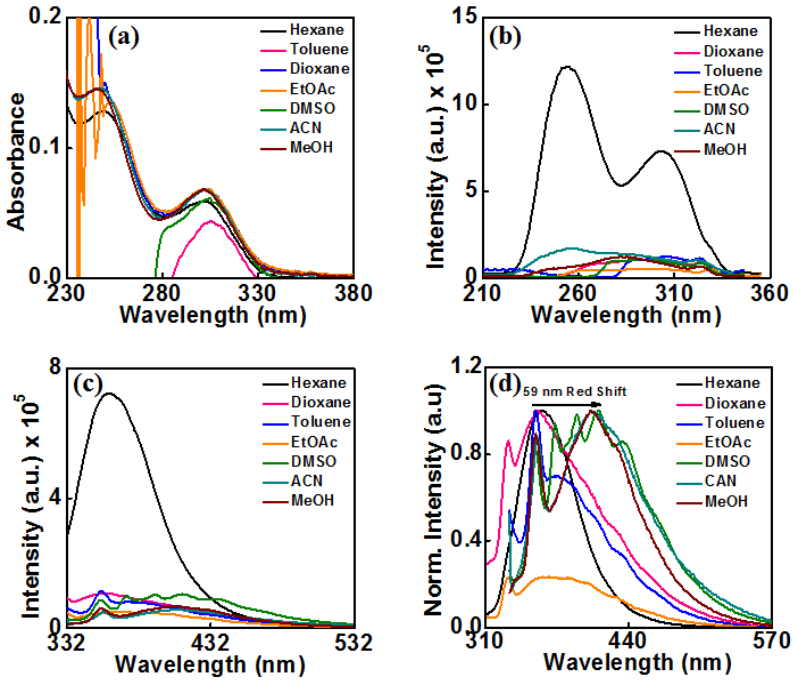

Figure 12. UV-Visible (a), excitation (b), fluorescence emission spectra (c), and normalized fluorescence emission spectra (d) of **3x** in different solvents [10 µM, r.t.; $\lambda_{ex} = \lambda_{max} \approx$ 300-305 nm in each solvent].

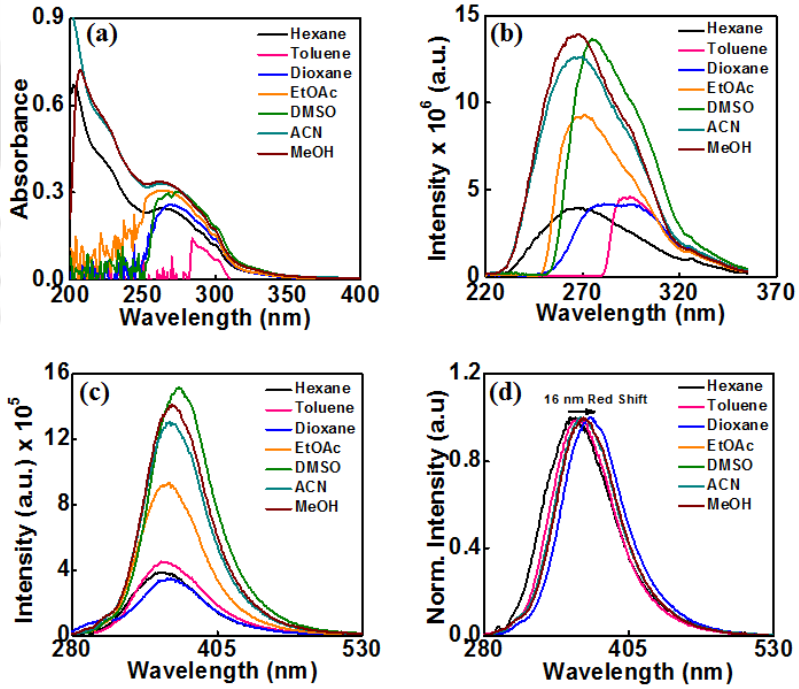

Figure 13. UV-Visible (a), excitation (b), fluorescence emission spectra (c), and normalized fluorescence emission spectra (d) of **3k** in different solvents [10 µM, r.t.; $\lambda_{ex} = \lambda_{max} \approx$ 263-272 nm in each solvent].

Table 3. Summary of Photophysical Properties of **3x** and **3k**

Entry	Solvents	Δf	UV-Visible & Fluorescence	
			λ_{max}^{abs} (nm)	λ_{max}^{fl} (nm)
3x	Hexane	0.001	249,301	361
	Toluene	0.013	305	358
	Dioxane	0.021	249, 303	355, 382
	EtOAc	0.201	253, 302	366
	DMSO	0.265	303	355, 375, 355
	ACN	0.307	247, 301	358, 407
	MeOH	0.309	245, 301	355, 407
3k	Hexane	0.001	203, 264	357
	Toluene	0.013	283	358
	Dioxane	0.021	269	364
	EtOAc	0.201	263	363
	DMSO	0.265	272	373
	ACN	0.307	263	366
	MeOH	0.309	207, 264	366

However, when pyrazole *N*-1 was substituted by the electron withdrawing group, dichlorophenyl, the compound **3x** showed very weak emission in the polar solvents with a strong red shift compared to highly non polar hexane (Figure 12, Table 3). The pyrazole derivative **3k**, exhibited strong absorbance in various organic solvents at around 265 nm.

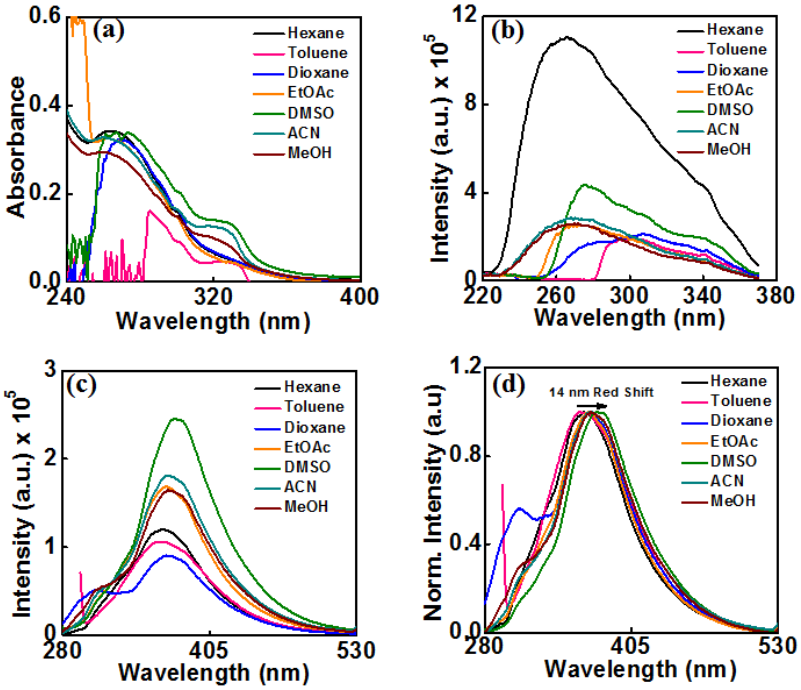

Figure 14. UV-Visible (a), excitation (b), fluorescence emission spectra (c), and normalized fluorescence emission spectra (d) of **3l** in different solvents [10 µM, r.t.; λ_{ex} = λ_{max} ≈ 260-270 nm in each solvent].

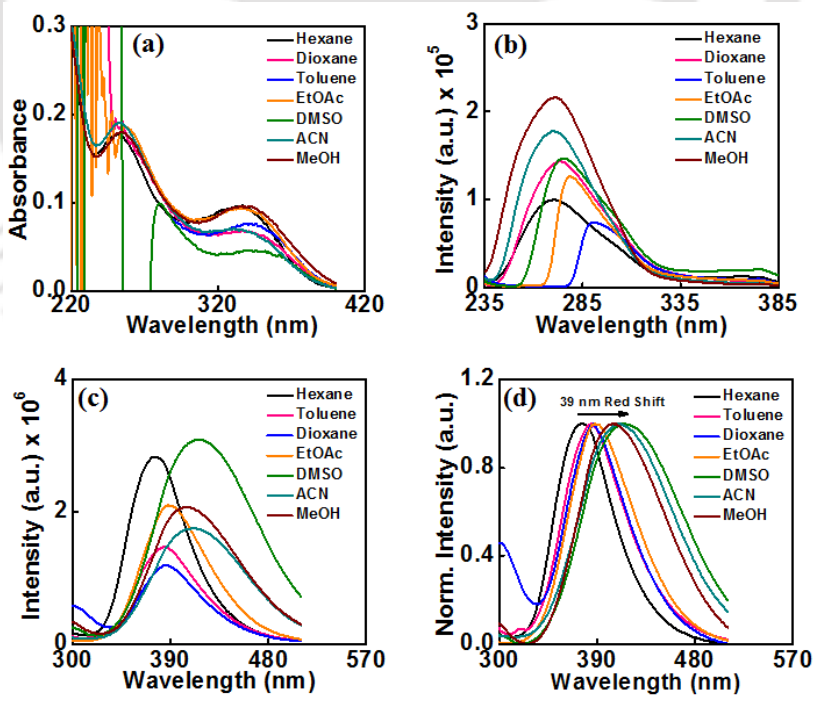

Figure 15. UV-Visible (a), excitation (b), fluorescence emission spectra (c), and normalized fluorescence emission spectra (d) of **3y** in different solvents [10 µM, r.t.; λ_{ex} = λ_{max} ≈ 251-256 nm in each solvent].

Table 4. Summary of Photophysical Properties of **3l**

Entry	Solvents	Δf	UV-Vis & Fluorescence	
			λ_{max}^{abs} (nm)	λ_{max}^{fl} (nm)
3l	Hexane	0.001	263,	363
	Toluene	0.013	285, 328	363
	Dioxane	0.021	269	370
	EtOAc	0.201	262	368
	DMSO	0.265	267, 327	377
	ACN	0.307	261, 325	371
	MeOH	0.309	260, 324	374

Table 5. Summary of Photophysical Properties of **3y**

Entry	Solvents	Δf	UV-Vis & Fluorescence		
			λ_{max}^{abs} (nm)	λ_{max}^{fl} (nm)	Φ_s
3y	Hexane	0.001	251, 335	376	0.007
	Toluene	0.013	253, 339	384	0.011
	Dioxane	0.021	339	385	0.009
	EtOAc	0.201	256, 334	388	0.007
	DMSO	0.265	280,344	415	0.017
	ACN	0.307	252, 330	409	0.008
	MeOH	0.309	254, 338	404	0.006

Upon excitation at individual absorption maxima (λ_{ex} = 263-272 nm) of each solvent, **3k** showed strong emission behaviour at around 365 nm with an increased intensity as the solvent polarity increases from hexane to methanol (Figure 13, Table 3). On the other hand, pyrazole **3l** containing the trimethoxyphenyl donor exhibited absorbance at around 265 and 325 nm. The charge transfer band at 325 nm showed increased intensity with red shifting behaviour as solvent polarity was increased. However, upon excitation at around 260-270 nm it showed strong emission at around 370 nm in various organic solvents with no regular trend (Figure 14, Table 4). The compound **3y** showed stronger absorbance at 255 nm and 335 nm than **3l**. The charge transfer band at 335 nm showed decreased intensity with a red shift as the solvent polarity was increased. Upon excitation at longer absorption band, it showed strong red shifted emission, characteristic of ICT at around 400 nm with a red shift of 39 nm as the solvent polarity was increased (Figure 15, Table 5).

The compound **3v** showed absorption at 260 nm in less polar solvent such as hexane with a shoulder at around 300 nm in polar solvents. It showed irregular emission behaviour at around 373 nm when excited as 260 nm (Figure 16, Table 6). On the other hand compound **3q** showed strong absorption band at around 262 nm which when excited at 262 nm showed structure less emission at around 375 nm with a red shift of 15 nm and decreased intensity as solvent polarity was decreased (Figure 17, Table 6).

From the above UV-visible and fluorescence study it was revealed that the pyrazole derivatives exhibited interesting fluorescent property and solvatochromicity. From this result, we become motivated to study the interaction behavior of pyrazole derivatives with biomacromolecule, such as BSA.

4.3.2 Studies on the Interaction of Two Pyrazoles with BSA Protein

UV-Visible and Fluorescence Study

Looking at the microenvironment sensitive emission characteristics of pyrazoles, **3a** and **3y**, we were next interested to study the interaction behaviour with BSA.[13] Absorption spectra of free **3a** and **3y** in phosphate buffer (20 mM, pH 7.0) showed maxima (λ_{max}) near 245, 299 nm and 243, 336 nm, respectively. Thus, upon addition of increasing concentration of BSA to the solution of pyrazole probe **3a**, we observed a

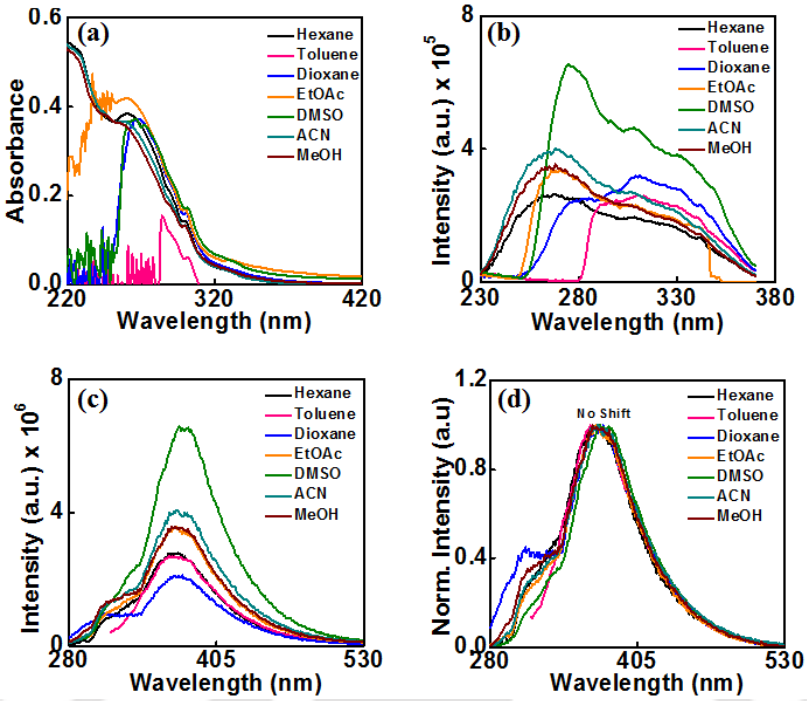

Figure 16. UV-Visible (a), excitation (b), fluorescence emission spectra (c), and normalized fluorescence emission spectra (d) of **3v** in different solvents [10 µM, r.t.; $\lambda_{ex} = \lambda_{max} \approx$ 258-268 nm in each solvent].

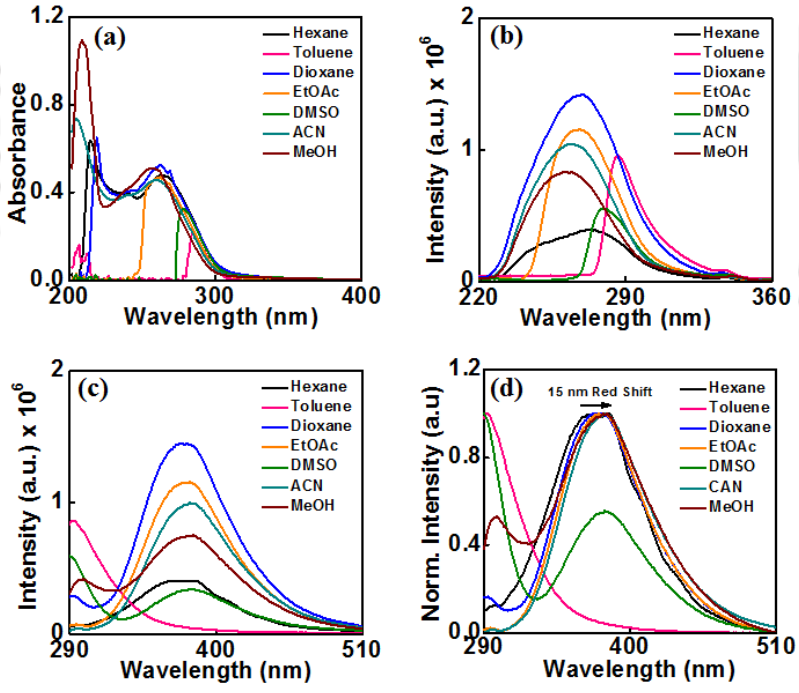

Figure 17. UV-Visible (a), excitation (b), fluorescence emission spectra (c), and normalized fluorescence emission spectra (d) of **3q** in different solvents [10 µM, r.t.; $\lambda_{ex} = \lambda_{max} \approx$ 262-265 nm in each solvent].

Table 6. Summary of Photophysical Properties of **3v** and **3q**

Entry	Solvents	Δf	UV-Visible & Fluorescence	
			λ_{max}^{abs} (nm)	λ_{max}^{fl} (nm)
3v	Hexane	0.001	260, 299	372
	Toluene	0.013	284, 301	372
	Dioxane	0.021	268, 301	372
	EtOAc	0.201	260, 300	373
	DMSO	0.265	265, 301	373
	ACN	0.307	259, 299	375
	MeOH	0.309	258, 299	373
3q	Hexane	0.001	214, 264	367
	Toluene	0.013	284	293
	Dioxane	0.021	219, 262	374
	EtOAc	0.201	262	377
	DMSO	0.265	278	290, 379
	ACN	0.307	205, 259	380
	MeOH	0.309	208, 257	297, 382

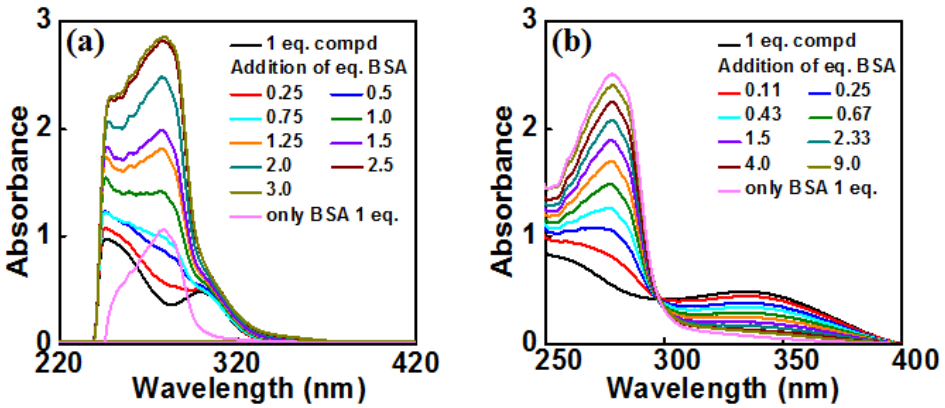

Figure 18. UV-Visible (a), of **3a** and (b), of **3y** in presence of increasing BSA concentration (20 mM phosphate buffer, pH 7.0, rt) at 298K. [Fluorophore (**3a)** and (**3y)**] = 30 μM and [BSA] = 0, 7.5, 15, 22.5, 30, 37.5, 45, 60, 75, 90 μM.

hyperchromicity with strong red shift of 12 nm in the UV-visible spectra indicating interactions between BSA and **3a** (Figure 18a, Table 7). On the other hand, pyrazole probe **3y** exhibited strong hypochromism with a red shift of about 8-10 nm of absorbance band in the UV-visible spectra upon gradual addition of BSA. The band in the UV-visible spectra at around 335 nm vanished when BSA concentration was 9 times the concentration of the probe. All these observations, along with an isosbestic point at 298 nm, clearly indicated strong ground state complex formation between **3y** and BSA (Figure 18b, Table 7).

To investigate the protein sensing ability and insight into the binding event of the probes, we then investigated the change in fluorescence upon addition of increasing concentrations of BSA to the individual probe's solution. Thus, it was observed that both the fluorescence intensity of the probe pyrazole **3a** decreased slowly with a little blue shift of emission maxima when excited at 302 nm (Fig. 19a, Table 7) indicating a binding of the probe in relatively hydrophobic site of the BSA. This observation was also evident from a blue shifted emission of the probe **3a** in various organic solvents as the solvent polarity decreases (Fig. 10c-d).[13,16] On the contrary, upon excitation at 335 nm, a gradual increase in fluorescence intensity at about 420 nm was the result when an increasing concentration of BSA solution was added gradually to a solution of probe pyrazole **3y** (Figure 19b, Table 7). This result indicated a binding interaction between the pyrazole **3y** and the BSA. Moreover, the nonperturbed nature of the isosbestic point suggested only one binding stoichiometry.

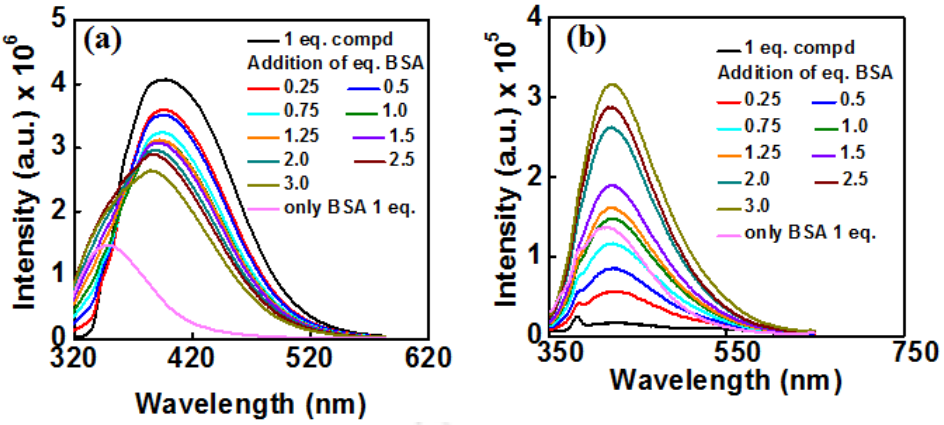

Figure 19. Fluorescence emission spectra (a), of **3a** and (b), of **3y** in presence of increasing BSA concentration (20 mM phosphate buffer, pH 7.0, rt) at 298K. [Fluorophore (**3a)** and (**3y)**] = 30 μM and [BSA] = 0, 7.5, 15, 22.5, 30, 37.5, 45, 60, 75, 90 μM. [$\lambda_{ex} = \lambda_{max} \approx 300$ nm (**3a**) and 340 nm (**3y**)]. Fluorescence titration of probe (**3a** and **3y**) with various concentration of BSA

Absorption Job's Plot from UV-Visible Study

To quantify the stoichiometry between fluorophore (**3a** and **3y**) and the BSA protein, the absorption measurement was carried out for Job's plot. For this purpose, an equal concentration of probe (**3a** and **3y**) and BSA protein solutions was prepared separately in Phosphate buffer. Then, the fluorophore and the BSA protein were mixed in different fraction of volume maintaining the total volume of mixture 1 mL. All the solutions were mixed well and kept for some time in room temperature. Then the absorbance spectra of the solutions of various pyrazoles in absence and in presence of BSA protein were recorded. To calculate the probe-BSA protein complexation ratio, [Probe-BSA protein] vs. X_{probe} were plotted, where [Probe -BSA protein] = $\Delta A/A0$ x [*probe*], {ΔA = (A-A0)}; and X_{probe} is the mole fraction of probe, {X_{probe} = [probe]/([*probe*] + [*BSA*])}. The Job's plot showed the point of maximum at the mole fraction of ~0.50 of both the probe (**3a** and **3y**) pyrazoles (Figure 20). The Job's plot for both the probes suggested a 1:1 binding complex between probes and BSA.

Table 7. Summary of Photophysical Properties of Interaction of **3a** and **3y** with BSA

Entry	**3a**		**3y**	
	UV-Visible & Fluorescence		UV-Visible & Fluorescence	
BSA : Probe	λ_{max}^{abs} (nm)	λ_{max}^{fl} (nm)	λ_{max}^{abs} (nm)	λ_{max}^{fl} (nm)
1:0	300	397	335	381, 420
1 : 0.25	300	395	335	381, 420
1 : 0.5	300	394	275, 335	381, 420
1 : 0.75	300	392	277, 335	381, 420
1 : 1	279, 300	391	277, 335	381, 420
1 : 1.25	278	391	277, 335	420
1 : 1.5	278	389	277, 335	421
1 : 2	277	387	277	421
1 : 2.5	277	385	278	421
1 : 3	277	385	278	421
0:1	277	346	278	412

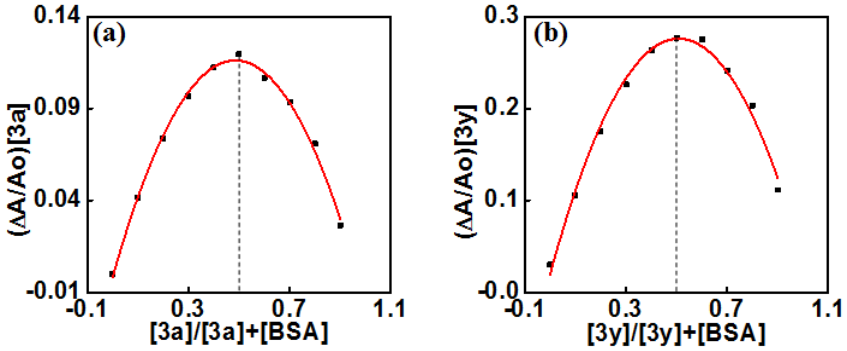

Figure 20. Job's plot (a), of probe **3a** and (b), of probe **3y** in presence of BSA protein indicates a 1:1 stoichiometry of the probe to BSA in the complex.

Steady State Anisotropy Study

Next, the fluorescence anisotropy was measured to confirm the binding event further. Thus, an enhancement of fluorescence anisotropy for the probe **3a** from 0.01 in aqueous buffer to 0.10 in presence of BSA was observed. This indicated that the probe **3a** bound strongly inside the hydrophobic pocket of BSA and experienced a highly restricted rotational motion (Figure 21a).[17] On the other hand, addition of BSA to a solution of **3y**, the anisotropy value increased initially from 0.18 to 0.31 indicating a strong binding between BSA and the probe (Figure 21b).[17]

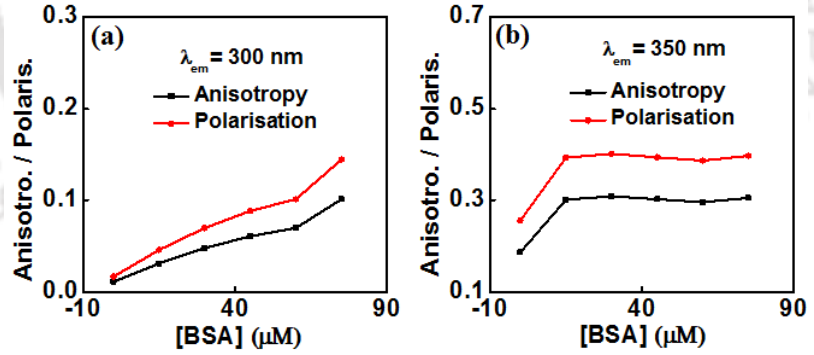

Figure 21. Fluorescence anisotropy and polarization change (a), of fluorophore **3a** and (b), of fluorophore **3y** in presence and absence of various concentration of BSA. [Fluorophore (**3a**) and (**3y**)] = 30 μM and [BSA] =0, 15, 30, 45, 60 and 75 μM.

Study of Circular Dichroism Spectroscopy

Circular dichroism spectra were recorded using a CD spectropolarimeter with a cell path length of 1 mm at 25 ^{o}C, samples concentration 60 μM. An increase in the %α -helicity of

BSA was observed from the CD spectra in the presence of both the pyrazoles. This indicated a possible conformational adjustment of BSA upon association with the pyrazoles (Figure 22).[13,16]

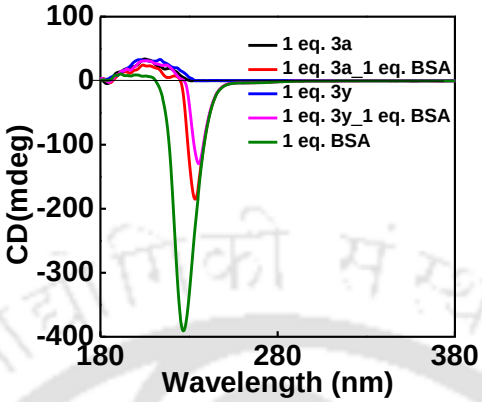

Figure 22. CD spectra of BSA in absence and in presence of synthesized compounds, **3a** and **3y**, respectively (60 µM concentration of each).

Determination of Protein–Probe Binding Constant

The quenching constant (K_{SV}) of protein-probe complex for quenching of fluorescence was determined by Stern-Volmer plot using the following equation 1.

$$I_0/I = 1 + K_{SV}[Q] \quad \text{..... (1)}$$

Where I_0 and I are the fluorescence intensities observed in the absence and presence, of the quencher respectively, and K_{SV} is the Stern-Volmer quenching constant. Thus, the plot of I_0/ I versus [BSA] yields a straight line with a slope equal to K_{SV} which was found to be 4.9 x 10^3 M^{-1}(Figure 23a). Next, the free energy of binding (ΔG) was calculated, which was found to be -5.03 kcal/mol.

The association constant (K) of protein-probe complex for pyrazoles **3y** was also determined from Benesi-Hildebrand plot using the following equation 2.

$$\frac{1}{(I - I_0)} = \frac{1}{(I_\infty - I_0)} + \frac{1}{(I_\infty - I_0)K[BSA]} \quad \text{..... (2)}$$

Where I_0, I and I_α are the emission intensities of pyrazole in the absence of BSA, and in the presence of intermediate and at an infinite concentration of BSA, respectively. From the slope (linear region's data points) of the plot of $1/(I - I_0)$ vs 1/[BSA] the binding constant K was determined, which was found to be 1.64 x 10^4 M^{-1}(Figure

23b). Next, Next, the free energy of binding (ΔG) was also calculated, which was found to be -5.74 kcal/mol.

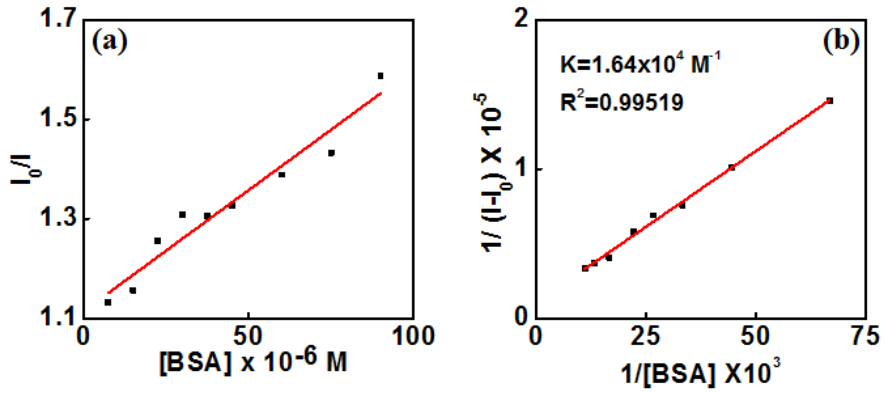

Figure 23. Stern-Volmer plot (a), of **3a** and Benesi-Hildebrand plot (b), of **3y** in presence of increasing BSA concentration. [Fluorophore (**3a**) and (**3y**)] = 30 µM and [BSA] = 0, 7.5, 15, 22.5, 30, 37.5, 45, 60 µM.

The association constants reflected that the compound **3y** binds with BSA more strongly than **3a**. Therefore, it is clear from the above bindings that the probe pyrazole **3y** is more efficient compared to **3a** in sensing BSA protein biomolecule via the generation of enhanced fluorescence intensity. The low fluorescence intensity of the probe in phosphate buffer in absence of biomolecules may be attributed to a radiationless channel assisted by intermolecular hydrogen bonding present in aqueous solution. However, in presence of BSA the nonradiative channels are possibly blocked and are less effective, as the probe interacts strongly with the protein, which ultimately leads to a fluorescence switch-on signal of enhanced intensity and quantum yields.

Molecular Docking Calculation

Docking calculations were carried out using Autodock4 (Bikadi, Hazai, 2009). The amino acid sequence of BSA protein was observed from the NCBI website, http://www.ncbi.nlm.nih.gov/protein/CAA76847.1 The 3D model of the BSA protein was built using the 3D structure 1AO6 chain 'A' as template using the ESyPred3D11 web server. This template shares 72.4% identities with the BSA sequence. Following is the BSA sequence which was used to generate the 3D model. >gi|3336842|emb|CAA76847.1| bovine serum albumin [Bos taurus]

MKWVTFISLLLLFSSAYSRGVFRRDTHKSEIAHRFKDLGEEHFKGLVLIAFSQYLQ
QCPFDEHVKLVNELTEFAKTCVADESHAGCEKSLHTLFGDELCKVASLRETYGD
MADCCEKQEPERNECFLSHKDDSPDLPKLKPDPNTLCDEFKADEKKFWGKYLYE
IARRHPYFYAPELLYYANKYNGVFQECCQAEDKGACLLPKIETMREKVLTSSAR
QRLRCASIQKFGERALKAWSVARLSQKFPKAEFVEVTKLVTDLTKVHKECCHGD
LLECADDRADLAKYICDNQDTISSKLKECCDKPLLEKSHCIAEVEKDAIPENLPPL
TADFAEDKDVCKNYQEAKDAFLGSFLYEYSRRHPEYAVSVLLRLAKEYEATLEE
CCAKDDPHACYSTVFDKLKHLVDEPQNLIKQNCDQFEKLGEYGFQNALIVRYTR
KVPQVSTPTLVEVSRSLGKVGTRCCTKPESERMPCTEDYLSLILNRLCVLHEKTP
VSEKVTKCCTESLVNRRPCFSALTPDETYVPKAFDEKLFTFHADICTLPDTEKQIK
KQTALVELLKHKPKATEEQLKTVMENFVAFVDKCCAADDKEACFAVEGPKLVV
STQTALA

The free energy of binding (ΔG) of pyrazole **3a**-BSA and **3y**-BSA complexes were found to be -6.38 and -6.91 kcal/mol respectively obtained from docking calculation (Table 8). These results closely matches with experimental values of -5.03 and -5.74 kcal/mol calculated from binding constant (K) value obtained from Stern-Volmer plot and Benesi-Hildebrand plot respectively. All the results suggested that hydrophobic interaction played an important role in the present BSA-pyrazole interaction process. The binding of the pyrazoles in the hydrophobic pocket of BSA was also supported by a molecular docking calculation with Autodoc programme[18] which clearly showed that pyrazole probes remained surrounded by hydrophobic amino acids of the hydrophobic pocket of subdomain IIIA of site II of BSA (Figure 24).

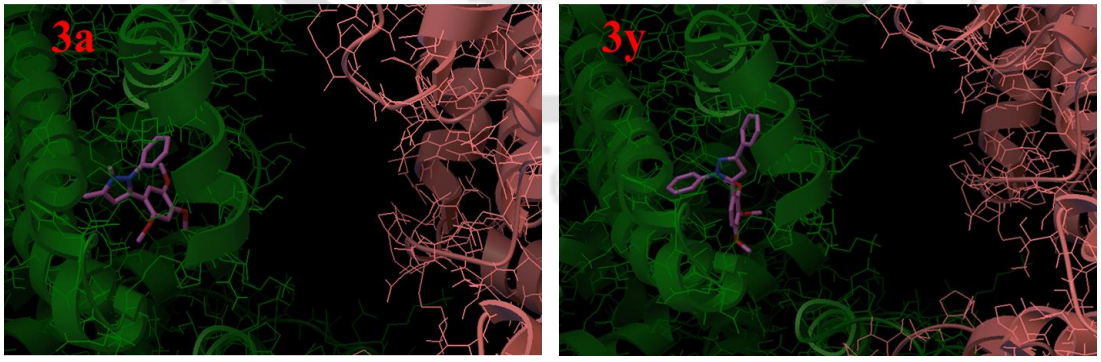

Figure 24. Docking pose of **3a** and **3y** in hydrophobic pocket of BSA.

Table 8. Energy of **3a-BSA** and **3y-BSA** complex obtained from Autodock4.

Interaction Energy	**3a-BSA** (kcal/mol)	**3y-BSA** (kcal/mol)
Estimated Free Energy of Binding	-6.38	-6.91
Final Intermolecular Energy	-7.88	-8.70
vdW + Hbond + desolv Energy	-7.78	-8.96
Electrostatic Energy	-0.10	+0.27
Final Total Internal Energy	-1.44	-1.89
Torsional Free Energy	+1.49	+1.79
Unbound System's Energy	-1.44	-1.89

In summary, the study of photophysical properties of the pyrazoles reflected their potential fluorophoric nature. We exploited such two pyrazoles for studying the interaction with BSA and found that both the pyrazoles bind with BSA strongly. While the interaction of pyrazoles **3y** with BSA led to switch-on fluorescence, a quenching of fluorescence was evident from an interaction of BSA with pyrazoles **3a**. From the association constants it was clear that the probe pyrazole **3y** is more efficient compared to **3a** in sensing BSA protein biomolecule via the generation of enhanced fluorescence intensity. Thus, this study will open new avenue for the further development of such biologically important small fluorescent pyrazoles which could be utilized for sensing of other biomolecules such as DNA, other class of proteins or study the interbiomolecular interaction with fluorescence switch-on response possibly at a longer wavelength region.

4.4 Experimental Section

Materials. BSA, Na_2HPO_4 and $NaH_2PO_4.H_2O$ (for preparation of phosphate buffer) were purchased from Merck, and used without further purification. Water was obtained from a Milli-Q purification system. All experiments were performed with freshly prepared solutions. The probe pyrazole compounds were synthesized and purified according to the procedure described in chapter 2.

UV-Visible and Fluorescence Measurements. All UV-visible spectra of the compound (10 μM) was measured in different solvents of varying dielectric constant by UV-visible spectrophotometer using 1 cm path length cell at 298 K. Fluorescence spectra of the compounds (10 μM) were measured in different solvents of varying dielectric constant by fluorescence spectrophotometer at 298 K using 1 cm path length cell. All the sample solutions were prepared just before doing the experiment. (Equqtion have to give or not)

$$\Phi_S = \Phi_R \frac{Fl_S^{Area}}{Fl_R^{Area}} \frac{Abs_R}{Abs_S} \frac{n_S^2}{n_R^2}$$

The fluorescence quantum yields (Φ_s) were determined using quinine sulphate as a reference with the known Φ_r (0.54) in 0.1 molar solutions in sulphuric acid. The above equation was used to calculate the quantum yield.

Preparation of Stock Solution. To prepare the BSA solution Milli-Q water was used. A 1000 μM of stock BSA solution was prepared by dissolving 0.198 gm of BSA in 3 mL Milli-Q water.

The stock solutions of pyrazoles derivatives were prepared in DMF because of the poor solubility in water. 0.97 mg of **3a** and 1.16 mg of **3y** was dissolved in 3 mL DMF to make stock probe solutions of each pyrazoles of concentration 1000 μM.

General Experimental on Interaction Study of BSA by UV–Visible Absorption and Fluorescence Spectroscopy. All the spectral measurements were carried out at room temperature. To study the interaction of compound with BSA, an aqueous solution (3% DMF) of compound (30 μM in 1mL solution) was titrated with different concentrations of BSA (ranging from 0, 7.5, 15, 22.5, 30, 37.5, 45, 60, 75, 90 μM). The total volume of the final solution for each sample was 1 mL. As the fluorophores are not soluble in water, 3% DMF is used to solubilize them. The presence of 3% DMF does not induce structural

changes to biomolecules. Each sample solution was mixed well before spectral measurements.

UV-Visible Study with BSA Protein. The UV-Visible absorbance measurements were performed using Shimadzu UV-2550 UV-Visible spectrophotometer with a cell of 1 cm path length at 298 K. All the UV-Visible studies were carried out in 20 mM phosphate buffer of pH 7.0 at 298 K. The measurements were taken in absorbance mode and the absorbance values of the sample solutions were measured in the wavelength region of 200-600 nm. All the experiments were carried out with freshly prepared sample solutions.

Fluorescence Study with BSA Protein. All fluorescence and steady state anisotropy experiments were performed using a Fluoromax4 spectrophotometer with a cell of 1 cm path length at 298 K. All the fluorescence studies were carried out in 20 mM phosphate buffer of pH 7.0 at 298 K. Steady state anisotropy of the solutions was measured using Fluoromax4 spectrophotometer.

4.5 References

1. (a) Kragh-Hansen, U. *Pharmacol. Rev.* **1981**, *33*, 17. (b) Beljaars, L.; Molema, G.; Schuppan, D.; Geerts, A.; De Bleser, P. J.; Weert, B.; Meijer, D. K. F.; Poelstra, K. *J. Biol. Chem.* **2000**, *275*, 12743. (c) Beljaars, L.; Molema, G.; Schuppan, D.; Geerts, A.; De Bleser, P. J.; Weert, B.; Meijer, D. K. F.; Poelstra, K. J. *J. Biol. Chem.* **2000**, *275*, 12743. (d) Sheffield, W. P. *Curr. Drug Targets Cardio*V*asc. Haematol. Disord.* **2001**, *1*, 1. (e) Rich, R. L.; Day, Y. S.; Morton, T. A.; Myszka, D. G. *Anal. Biochem.* **2001**, *296*, 197. (f) Buchholz, L.; Cai, C.-H.; Andress, L.; Cleton, A.; Brodfuehrer, J.; Cohen, L. *Eur. J. Pharm. Sci.* **2002**, *15*, 209. (g) Kratochwil, N. A.; Huber, W.; Muller, F.; Kansy, M.; Gerber, P. R. *Biochem. Pharmacol*. **2002**, *64*, 1355.
2. (a) Ghuman, J.; Zunszain, P. A.; Petitpas, I.; Bhattacharya, A. A.; Otagiri, M.; Curry, S. *J. Mol. Biol.* **2005**, *353*, 38. (b) Simard, J. R.; Zunszain, P. A.; Ha, C. E.; Yang, J. S.; Bhagavan, N. V.; Petitpas, I.; Curry, S.; Hamilton, J. A. *Proc. Natl. Acad. Sci. U.S.A.* **2005**, *102*, 17958. (c) Ascenzi, P.; Bocedi, A.; Notari, S.; Fanali, G.; Fesce, R.; Fasano, M. *Mini Rev. Med. Chem.* **2006**, *6*, 483. (d) Simard, J. R.; Zunszain, P. A.; Hamilton, J. A.; Curry, S. *J. Mol. Biol.* **2006**, *361*, 336.

3. (a) Gellman, S. H. *Chem. Rev.* **1997**, *97*, 1231. (b) Lyon, C. E.; Suh, E. S.; Dobson, C. M.; Hore, P. J. *J. Am. Chem. Soc.* **2002**, *124*, 13018. (c) Schneider, H.-J.; Yatsimirsky, A. K. *Chem. Soc. Re*v. **2008**, *37*, 263.

4. (a) Gelamo, E.L.; Silva, C.H.; Imasato, H.; Tabak, M. *Biochim. Biophys. Acta* **2002**, *1594*, 84. (b) Klajnert, B.; Bryszewska, M. *Bioelectrochem* **2002**, *55*, 33e5. (c) Cui, F.L.; Fan, J.; Li, W.; Fan, Y.C.; Hu, Z.D. *J. Pharm. Biomed. Anal.* **2004**, *34*, 189.

5. Ibrahim, N.; Ibrahim, H.; Kim, S.; Nallet, J.-P.; Nepveu, F. *Biomacromolecules* **2010**, *11*, 3341

6. (a) Sjoholm, I.; Ekman, B.; Kober, A.; Ljungstedt-Pahlman, I.; Seiving, B.; Sjodin, T. *Mol. Pharmacol*. **1979**, *16*, 767. (b) Berde, C. B.; Hudson, B. S.; Simoni, R.D.; Sklar, L.A. *J. Biol. Chem.* **1979**, *254*, 391. (c) He, X. M.; Carter, D.C. *Nature* **1992,** *358*, 209. (d) Nowak, I.; Shaw, L. M. *Clin. Chem.* **1995**, *41*, 1011. (e) Valle, M.; Estaban, M.; Rodriquez-Sasiain, J. M.; Calvo, R.; Aquirre, C. *Res. Commun. Mol. Pathol. Pharmacol.* **1996**, *94*, 73. (f) Yamasaki, K.; Maruyama, T.; Kragh-Hansen, U.; Otagiri, M. *Biochim. Biophys. Acta* **1996**, *1295*, 147. (g) Gelamo, E. L.; Tabak, M. *Spectrochim Acta A*, **2000**, *56*, 2255. (h) Gelamo, E. L.; Silva, C. H.; Imasato, H.; Tabak, M. *Biochim. Biophys. Acta* **2002**, *1594*, 84.

7. (a) Benyamini, H.; Shulman-Peleg, A.; Wolfson, H.J.; Belgorodsky, B.; Fadeev, L.; Gozin, M. *Bioconjugate Chem*. **2006**, *17*, 378. (b) Mandeville, J. S.; Tajmir-Riahi, H. A. *Biomacromolecules* **2010**, *11*, 465.

8. (a) Carter, D. C.; He, X. M. *Science* **1990**, *249*, 302. (b) He, X. M.; Carter, D. C. *Nature* **1992**, *358*, 209. (c) Carter, D. C.; Ho, J. X. *Adv. Protein Chem*. **1994**, *45*, 153. (d) Dockal, M.; Carter, D. C.; Ruker, F. *J. Biol. Chem*. **1999**, *274*, 29303.

9. (a) Moriyama, Y.; Ohta, D.; Hachiya, K.; Mitsui, Y.; Takeda, K. *J. Protein Chem*. **1996**, *15*, 265. (b) Huang, B.X.; Kim, H.-Y.; Dass, C. *J. Am. Soc*. **2004**, *15*, 1237.

10. (a) Lhiaubet-Vallet, V.; Sarabia, Z.; Bosca, F.; Miranda, M. A. *J. Am. Chem. Soc*. **2004**, *126*, 9538. (b) Jimenez, M. C.; Miranda, M. A.; Vaya, I. *J. Am. Chem. Soc*. **2005**, *127*, 10134.

11. For examples, see: (a) Chu, C. K.; Cutler, J. J. *Heterocycl. Chem*. **1986**, *23*, 289. (b) Janus, S. L.; Magdif, A. Z.; Erik, B. P.; Claus, N. *Monatsh. Chem*. **1999**, *130*, 1167. (c) Tewari, A. K.; Mishra, A. *Bioorg. Med. Chem*. **2001**, *9*, 715. (c) Mohammed, K.

O.; Nissan, Y. M. *Chem. Biol. Drug. Des*. **2014**, *84*, 473. (d) Ghorab, M. M.; Ragab, F. A.;Heiba, H. I.; El-Gazzar, M. G.; Zahran, S, S. *Eur. J. Med. Chem*. **2015**, *92*, 682.

12. (a) Baraldi, P. G.; Balboni, G.; Pavani, M. G.; Spalluto, G.; Tabrizi, M. A.; Clercq, E. D.; Balzarini, J.; Bando, T.; Sugiyama, H.; Romagnoli, R. *J. Med. Chem*. **2001**, *44*, 2536. (b) Kulkarni, N. V.; Kamath, A.; Budagumpi, S.; Revankar V. K. *J. Mol. Struct*. **2011**, *1006*, 580.
13. For examples, see: (a) Tse, W. C.; Boger, D. L. *Acc. Chem. Res*. **2004**, *37*, 61. (b) Wu, J.; Liu, W.; Ge, J.; Zhang, H.; Wang, P. *Chem. Soc. Rev*. **2011**, *40*, 3483.
14. (a) Yuan, C.-X.; Tao, X.-T.; Wang, L.; Yang, J.-X.; Jiang, M.-H. *J. Phys. Chem. C* **2009**, *113*, 6809. (b) Xu, Y.; Li, Z.; Malkovskiy, A.; Sun, S.; Pang, Y. *J. Phys. Chem. B* **2010**, *114*, 8574. (c) Wang, J.-X,; Chen, Q.; Bian, N.; Yang, F.; Sun, J.; Qi, A.-D.; Yan C.-G.; Han,B.-H. *Org. Biomol. Chem.* **2011**, *9*, 2219. (d) Banerjee, M.; Pal, U.; Subudhhi, A.; Chakrabarti, A.; Basu, S. *J. Photochem. Photobiol. B: Biology* **2012**, *108*, 23. (e) Zhang, Y.; Yue, X.; Kim, B.; Yao, S.; Bondar, M. V.; Belfield, K. D. *ACS Appl. Mater. Interfaces* **2013**, *5*, 8710. (f) Anees, P.; Sreejith, S.; Ajayaghosh, A. *J. Am. Chem. Soc*. **2014**, *136*, 13233.
15. (a) Hu, Y.-J.; Liu, Y.; Zhang, L.-X.; Zhao, R.-M.; Qu, S.-S. *J. Mol. Struct*. **2005**, *750*, 174. (b) Ojha, B.; Das, G. *Chem. Commun*. **2010**, *46*, 2079. (c) Jana, S.; Dalapati, S.; Ghosh, S.; Guchhait, N. *J. Photochem. Photobiol A: Chemistry* **2012**, *231*, 19. (d) Pisoni, D. d. S.; Abreu, M. P. d.; Petzhold, C. L.; Rodembusch, F. S.; Campo, L. F. *J. Photochem. Photobiol A: Chemistry* **2013**, *252*, 77. (e) Li, X.; Chen, D.; Wang, G.; Lu, Y. *J. Lumin*. **2014**, *156*, 255. (f) Hu, Y.; Zhang, G.; Yan, J. *Mol. Biol. Rep*. **2014**, *41*, 1693. (g) Li, W.; Chen, D.; Wang, H.; Luo, S.; Dong, L.; Zhang, Y.; Shi, J.; Tong, B.; Dong, Y. *ACS Appl. Mater. Interfaces* **2015**, *7*, 26094.
16. For examples, see: (a) Xu, Y.; Li, Z.; Malkovskiy, A.; Sun, S.; Pang, Y. *J. Phys. Chem. B* **2010**, *114*, 8574. (b) Banerjee, M.; Pal, U.; Subudhhi, A.; Chakrabarti, A.; Basu, S. *J. Photochem. Photobiol. B: Biol*. **2012**, *108*, 23. (c) Bag, S. S.; Kundu, R.; Jana, S. *Tetrahedron Lett*. **2013**, *54*, 2627.
17. For examples, see: (a) Bi, S.; Song, D.; Tian, Y.; Zhou, X.; Liu, Z.; Zhang, H. *Spectrochim. Acta A* **2005**, *61*, 629. (b) Lakowicz, J. R. In *Principles of Fluorescence Spectroscopy*, 3rd ed., Kluwer Academic/Plenum Publishers, New York, 2006.

18. Morris, G. M.; Huey, R.; Lindstrom, W.; Sanner, M. F.; Belew, R. K.; Goodsell, D. S.; Olson, A. J. *J. Comput. Chem*. **2009**, *16*, 2785.

Conclusions

In chapter I, synthesis of bisarylnitromethyl sulfones is described from bisarylsulfonyl hydrazones in presence of $Fe(NO_3)_3 \cdot 9H_2O$ via a radical C-N/S bonds formation at moderate temperature. The reaction is simple, general and tolerates an array of functionality. The reaction pathway has been demonstrated using DFT calculations.

In chapter II, synthesis of trisubstituted pyrazoles is presented via *C-N* cross-dehydrogenative coupling of alkenyl hydrazones in presence of V(IV) catalyst using air as the oxidant at room temperature. The synthesis of Celebrex drug using this protocol is also demonstrated.

In chapter III, a metal-free C-H oxidative procedure for the synthesis of highly substituted pyrazoles using TEMPO and NBS system is described under mild reaction conditions. In the absence of TEMPO, the process leads to the selective formation of 4-bromopyrazoles. The presence of bromine at 4-position can permit further elaboration of the products into the complex derivatives.

In chapter IV, photophysical and binding studies of some of the pyrazoles towards BSA protein have been presented.

List of Publications

1. **“**Iron(III)-catalyzed aerobic dioxygenation of Styrenes Using *N*-hydroxyphthalimide and *N*-hydroxybenzotriazole” Bag, R.; **Sar, D.**; Punniyamurthy, T. *Org. Biomol*. Chem. **2016**, *14*, 3246.

2. "Synthesis of Functionalized Pyrazoles via Vanadium-Catalyzed C-N Dehydrogenative Cross-Coupling and Fluorescence Switch-On Sensing of BSA Protein" **Sar**, **D.**; Bag, R.; Yashmeen, A.; Bag, S. S.; Punniyamurthy, T. *Org. Lett*. **2015**, *17*, 5308.

3. "Copper(II)-Catalyzed Direct Dioxygenation of Alkenes with Air and *N*-Hydroxyphthalimide: Synthesis of *β*-Keto-*N*-alkoxyphthalimides", Bag, R.; **Sar, D.**; Punniyamurthy, T. *Org. Lett*. **2015**, *17*, 2010.

4. "Iron(III)-Mediated Radical Nitration of Bisarylsulfonyl Hydrazones: Synthesis of Bisarylnitromethyl Sulfones", **Sar, D.**; Bag, R.; Bhattacharjee, D.; Deka, R. C.; Punniyamurthy, T. *J. Org. Chem*. **2015**, *80*, 6676.

5. "Synthesis of Substituted Pyrazoles from Vinylhydrozones via Bromoamination and Hydroamination with 2,2,6,6-Tetramethylpiperidine-1-oxyl and *N*-Bromosuccinimide", **Sar, D.**; Paul, R.; Sengoden, M.; Punniyamurthy, T. *Asian J. Org. Chem*. **2014,** *3*, 638.

6. "Oxidative Aromatic C-H Functionalization Promoted by Phenyliodine(III) Diacetate to form C-N, C-S, and C-Se Bonds" Kumar, R. K.; Manna, S.; Mahesh, D.; **Sar, D.**; Punniyamurthy, T. *Asian J. Org. Chem.* **2013**, *2*, 843.

Conferences

1. "Vanadium-Catalyzed C-H Oxidative Synthesis of Substituted Pyrazoles and Fluorescence Switch-On Sensing of BSA Protein" **Sar, D.**; Bag, R.; Yashmeen, A.; Bag, S. S.; Punniyamurthy, T. *19th CRSI National Symposium in Chemistry* 2016, July 14-16, University of North Bengal.

2. "Synthesis of Bisarylnitromethyl Sulfones Using $Fe(NO_3)_3 \cdot 9H_2O$ with Aryl Aldehydes and Aryl Sulfonyl Hydrazides" **Sar, D.**; Bag, R.; Bhattacharjee, D.; Deka, R. C.; Punniyamurthy, T. *11th J-NOST Conference for Research Scholars 2015*, December 14-17, NISER Bhubaneswar, India.

3. "Synthesis of Substituted Pyrazoles from Vinyl hydrazones via Bromoamination and Hydroamination with 2,2,6,6-Tetramethylpiperidine-1-oxyl (TEMPO) and *N*-Bromosuccinimide (NBS)" **Sar, D.**; Paul, R.; Sengoden, M.; Punniyamurthy, T. *International Symposium on Nature Inspired Initiative In Chemical Trends* 2014, March 02-05, IICT Hyderabad, India.